Linking Scales: Investigations on the interactions between environmental conditions, humans, and a fossorial rodent species across space and time

Dissertation

„kumulativ"

zur Erlangung des Grades eines

Doktor der Naturwissenschaften

(Dr. rer.nat.)

des Fachbereichs Biologie der Philipps-Universität Marburg

Vorgelegt von

Victoria Michelle Reuber

aus Siegen

Marburg, September 2023

Linking Scales: Investigations on the interaction between environmental conditions, humans, and a fossorial rodent species across space and time

Dissertation

„kumulativ"

zur Erlangung des Grades eines

Doktor der Naturwissenschaften

(Dr. rer.nat.)

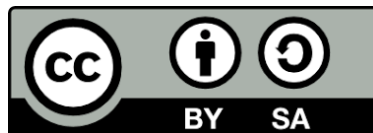des Fachbereichs Biologie der Philipps-Universität Marburg

Vorgelegt von

Victoria Michelle Reuber

aus Siegen

Marburg, September 2023

Die vorliegende Dissertation wurde von Oktober 2019 bis September 2023 am Fachbereich Biologie der Philipps-Universität Marburg unter Leitung von Prof. Dr. Dana G. Schabo angefertigt.

Vom Fachbereich Biologie der Philipps-Universität Marburg (Hochschulkennziffer 1180) als Dissertation angenommen am _____

Erstgutachter(in):   Prof. Dr. Dana G. Schabo

Zweitgutachter(in):   Prof. Dr. Nina Farwig

Tag der Disputation: _____

Table of content

Declaration of author contributions

The thesis *'Linking Scales: Investigations on the interaction between environmental conditions, humans, and a fossorial rodent species across space and time'* is based on the work I carried out from October 2019 to September 2023 at the Philipps University of Marburg, under the supervision of Dr. Dana G. Schabo and Prof. Dr. Nina Farwig. Chapters 2 - 5 of this thesis include four independent scientific manuscripts, each with co-authorship, and have been published or will be published in peer-reviewed journals. My contributions to other manuscripts relevant for my research topic, but not being included as chapters in this dissertation, are also described. The contributions of the authors for each manuscript or project are stated as following:

The activity of a subterranean small mammal alters Afroalpine vegetation patterns and is positively affected by livestock grazing

Addisu Asefa*, **Victoria M. Reuber***, Georg Miehe, Melaku Wondafrash, Luise Wraase, Tilaye Wube, Nina Farwig, Dana G. Schabo.

* These authors contributed equally to this study

Published in *Basic and Applied Ecology* |DOI: 10.1016/j.baae.2022.09.001

AA and VMR contributed equally to this work. AA collected field data, VMR conducted the data analyses and visualized results, NF and DGS secured the project funding,. AA, VMR, GM, LW, TW, NF and DGS designed the research concept. AA and VMR drafted the manuscript with contributions from all authors.

Remote sensing-supported mapping of a subterranean landscape engineer across an afro-alpine ecosystem

Luise Wraase*, **Victoria M. Reuber***, Philipp Kurth, Mekbib Fekadu, Sebsebe Demissew, Georg Miehe, Lars Opgenoorth, Ulrike Selig, Zerihun Woldu, Dirk Zeuss, Dana G. Schabo, Nina Farwig & Thomas Nauss

* These authors contributed equally to this study

Published in *Remote Sensing in Ecology and Conservation* |DOI: 10.1002/rse2.303

LW and VR contributed equally to this work. PK and MF mapped the GRR mounds and sampled the vegetation on the GRR presence and absence plots. LW, VR and PK processed the vegetation survey data that was collected. VR conducted the statistical vegetation analysis. US did the temperature modelling of the Landsat-8 images. LW and TN performed the statistical and spatial modelling and prediction. LW, VR, PK, MF, SD, GM, LO, ZW, DZ, DS, NF, and TN designed the research concept, LW and VR drafted the manuscript and figures with contributions from all authors.

Topographic barriers drive the pronounced genetic subdivision of a range-limited fossorial rodent

Victoria M. Reuber, Michael V. Westbury, Alba Rey-Iglesia, Addisu Asefa, Nina Farwig, Georg Miehe, Lars Opgenoorth, Radim Sumbera, Luise Wraase, Tilaye Wube, Eline D. Lorenzen* and Dana G. Schabo*

* These authors contributed equally to this study

VMR, AA, LW and DGS captured specimens in the field. VMR and AR-I conducted lab work. VMR, AR-I and MVW analysed the data with contributions from RS, EDL, and DGS for genetic and ecological interpretation. LW generated raster layers for landscape genetic analyses. NF, LO and DGS secured the project funding. VMR, NF, GM, LO, TW, EDL and DGS designed the research concept. VMR, EDL and DGS wrote the manuscript with contributions from all co-authors. All authors gave final approval for publication and agreed to be held accountable for the work carried out within this publication.

Evolutionary history of fossorial rodent species reveals insights into Middle Stone Age foragers' resource-use and high-altitude residency under Late Pleistocene climate change

Victoria M. Reuber, Alba Rey-Iglesia, Michael V. Westbury, Mona Schreiber, Addisu Asefa, Nina Farwig, Alexander Groos, Georg Miehe, Dana G. Schabo, Paul Szpak, Tilaye Wube, Götz Ossendorf, Lars Opgenoorth* and Eline D. Lorenzen*

* These authors contributed equally to this study

Not published

VMR and AR-I conducted lab work, VMR analysed the data with the help from AR-I, and with help in data generation from MVW, and analytic support from AG, GO, MVW, MS, PS, LO and EDL. GO conducted excavations and collected ancient bone samples, AA collected contemporary bone samples. PS compiled radiocarbon and stable isotope data. NF, DGS and LO secured the project funding. VMR, NF, AG, GM, GO, DGS, TW, LW, EDL and LO designed the research concept. VMR, LO and EDL wrote the manuscript with contributions from all co-authors.

Other (co-)authors' contributions

Complete mitochondrial genome of the giant root-rat (*Tachyoryctes macrocephalus*)

Victoria M. Reuber, Alba Rey-Iglesia, Michael V. Westbury, Andrea A. Cabrera, Nina Farwig, Mikkel Skovrind, Radim Šumbera, Tilaye Wube, Lars Opgenoorth, Dana G. Schabo, Eline D. Lorenzen

Published in *Mitochondrial DNA Part B*| DOI: 10.1080/23802359.2021.1944388.

VMR captured specimens in the field with the help from DGS. VMR, AR-I, AAC, MS and conducted lab work. VMR, AR-I and MVW analysed the data with input for interpretation from RS, EDL and DGS. NF, LO and DGS secured the project funding. VMR, EDL and DGS wrote the manuscript with contributions from all co-authors. All authors gave final approval for publication and agreed to be held accountable for the work carried out within this publication

---

Human activities modulate reciprocal effects of a subterranean ecological engineer rodent, *Tachyoryctes macrocephalus*, on Afroalpine vegetation cover

Addisu Asefa, **Victoria Reuber**, Georg Miehe, Luise Wraase, Tilaye Wube, Dana G. Schabo, Nina Farwig

Published in *Ecology and Evolution*| DOI: 10.1002/ece3.10337

AA collected field data, conducted the data analyses and visualized results with help from VMR, NF and DGS. NF and SGS secured the project funding. Validation and review were key stages in the research process, and these tasks were expertly handled by VMR, GM, LW, TW, DGS and NF. AA, DGS, and NF took the lead in crafting the original draft,

---

Giant root-rat engineering and livestock grazing activities regulate plant functional trait diversity of an Afroalpine vegetation community in the Bale Mountains, Ethiopia

Addisu Asefa, **Victoria M. Reuber**, Georg Miehe, Luise Wraase, Tilaye Wube, Nina Farwig, Dana G. Schabo

Under revision in *Oecologia*

AA collected data and conducted the analyses with support from VMR, DGS and NF. AA visualized the results with support from VMR, DGS, NF. AA wrote the original draft with contributions from all co-authors. AA, VMR, GM, LW, TW, NF and DGS designed the research concept. NF and DGS secured the project funding.

Summary

Interactions between species and their environment build the backbone of biodiversity and ecosystem stability. Species-environment interactions shape species' spatial distributions and population dynamics, with present and past environmental conditions, as well as evolutionary mechanisms such as dispersal ability playing pivotal roles. Understanding how species are shaped by the environment and human activities across spatial scales and time, is a precondition to predict and reverse the ongoing decline of global biodiversity.

Fossorial species usually exhibit a tight interaction with the environment. Their burrowing activity shapes ecosystems processes but at the same time, limits their ability to disperse. This may be exacerbated in mountain ecosystems where the geomorphology of the landscape further restricts dispersal and distribution ranges. Additionally, human induced habitat degradation and environmental change in mountain ecosystems may affect the persistence of many species.

In order to disentangle complex species-environment interactions under human activities, a combination of methods is required covering varying spatial scales, including how the environment over time has shaped the species we observe today. This thesis explores the case of the giant root-rat (*Tachyoryctes macrocephalus*), an endemic, fossorial rodent species with a limited range in the afro-alpine Bale Mountains in southern Ethiopia. By combining spatially explicit ecological and genetic analyses, I assessed the intricate interplay between the environmental conditions and human activities across time that have shaped the species' local and range-wide distribution at the landscape scale, as well as its population genetic structure, diversity, and demography.

Through a combination of methods, my results revealed a scale dependency of species-environment interactions, with historical and evolutionary factors shaping interactions differently on local and landscape scales. Ecological field studies revealed (Chapter II) a tight interaction between the giant root-rat, the local environmental conditions and human land use. Giant root-rat activity reduced vegetation cover, while the local species' activity increased with decreasing vegetation cover and elevated livestock grazing, indicating the species' preference for open habitats. However, extending our inquiry to the landscape scale using satellite-based remote sensing and vegetation data (Chapter III), we found that texture metrics describing topographic differences across the landscape determined the species' range-wide distribution. Hence, environmental conditions shaping the local activities, differed from those influencing the species' overall distribution.

Population genetic studies of genetic subdivision and diversity (Chapter IV), further demonstrated the effect of topography on the species distribution and dispersal ability. I found a pronounced subdivision of the species into a northern and southern population, with no sign of gene flow between them. Landscape genetic analyses revealed that topographic barriers were the driving force on the landscape scale, hindering dispersal between north and south. Environmental conditions played a subordinate role, at least for local species' genetic substructure and dispersal within populations.

With the analyses of giant root-rat subfossil remains from the Late Pleistocene era (Chapter V), I expanded the examination of the species' interaction with the environment and humans on a temporal scale. Notably, radiocarbon dating of these subfossils provided insights into human presence in the Bale Mountains, indicating nearly continuous human habitation in the region from 47,000 to 31,000 years ago. Ancient DNA studies revealed that both environmental changes and human activities played pivotal roles in driving phylogenetic lineage divergence and shaping the demographic history of the species over thousands of years. The last glaciation of the Bale Mountains and human hunting practices during that period likely led to a population decline in the northern and southern regions, respectively. Additionally, I observed an ongoing population decline and reduced nucleotide diversity in the northern population since the end of the last glacial period, possibly resulting from habitat reduction caused by environmental changes.

The presented studies in this thesis collectively demonstrate the direct effect of local environmental conditions and human activity on the occurrence of the species. The joint consideration of my research findings emphasized that the giant root-rat may have a limited ability to shift its range under changing environments due to its limited dispersal ability, which hinders the traversal of pronounced topographic barriers in the landscape. Understanding these complex relationships is essential for effective conservation management for preserving mountain biodiversity and ecosystem functionality, of the afro-alpine ecosystem and other similar environments where species and their habitats are deeply interconnected.

.

Chapter I — General introduction

The earth is currently undergoing a severe biodiversity crisis as a direct consequence of human activities (Ceballos et al. 2015; IPBES 2019). Land use and climatic change are the main drivers for environmental change which disrupts ecosystem processes on a global scale (Foley et al. 2005; IPBES 2019; Pielke et al. 2011). Therefore, it is essential to effectively protect species, but this first requires profound understanding on how species interact with their environment (hereafter species-environment interaction), and how this interaction might differ across spatial scales and time. Additionally, comprehensive knowledge is needed on the present impact of human activities on species and how humans might have shaped species' distributions and dynamics in the past (Mertes and Jetz 2018).

Species that often have a tight interaction with their environment are ecosystem engineers, which continuously shape and re-shape the spatial and temporal structure of the environment (Hastings et al. 2007; Jones, Lawton, and Shachak 1994). One important group of ecosystem engineers are fossorial species. Due to soil perturbation, they redistribute nutrients in the soil and change soil texture which influences the aboveground vegetation (Jones, Lawron, and Shachak 1997; Jones et al. 1994; Lawton 1994; Romero et al. 2015). Hence, their fossorial activity has clear implications for ecosystem functionality (Hastings et al. 2007). Concurrently, fossorial species with a predominant below-ground activity are often tightly linked to the prevailing climatic conditions, local soil types and food resources due to their low mobility (Crawford, Mackay, and Cepeda-Pizarro 1993; Eldridge and Whitford 2014; Reichman 1975; Vlasatá et al. 2017). For instance, while mammals and ants are the most present fossorial animals in arid areas, earthworms are dominating in humid areas (Wilkinson et al., 2009); in arid and semi-arid regions, the activity of fossorial animals is positively correlated to vegetation cover (Eldridge and Whitford 2014).

Such species-environment interaction of fossorial species may be exacerbated in harsh mountain ecosystems, where they already exhibit small distribution ranges and effective population sizes (Badgley et al. 2017; Brown 2001). Moreover, the geomorphology of the landscape limits habitat availability and dispersal opportunities especially for species close to mountain tops (Gaston 2003; Rahbek, Borregaard, Antonelli, et al. 2019; Rahbek, Borregaard, Colwell, et al. 2019). Therefore, species in mountain ecosystems may have limited potential to adapt to changing environmental conditions and are particularly prone to extinction, especially since mountain ecosystems face increasing threats from land use and climate change-induced

habitat shifts (Davies, Purvis, and Gittleman 2009). This highlights the importance of investigating species-environment interactions in order to preserve the high biodiversity in mountain ecosystems. However, exploring fossorial species in mountain ecosystems and their interaction with the environment is demanding, especially due to the inherent challenges in assessing remote areas and observing those species in their natural habitat below-ground.

Exploring species' interactions with environmental conditions, and how these shape species' spatial distributions and population dynamics is a fundamental inquiry in both ecology and evolutionary biology (Brown, Stevens, and Kaufman 1996; Graham et al. 1996; Grinnell 1917; Sandel et al. 2011). The distribution and dynamics of species are determined by the combined effects of present and past environmental conditions, and evolutionary mechanisms such as a species' dispersal ability (Boulangeat, Gravel, and Thuiller 2012; Wisz et al. 2013). Abiotic and biotic factors, for instance species-specific habitat and food requirements, or landscape structures such as topographic barriers coupled with the species' dispersal ability, determine the continuous distribution of individuals across space (Boulangeat et al. 2012; Cunningham et al. 2016; Gaston 2009; Graham, Moritz, and Williams 2006; Sexton et al. 2009).

Such species-environment interactions display variability, exhibiting significant differences across species, spatial scales and time (Hewitt, Thrush, and Lundquist 2017; Mertes and Jetz 2018; Sandel 2015). The distribution and dynamics of species observed today are, in part, a consequence of their interactions with the present environment. However, within a species, environmental conditions shaping the local abundances may diverge from those affecting the species' overall distribution. For instance, the abundance of red-backed voles *Myodes gapperi* in boreal forests is strongly associated with the amount of coarse woody debris on a <250 m scale, but this effect diminishes on larger scales (Fauteux et al. 2012; Orrock et al. 2000; Sandel 2015). Moreover, the strength of a species-environment interaction depends on the range size of a species. Environmental conditions may have a more pronounced impact on species with limited distribution ranges and dispersal abilities, such as many fossorial species (Kelt and Van Vuren 1999; Šklíba et al. 2020; Tucker, Ord, and Rogers 2014), due to their specific ecological requirements (Slatyer, Hirst, and Sexton 2013). In contrast, species with broader ranges and higher dispersal abilities are generally more adaptable and can tolerate a wider range of environmental conditions (Slatyer et al. 2013). Additionally, species distribution and dynamics are shaped by past environmental conditions. Climatic changes over millennia caused habitats to shifts, expand or disappear and thereby played a significant role in shaping the current patterns of species distributions (Graham et al. 2006; Rosenzweig 1995). For example, regions

7

with long-term climate and vegetation stability often harbour a higher number of small-ranged species (Graham 1996, Graham, Moritz, and Williams, 2005).

Next to environmental conditions, present human activities exert a direct influence on species distribution and dynamics. The consequences for many species include population declines or altered natural predator-prey dynamics due to habitat degradation or hunting (Benítez-López et al. 2017; Palmeirim, Santos-Filho, and Peres 2020). Such human impacts extend far beyond recent times, spanning thousands of years (Boivin et al. 2016; Koch and Barnosky 2006). During the Late Pleistocene and Holocene, many species suffered from human hunting activities, shaping their population dynamics and causing their extinction or pushing them close to it (e.g. Hempel et al. 2022; Lorenzen et al. 2011). Conversely, some species, including domesticated ones such as sheep or cattle, benefited from humans (Boivin et al. 2016). In conclusion, present and past environmental changes along with human activities have significantly shaped the species distributions and dynamics observable today. Given the dependence on spatial and temporal scales, unravelling species-environment interactions in relation to human influences requires integrating diverse methods across various spatial and temporal contexts.

Ecological field studies offer valuable insights into present species-environment interactions at local scales. Through on-site observations and direct measurements, researchers obtain detailed knowledge about the direct influence of factors such as food resources, habitat availability, climatic conditions, or human activity on the local occurrence of a species across short time periods (Kraus et al. 2022; Rehling, Delius, et al. 2023; Tang et al. 2019; Vlasatá et al. 2017). Long-term monitoring in the field further provides details on how species respond to environmental change. In turn, field-based evidence reveals a species' impact on its surrounding environment and on other organisms, which helps to assess the species' contribution to ecosystem functionality (e.g. Rehling, Jongejans, et al. 2023; Reichman and Seabloom 2002; Šklíba et al. 2017). By studying the reciprocal relationships between species, their local environment, and human activity, researchers may disentangle the intricate ecological dynamics at play, which shape a species' distribution and dynamics (Asefa et al. 2023; Brown et al. 1996; Feng et al. 2020; Stewart et al. 2015). This knowledge of species-environment interactions is invaluable for effective conservation and management efforts, as it aids in identifying critical habitats, potential threats, and strategies for safeguarding the species' well - being in their natural ecosystems.

To extend this knowledge of local field studies on large spatial scales, inferences can be made using satellite-based remote sensing data (Barber-Meyer, Kooyman, and Ponganis 2007; Wang, Shao, and Yue 2019). Machine learning models link spectral remote sensing observations with field-based occurrence data of species (Estes et al. 2010; Fretwell et al. 2012). Thereby, environmental conditions that shape species' occurrences are identified and upscaled on the landscape scale to predict the species distribution, which is usually not feasible with traditional field studies (Pöyry et al. 2018; Wakulińska and Marcinkowska-Ochtyra 2020). Predicting the range-wide distribution of small-sized species or those with low visibility on a landscape scale can be achieved by utilizing for instance vegetation composition or geomorphological properties as indicators for habitat suitability, or by identifying discrete habitat changes caused by these animals (Culbert et al. 2012; Estes et al. 2010; Grigusova et al. 2021; Koshkina et al. 2020). This approach enables the prediction of species distribution across large spatial extents, also under future climate scenarios (e.g. Latinne et al. 2015; Taylor et al. 2016).

The integration of population genetic studies in ecological and remote sensing findings adds a temporal perspective into species-environment interactions across time. Population genetic studies illuminate how environmental conditions and human activities have shaped species over time, as the long-term impact of the environment is reflected in the species' genetic population subdivision, diversity and demography (e.g Berthier et al. 2005; Lorenzen et al. 2011; Mirol et al. 2010). Species-specific requirements such as temperature or food availability, or topographic barriers impede the continuous distribution of individuals and thereby reduce gene flow between populations (Boulangeat et al. 2012; Cunningham et al. 2016; Cushman and Lewis 2010; Sexton et al. 2009). Consequently, natural selection, genetic drift, and inbreeding particularly in smaller isolated populations, may result in a heterogeneous pattern of genetic variability across space (Wright 1969). Thereby, researches can uncover historical patterns such as migration or adaptation, allowing for a deeper understanding of how species-environment interactions have shaped the genetic diversity and population dynamics of species on a temporal scale. Thereby, population genetic studies complement the more immediate snapshots provided by ecological and remote sensing studies.

To elucidate evolutionary and ecological history of populations ancient biomolecular analysis of subfossil faunal remains provide a powerful tool (reviewed in Rosengren et al., 2021; Swift et al., 2019). Ancient DNA analyses can be used to reconstruct demographic histories or phylogenetic lineage divergence (Campos et al. 2010; Ersmark et al. 2019; Faith 2014; Lorenzen et al. 2011). Thereby, the timing and magnitude of species' responses to external

factors such as to environmental changes or human activities is elucidated, which mirrors species-environment interactions over millennia (Rosengren et al. 2021). At the same time ancient biomolecule analysis of subfossil faunal remains can indicate human presence and resource-use in the past (Lazagabaster et al. 2021; Wan et al. 2019; Yu et al. 2022). For instance, paleogenomic analysis of archaeological mice and rats specimens have been used to track human migration (e.g. Jones et al. 2012; Yu et al. 2022). Such comprehensive knowledge of long-term interactions between species and humans is important as it can help to predict species persistence under anthropogenic stressors.

1.1 Aims of the thesis

In this thesis, I employed complementary ecological and genetical methods, to explore the link between environmental conditions, human activities, and the distribution and population dynamics of the giant root-rat (*Tachyoryctes macrocephalus*; Rüppel 1942), a fossorial rodent species endemic to the afro-alpine Bale Mountains in southern Ethiopia (Yalden 1985). I have chosen a combination of methods which encompass species-environment interactions and human activities across spatial scales and time. Integrating several approaches might allow us to forecast how species-environment interactions will develop in the future and contribute to our understanding of a species' abilities to adapt and persist. Such insights are important to effectively protect species and reverse the ongoing decline in biodiversity worldwide.

My research focused on i) the interrelation between present environmental conditions, human land use and the activity of the giant root-rat on a local scale; ii) predicting the species' range-wide distribution to the landscape scale using vegetation field data in combination with and remotely derived satellite data; iii) the genetic subdivision and diversity of the species locally and across its distribution range on the landscape scale, linked to long-term impact of environmental conditions and topographic structures; iv) the relation between Late Pleistocene environmental changes and human activities in the Bale Mountains on the genetic subdivision, diversity and demography of the giant root-rat over a millennial time.
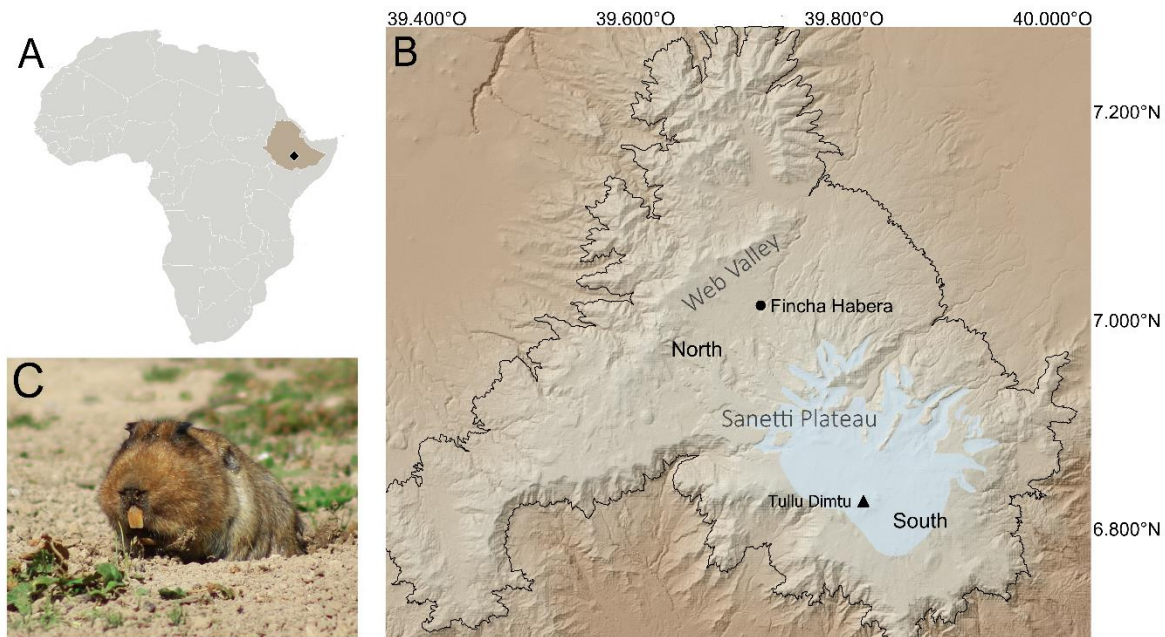
Figure 1.1: Figure 1.1: A) B) Map of Africa showing Ethiopia in brown and indicating location of Bale Mountains National Park; B) Map of study area. Black line indicates 3,000 m above sea level, which is the lower distribution margin of the giant root-rat. Blue shading on southern area indicates local last glacial maximum ~42,000 -28,000 years ago (Groos et al., 2021); C) Giant root-rat, photography by Philipp Kurt.

The study took place in the Bale Mountains (6.508–7.178 N, 39.508–39.928 E) which represent the largest area of afro-alpine and subalpine ecosystem above 3,000 m above sea level (a.s.l.) in Africa (Groos et al. 2021; Miehe and Miehe 1994). The evolution and persistence of many flora and fauna species, and high numbers of endemic species, characterise the region as a biodiversity hotspot (Hillman 1986; Miehe and Miehe 1994; Williams et al. 2004, Yalden and Largen 1992). One main characteristic of the region, the Sanetti plateau, encompasses an elevation range of 3,800–4,377 m a.s.l. to its highest peak and second highest mountain in Africa, the Tullu Dimtu (Figure 1.1). During the Late Pleistocene, between 42,000 to 16,000 years ago, significant parts of the plateau and adjacent valleys were covered by ice (Groos et al., 2021; Ossendorf et al., 2019, Figure 1.1). The northern region of the national park, the Web Valley, lies at a lower elevation of approximately 300 - 500 m and consists of broad valleys and plains with afro-alpine vegetation (Miehe and Miehe 1994). (Figure 1.1).

As mentioned above, one of the endemic species of the Bale Mountains is the giant root-rat. The predominant below-ground activity of the species, and its distribution in the Bale Mountains define a unique setting for joint investigations about species-environment interactions across spatial scales and time. The giant root-rat has a rather limited and enclosed distribution range across the Bale Mountains massif of ~1,000 km^2 between 3,000 and 4,150 m

a.s.l. (Sillero-Zubiri, Tattersall, and Macdonald 1995; Yalden 1975; Yalden and Largen 1992). Therefore, studies can cover the entire distribution range studies of the species on the landscape scale, which is often not feasible due to logistic constrains. Secondly, due to their restricted distribution range, the giant root-rats presumably have a tight interaction with local environmental conditions allowing allows small-scale analyses (Slatyer et al. 2013). Locally, the species occurs in high abundancies, but has small home-ranges due to their limited dispersal abilities, which facilitates direct field observations (Šklíba et al. 2017, 2020). Further, due to a joint effect of soil perturbation and herbivory the species largely influences its surrounding environment as ecosystem engineer, contributing to the ecosystem functionality of the region (Sillero-Zubiri et al. 1995; Šklíba et al. 2017; Yalden 1975).

The rationale that giant root-rats have a long-term history of interactions with humans provides an opportunity to examine the long-term impact of human activities on the species (Ossendorf et al. 2019; Vial, Macdonald, and Haydon 2011). Over the last decades, human settlements and livestock grazing intensified in the Bale Mountains which potentially threatens the persistence of giant root-rats (Gashaw 2015; Mekonen 2020; Stephens et al. 2001; Vial et al. 2011). In addition to this present human influence on the species, humans have already shaped the giant root-rat in the Late Pleistocene (Ossendorf et al. 2019, 2023). Archaeological findings evidence that the giant root-rat was a key food resource to Middle Stone Age foragers, and thereby facilitated the occupation of the world's earliest known human high-altitude residential site 47,000 – 31,000 years ago, the Fincha Habera rock shelter in the Web valley of the Bale Mountains (Figure 1.1) (Groos et al. 2021; Ossendorf et al. 2019). Radiocarbon dating of giant root-rat subfossils and other archaeological remains indicate that the rock shelter was occupied for three longer phases during that time (Ossendorf et al. 2023). Taken together, the species' key role as an ecosystem engineer combined with its limited dispersal ability and restricted distribution range in a changing mountain ecosystem, and its long-term interaction with humans makes it an ideal model organism for exploring species-environment interaction across spatial scales and over time. This is a precondition to preserve mountain biodiversity and ensure ecosystem functioning in the Bale Mountain region.

To reach the aims of my thesis, I have worked in separate chapters. This dissertation is cumulative in nature. Subsequent to this general introduction (Chapter I), Chapters II-V present and discuss scientific background, material and methods, as well as results independently in each chapter, and therefore can be read as standalone sections. It is important to note I use the term "we" in Chapter II and III, to indicate the collaborative work of two main authors (please

refer to author contribution as well). Chapter VI provides individual summaries for each of the chapters (II-V) and presents an overarching summary. Chapter VII gives perspectives for future research.

In the second chapter (Chapter II), we used ecological field studies to assess the interrelation of giant root-rat burrow density (as proxy for giant root-rat activity), vegetation cover and plant species richness, and how these reciprocal effects might by modulated by the present climatic conditions (temperature), soil moisture (habitat availability) and livestock grazing (human activity). We expected that giant root-rat activity increases with reduced vegetation cover, and with increasing soil moisture and temperature due to their habitat requirements of open space and wet soils for digging. We also expected the species activity to decrease with increasing livestock intensity. To test the hypotheses, we established eight study locations across the Bale Mountains, at which we recorded vegetation data, temperature and soil moisture, giant root-rat activity, and livestock intensity over a total of 62 plots scattered across the species distribution range.

In the third chapter (Chapter III), we used plant species composition data from the field, and combined these with satellite-based remote sensing data to predict the species' distribution on the landscape scale. We compared three different machine learning models, using i) remote sensing imagery on which we visually selected data points of giant root-rat presence; ii) GPS logged giant root-rat presence data from field observations of the species in combination with remote sensing data; ii) detailed vegetation composition data collected over 94 plots of giant root-rat presence and absence (47 each). Our aim was to predict the species distribution, and compared the prediction outcome of each model in terms of reliability. We expected that more detailed field data improves the species distribution prediction.

In my fourth chapter (Chapter IV), I analysed the genetic subdivision and diversity of the giant root-rat and how these are impacted by environmental conditions and topographic barriers. I expected strong genetic subdivision on small spatial scales, due to the predominantly below-ground activity of the species. Owing to the pronounced environmental heterogeneity of the Bale Mountain ecosystem, I expected that food and habitat availability, and topographic structures across the species' range cause genetic subdivision of the species. In detail, I used complete mitochondrial genomes and low-coverage nuclear genomes from 77 giant root-rat individuals from nine sampling localities in the Bale Mountains to assess genetic subdivision and diversity. I applied landscape genetic analyses to identify how mitochondrial gene flow is affected by geographic distance, by vegetation and soil moisture (food and habitat availability),

13

and by slope and elevation (topographic barriers). Fundamental to this study was the generation of the first complete mitochondrial genome of the species, which I did prior to this study (see Supplementary material, Reuber et al. 2021).

In the fifth chapter (Chapter V), I aimed at a comprehensive analysis of the species' temporal patterns in the phylogeny, diversity, and demographic history in relation to Middle Stone Age foragers resource utilisation and high-altitude residency, and Late Pleistocene climatic change. I used biomolecular approaches of ancient DNA, radiocarbon dating, and stable carbon and nitrogen isotope analyses of 18 faunal subfossil remains of the species. Subfossil remains were excavated from anthropogenic fire pits of the Fincha Habera rock shelter, which was occupied by the Middle Stone Age foragers in the Late Pleistocene. To contextualize the data, I integrated contemporary mitochondrial data from Chapter IV, and stable isotopes of 30 contemporary bone samples that were collected across the species range. I expected that the ages of subfossils indicate three human occupation periods at Fincha Habera, between 47,000 and 31,000 years ago. Further, I expected that the regular exploitation of the species by Middle Stone Age foragers reduced the population of the northern individuals and that Late Pleistocene climatic change, specifically the glaciation of the Bale Mountains 42,000 – 16,000 years ago, profoundly decreased the population in the southern part of the study region.

The activity of a subterranean small mammal alters Afroalpine vegetation patterns and is positively affected by livestock grazing

by

Addisu Asefa*, **Victoria M. Reuber***, Georg Miehe, Melaku Wondafrash,

Luise Wraase, Tilaye Wube, Nina Farwig, Dana G. Schabo

* These authors contributed equally to this study

ABSTRACT

Subterranean rodents can act as ecosystem engineers by shaping the landscape due to soil perturbation and herbivory. At the same time, their burrow density is affected by environmental conditions, vegetation and anthropogenic factors. Disentangling this complex interplay between subterranean rodents and their environment remains challenging. In our study, we analysed the interplay of abiotic conditions, vegetation patterns and human land-use and the burrow density of the giant root-rat (GRR; *Tachyoryctes macrocephalus*), a subterranean rodent endemic to the Afroalpine ecosystem of the Bale Mountains in south-east Ethiopia. Specifically, we examined the effects of GRR on plant species richness and vegetation cover and *vice-versa*, and how these reciprocal effects might be modulated by temperature, habitat wetness and grazing. Our results showed that increasing GRR burrow density led to decreased vegetation cover, and that effects of GRR on vegetation cover were slightly stronger than *vice-versa*. Considering the reciprocal causation models, we found that increasing plant species richness led to increased GRR burrow density, while GRR burrow density decreased as vegetation cover increased. Increases in habitat wetness and livestock grazing intensity also directly led to increased GRR burrow density. Our results stress the importance of subterranean ecosystem engineers on vegetation and highlight the vulnerability of these complex interactions to human activity.

2.1. Introduction

Ecosystem engineer species constantly create habitats and therefore drive structures of plant and animal communities and ecosystem dynamics (Jones et al. 1997; Lawton 1994; Romero et al. 2015). Particularly, herbivorous subterranean rodents have a high impact on ecosystems due to a joint effect of soil perturbation and herbivory (Hagenah and Bennett 2013; Jones et al. 1997). The creation of subterranean tunnel systems by rodents with deposition of soil mounds at the ground surface facilitates sediment transport; alters nutrient availability, soil texture and moisture content; and creates habitats for other animal and plant species (Gabet, Reichman, and Seabloom 2003; Huntly and Reichman 1994; Reichman and Seabloom 2002; Sherrod and Seastedt 2001; Zhang and Liu 2003). Studies have found that such mosaics of nutrients and soil conditions created by subterranean rodents boost plant species diversity (Hagenah and Bennett 2013). However, tunnelling and mound creation itself reduces the overlying vegetation because short, ground layer plant species are buried (Mokotjomela, Schwaibold, and Pillay 2009; Reichman and Smith 1985). In addition, subterranean rodents also impact vegetation directly

16

as they feed on plant material, with consequences for plant community composition and structure. Through direct herbivory, rodents are known to reduce plant cover and diversity on top of their burrows (Šklíba et al. 2017).

The direction and magnitude of the impacts of subterranean animals in shaping and maintaining vegetation patterns depend on a number of factors, including local soil characteristics and climatic conditions (e.g. Hagenah & Bennett 2013; Jones et al. 1997). Firstly, the activities of subterranean rodents seem to be negatively related to temperature in arid and semi-arid regions (Huntly & Reichman 1994), but are positively linked in the high altitude (Vlasatá et al. 2017). Secondly, soil moisture determines rodent burrowing activity, as it defines the energy needed for the excavation (Marcy et al. 2013; Price and Podolsky 1989; Vleck 1979). Finally, while subterranean rodents shape vegetation patterns, their burrow density is at the same time strongly determined by vegetation structure, diversity and composition of their habitat (Huntly and Reichman 1994; Reichman and Seabloom 2002; Zhang and Liu 2003). For instance, the activities of rodents in dry regions are shown to increase with increasing vegetation cover (Zhang, Zhang, and Liu 2003) and plant productivity is also shown to positively affect the abundance of rodents (Šklíba et al. 2017).

The above-mentioned complex interplay between subterranean rodents, abiotic factors and vegetation patterns is modified by human land-use, such as livestock grazing. Soil compaction due to the presence of livestock may impact the construction and maintenance of their foraging tunnels (Torre et al. 2007). Additionally, selective removal and damage of plants by livestock grazing and threading, alter plant community composition and reduce plant biomass (Vial et al. 2011). As a consequence, in addition to inducing food competition, livestock activities can cause alterations of suitable habitats for rodent species and their abundance, distribution and ecological functions. In contrast to the negative effects of livestock grazing on subterranean rodents (Vial et al. 2011), some other studies show that livestock grazing, especially following burning of shrubby vegetation, influence the distribution of many rodent species due to enlargement of their natural, open-landscape habitat (Miehe and Miehe 1994). So far, studies investigating the interplay between subterranean rodents and their environment have mostly looked at distinct relationships between few of the above-mentioned factors (e.g. Šklíba et al. 2017; Vial et al. 2011; Vlasatá et al. 2017). However, to gain a comprehensive picture of how subterranean rodents shape an ecosystem, analyses taking the complexity of the interrelations among environmental factors, land use, rodent activities, and vegetation patterns are needed.

In this study, we examined the ecosystem engineering role of the endemic giant root-rat (GRR; *Tachyoryctes macrocephalus*, RÜPPELL 1842), an Afroalpine specialist rodent in the Bale Mountains, south-eastern Ethiopia. GRR, via their burrowing and herbivory activities, strongly shape the Afroalpine landscape of the Bale Mountains, where they have a long history of interaction with humans (Miehe and Miehe 1994; Ossendorf et al. 2019) and where the number of people is still rising (BMNP [Bale Mountains National Park] 2017). Its subterranean and above-ground herbivory activities in the immediate vicinity of the burrow opening cause changes in soil properties and vegetation structure (Sillero-Zubiri et al. 1995). Currently the GRR is classified by the IUCN as globally endangered due to habitat change/degradation induced by livestock grazing (Teshome, Randall, and Kinahan 2011). Understanding the interactions among environmental factors, human activities and GRR activities in structuring the Afroalpine ecosystem has been identified as one of the top priority research topics by the BMNP management to aid effective management decisions (BMNP 2017). Thus, the GRR is a perfectly suitable species to understand the linkages between abiotic conditions, vegetation patterns, rodent burrow density and human land-uses. Previous research on the impact of the GRR on vegetation in some parts of the Afroalpine zone of the Bale Mountains have shown that burrowing activity of GRR causes altered plant species composition and reduced cover (Šklíba et al. 2017; Yaba et al. 2011). However, so far, it is poorly understood how these effects might be influenced by environmental factors and land-use across the species distribution range. Our aims were to determine the role of GRRs as ecosystem engineers through the interrelations between environmental conditions, land-use, GRR burrow density, and vegetation variables. More specifically, we analysed, using path analysis: i) the direct and indirect effects of temperature, habitat wetness, livestock grazing and GRR burrow density on plant species richness and vegetation cover, and ii) the direct and indirect effects of temperature, habitat wetness, livestock grazing, plant species richness and vegetation cover on GRR burrow density. Comparing the effect of the GRR burrow density on vegetation and *vice-versa*, we aimed to reveal which factor is more strongly influenced by the other. We hypothesize: i) reduced vegetation cover and plant species richness in areas with elevated GRR burrow density; ii) increased plant species richness and vegetation cover, directly or indirectly via GRR burrow density, but a decrease with increasing surface temperature and habitat wetness, but decreased with increasing livestock grazing intensity; iii) a decrease in GRR burrow density with increasing plant cover due to the need for open spaces and an increase in GRR burrow density with increased plant species richness due to the need to access and select high quality resources; and iv) an increase of GRR burrow density with, directly or indirectly via species richness and

vegetation cover, increasing surface temperature, habitat wetness, and livestock grazing intensity.

2.2. Material and methods

Study species

The giant root-rat (GRR) is one of the 13 to 14 African root-rat species of the genus *Tachyoryctes* Rüppel, 1842 in the family Spalacidae (Šumbera et al. 2018). It is easily distinguished from the other congeneric species by its large body mass (around 1 kg) and eyes on top of the head, considered as an adaptation to detect predators in open habitats (Šumbera et al. 2018; Yalden 1975).

GRR is endemic to <1,000 km^2 area in the Bale Mountains of Ethiopia at altitudes from 3,000 to 4,150 m asl (Yalden 1985; Yalden and Largen 1992), where it is the main prey of the endangered Ethiopian Wolf (*Canis simensis*) and numerous raptor species (Sillero-Zubiri, Tattersall & Macdonald 1995). GRRs are naturally confined to open, Afroalpine *Helichrysum* dwarf-shrub heathlands, seasonally waterlogged short grassland and swamps (Sillero-Zubiri et al. 1995; Tallents and Macdonald 2011). The species is diurnal and constructs large underground burrows including an extensive tunnel system (Sillero-Zubiri et al. 1995; Yalden 1975). The burrow system of an individual GRR may extend to 34 m (Beyene 1986; Yaba et al. 2011; Yalden 1975). The tunnels are characterized by extensive soil perturbation aboveground and have holes through which GRRs are able to forage and bask on the ground surface (Beyene 1986; Bryja et al. 2019; Sillero-Zubiri et al. 1995). During foraging, GRR stays with its back in the hole and collects plants surrounding it (Vlasatá et al. 2017). It largely feeds on *Alchemilla abyssinica*, an abundant forb species in the area (Vlasatá et al. 2017).

Study area

Our study was conducted in the Afroalpine ecosystem of the BMNP across the Sanetti Plateau and Web Valley in South-Eastern Ethiopia (Fig. 1), during the dry season in January/February 2020. The Bale Mountains represent the largest area of Afroalpine vegetation in Africa (Miehe and Miehe 1994; Yalden 1983) and encompass an elevation range of 1,500–4,377 m asl. There are two rainy seasons, with short rains from March to June and the long rains from July to October, and a dry season between November and February; mean annual rainfall is approximately 1,000 mm (Miehe and Miehe 1994). The BMNP is included in Conservation

International's Eastern Afromontane Biodiversity Hotspot (BMNP 2017).

Study design

To assess the interplay between environmental conditions, livestock grazing, vegetation and GRR burrow density, we established eight study locations scattered over an area of 1,000 km^2. Three locations were established in the Web Valley and five in the Sanetti Plateau of the BMNP (Fig. 1). We chose suitable localities for study locations in accessible areas with flat terrain, encompassing major habitat types known to host populations of the target species, before going to the field. The pairwise distance between study locations ranged from 5–30 km. At each study location, we defined two (n= 3 locations) to three (n=5 locations) transects of 1.5 km length in different directions, to maximize representation of various habitats (see Tallents and Macdonald 2011), at a minimum angle of 100 degrees. Major habitat types covered by study locations and transects included: open-grassland, grassland dotted with *Artemisia afra* shrub, *Helichrysum* dwarf-scrub, *Alchemilla* meadow, *Lobelia rhychopetalum*, and wetlands, such as alpine lakes, rivers, swamps and seasonal wetland grasslands (Tallents and Macdonald 2011). Along each transect, we established three 25 m × 25 m plots at a minimum distance of 500 m from each other, and placed plots within a homogeneous habitat type, at least 5 m away from habitat edges. Due to logistic constraints, one location was missing one plot within one transect. Overall, we thus had 62 plots covering an area of 38,750 m^2.

Data collection

At each plot, we recorded data on GRR burrow density, vegetation patterns, livestock grazing and habitat wetness. As indicator for GRR burrow density we counted the numbers of: a) GRR fresh burrows, which are surrounded by or plugged with fresh soil; b) old burrows, which are abandoned GRR burrows, with holes open or plugged with old soil, without freshly perturbated soil, partially or wholly covered by vegetation regrowth, and sometimes occupied by other small rodents (Sillero-Zubiri et al. 1995), and c) the proportion of the plot area covered by GRR soil perturbation. The often smaller diameter of other rodents holes and presence of rodents' droppings and pathways connecting burrow openings were used to distinguish fresh and old GRR burrows (Šklíba et al. 2017). As density of fresh burrows, old burrows and the proportion of perturbated soil cover were positively correlated, only the density of fresh burrows was incorporated in further analyses (Spearman's correlation test, $\rho > 0.65$, $P < 0.001$). To estimate

livestock grazing on the plateau, we recorded the number of cow droppings within the 25 m × 25 m plots. We estimated habitat wetness, as an ordinary variable, at each plot as absent (1), seasonally waterlogged (2), along perennial rivers drainage line (3), and wetland (4).

To record vegetation data, we established two 10 m × 10 m subplots at opposite corners of each 25 m × 25 m plot, the first subplot being randomly selected. In each of these subplots, we identified all plants to species level, except senescent plants which were not recorded and grasses which were recorded as a single morpho-species. We recorded estimated cover of each species in 5% intervals and subsequently summed cover estimations of all species recorded on a subplot. For further analyses, we calculated the mean number of species and summed vegetation cover on the plot level. We also calculated the Shannon diversity at the 25 m × 25 m plot scale, but excluded it from the analysis as it was correlated to species richness (correlation coefficient = 0.75). To make sure that GRR burrow density matches vegetation sampling, we also recorded GRR burrow density at the 10 m × 10 m plots. GRR burrow density as well as vegetation parameters positively correlated between the two plot sizes (all correlation coefficient > 0.83, Supplementary file Table S1). Therefore, as we recorded all other environmental data on the 25 x 25 m scale, we used GRR burrows and estimated vegetation parameters on the 25 m × 25 m plot level for further analyses.

In addition, we derived temperature data for each plot using remote sensing data and temperature records from ten weather stations positioned over the whole BMNP and covering the time period from January to December 2017. For remote sensing data, we used thermal Landsat-8 satellite imagery in 30 m resolution from the USGS Earth Explorer (www.earthexplorer.com). Then, the bi-monthly Landsat-8 imagery and daily local temperature recordings were aggregated to monthly means and were spatially predicted for the whole study area, following Kuhn and Johnson (2013).
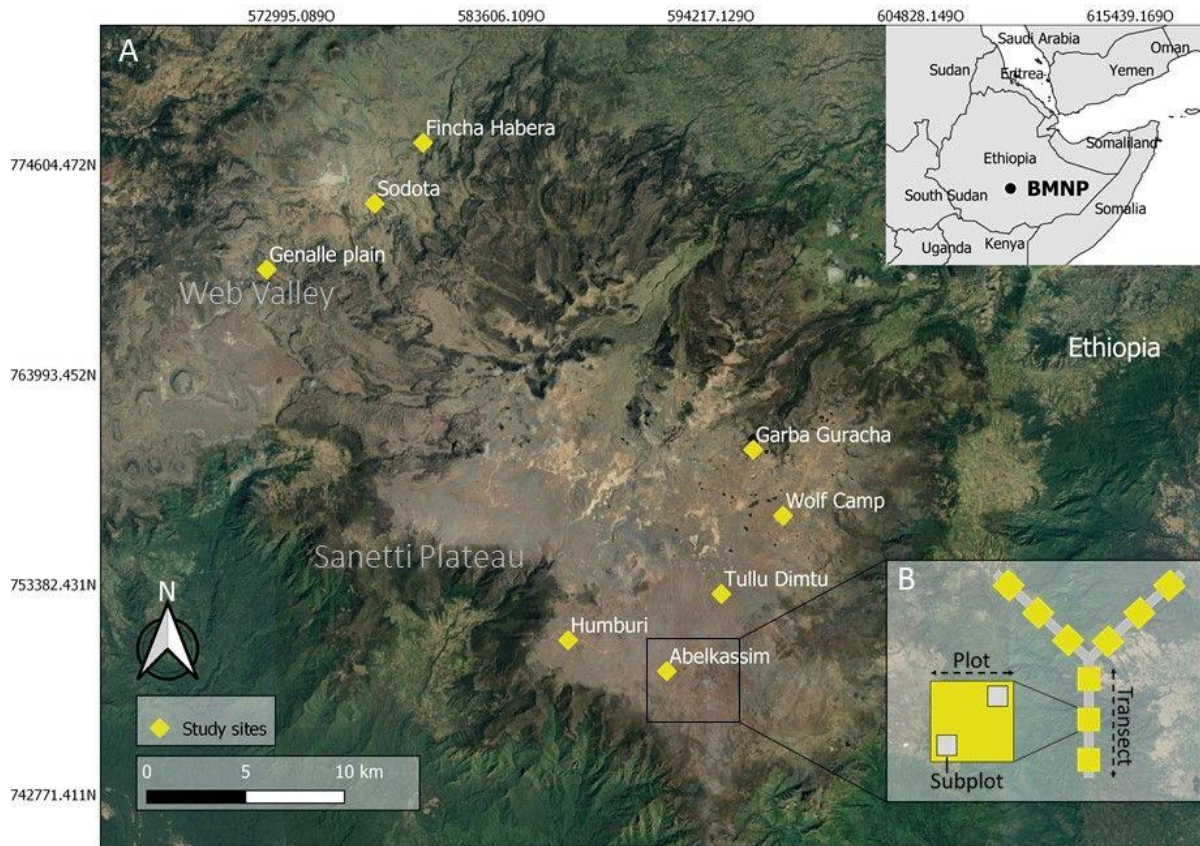
Fig. 1. (A) Overview map of the Bale Mountains National Park (BMNP) in southern Ethiopia with eight study locations; and (B) Detailed map showing the set-up of one study location with three transects of 1.5 km length and 3 study plots along each transect (for detailed description see Methods section "Study area").

Data analyses

We *a priori* defined sets of two alternative path models to disentangle the effect of GRR burrow density on vegetation patterns and *vice-versa* using Shipley's test of directed separation (Shipley 2009). In a first set of path models, we analysed the direct and indirect effects of temperature, habitat wetness, livestock grazing and GRR burrow density on plant species richness and vegetation cover, whereby two separate models were calculated for plant species richness and vegetation cover as response variables (path models "effect of GRR burrow density on vegetation patterns"). In a second set of path models, we reversed the direction of causal paths between vegetation patterns and GRR burrow density, and analysed the direct and indirect effects of temperature, habitat wetness, livestock grazing and vegetation cover or plant species richness on GRR burrow density (path models "effect of vegetation patterns on GRR burrow density"). Again, separate models were run for plant species richness and vegetation cover, resulting in a total of four path models. Prior to the analysis, all predictor variables were

tested for collinearity using Spearman's correlation test (Supplementary file Table S2). The analyses were conducted in the R environment (R Core Team 2021).
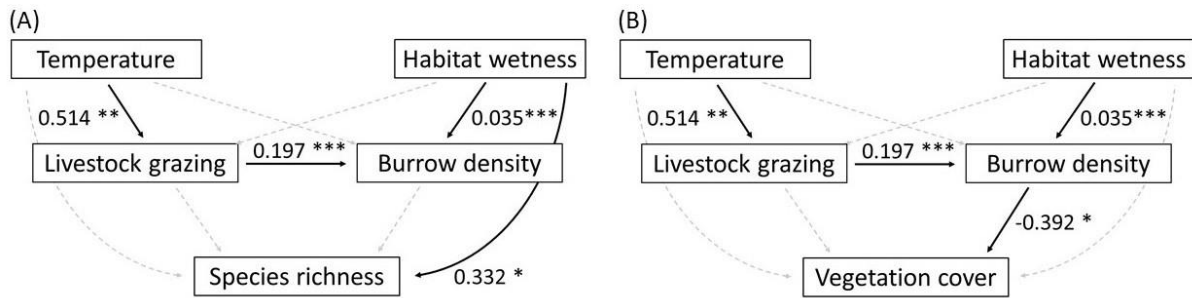
Fig. 2. Path models testing for the effect of giant root-rat (GRR) burrow density on vegetation patterns, showing relationships between temperature, habitat wetness, livestock grazing, GRR burrow density and (A) plant species richness and (B) vegetation cover. Significant paths are depicted by solid, black arrows. Values show standardized effect sizes with asterisks indicating the significance levels (*P < .05, **P < .01, ***P < .001). Dotted, grey arrows indicate non-significant relationships
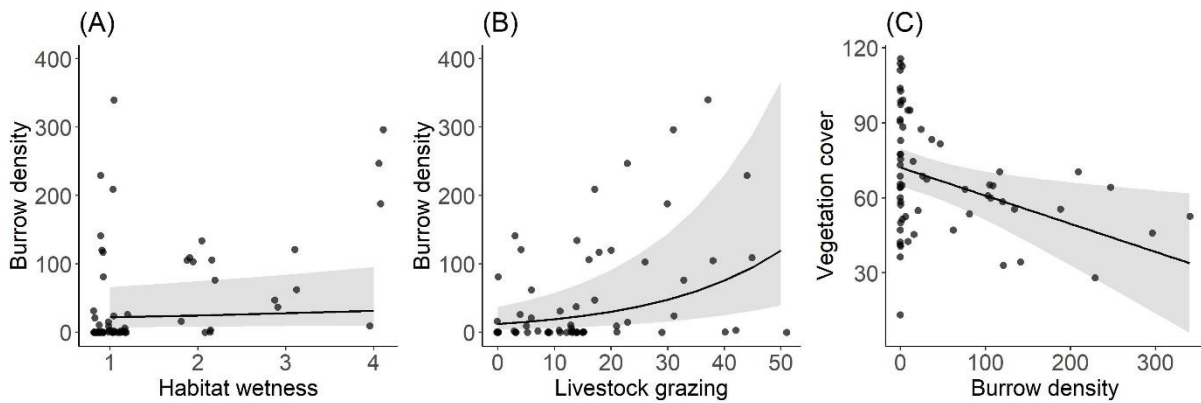
Fig. 3. Increasing giant root-rat (GRR) burrow density with increasing habitat wetness (A) and livestock grazing intensity (B) and decreasing vegetation cover with increasing GRR burrow density (C). Shown are effects of model outputs and 95% intervals based on generalized mixed effects models and underlying raw data.

Each path model consisted of three mixed effects regressions, testing the initially assumed relationships between the variables (see Figures 2–5). We used generalized- and linear mixed effect models (GLMM and LMM, respectively), including transects nested within study locations as random effects in each regression. Analysing the effect of GRR burrow density on vegetation patterns, the first regression was a GLMM with a negative binomial family to correct for overdispersion, which analysed the effect of temperature and habitat wetness on livestock grazing (package glmmTMB, function glmmTMB, Brooks et al. 2017). The second regression included livestock grazing as fixed effect with GRR burrow density as response, using a GLMM accounting for zero-inflation. The third regression included GRR burrow density as fixed effect, and either plant species richness or vegetation cover as response variables in two separate

23

LMMs with normal error distribution (R package NLME, function lme; Pinheiro and Bates 2019). For the models with interchanged path direction, revealing the effect of vegetation on GRR burrow density, the first regression was identical as for previous path models. The second regression modelled species richness or vegetation cover including livestock grazing as fixed effect using LMMs, in two separate path models. The third regression included species richness or vegetation cover as additional predictor variables, predicting GRR burrow density, using GLMMs with Poisson distribution accounting for zero-inflation. The model diagnostics were made using the DHARMa package (Hartig 2021).

Fig. 4. Path models testing the effects of vegetation patterns on giant root-rat (GRR) burrow density, showing: relationships between temperature, habitat wetness, livestock grazing with (A) species richness, and (B) vegetation cover on GRR burrow density. Significant paths are depicted by solid, black arrows. Values show standardizes effect sizes with asterisks indicating the significance levels (*P < .05, **P < .01, ***P < .001). Dotted, grey arrows indicate non-significant relationships.
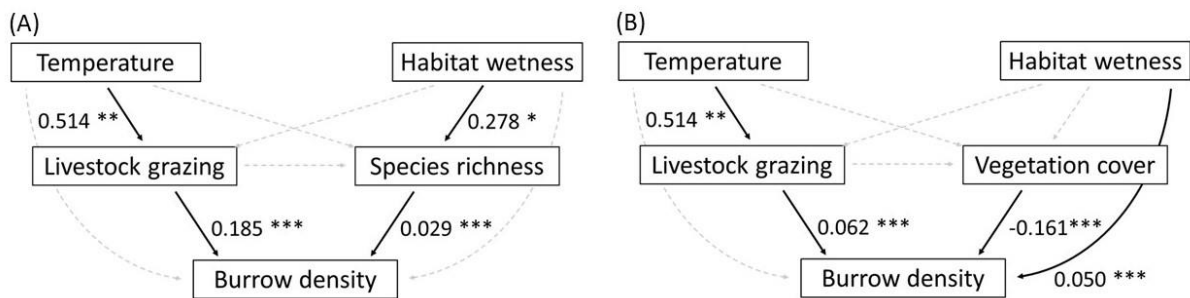

Fig. 5. Increasing giant root-rat (GRR) burrow density with increasing species richness (A) and decreasing GRR burrow density with increasing vegetation cover (B). Shown are effects of model outputs and 95% intervals based on generalized mixed effects models and underlying raw data.
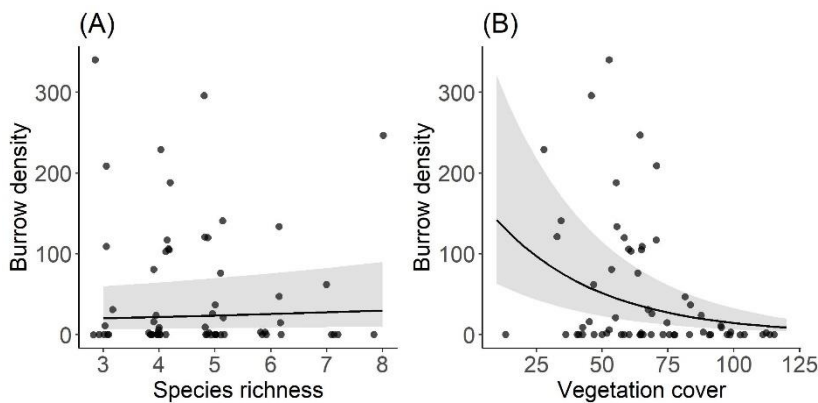
A model-wide comparison of effect sizes across the regressions was achieved by scaling path coefficients, which is appropriate for path analysis including non-normally distributed response variables. In a regression with normally-distributed response, we standardized the path coefficient by the ratio of the standard deviation of the predictor over the standard deviation of the response. For non-normally distributed response variable, we followed the observation-empirical approach by Lefcheck (2021). For the estimated path coefficients of each regression

in a path model, we derived the *p*-values using the cftest function from the multcomp package (Hothorn et al. 2021). If a response variable was hypothesized to be independent from a predictor variable, a d-separation test was applied to test this independence claim. For each claim we tested if the response was independent from the predictor by testing if its partial slope deviated significantly from zero, using the LMM or GLMM applied for that response in the path model. For each path model separately, the null-probabilities of all independence claims were combined using C-statistics (Shipley 2009). A Chi^2 test was run on the C-statistics to derive a model-wide *p*-value (Shipley 2009). We also estimated the indirect effects of temperature, habitat wetness and livestock grazing on each vegetation variable via GRR burrow density, as well as on GRR burrow density via each vegetation variable (Shipley 2009). We tested the significance of these indirect effects using the Sobel Test in a freely available online application provided by Soper (2021).

We compared both competing sets of path models (effect of GRR burrow density on vegetation patterns *vs*. effect of vegetation patterns on GRR burrow density) using the Akaike's information criterion (AIC) as model selection technique for d-separation tests (Shipley 2009).

2.3. Results

The number of GRR fresh burrow ranged from 0 to 340 across plots (mean ± SD: 48.78 ± 79.43), with a density of 780.50 ± 1270.81 burrows per ha. We recorded 38 plant species across all plots, with species richness per plot varying between three and eight species (4.72 ± 1.25). Vegetation cover ranged from 13% to 115 % (68.03 ± 22.86). The number of cow dungs ranged between 0 and 51 (16.23 ± 14.03). Across plots, the temperature varied between 2.6 °C and 8.3 °C (5.2 ± 1.5).

Path models: Effect of GRR burrow density on vegetation

While habitat wetness had a direct positive effect on plant species richness, we neither found a significant effect of temperature nor of livestock grazing or GRR burrow density on plant species richness (Fig. 2A; Table 1). We found a direct and negative effect of increasing GRR burrow density on vegetation cover (Figs. 2B & 3C). However, neither a direct effect of increasing temperature nor of grazing or habitat wetness on vegetation cover was observed (Table 1). Yet, we found significant indirect negative effects of habitat wetness and livestock grazing, both via GRR burrow density, on vegetation cover (Supplementary file Table S3). Both

path models with the different vegetation variables reproduced the data well as proven by the Chi-squared test for independence (path model for species richness: Chi-squared = 13.04, P = 0.22; vegetation cover: Chi-squared= 9.48; P = 0.48).

Table 1. Results of path models analysing the effects of temperature, habitat wetness, livestock grazing and GRR burrow density on plant species richness and vegetation cover. Given are values of unstandardized path coefficients and their standard errors (Ustd. Estimate § SE), standardized path coefficients (Std. Estimate) and R^2. Values of Std. Estimates with asterisk indicate significant effects at significance levels of * = $P < 0.05$, **$P < 0.01$, ***$P < 0.001$).

Variables	Ustd. Estimate ± SE	Std. Estimate	R^2
Level 1: Livestock grazing			0.37
Habitat wetness	0.204 ± 0.132	0.245	
Temperature	0.249 ± 0.083	0.514**	
Level 2: GRR burrow density			0.38
Livestock grazing	0.046 ± 0.003	0.197***	
Habitat wetness	0.121 ± 0.024	0.035***	
Temperature	0.044 ± 0.056	0.022	
Level 3: Plant species richness			0.51
GRR burrow density	-0.003 ± 0.002	-0.208	
Livestock grazing	-0.004 ± 0.015	-0.036	
Habitat wetness	0.474 ± 0.187	0.332*	
Temperature	0.136 ± 0.164	0.163	
Level 3: Vegetation cover			0.20
GRR burrow density	-0.113 ± 0.044	0.044*	
Livestock grazing	0.040 ± 0.278	0.023	
Habitat wetness	2.352 ± 3.578	0.090	
Temperature	1.134 ± 2.471	0.074	

Path models: Effect of vegetation on GRR burrow density

We found a positive effect of plant species richness on GRR burrow density (Fig 4A & Fig. 5A), and a negative effect of vegetation cover on the rodent's burrow density (Fig 4B & Fig. 5B; Table 2). Livestock grazing had a positive direct influence on GRR burrow density in both path models, as well as habitat wetness in the path model testing the effect of plant species richness on GRR burrow density (Table 2). No indirect effect of grazing either through species richness or vegetation cover on GRR burrow density was detected (in all cases, Sobel test statistic = -1.27–0.31; P = 0.204–0.762; Supplementary file Table S3). The assumptions of both

path models were supported by the Chi-squared test for independence (path model for species richness: Chi-squared = 14.33, P = 0.16; vegetation cover: Chi-squared = 10.46; P = 0.40).

Table 2. Results of path models analysing the effects of temperature, habitat wetness, livestock grazing and plant species richness, or vegetation cover on GRR burrow density. Given are values of unstandardized path coefficients and their standard errors (Ustd. Estimate § SE), standardized path coefficients (Std. Estimate) and R^2. Values of Std. Estimates with asterisk indicate significant effects at significance levels of * = $P < 0.05$, **$P < 0.01$, ***$P < 0.001$).

Variables	Ustd. Estimate ± SE	Std. Estimate	R^2
Level 1: Livestock grazing			0.37
Habitat wetness	0.204 ± 0.132	0.245	
Temperature	0.249 ± 0.083	0.514**	
Level 2: Species richness			0.51
Livestock grazing	-0.011 ± 0.014	-0.109	
Habitat wetness	0.398 ± 0.018	0.278*	
Temperature	0.172 ± 0.612	0.206	
Level 3: GRR burrow density			0.29
Species richness	0.079 ± 0.024	0.029***	
Livestock grazing	0.049 ± 0.003	0.185***	
Habitat wetness	0.051 ± 0.032	0.013	
Temperature	0.005 ± 0.057	0.002	
Level 2: Vegetation cover			0.15
Livestock grazing	-0.234 ± 0.269	-0.131	
Habitat wetness	-1.057 ± 3.462	-0.040	
Temperature	2.354 ± 2.592	0.154	
Level 3: GRR burrow density			0.18
Vegetation cover	-0.025 ± 0.001	-0.161***	
Livestock grazing	0.017 ± 0.002	0.062***	
Habitat wetness	0.204 ± 0.018	0.050***	
Temperature	-0.051 ± 0.048	-0.021	

Comparison of path models

We compared both sets of path models for each of the vegetation variables, i.e., plant species richness or vegetation cover. The path model testing the effect of plant species richness on GRR burrow density (AIC: 75.04) showed a slightly better AIC value than the model testing the effect of GRR burrow density on species richness (AIC: 78.33; ΔAIC: 3.29). In contrast, the path model testing the effect of GRR burrow density on vegetation cover (AIC: 62.46; ΔAIC:

3.02) produced slightly better AIC values, than that testing the effect of vegetation cover on GRR burrow density (AIC: 65.48).

2.4. Discussion

Our results show that increasing GRR burrow density led to decreased vegetation cover. Considering the reciprocal causation models, we found that increasing plant species richness led to increased GRR burrow density, while GRR burrow density decreased as vegetation cover increased. The latter finding is particularly interesting, because GRR's preference of sites with lower vegetation cover has been less known unlike the well-known decrease of vegetation cover by root-rat activity (Šklíba et al. 2017). However, the AIC statistics of the alternative models are too similar to make any conclusion(s) about which causal effect is more likely; hence, both directions are presumably at equilibrium. Increases in habitat wetness and livestock grazing intensity also directly led to increased GRR burrow density.

In line with our prediction, our results showed that vegetation cover decreased with increasing GRR burrow density. Obviously, both bioturbation and direct herbivory of GRR lead to reduced vegetation cover, in agreement with reports of previous studies on other species (Haussmann 2017; Wu et al. 2015). Our findings are also in line with studies on the GRR (Beyene 1986; Sillero-Zubiri et al. 1995; Šklíba et al. 2017; Yalden 1975) and reduced *A. abyssinica*, GRR's favoured food plant, at active GRR burrows. Yet, we did not find a significant effect of GRR burrow density on plant species richness, which partly contradicts out initial prediction but is in line with many similar studies demonstrating inconsistent results (Haussmann 2017; Jones et al. 1997; Romero et al. 2015; Wu et al. 2015). Our result in this regard may suggest that plant damage during mound excavation and foraging does not lead to reduced species richness. This might be true in the latter case because subterranean rodents are well-known to be food generalists (Nevo 1999). Studies on food consumption of GRRs (Beyene 1986; Yaba et al. 2011) showed that they feed on any available plants around burrows even though they amply forage on abundantly available herb plant species (e.g. *A. abyssinica*) and grasses (Vlasatá et al. 2017). This suggests that GRR might be a food generalist predominantly foraging on abundantly available forbs, which in turn might minimize the risk of local extinction of rare species and may explain the lack of impact of the rodent's burrow density on plant species richness.

Analysing vegetation effects on GRR burrow density, we found increased GRR burrow density with increasing plant species richness and with decreasing vegetation cover. The increased GRR activity with increasing plant species richness is not clear, because, as discussed above, GRRs feed on any available plants around burrows (Beyene 1986; Yaba et al. 2011). Despite this, Šklíba et al. (2020) showed that GRRs shifted their home ranges, during the late dry season when forage was in short supply, from shorelines into the wetlands to increase their food supply. Thus, given the positive associations we found between habitat wetness and both GRR burrow density and plant species richness, our result of GRR's association with richness could be a by-product of GRR's preference for microhabitats, such as wetlands that are characterized by high species richness (Sillero-Zubiri et al. 1995; Yalden 1975). The increased GRR burrow density with decreasing vegetation cover clearly reveals GRR's preference for open habitats ((Sillero-Zubiri et al. 1995; Vlasatá et al. 2017). In fact, they are morphologically, physiologically and behaviourally adapted to life in open Afroalpine habitats (Bryja et al. 2019; Sillero-Zubiri et al. 1995; Yaba et al. 2011). Overall, our results demonstrate that effects of GRR on vegetation cover were stronger than *vice-versa*, and that the cause-effect relationship between plant species richness and GRR was only in one direction (richness on GRR).

The significant positive effect of livestock grazing on GRR burrow density is in agreement with our prediction and has not been well known although previously suggested (Šklíba et al. 2017), and fits with the rodent's preference for open habitats (Beyene 1986; Lavrenchenko and Kennerley 2016). A study on Plateau zokor (*Myospalax baileyi*) in the Tibetan Plateau, China, has also shown such increase in burrow density with increasing livestock grazing activity, but the effects were found to be dependent on the seasonality, grazing system and stocking rate of grazing practices (Wang et al. 2020). Our result, however, is in contrast to results of other studies reporting a non-significant or negative effect of livestock grazing on GRR and other subterranean rodents (Torre et al. 2007). These inconsistences in results across studies indicate a spatiotemporal context-dependence of the complex interplays between livestock grazing, vegetation patterns and subterranean rodents. In our study system, the effect of livestock grazing on GRR is assumed to be attributable to a livestock herbivory-induced decrease in vegetation cover (Vial 2011). The GRR could thus, potentially benefit from livestock-induced enlargement of their habitat. Yet, our results are based on assessments in the dry season; grazing intensity and its effects on GRR burrow density may differ in the wet season, when food abundance for livestock is higher (Vial 2011). In addition, our study did not cover the potential effects of other domestic animals. Thus, our result should be interpreted cautiously because, despite the long-time associations of humans and GRRs in the Bale Mountains (Ossendorf et

al. 2019), concerns over the increasing livestock grazing encroachments in the Bale mountains have been growing (BMNP 2017; Vial 2011). Particularly, unregulated overstocking of livestock has been considered as the major threat to several globally threatened species, including the GRR. Thus, future research should focus on the spatiotemporal intensity of domestic animals grazing tolerable by the GRRs to inform management decisions.

The increased GRR burrow density with increasing habitat wetness found in our study is consistent with our prediction and findings in other studies (Sillero-Zubiri et al. 1995; Šklíba et al. 2017, 2020; Vlasatá et al. 2017) that reported that wetland habitats are dry-season preferred habitats of GRRs. This habitat type provides better forage quality, and easily workable soil (Sillero-Zubiri et al. 1995; Šklíba et al. 2017; Vlasatá et al. 2017). A similar positive association between moisture and mound density has been reported for Plateau Zokor (Zhang and Liu 2003). In contrast to our prediction, but in consistence with findings on the GRR (Vlasatá et al. 2017) and on other species (e.g. Hagenah and Bennett 2013; Hart et al. 2021), we did not observe any effect of temperature on GRR burrow density. Our result could be attributed to the species' adaptation to local climatic conditions within its range.

Conclusions

With our study on GRR, we could show the reciprocal impact of a subterranean ecosystem engineering rodent on its environment, and *vice versa.* Surprisingly, we found positive influences of human activities in terms of livestock grazing on GRR burrow density. Our results highlight the complex interplay between environmental factors, humans and ecosystem engineering species, especially in light of an extreme environment such as Afroalpine ecosystem. Given the unregulated ongoing human activity in the Afroalpine ecosystem of the Bale mountains, research focusing on the influences of different grazing seasons and stocking rate on the GRR and its engineering role would be important to inform effective ecosystem management.

Acknowledgements

Supplementary material

Supplementary material to this chapter can be found in Supplementary material Chapter II.

Remote sensing-supported mapping of a subterranean landscape engineer across an afro-alpine ecosystem

by

Luise Wraase*, **Victoria M. Reuber***, Philipp Kurth, Mekbib Fekadu, Sebsebe Demissew, Georg Miehe, Lars Opgenoorth, Ulrike Selig, Zerihun Woldu, Dirk Zeuss, Dana G. Schabo, Nina Farwig & Thomas Nauss

* These authors contributed equally to this study

ABSTRACT

Subterranean animals act as ecosystem engineers, for example, through soil perturbation and herbivory, shaping their environments worldwide. As the occurrence of animals is often linked to above-ground features such as plant species composition or landscape textures, satellite-based remote sensing approaches can be used to predict the distribution of subterranean species. Here, we combine in-situ collected vegetation composition data with remotely sensed data to improve the prediction of a subterranean species across a large spatial scale. We compared three machine learning-based modeling strategies, including field and satellite-based remote sensing data to different extents, in order to predict the distribution of the subterranean giant root-rat GRR, *Tachyoryctes macrocephalus*, an endangered rodent species endemic to the Bale Mountains in southeast Ethiopia. We included no, some and extensive fieldwork data in the modeling to test how these data improved prediction quality. We found prediction quality to be particularly dependent on the spatial coverage of the training data. Species distributions were best predicted by using texture metrics and eyeball-selected data points of landscape marks created by the GRR. Vegetation composition as a predictor showed the lowest contribution to model performance and lacked spatial accuracy. Our results suggest that the time-consuming collection of vegetation data in the field is not necessarily required for the prediction of subterranean species that leave traceable above-ground landscape marks like the GRR. Instead, remotely sensed and spatially eyeball-selected presence data of subterranean species could profoundly enhance predictions. The usage of remote sensing-derived texture metrics has great potential for improving the distribution modeling of subterranean species, especially in arid ecosystems.

3.1. Introduction

Subterranean animals act as ecosystem engineers as they shape and maintain grassland ecosystems worldwide. By burrowing, they rework sediments, redistribute nutrients in the soil and change vegetation patterns and when taken together, create and modify habitats for other organisms (Corenblit et al. 2011; Gabet et al. 2003; Hastings et al. 2007; Jones et al. 1994; Reichman and Seabloom 2002). At the same time, the distribution of subterranean animals and the species' functions for biodiversity and ecosystems are affected by human-induced habitat modification and degradation, such as changes in vegetation cover caused by livestock grazing (Bakker, Olff, and Gleichman 2009; Keesing 1998; Vial 2011). Studies on the distribution and

abundance of subterranean animals remain rare despite their importance for ecosystems and the increasing demand for detecting and predicting ecosystem changes.

The giant root-rat (GRR; *Tachyoryctes macrocephalus*, Rüppel, 1842 by Yalden 1985) is a prime example of an animal ecosystem engineer. By creating extensive underground burrows and tunnel systems, it has a strong impact on the environment, particularly on the surrounding soil structure and vegetation (Šklíba et al. 2017; Yalden 1985). The rodent is endemic to the afro-alpine ecosystem of the Bale Mountains of southeast Ethiopia, stretching between elevations of 3,000 and 4,150 m a.s.l., in lawns of *Alchemilla abyssinica*, which is their preferred diet (Yaba et al. 2011; Yalden 1985; Yalden and Largen 1992). Over time, the subterranean activity of the GRR changes the vegetation and soil structure of the prevailing open dwarf shrublands of *Helichrysum splendidum*, the Cyperaceae swamps and grasslands into discrete opensoil mounds (Miehe and Miehe 1994; Yalden and Largen 1992). Due to soil texture changes, these discrete mounds are distinguishable from the characteristically flat areas marked by an absence of GRR activity. Further, the species affects plant species richness, composition and biomass in its direct vicinity due to soil perturbation and above-ground herbivory (Sillero-Zubiri et al. 1995; Šklíba et al. 2017; Yalden and Largen 1992). The changes in soil structure and vegetation patterns underpin the GRR's influence on the landscape and ultimately, their strong impact on an ecosystem and its processes. The ecological role of the species is even broader as GRRs are the predominant prey of the endangered Ethiopian wolf *Canis simensis* (Sillero-Zubiri and Gottelli 1995). Moreover, the GRR is currently listed as endangered and is especially sensitive to increasing human-induced habitat degradation in the Bale Mountains (Lavrenchenko and Kennerley 2016). Therefore, assessing the distribution of GRRs on the landscape scale is equally important for estimating their effectiveness as an ecosystem engineer as it is for evaluating the endangerment of the species. Here, we used satellite-based remote sensing to upscale the ecosystem engineering signs and quantify ground burrows across large extents (i.e., assessing the species distribution across the Bale Mountains).

Many satellite-based remote sensing studies have predicted particularly large animal species that are easily detectable from space either via direct observations across large extents or indirectly by predicting discrete structures or habitat changes caused by these animals, for example, elephants, penguins, or lions (Barber-Meyer et al. 2007; Fretwell et al. 2012; Fretwell, Staniland, and Forcada 2014; Hollings et al. 2018; Kellenberger, Marcos, and Tuia 2018; LaRue et al. 2014; Loarie, Tambling, and Asner 2013; Wang et al. 2019). To predict smaller-sized or species with low visibility such as birds, invertebrates, or subterranean animals, remote sensing

approaches must rely on vegetation cover and composition, or geomorphological properties as proxies for habitat suitability and probability of the species' presence (Culbert et al. 2012; Estes et al. 2010; Farwell et al. 2021; Gabet et al. 2003; Grigusova et al. 2021; Koshkina et al. 2020; Porcasi et al. 2005). Generally speaking, predicting the presence of an animal species becomes increasingly difficult as its visibility decreases, for example, due to small body size or fast movement; this is particularly true for subterranean animals in homogenous grasslands. Hence, in order to predict GRR distribution, the focus should be on changes in vegetation patterns or soil structure (i.e., on the mounds created by the species) (Grigusova et al. 2021; Koshkina et al. 2020)

Machine learning has recently been used to bridge the gap between grain and extent. In our approach, we opted for statistical classification models, which can be trained on the local field data that link spectral remote sensing observations or other area-wide data sets, such as digital elevation models, with the occurrence of GRRs. This approach is regularly used to scale surveys across large areas (Pöyry et al. 2018; Wakulińska and Marcinkowska-Ochtyra 2020). However, the performance of a given model depends on numerous factors, such as the observed environment and the species it aims to predict (Aguirre-Gutiérrez et al. 2014; Fiedler et al. 2008). Some studies show that including plant species composition as an additional independent variable can improve the predictability of animal species distribution or diversity (Schaffers et al. 2008; Wallis et al. 2017). In this specific context, if plant species composition and its change over space (i.e., turnover) are caused by a subterranean engineer, the turnover indicates the distribution of the species. However, this requires a labor-intensive field campaign to collect sufficient training data to directly predict the species composition in space as a surrogate for the animals' distribution. Thus, comparing remote sensing models that integrate field survey data to different extents with a model solely trained on readily available data could determine whether integrating time intensive field observations improves the prediction of a subterranean ecosystem engineer (e.g., GRRs) across large extents.

In this study, we map GRRs distribution across the Bale Mountains using three different modeling strategies that require no (method 1, M1), some (M2) and very intensive (M3) fieldwork to collect training data. First, we hypothesize that in-situ collected GPS coordinates (M2), which accurately depict GRR presence and absence, improve the classifications exclusively based on training areas selected with the eyeball method (M1). Second, we hypothesize that using plant species composition data (M3) and remotely sensed observations improve the classification outcome. Our comparative approach demonstrates methodological

tools for mapping the current distribution of a subterranean species. Therewith, we provide insights into how GRRs shape the afro-alpine Bale Mountains ecosystem across their entire distribution range.

3.2. Material and methods

Field survey

The field survey was conducted in October and November 2017 across the Sanetti Plateau, and Web Valley of the Bale Mountains National Park in Ethiopia (6°29′N–7°10′N and 39°28′ E–39°57′ E; Fig. 1B). The highest peak of the study area was the Mount Tullu Dimtu at 4,377 m a.s.l. The climate of the study area is characterized by two consecutive wet and warm seasons (April–September) and a dry and colder season (November–March) with annual rainfall of approximately 1,000 mm (station records of the DFG Research Unit Bale Exile at 10 sites). The slopes of the Bale Mountains are covered in moist mountain forests merging into the Ericaceous Belt around 3,000 m a.s.l. At the upper reaches, these ericaceous shrubland and dwarf forests of *Erica trimera* again merge in an extended ecotone into the afro-alpine ecosystem between 3,800 and 4,000 m with the highest Erica outposts at approximately 4,250 m a.s.l. The afro-alpine ecosystem consists of species-poor open dwarf shrublands of *Alchemilla haumannii* and *Helichrysum citrispinum* in the northern part and *H. splendidum* in the southern highlands. *Lobelia rhynchopetalum*, a giant rosette plant, is scattered across the entire afro-alpine ecosystem (Chala et al. 2016). In addition to the GRR, other wild herbivores such as mountain nyalas *Tragelaphus buxtoni*, bohor reedbucks *Redunca redunca* and rock hyraxes *Procavia capensis capillosa* feed upon vegetation (Mekonen 2020; Teklehaimanot and Balakrishnan 2018). Furthermore, growing human presence in the Bale Mountains National Park followed by livestock and associated grazing, human settlements, grass collection or frequent fire and bush encroachment impact the landscape of the Bale Mountains National Park (Mekonen 2020). The impact GRRs have on the landscape can be clearly separated from the impact of other species as a result of the pronounced effect they have on soil structure creating discrete mounds and a "spongy" ground (Fig. 1C and D) (Miehe and Miehe 1994; Sillero-Zubiri et al. 1995).
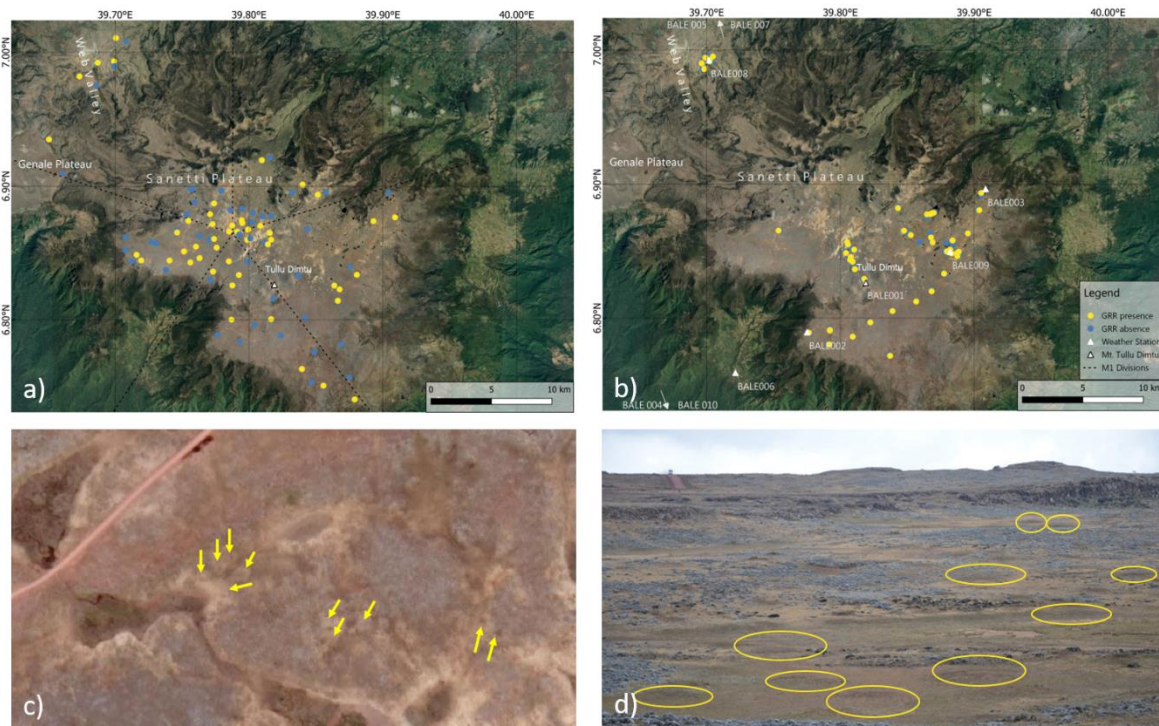
Figure 1. Locations of training areas with presence (yellow dots) and absence (blue dots) of giant root-rat (GRR) activity used in the different model strategies based on (A) Google Earth (M1) and (B) local GPS records (M2 and M3). Black dotted lines in (A) show sectors, in which training areas were selected, and white triangles in (B) show the location of climate stations; for details, see the methods section. (C) Shows GRR mounds as observable in Google Earth and (D) in the field.

In the field survey, we selected 94 GPS points and sampled plant species composition data in a pairwise plot design at the GPS points, in areas with and without GRR activity for later machine learning analyses (47 presence and 47 absence plots; GPS: Garmin eTrax30, precision 3 m). The survey was conducted along the main track of the Sanetti Plateau, the northern and northeastern parts of the Sanetti Plateau, and the Web Valley. The track was unpaved and infrequently used, and thus, the impact on plant species composition or GRR activity was presumably insignificant. Plots following the main track were established in a 2 km interval with a minimum of 100 m distance to the main track and a minimum of 50 m between presence and absence plots. The presence and absence plots were and carefully distinguished by the observers in GRR presence or absence areas (two persons with each 25 days and 10 h observations per day; PK and MF). Areas of GRR presence were clearly detectable as mound structures, which showed altered vegetation patterns in comparison to areas where GRR were absent and thus, areas without GRRs were also clearly identifiable. One mound was approximately 20 m in diameter (personal observation), with several burrow openings scattered across one mound. The immediate surrounding of GRR burrow openings was characterized by bare vegetation, while herbaceous vegetation covered the rest of the mound (Miehe and Miehe

37

1994). For each mound, GRR activity could further be identified by fresh burrow openings (Leyer and Wesche 2007), whereby one GRR individual used several burrow openings. The burrow openings from other subterranean species were smaller in diameter and thus distinguishable from GRR burrows, wherefore presence and absence of GRR activity areas were clearly specifiable. Nonetheless, past GRR activity at absence points could theoretically not be ruled out entirely; however, the impact on our analyses should be negligible, as the aim was to map current GRR presence and absence. We documented the plant species composition on each plot of 5 × 5 m size, and estimated the cover fraction in intervals of 5%, following a typical Mueller-Dombois and Ellenberg (1974) design. In addition, specialists identified plant species that could not be determined in the field (MF and SD). As a result, we found 60 (63) different plant species on GRR presence (absence) plots and 79 different plant species in total. The most abundant plant species for both areas with and without GRR activity was *A. abyssinica*. The abundance of other plant species varied between both areas.

Pre-processing

Species composition analysis

To compare the plant species composition between plots with and without GRR activity, we used constrained correspondence analysis (CCA) as an ordination method, based on the correlation matrix of the 79 plant species (rare species included) across all 94 plots (Fig. 1B). In general, ordination techniques can be used for assessing the main environmental gradients driving plant composition turnover across sites, using raw data of species richness and abundance. The gradients are projected into axes and displayed in a multidimensional ordination space with the first axis explaining the largest variance in the changes of plant composition by a gradient, with decreasing variance explained by the subsequent axes (Feilhauer and Schmidtlein 2009; Leyer and Wesche 2007). A constrained ordination method assumes that the variation in the vegetation data is displayed by a priori chosen environmental gradient (i.e., constraints) (Leyer and Wesche 2007), which are included in the first constrained axis. Further, a CCA assumes that a species' response to environmental gradients is unimodal and not linear. CCAs can deal with zero-inflated data and are therefore suited for our species composition data set (ter Braak 1987; Leyer and Wesche 2007). As temperature is a main driver for plant species composition (Keller, Kienast, and Beniston 2000; Nottingham et al. 2018), the satellite-predicted mean air temperature of 2017 was used as a constraining variable on the first CCA axis (CCA: Fig. S1A; for Landsat-8 temperature prediction see Appendix S1;

Supplementary Method 1). By constraining species compositions on temperature, we removed the effect of temperature on species composition from the remaining unconstrained axes. The ordination scores of the first two unconstrained axes (CA1 and CA2 axes; Fig. S1B) were used in subsequent machine learning steps, herein referred to as CA1 and CA2 scores. Thus, the CA scores present plant species composition across survey sites corrected for the effects of temperature on vegetation composition. Temperature as a constraining variable explained 5% of the plant species composition. The package vegan (Oksanen et al. 2020) was used for the analysis in R version 4.0.2 (R Core Team 2021).

Sentinel-2 observations for spatial prediction of GRR presence

An almost cloud-free (3.5% cloud cover) Sentinel-2 scene from December 15, 2017 at 07:54:34 UTC was retrieved from the USGS Earth Explorer repository and used as a basis for predicting GRR mounds in the study area. The data were atmospherically corrected using the Sen2cor algorithm (Filipponi 2018) . We used Sentinel-2 observations of the red, green, blue, red edge, near-infrared bands – each with 10 m resolution – and short-wave infrared satellite bands with 20 m resolution to include multiple indices with different foci on vegetation, soil and water, which best represent the grassland habitat of the GRR. The 10 m bands (three visible and one near-infrared) were resampled to match the 20 m resolution of the near- and short-wave infrared bands, to characterize the GRR presence in the study area. Spectral indices that highlight different vegetation and environmental characteristics (e.g., soil wetness) were computed from the individual band observations using the RStoolbox (Leutner et al. 2017). In addition, the k-mean distance from the centroid (KMDC) was computed in each case on every band and generated an index raster image (Table S1). Since GRR activity leads to hill-like structures, such as mounds, a group of grey-level co-occurrence matrix features (GLCM) and Rao's Q (Rocchini et al. 2018) were also compiled. For the GLCM, the entropy, homogeneity, and second moment (Haralick, Shanmugam, and Dinstein 1973) for three different window sizes (3 × 3, 11 × 11 and 31 × 31 pixels) were derived separately for both KMDC indices that were reduced to 32 grey levels. Different texture metrics are helpful to detect similarities and differences, and also patterns in the topography that simple satellite bands and vegetation indices cannot depict as accurately (Kupidura 2019; Mishra et al. 2019). For depicting topographical differences, especially in soil texture and soil type from space, a pre-processing step with k-means cluster analysis was conducted using the Hartigan and Wong (1979), set center = 1 and squared the fitted result which was multiplied by 2, in R-version 4.0.2 (Brus

2019; Brus, de Gruijter, and van Groenigen 2006; Hartigan 1975). Rao's Q (Rao 1982) was determined based on the combined set of original bands, the scaled vegetation indices, and the results from KMDC (Table S1).

Modeling workflow

We followed three different modeling strategies to map the presence and absence of GRR activity, that is, by identifying locations with or without mound occurrences (Fig. 2; Table S2). All three strategies, hereafter referred to as M1, M2 and M3 utilized the Sentinel-2-based spectral indices and texture metrics as predictor variables. M1 was based on 94 training data points (i.e., 47 presence and 47 absence points) that were visually chosen from Google Earth. The visually chosen training data points (i.e., mounds for GRR presence and no mounds for GRR absence) were taken in the middle of a mound (presence) and in landscapes visually without mounds (absence). Mounds (Fig. 1C and D) were selected visually by one person (LW) and cross-checked by a second person (TN) in a two-day process from Google Earth imagery, using their specific non-edge landscape characteristics and often repetitive appearance. M2 used in-situ collected GPS points as training data instead, with 94 training data points in total that were composed of 47 presence and 47 absence points. The GPS points (i.e., the training data) in M2 were taken in the middle of each mound and in areas without mounds. Finally, M3 employed the same *in-situ* collected training data points as in M2 (i.e., 94 points in total, 47 presence and 47 absence points); however, the CA1/CA2 scores derived from vegetation composition (CA prediction) into space were first predicted using the Sentinel-2-based variables. Next, the GRR activity was classified into a binary presence and absence map by a second model trained on the CA1/CA2 maps (M3, CA classification).
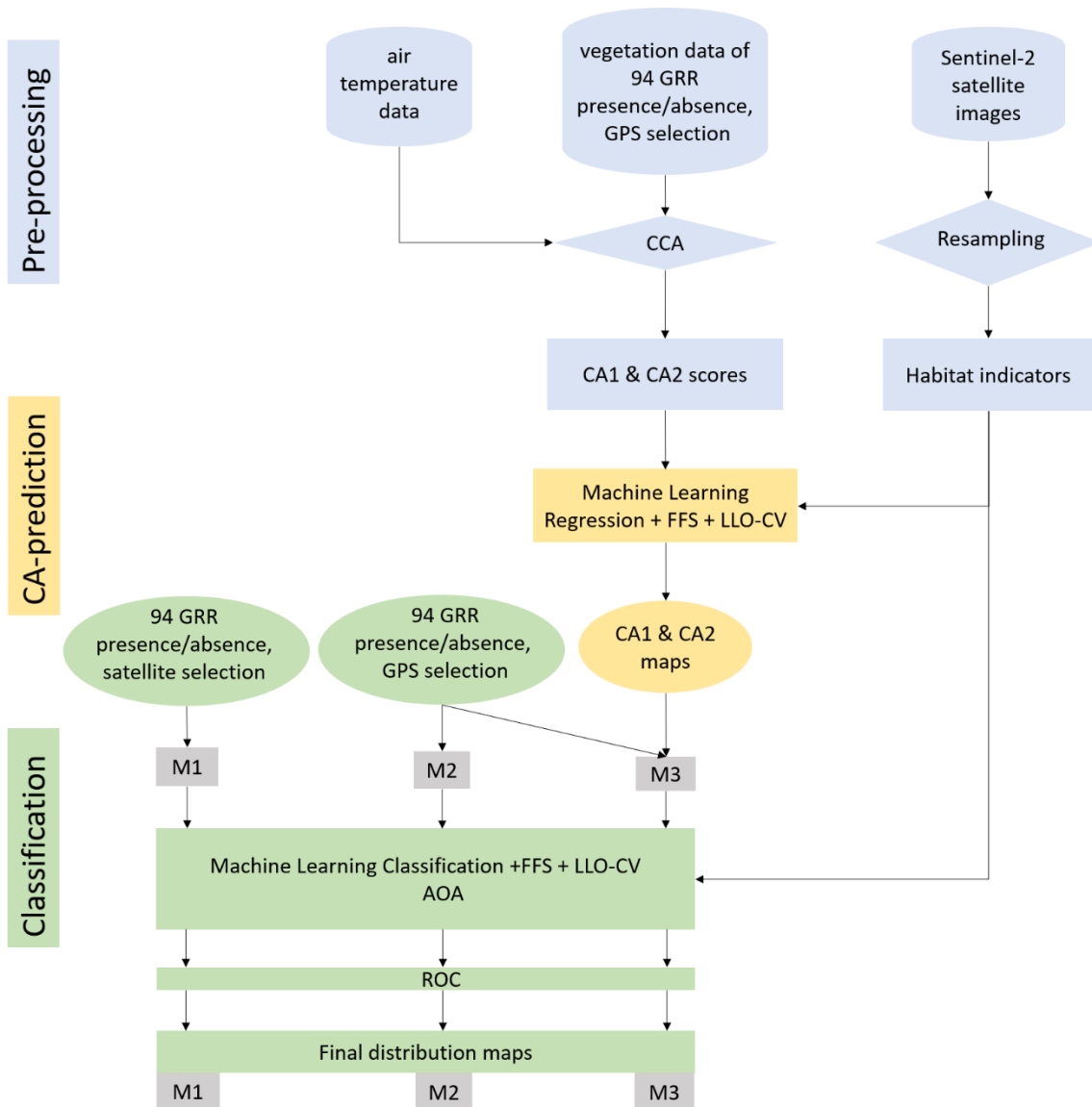
Figure 2. Modeling workflow showing the pre-processing (blue), the CA prediction (yellow, M3 only) and the classification (green). Pre-processing: Air temperature and habitat indicators were processed for downstream analyses; field-based plant species composition data was used in constrained correspondence analysis (CCA) to retrieve CA scores; CA-prediction: A machine learning regression model was used to predict CA1/CA2 scores into space with Sentinel-2 variables. Using forward feature selection (FFS) and a 10-fold leave-location-out (LLO) cross-validation (CV) to compile the CA1/CA2 maps, which were used in subsequent classification for M3; Classification: Machine learning models were applied, using FFS and 10-fold LLO-CV for predicting species distribution maps. The boxes with the numbers M1, M2 and M3 depict the three model strategies compared in this paper, with M1 supplied by image-selected classification categories, M2 using in-situ collected GPS coordinates and M3 using the same settings as M2 and also additionally the predicted CA scores as a predictor for the modeling process (see section Pre-processing). The area of applicability (AOA) method was used to calculate the validity of prediction error in space.

Our approach for M1 and M2 included using a random forest classifier (Breiman 2001) in a forward feature selection (FFS), a 5-fold external leave location-out-(LLO) and 10-fold internal cross-validation (CV). Within each of the five iterations, 70% of the data was used for training and 30% data was withheld for independent testing. For M3, the CA1/CA2 scores were first predicted into space using a random forest regression model (CA prediction step) using the

41

same FFS, LLO and CV settings as in M1 and M2. For the second step, the variables CA1 and CA2 were added as predictors. Lastly, for the M3 approach, the same model settings were used as for M1 and M2. The FFS used in M1, M2 and M3 always starts by identifying the two best-performing variables based on the LLO error estimates. Subsequently, the algorithm incrementally increases the number of predictor variables and tests for each additional predictor variable if it is improving the current model further. The model stops training when adding another variable no longer increases the overall performance. For details on FFS, see Meyer et al. (2018). Previous studies identified the random forest classifier robust (Kuhn and Johnson 2013; Meyer et al. 2018). The classification model performance was measured by Cohen's Kappa (Cohen 1960), while the root mean square error (RMSE) was used for the regression models. Finally, the GRR presence and absence was classified after receiver operator characteristic (ROC) analysis for each of the three modeling strategies M1, M2 and M3 (Fig. S5). Since models are generally restricted to the information dimension of the input data sets (i.e., the spectral range of the Sentinel-2 data across the 94 extracted training areas) and a certain level of uncertainty generally remains after the final prediction, it is necessary to consider those (Jansen et al. 2022). Here, the area located outside of the actual area of applicability (AOA) of the model was masked and not further considered, following the approach from Meyer et al. (2018) and Meyer and Pebesma (2021) as implemented in the CAST package. Besides the random forest-based methods M1–M3, a Maximum Entropy (MaxEnt) (Phillips, Anderson, and Schapire 2006) machine learning model software accessed by the R-Package dismo (Hijmans et al. 2017) was conducted to further evaluate and cross-check the results of our three machine learning modeling strategies. In short, we used the same model settings and input data including the predicted CA variables as in M2 and M3, with the exception of the absence data (also 47 points) in MaxEnt which was selected randomly within the raster extent. The MaxEnt and random forest models were compared by the area under a receiver operating characteristic curve (AUC) value. If available, true presences and absences should be considered first in any modeling of species distributions (Elith et al. 2011; Guillera-Arroita, Lahoz-Monfort, and Elith 2014; Zaniewski, Lehmann, and Overton 2002) . Thus, the random forest model we used was the preferred method over the MaxEnt model, as it used true presences and true absences in our data. In contrast, absence points (or "background" points) in MaxEnt were randomly sampled across the whole area (Massada et al. 2012; Oppel et al. 2012) and may, by chance, also depict single presence points, which might influence the model results. Nevertheless, in other comparative studies, both machine learning-based methods tend to perform similarly (Acharya et al. 2019; Bektas et al. 2022; Kaky et al. 2020; Kaky and Gilbert 2016; Mi et al. 2017; Zhao

et al. 2022). As also in our case, the results of the MaxEnt and the modeling strategy M1 (the best of the random forest models) were qualitatively similar, we only present the results of the random forest machine learning approaches in the results section. The model performance, evaluation and final predictor variable selection of the MaxEnt model can be found in Appendix S1, Supplementary Method 2.

3.3. Results

CA prediction

Predicting CA1/CA2 values in M3 resulted in relatively high RMSE values with CA2 (0.882) exceeding CA1 (0.715); the R2 (coefficient of determination) values provided a slightly contrary perspective (CA1: 0.188 and CA2: 0.129). The difference between the mean absolute error (MAE) values in CA1 (0.445) and CA2 (0.770) was more pronounced than for the RMSE and R2. The predicted CA1 scores overlapped more with the original scores than CA2 (Fig. 3). The two most important predictors for CA1 were the Normalized Difference Vegetation Index (NDVI) and Land Surface Water Index (LSWI); for CA2 they were the Sentinel-2 band 3 (blue) and GLI (Table S3; Fig. S2). Three of the six (CA1) and five of the eight (CA2) variables were composed based on the pixels' surroundings (Table S3; Fig. S2).
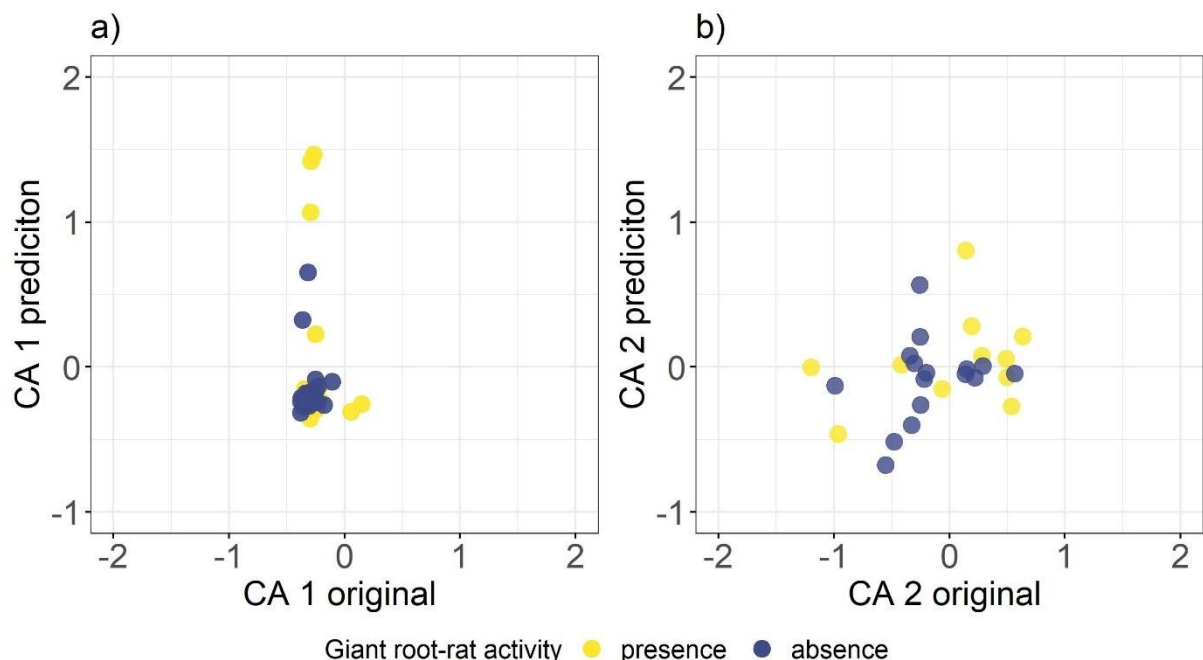
Figure 3. Correlation between original and predicted CA scores of (A) CA1 and (B) CA2 by M3 for each of the 47 GRR presence and absence locations. This figure displays a randomly chosen test set of 27 data points.

Giant root-rat classification

In terms of predicting the presence and absence of GRR activity, the model accuracies showed considerable differences with M1 (Cohen's Kappa: 0.777) and M2 (0.494) outperforming M3 (0.375) (Table 1b). Models M1 and M2 shared similarities, for example, they each included at least two texture metrics, representing information computed on window sizes of 3×3 or 11×11 pixels, which cover an extent of 60 and 220 m, respectively (Fig. 4). In M1, the most important predictor variable was the KMDC indices stack (k-means distance from the center of indices stack) and the second most important predictor was the texture metric of Rao's Q KMDC indices stack. The texture metrics were the most important predictor group of M1, with seven texture metrics selected in total (Fig. 4A). Compared to M1, the difference in the importance of the top four predictors in M2 was more gradual. The final model of M2 included two predictor variables less than M1, including the Visible Vegetation Index (VVI), two Sentinel-2 bands and two texture metrics based on a 3×3 window size of 60 m2 as predictor variables for the GRR distribution (Fig. 4B). In M3, only the predicted CA2 axis scores were chosen in combination with texture Rao's Q KMDC (Sentinel-2 band stack) as the second most important predictor (Fig. 4C). Model tuning resulted in five (M1), three (M2) and two (M3) variables used for splitting at each tree node of the random forest classifier (i.e., mtrys, Fig. S3). The error matrix, which depicts how much of each class is assigned correctly (i.e., GRR presence or absence), determined that M1 outperformed M2 and M3.

Table 1. Comparison of the three model strategies (M1–M3); Google Earth (M1) and local GPS records (M2 and M3 with M3 additionally including CA scores as predictors, see section Modeling workflow for details) by depicting the (a) error matrix and (b) accuracy values. (a) shows which response, that is, presence or absence of giant root-rat (GRR) activity, explains how much percentage of its own or the other classes. (b) shows each model's performance for the applied classifications (ROC threshold as graph, see Figure S5).

	(a) Error matrix			(b) Accuracy values			
	Prediction	Presence	Absence	Accuracy	Cohen's Kappa	AUC	ROC threshold
M1	Presence	49.3	6.0	0.895	0.777	0.849	0.555
	Absence	4.5	40.3				
M2	Presence	41.8	13.4	0.750	0.494	0.640	0.575
	Absence	11.9	32.8				
M3	Presence	38.8	16.4	0.691	0.375	0.654	0.581
	Absence	14.9	29.9				
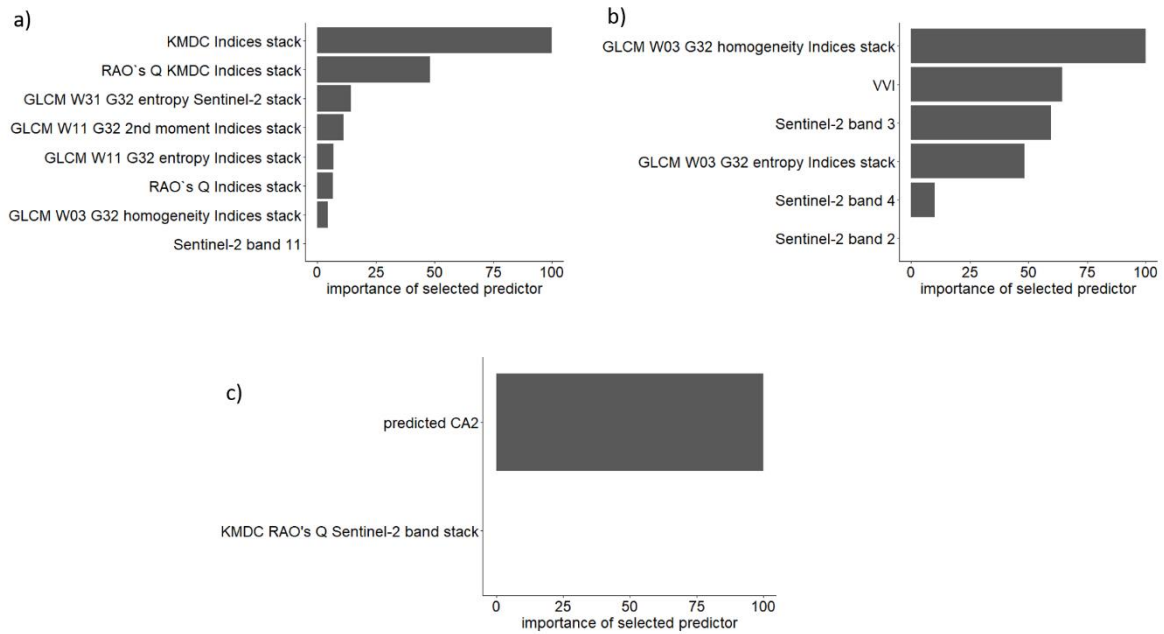
Figure 4. Selected predictors in order of importance and their explanatory power in percent (%) for each of the three model strategies M1–M3 (A–C); training areas based on Google Earth (M1; A), local GPS records (M2; B) and (M3; C). M3 additionally included CA scores as predictors (see section Modeling workflow for details; predictor names: Table S1).

Distribution of the giant root-rat

The three model strategies predicted GRR presence and absence across the Sanetti Plateau and Web Valley. M1 and M2 both predicted a strong concentration of GRR presence on the central Sanetti Plateau and the northwestern descent toward the Web Valley and the lower plateau area (Fig. 5). While M1 predicted a higher presence of GRR activity in the middle of the Sanetti Plateau and resulted in an area of 28,366 ha for GRR presence (i.e., 19% of the total area of 147,963 ha). M2 showed a higher concentration around the upper northwestern parts and less concentration on the Sanetti Plateau with 55,589 ha of GRR presence. The classification map of M3 predicted 84,859 ha of GRR presence centered around the plateau area and with extra parts in the north–northwestern area. These values were based on prediction probability ROC thresholds of 0.555 (M1), 0.575 (M2) and 0.581 (M3) for delineating presence and absence locations (Fig. S5). In general, the plateau area was more likely to be predicted for the three methods (Fig. 5A–C). These values were also corrected for the models AOA (Fig. 5). For M1, 41.35% of the entire satellite image extent fell into the valid area; this percentage was much greater for M2 (62.73%) and M3 (86.82%). Areas in white were not considered applicable for the model results and areas in transparent displayed overlap. For M1, the AOA partly aligned with the prediction results (orange) but excluded some distinct, concentrated parts in the

southern section. For M2, the AOA also aligned with the prediction result with a greater AOA at an area west adjacent to the Sanetti Plateau and northern parts the Web Valley. In general, the AOA for M3 covered more area than M1 and M2, excluding larger areas in the south and southwestern parts adjacent to the Sanetti Plateau. The AOA also eliminated all areas that did not exhibit GRR mound structures.
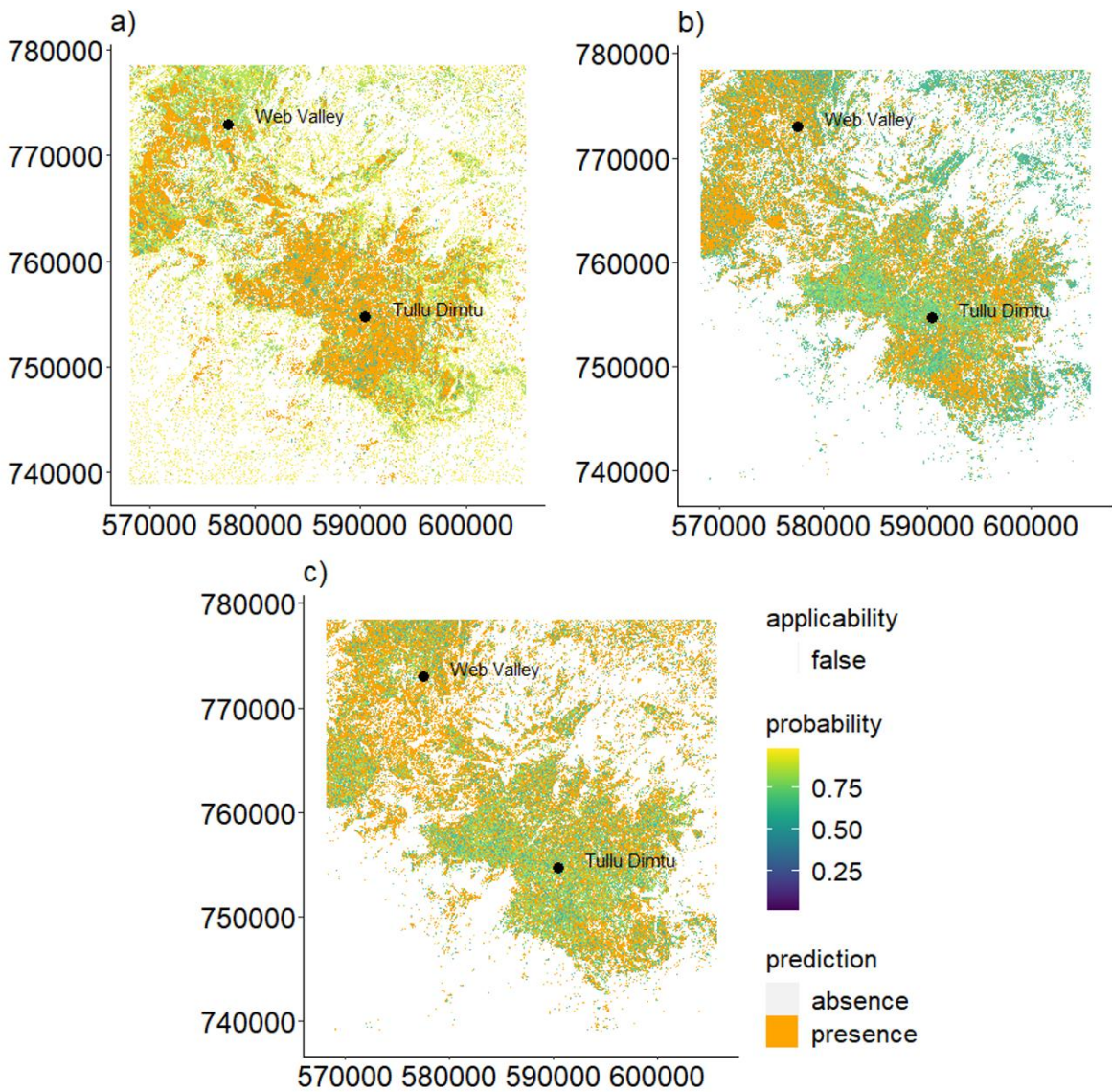
Figure 5. Spatial predictions of giant root-rat (GRR) presence across the Bale Mountains. Each map depicts the distribution of the GRR with a different model strategy M1 (A), M2 (B) and M3 (C). The prediction layer of GRR distribution shows presence in orange and absence in dark grey. The probability of GRR presence in an area is indicated from 1 (presence, yellow) to 0 (absence, dark purple). This is based on the best fitting threshold from each model strategy defined by a receiver operating characteristic (ROC) curve analysis (see Table 1 and Fig. S4 for plotted ROC curves). The validity of the prediction result for GRR presence using the area of applicability method (AOA) is displayed with a transparent mask; white areas lie outside the AOA – and predictions in this area should not be considered.

3.4. Discussion

Comparing subterranean species prediction methods that include field data to a different extent helps to elucidate whether integrating detailed plant species composition data improves predictions across space. Contrary to our first and second hypotheses, our study showed that in-situ collected GPS coordinates of GRR presence and absence and additional plant species composition information did not improve the landscape-scale prediction of the distribution of a subterranean rodent in a homogenous afro-alpine environment. Remotely sensed textural metrics and vegetation indices significantly improved models for predicting the presence of the subterranean GRR. The model strategy based on training areas visually selected on Google Earth images (M1), outperformed training areas using in-situ collected GPS coordinates (M2). In the overall comparison, the complex model M3, including CA scores for plant species composition as a model predictor, had the lowest accuracy. Hence, detailed vegetation surveys are superfluous for predicting the distribution of the GRR, a species that leaves distinct above-ground, and remotely distinguishable landscape marks therefore it is advisable to focus on remote sensing analyses.

Model performance

Overall, M1 had a considerably higher accuracy (Cohen's Kappa) compared to M2 and M3. Comparisons revealed that the spatial coverage of the training data was decisive in improving the quality of the models. As such, M1 performed better given that the training data points covered the entire extent of the Sanetti Plateau and were possibly more heterogeneous. Previous studies have shown that the more spatial representative the training data, the better the resulting models (Berhane et al. 2019; Hengl 2007; Warren et al. 2014). Future field campaigns should focus on covering the entire study area to generate a heterogenous data set. Furthermore, M1 only used training points that were clearly identifiable as locations with GRR presence or absence in the Google Earth images. This selection of training points may skew towards large or characteristic features, which is concomitant with deficits in mapping the potential variability of the GRR locations. The visual selection of training data (M1) works if the species makes a tremendous impact on its landscape, like the GRR. In contrast, the training data in M2 and M3 were restricted to in-situ collected GPS coordinates and plant species composition data of GRR presence and absence areas (only M3). *In-situ* sampling was subject to human labor and temporal constraints on the extensive and partly difficult to access mountain plateau. An extended field period in remote areas at high elevations (4,000 m a.s.l.) would require several

months of physically challenging work conditions to collect a sample comparable to M1, for which the data was retrieved within a few office days.

Predictor importance

M1 and M2 shared similarities as both methods chose texture metrics as predictors of 3×3 and 11×11 pixel window sizes. The texture metrics as the most frequently chosen predictors, likely reflect the topographic pattern of the GRR (i.e., the mounds created by GRR activity). These mounds are distinct from the relatively flat surroundings and, hence, detectable from space. Numerous studies have demonstrated the use of environmental structural heterogeneity for predicting a broad range of plant and animal species (Bellis et al. 2008; Farwell et al. 2021; Tuanmu and Jetz 2015; Wood et al. 2013). The impact of the GRR on soil structure is extreme compared to other species; however, we would recommend using texture metrics in future predictions of subterranean rodents, for example, the east African root-rat, north American pocket gophers or Mongolian marmots (Gabet et al. 2003; Huntly and Reichman 1994; Koshkina et al. 2020), which also leave above-ground marks.

In direct comparison, M1 selected two more predictors for the final model than M2. The importance of the predictors was less abrupt for M2 than for M1. For M1, the most interpretable variable is Rao's Q, which can be linked to plant functional types (i.e., grouping plant species with similar structural features) (Botta--Dukát 2005; Rocchini et al. 2018). The presence of GRRs is related to grasslands where *Alchemilla* is the predominant species, whereas the species' absence is characterized by other habitat features, such as denser shrubland or Erica-thickets (Miehe and Miehe 1994).

For M2, the VVI and Sentinel-2 bands were chosen along with texture metrics. VVI is typically used to predict biomass and can be linked to GRR presence and absence because the species keeps vegetation low and in pioneer stages through soil perturbation, its herbivorous diet (Miehe and Miehe 1994) and reduced vegetation covers at the top of burrows. Furthermore, the abundance and activity of herbivorous rodents are affected by vegetation as their primary food resource. Hence, they are typically more abundant in areas with higher plant productivity (Eldridge and Whitford 2014; Huntly and Reichman 1994; Zhang and Liu 2003). Further, the reduced food supply during the dry season causes GRRs to change their home range to food-rich periodic wetlands in the Bale Mountains (Šklíba et al. 2020; Vlasatá et al. 2017). Thus, selecting a vegetation index describing biomass is in accordance with the ecology and habitat

preferences of the target species and emphasizes our findings that GRR distribution can be predicted using remote sensing.

In M3, the predicted CA2 scores describing species composition were chosen as a predictor for GRR presence and absence, indicating the effect that the GRR has on species composition. For instance, the species reduces *A. abyssinica* but fosters *Salvia merjame* (Šklíba et al. 2017). In general, the vegetation and texture metrics selected for predicting the CA scores can be related to the rodent's ecological function. The selected vegetation index is sensitive to chlorophyll concentration, the reflectance of which can be related to the distribution of herbivorous species as they correlate to plant biomass (Gitelson et al. 2009; Olofsson, Tommervik, and Callaghan 2012) and, hence, available food resources (Reichman and Seabloom 2002). However, including vegetation data in the form of CA scores did not explain GRR presence as accurately as the purely remote sensing-based approach in M1, even when combined with remote sensing-based predictors. The prediction of the area of M2 and M3 only approximates to the final distribution map of M1 when the AOA layer is included, which masks areas where the prediction should not be considered.

Despite the well-known impact of GRRs on vegetation (Miehe and Miehe 1994; Sillero-Zubiri et al. 1995; Šklíba et al. 2017; Yalden 1985), the in-situ collected raw plant species composition data, surprisingly did not enhance the prediction of GRR distribution. One explanation might be that the spectral difference of plant species between areas with and without current GRR activity was not pronounced enough to be detected remotely and to be a reliable predictor for GRR distribution. In fact, the most abundant plant species in both presence and absence areas was *A. abyssinica*. The less abundant plant species differed between GRR presence and absence areas; however, their spectral signature was presumably not pronounced enough or masked by the spectral signature of the dominant plant species *A. abyssinica*. Our results demonstrate that textural metrics can reliably predict the presence and absence of the species via their impact on soil structure. However, more subtle impacts of the GRR on its biotic environment, such as the vegetation composition, could not be assessed from space. Hence, field assessments are indispensable if subtle impacts of a species on ecosystem functionality are the primary focus. Yet, we emphasize that remote sensing is a promising tool for predicting the presence of a subterranean species based on texture metrics, while field-based knowledge about plant species composition is not required to predict the distribution of the GRR. Predicting the current distribution with minimized effort is particularly relevant considering the endangerment of the species and its ecological role as ecosystem engineer.

To summarize, our aim to predict the spatial distribution of the focal subterranean animal species was best conducted with textural and vegetation indices; detailed knowledge of the vegetation composition around the mounds was not required. As such, remote sensing and machine learning approaches can facilitate spatial modeling of subterranean species that create distinctive above-ground landscape structures. In this study, we examined tools to meet the complex challenge of predicting less visible species. This could be particularly valuable for spatial modeling in remote areas and environments with low structural heterogeneity. Our approach may be applicable to other arid ecosystems, where vegetation stands are low and sparse. Here, subterranean rodents are present frequently with important implications for ecosystem processes (Contreras et al. 1993; Desmet and Cowling 1999; Kerley, Whitford, and Kay 2004; Lacey and Wieczorek 2003; Miranda et al. 2019), which is particularly critical if the ecosystems are difficult to access. Yet, further studies need to confirm if our approach is applicable for other subterranean species, for instance for the GRR's sister species T. splendens, subterranean mammals in the Tibetan and Mongolian grasslands, or other cryptic species such as social-insect colonies that create vegetation patterns like the Namibian and Australian fairy circles.

Data Availability Statement

The corresponding data set is available here:10.5281/zenodo.5704707

Acknowledgements

cooperation and kind permission to conduct fieldwork. We are grateful to Awol Asefa, Wege Abebe, Katinka Thielsen, Tiziana Li Koch, Kevin Frac, Terefe Endale, Geremew Mebratu for helping to prepare the fieldwork and this manuscript.

Supplementary material

Supplementary material to this chapter can be found in Supplementary material Chapter III.

Topographic barriers drive the pronounced genetic subdivision of a range-limited fossorial rodent

by

Victoria M. Reuber, Michael V. Westbury, Alba Rey-Iglesia, Addisu Asefa, Nina Farwig, Georg Miehe, Lars Opgenoorth, Radim Sumbera, Luise Wraase, Tilaye Wube, Eline D. Lorenzen* and Dana G. Schabo*

* These authors contributed equally to this study

ABSTRACT

Due to their limited dispersal ability, fossorial species with predominantly belowground activity usually show increased levels of population subdivision across relatively small spatial scales. This may be exacerbated in harsh mountain ecosystems, where landscape geomorphology limits species' dispersal ability and leads to small effective population sizes, making species susceptible to environmental change. The giant root-rat (*Tachyoryctes macrocephalus*) is a highly fossorial rodent confined to the afro-alpine ecosystem of the Bale Mountains in Ethiopia. Using mitochondrial and low-coverage nuclear genomes, we investigated 77 giant root-rat individuals sampled from nine localities across its whole ~1,000 km2 range. Our data revealed a distinct division into a northern and southern subpopulation, with no signs of gene flow, and higher nuclear genetic diversity in the south. Landscape genetic analyses of the mitochondrial genomes indicated that population subdivision was driven by steep slopes and elevation differences of up to 500 m across escarpments separating the north and south, potentially reinforced by glaciation of the south during the Late Pleistocene (~42,000 to 16,000 years ago). Despite the pronounced subdivision observed at the range-wide scale, weak geographic structuring of sampling localities within subpopulations indicated gene flow across distances of at least 16 km, suggesting aboveground dispersal and high mobility for relatively long distances. Our study highlights how topographic barriers can lead to the genetic subdivision of fossorial species, despite their potential to maintain gene flow at the local scale. These factors can reduce genetic variability, which should be considered when developing conservation strategies.

4.1. Introduction

The genetic subdivision and diversity of a species across space are determined by the combined effects of the environment and the ability of a species to disperse (Berthier et al. 2005; Manel et al. 2012; Quaglietta et al. 2013; Ruiz-Gonzalez et al. 2015). Dispersal ability can be limited by topographic barriers such as mountains or steep slopes, and by species-specific abiotic or biotic requirements, such as temperature or food availability, which may prevent the continuous distribution of individuals and reduce gene flow (Boulangeat et al. 2012; Cunningham et al. 2016; Cushman and Lewis 2010; Sexton et al. 2009). As a consequence, natural selection, genetic drift, and inbreeding in smaller isolated populations may lead to heterogeneous patterns of genetic variability and population subdivision (Wright 1969). Species with low dispersal

ability such as those with low mobility and a burrowing lifestyle, are especially prone to these processes.

Fossorial rodents engineer elaborate underground burrow systems. In many species, activities including searching for mates, reproduction, and foraging, occur below-ground (Nevo 1999). Therefore, these rodents are often restricted to specific soil types and available food resources (Begall et al., 2007; Nevo, 1999; Reichman, 1975). Apart from these notable constraints in habitat and resource availability, the low mobility of fossorial species leads to small home ranges and limited dispersal (Harestad and Bunnel 1979; Tucker et al. 2014). As a result, fossorial rodents often have a localised and patchy distribution. Moreover, in the case of solitary species, mature individuals meet mainly during the mating season, which further limits conspecific encounters. Combined, these characteristics lead to small and isolated subpopulations, with low genetic variation and genetic differentiation across relatively small scales and rapid inter-population divergence, as shown for instance in several tuco-tuco species (*Ctenomys sp.,*) and common voles *(Microtus arvalis)* (Mapelli et al. 2012; Mirol et al. 2010; Nevo 1999; Schweizer, Excoffier, and Heckel 2007).

These genetic and ecological patterns may be exacerbated in harsh environments, such as in mountain ecosystems, where the geomorphology of the landscape and the availability of suitable habitats, limits dispersal opportunities and leads to restricted species distribution ranges and small effective population sizes (Badgley et al. 2017; Brown 2001; Gaston 2003; Rahbek, Borregaard, Colwell, et al. 2019). As a result, mountain regions have been recognized as hotspots for genetic differentiation and speciation, contributing disproportionately to terrestrial biodiversity, at least in the tropics (Rahbek, Borregaard, Antonelli, et al. 2019; Rahbek, Borregaard, Colwell, et al. 2019; Sandel et al. 2011). However, species with limited distribution ranges and small population size, such as those found in mountain ecosystems, are at particular risk of extinction (Davies et al. 2009; Gaston 2003). Small populations tend to exhibit accumulations of deleterious mutations, low intraspecific diversity, or loss of adaptive potential, making them susceptible to environmental change and habitat shifts (Hoffmann, Sgrò, and Kristensen 2017; Lande 1988; Willi, Van Buskirk, and Hoffmann 2006). Additionally, upslope habitat shifts are limited for mountain species, especially for those occurring near mountaintops (Parmesan 2006; Wilson and Gutiérres 2016). Mountain ecosystems face increasing threats from land use and climate change-induced habitat shifts. Therefore, it is imperative to understand the impact of species-environment interactions on genetic diversity to effectively establish conservation targets, however, thorough understanding

is still lacking. Studying species in mountain ecosystems remains a challenge, especially for fossorial rodents, due to the difficulty of accessing remote areas and the inherent challenges in assessing these species in their natural habitats.

Our study addresses this knowledge gap by elucidating how landscape features drive the genetic subdivision and diversity of the giant root-rat (*Tachyoryctes macrocephalus*), a fossorial rodent endemic to the afro-alpine and afro-montane ecosystem of the Bale Mountains in southeast Ethiopia (Figure 1). The species has a limited distribution range of ~1,000 km^2 across the Bale Mountains massif and is found between 3,000 and 4,150 m above sea level (a.s.l.) (Sillero-Zubiri et al. 1995; Yalden and Largen 1992). Giant root-rats have specific habitat requirements, occurring in grasslands in areas with good soil depth, especially along wetland shores and flooded valleys (Sillero-Zubiri et al. 1995; Šklíba et al. 2017). Grassland in river valleys that spread through shrubs and forest zones into lower elevations, allow the species to expand down to about 3,000 m a.s.l. (Yalden 1985). Their relatively small home ranges (about 100 m^2) can shift throughout the year depending on food availability (Šklíba et al. 2020). Giant root-rats are significant ecosystem engineers creating large underground burrow systems, in which they live solitarily. Through their combined effect of soil perturbation and herbivory, they alter nutrient availability, soil texture and moisture, and create their own habitat and that for other plant and animal species (Asefa et al. 2022; Miehe and Miehe 1994; Šklíba et al. 2017; Yalden 1985). By using below-ground burrows, the species circumvents the harsh environmental conditions of the mountain ecosystem, which include strong winds and temperatures below 0 C°, and limits the risk of being preyed upon by its main predator the Ethiopian wolf (*Canis simensis*) (Sillero-Zubiri and Gottelli 1995; Šumbera et al. 2020; Vlasatá et al. 2017; Yalden 1985). Taken together, the species' key role as ecosystem engineer combined with its limited range in a changing mountain ecosystem, makes it an ideal model organism for investigating the connection between genetic patterns and landscape features, so as to preserve mountain biodiversity and ensure ecosystem functioning.

In the present study, we analysed the spatial genetic subdivision and diversity in the giant root-rat across its distribution range. To achieve this, we analysed both mitochondrial genomes (mitogenomes) and nuclear genomes, and further utilized mitogenomes to investigate the relationship between genetic differentiation and landscape features. We generated complete mitogenomes and low-coverage nuclear genomes from 77 individuals collected across nine sampling localities in the Bale Mountains (Figure 1). We applied two different landscape genetic approaches to evaluate how mitochondrial gene flow of the species is impacted by

geographic distance, by vegetation and soil moisture (used as proxies for food and soil availability), and by slope and elevation (used as proxies for topographic barriers). Due to the predominantly below-ground activity and patchy distribution of the giant root-rat, we hypothesise strong genetic subdivision across small spatial scales. Owing to the pronounced heterogeneity of the environment in the Bale Mountains, we hypothesise that genetic structuring is driven by habitat availability, and by topographic structures across the species' range.

4.2. Material and methods

4.2.1 Study area

The Bale Mountains in southeast Ethiopia (6º29'N – 7º10'N and 39º28'E – 39º57') represent Africa's largest afro-alpine ecosystem, comprising ~8 % of the continent's area above 3,000 metres above sea level (m a.s.l) (Groos et al., 2021, Figure 1A-C). In order to protect the unique afro-montane and afro-alpine ecosystem of the Bale Mountains, the area above ~3,200 m a.s.l. became a national park in 1970. The Bale Mountains are characterised by two rainy seasons and one dry season per year, with short rains from March to June, long rains from July to October, and a dry season from November to February. The vegetation of the Bale Mountains shows an elevational zonation from moist montane forest (~1,500 - 3,500 m a.s.l.) over ericaceous shrubland and dwarf forest (~3,500 - 4,000 m a.s.l.) to afro-alpine vegetation with open grassland and *Erica* outposts (above 4,000 m a.s.l.). Dwarf-scrub vegetation, such as *Helichrysum* associated with *Lobelia*, is the main plant formation in the afro-alpine vegetation but does not cover the whole area, leaving open spaces for herbaceous plants like *Senecio*, *Alchemilla* or *Salvia* (Miehe and Miehe 1994; Tallents and Macdonald 2011).

Characteristic of the Bale Mountains National Park is the afro-alpine Sanetti Plateau, which spans elevations from approximately 3,800 m a.s.l, to 4,377 m a.s.l. at the peak of the mountain Tullu Dimtu (Figure 1C). Large parts of the plateau were glaciated during the Late Pleistocene, between 42,000 to 16,000 years ago (Groos et al. 2021). The plateau is bounded by several outlet valleys in the north and the east with slopes that are covered by dense, shrubby *Erica* vegetation and by congealed lava flows at its northwestern margins. These topographic structures distinguish the plateau from the northern region of the national park, which is ~300 - 500 m lower in elevation and comprises broad valleys and plains with afro-alpine vegetation (Miehe and Miehe 1994). In comparison to the plateau, the north has higher moisture availability and milder temperatures.

4.2.2 Sampling

We collected tissue samples from 77 live giant root-rat individuals at nine localities across the Bale Mountains National Park, covering the distribution range of the species (Figure 1C, supporting information Table S1). The sampling localities were distributed across the two topographically distinct regions in the national park, in the north (localities N1-N3) and in the south (localities S1-S6). The southern localities are scattered across the centre and south of the Sanetti Plateau. Localities sampled in the north of the plateau lie at a lower elevation (~3,500 m a.s.l) than localities sampled in the south (~3800 - 4000 m a.s.l.). Sampling localities between regions were separated by 15.3 to 28.3 km, and localities within regions were separated by 2.6 km to 16.0 km.

We captured 7-9 giant root-rat individuals per locality (except locality S4 with n=1). The samples were collected in January and February in two consecutive years (2020, 2021) under the permit of the Ethiopian Wildlife Conservation Authority. Individuals were caught with snare traps that were monitored by the capture team at all times to guarantee no harm to the animals. A ~0.5 cm^2 piece of skin from the hind leg was cut with sterilised scissors and stored in 96% ethanol or DNAgard® for blood and tissue (Biomatrica, Inc.) for genomic analyses. After sterilising the wound, the animals were immediately released back into their burrow systems.
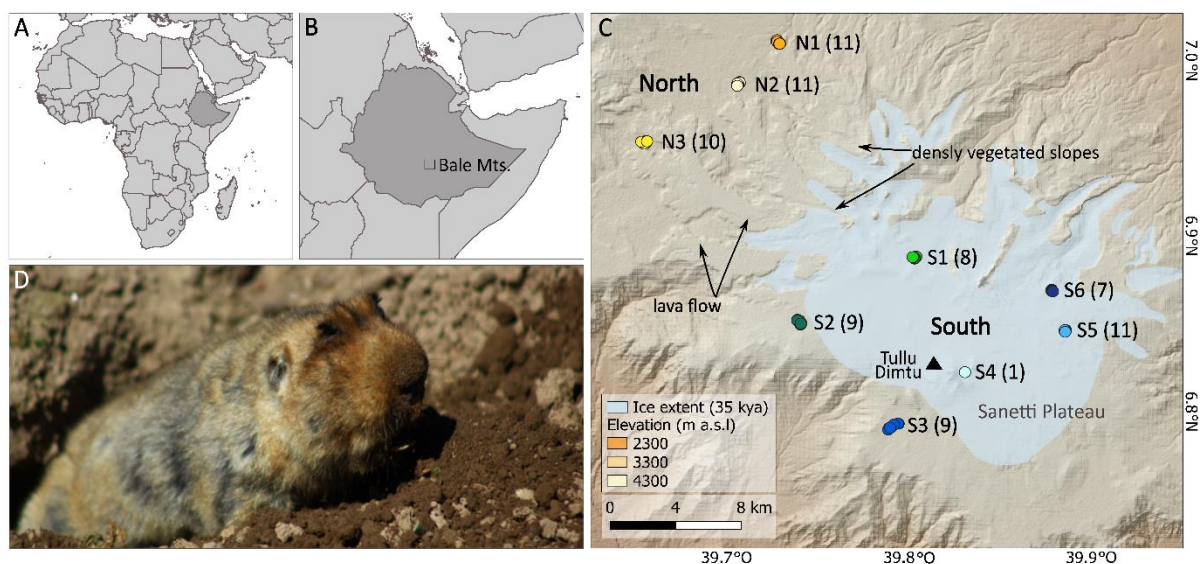
Figure 1: Sampling localities of giant root-rats within Bale Mountains National Park, Ethiopia. A) Map of Africa showing Ethiopia in dark grey; B) Map of Ethiopia indicating location of Bale Mountains National Park, C) Map of the nine sampling localities from two distinct geographic regions. The north (~3,500 m above sea level [m a.s.l]), and south (~3,800-4,000 m a.s.l, Sanetti Plateau) are separated by steep slopes covered with dense Erica thickets and congealed lava flows. Sample size of each locality is indicated in brackets. Tullu Dimtu is the highest peak in the Bale Mountain National Park at 4,377 m a.s.l., and is indicated with a filled triangle. Region with light blue shading indicates the glacial extent within Bale Mountains National Park ~35±7.1 thousand years ago (kya) (Groos et al. 2021; Ossendorf et al. 2019); D) Burrowing giant root-rat, photography by V. Reuber.

4.2.3 Laboratory analyses

We extracted DNA from the tissue samples using the Qiagen DNeasy® Blood and Tissue Kit following the manufacturer's protocol (Qiagen Ltd.). 60 of the samples were processed in-house in the modern DNA labs at Globe Institute, University of Copenhagen. The DNA concentration of the extracts was measured using QubitTM dsDNA HS (Invitrogen). After quantification, we diluted the extracts to a concentration of 6 ng/µl in a total volume of 50 µl. DNA was sheared to ~400 base pair (bp) fragment lengths using the Covaris M220 ultrasonicator. We built DNA fragments into an Illumina library following the protocol from Carøe et al., (2018) and double-indexed them using AmpliTaq Gold Polymerase (ThermoFisher) during the indexing PCR step. Index PCR reactions were performed in 100 µl, using 1x PCR buffer, 2.5 mM of MgCl (25 mM), 0.2 mM of dNTPs (25 mM), 0.2 µM of index primer mix (10 µM), and 0.1 U/ µl of polymerase (5 U/µl). PCR cycling conditions were 95 °C for 10 min; 10 - 18 cycles of 95 °C for 30 s, 50 °C for 30 s and 72 °C for 1 min followed by 72 °C for 5 min. The number of cycles for the index PCR was determined from qPCR analysis. Post-amplification, libraries were purified using SPRI beads as in Carøe et al., (2018). The purified indexed libraries were quantified on a QubitTM dsDNA HS (Invitrogen), and quality-checked on either an Agilent 2100 Bioanalyser or an Agilent Fragment AnalyzerTM. Libraries were pooled equimolarly and sequenced on an Illumina NovaSeq 6000 using paired-end (PE) 150 bp technology (Novogene Europe, http://en.novogene.com).

For the remaining 17 samples, DNA was extracted and processed to libraries by Novogene and sequenced on a NovaSeq 6000, using paired end 150 bp technology.

4.2.4 Data generation of mitochondrial and nuclear DNA

We trimmed adapters and removed reads shorter than 30 bp for each individual using skewer v0.2.2. (Jiang et al. 2014). We merged overlapping paired-end reads using FLASHv1.2v11 (Magoč and Salzberg 2011) with default parameters. We mapped both merged and unmerged reads to the hoary bamboo rat (*Rhizomys pruinosus*) nuclear genome (Genbank accession: VZQC00000000.1; Guo et al. 2021) which is the nearest relative of the giant root-rat with an available genome, combined with the giant root-rat mitogenome (Genbank accession: MW751806; Reuber et al., 2021). We used BWA v0.7.15 (Li and Durbin 2009) utilising the mem algorithm and default parameters. We parsed the alignment files, and removed duplicates and reads of mapping quality score <30 using SAMtools v1.6 (Li et al. 2009). We built consensus mitogenomes from each individual using a majority rules approach (-doFasta 2) in

ANGSD v0.921 (Korneliussen, Albrechtsen, and Nielsen 2014) only considering bases with a base quality score greater than 30 (-minq 30), reads with a mapping quality score greater than 30 (-minmapq 30), and sites with at least 10x coverage (-minInddepth 10). The mitogenomes are available under GenBank accessions OQ207545 - OQ207620.

4.2.5 Genetic subdivision

4.2.5.1 Mitochondrial DNA analysis

Haplotype network
The mitogenomes were aligned with Mafft v.7.392 (Katoh and Standley 2013). We constructed a median-joining haplotype network to investigate the relationships among the 77 mitogenomes using the software PopArt v.1.7 (Leigh and Bryant 2015).

Phylogenetic analysis
We constructed a Bayesian phylogeny with the 48 mitogenome haplotypes identified in the network analyses, using MrBayes v.3.2.7a (Ronquist and Huelsenbeck 2003). We used the GTR + I + G model of evolution, which was defined as the best model with PartitionFinder v. 2.1.1 (Lanfear et al. 2017) prior to the analysis. The MCMC algorithm was run twice with four chains of 10 million generations, sampled every 1,000 generations and with a 10 % burn-in. The trees were combined following the majority-rule consensus approach, to assess the posterior probability of each clade. The resulting tree was visualised in FigTree v.1.4.4 (http://tree.bio.ed.ac.uk/software/figtree/; supporting information Figure S1).

Fixation statistics and AMOVA
We calculated the pairwise differentiation between eight of the nine sampled localities (omitting S4 as n=1) with the F_{ST} -estimator of the software Arlequin v. 3.5.2.2 with 10,000 permutations (Excoffier and Lischer 2010); *p*-values of F_{st} estimates were adjusted using the Bonferroni correction (Rice 1989), controlling for a false-positive discovery rate (R Core Team 2021). Additionally, we conducted a hierarchical analysis of molecular variance (AMOVA), also in Arlequin, with localities grouped into their provenance in the regions north and south (Figure 1C).

4.2.5.2 Nuclear DNA analysis

We investigated population subdivision of the nuclear data using principal component analysis (PCA) and admixture proportion analysis. We generated genotype likelihoods in ANGSD (Korneliussen et al. 2014) for all individuals using the following filters and parameters: call genotype likelihoods using the GATK algorithm (-GL 2), output a beagle file (-doGlf 2), only include reads with mapping and base qualities greater than 30 (-minmapQ 30 and -minQ 30), only include reads that map to one location uniquely (-uniqueonly 1), a minimum minor allele frequency of 0.05 (-minmaf 0.05), only call a SNP if the p-value is greater than $1e^{-6}$ (-SNP_pval 1e-6), infer major and minor alleles from genotype likelihoods (-doMajorMinor 1), only include sites if at least 40 individuals are covered (-MinInd 40), remove scaffolds shorter than 100 kb (-rf), and remove secondary alignments (-remove_bads 1). To compute the PCA, we constructed a covariance matrix from the genotype likelihoods using PCAngsd v0.98 (Meisner and Albrechtsen 2018). Admixture proportions were calculated using the same genotype likelihoods with NGSadmix (Skotte, Korneliussen, and Albrechtsen 2013). We ran NGSadmix specifying K=2 and K=3. To evaluate the reliability of the NGSadmix results, we ran each *K* up to 100 times independently. If we retrieved consistent log-likelihoods from at least two independent runs, the corresponding K was considered reliable.

To estimate levels of differentiation among localities, we computed F_{ST} from a consensus haploid call file created using ANGSD (-dohaplocall 2) and the same filtering parameters as the PCA and admixture proportions above. We calculated the F_{ST} using an available python script https://github.com/simonhmartin/genomics_general/blob/master/popgenWindows.py) and specifying a window size of 1Mb, and a minimum number of sites per window as 1,000 bp.

Gene flow

The mitogenomes of two individuals (WM07 from locality S1 and GG01 from locality S6) grouped with individuals from the north in the haplotype network and phylogeny. We therefore used D-statistics (also known as ABBA/BABA, Durand et al., 2011) to test whether the results were driven by ancient gene flow between regions north and south, or by incomplete lineage sorting. We tested several topologies [[H1, H2], H3], with branch H1 being one of the two putative introgressed individuals, and branches H2 and H3 being individuals from one region north or south, or one from each region. A negative D-score illustrates a closer relationship between H1 and H3 than H2 and H3, while a positive D-score indicates that branches H2 and H3 are more closely related than H1 and H2. This setup can also be used to uncover population

subdivision, as the incorrect input topologies would lead to elevated D-scores due to more recent common ancestry, as opposed to gene flow (Westbury et al. 2018).

We performed the D-statistic tests using a random base-call approach in ANGSD (-doAbbababa 1). We implemented the same filtering approach as for the above analyses but only included scaffolds >1 megabase (Mb) in size, a block size of 1 Mb (-blocksize 1000000), and the hoary bamboo rat (*Rhizomys pruinosus*, GenBank accession VZQC00000000.1, Guo et al. 2021) as the ancestral state/outgroup (-anc). To assess the significance of our results we used a block jackknife test with the script jackKnife.R which is available with the ANGSD tool suite.

4.2.6 Diversity

Based on the mitochondrial genomes, we calculated nucleotide diversity (π) per region, and separately for eight of the nine localities using DnaSp v.6 (omitting S4 as n=1) (Rozas et al. 2003). We tested differences in nucleotide diversity between the two geographic regions, and among localities using genetic_diversity_diffs v. 1.0.3 (Alexander 2017).

The python script used to calculate nuclear F_{ST} above simultaneously computes nucleotide diversity per region and per locality. To test for significant differences in levels of nucleotide diversity between regions and between localities, we used a Welch-test (unpaired t-test), accounting for unequal variance.

4.2.7 Landscape genetic analysis

We applied two landscape genetic approaches to investigate the effects of landscape features on the observed genetic differentiation between localities based on F_{ST} estimates of the mitogenomes. We exclusively used mitogenomes due to their higher mutation rates and lack of recombination compared to nuclear genomes, which result in faster responses to environmental changes and increased resolution (Avise 2000; Birky, Maruyama, and Fuerst 1983). The limited number of sampling localities prevented us from analysing the north and south regions separately.

We selected four environmental variables (vegetation, soil moisture, slope, elevation), which were based on satellite-based remote sensing data, as predictors for genetic differentiation of the giant root-rat. For vegetation and soil moisture, we used observations from satellite Sentinel-2, captured on an almost cloud-free day on December 15, 2017, and derived from the

USGS Earth Explorer repository. We used the red, green, blue, red and near infrared bands of from the Sentinel-2 observations and with those computed raster layers of the Normalised Differentiation Vegetation Index (vegetation index) and Land-Surface Water Index (soil moisture index, for details see Wraase et al., 2022) using the Rtoolbox, as proxies for food and soil availability for giant root-rats (Sillero-Zubiri et al. 1995; Šklíba et al. 2017; Yaba et al. 2011; Yalden and Largen 1992). To determine whether topographic structures act as barriers for burrowing giant root-rats, we included the variables slope and elevation in our analysis. Raster layers for slope and elevation were obtained from a Shuttle-Radar-Topography-Mission digital elevation model from the USGS Earth explorer (www.earthexplorer.usgs.gov). The generated raster layers of all four environmental variables had a 30 x 30 m resolution and were cropped on extent 567910.0, 605990.0, 738620.0, 778750.0. Our analyses were conducted in R environment version 4.2.1 (R Core Team 2021).

Partial Mantel tests

Using partial Mantel tests, we analysed if the genetic differentiation between eight of the nine sampling localities (omitting S4 as n=1) was correlated with geographic distance, vegetation, soil moisture, slope and elevation (see above). Therefore, we constructed distance matrices. The genetic distance matrix was generated by linearizing the pairwise genetic differentiation estimates between localities, i.e the F_{ST} -estimates ($[F_{ST}/(1- F_{ST})]$; Rousset 1997). The geographic distance matrix was calculated in Euclidean distances and log-transformed to linearize the relationship with genetic distance. For each environmental variable, we extracted their values from the computed raster layers at the coordinates of the sampling localities and therewith generated the environmental distance matrices. We then applied a pairwise reciprocal causal modelling approach. Reciprocal causal modelling compares partial Mantel tests of a focal environmental model, removing the influence of a competing, alternative model (Cushman et al. 2006; Cushman and Landguth 2010). In this approach, the correlation between one environmental distance matrix and genetic distance is controlled by a second matrix (e.g. focal model: genetic distance~geographic distance|elevation distance) and in a next step, both environmental distance matrices are interchanged (e.g. alternative model: genetic distance~elevation distance|geographic distance). In that way, we were able to account for high correlation among matrices (Cushman et al. 2006; Cushman and Landguth 2010). To assess which of the two models explains genetic distance better, the relative support of the focal and alternative model was calculated by estimating the difference between the correlation values of the two models. If the difference in correlation factors was positive, we assumed that the focal

hypothesis was correct. The partial Mantel tests were performed with 9,999 permutations in the vegan R package v.2.6-4. (Oksanen et al. 2020).

Raster layer optimization framework to generate resistance surfaces

We used a raster layer optimization framework developed by Peterman et al. (Peterman 2018; Peterman et al. 2014), to further identify landscape features that explain mitochondrial genetic differentiation, using the R package ResistanceGA (Peterman 2018). In this framework, the raster layers of the environmental variables (see above) were transformed into resistance surfaces, with the ResistanceGA package utilising a genetic algorithm from the GA R package (Scrucca 2013). A resistance surface is a spatial layer that assigns values to each grid in the raster layer of the selected environmental variable. Those values are used to estimate the cost of dispersal and mirror to what extent the selected variable hinders or facilitates the connectivity of a species between two localities (pairwise resistance distances). Thereby, there are no *a priori* assumptions about the relationship between the environmental variable and the species' dispersal characteristics. The genetic algorithm in the optimization framework is used to maximise the relationship between the resistance distances of each raster layer, and the pairwise genetic differentiation (F_{ST}) between localities. The process of generating resistance surfaces is repeated, and in every iteration, the resistance distances are fitted against the genetic distances in a mixed effect model, until the objective function, the AIC (Akaike's information criterion; Akaike, 1974) of the mixed effect model does not improve further. The mixed-effect models are conducted using a maximum likelihood population effect parameterization to account for the non-independence of the predictor variables and to account for spatial autocorrelation (Clarke, Rothery, and Raybould 2002; Peterman et al. 2014; Shirk, Landguth, and Cushman 2018). This iterative process works towards identifying the best-fit landscape resistance surface. In our optimization framework, we used a single surface optimization approach, where the resistance surfaces of the raster layers of each selected environmental variable (i.e. vegetation index, soil moisture index, slope and elevation) were optimised individually, using eight transformation functions (Monomolecular and Ricker functions) and the default parameters (Peterman 2018). In this step, the pairwise resistance distance between localities was estimated by assuming that individuals can use several paths to disperse. Resistance distances were generated with the *costDist* function implemented in the ResistanceGA package and movements between localities were allowed in eight directions during resistance distance calculation. Because Euclidean distance is incorporated in the resistance distances, it was not included as an additional variable. In the optimization process, the mixed-effect models were

calculated, fitting the pairwise genetic differentiation as a response against the resistance distances as single fixed effects, using the AIC for model evaluation and including sampling localities as a random effect to account for spatial autocorrelation. We did two independent optimization runs to confirm convergence across runs. The run containing the mixed-model with the greatest log-likelihood value is presented in the results section (Table 1). After the optimization, we used bootstrap model selection with 75% of the samples and 10,000 iterations. The bootstrap model selection refits the mixed-effect models and calculates fit statistics for each model, showing the average AIC and percentage each resistance surface has been selected as a top rank model across all bootstrap iterations (Peterman 2018).

4.3. Results

We generated complete mitogenomes from all 77 giant root-rat individuals, with a depth of coverage ranging between 24.94x and 383.22x, and a length of 16,646 bp. For the nuclear genomes, we obtained coverages ranging from 0.12x to 0.77x (supporting information Table S2).
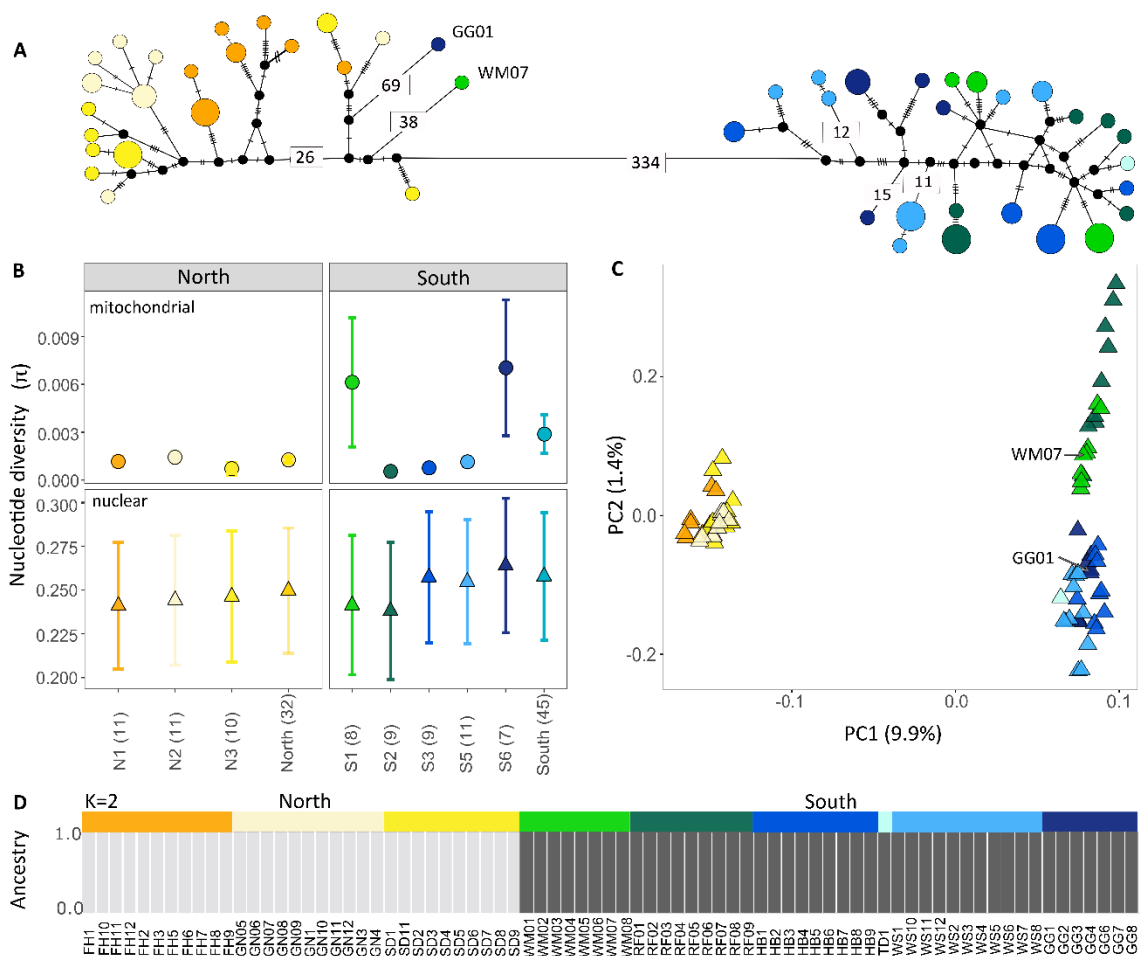
Figure 2: Patterns of genetic diversity and subdivision of giant root-rats across their range. A) Network of the 48 mitochondrial haplotypes present among the 77 sampled individuals. Each circle represents a haplotype, and the relative size of each circle represents haplotype frequency. Numbers on branches show the number of segregating sites between haplotypes for >10. Black dots indicate intermediate haplotypes not present in the data. Distances between haplotypes are not to scale. B) Diversity levels within the sampled localities and subpopulations based on mitogenomes (circles) and nuclear data (triangles). Sample sizes are shown in brackets. C) PCA based on 77 low-coverage nuclear genomes. The percentage of the diversity of each principal component is shown in brackets. D) Ancestry proportions based on the nuclear data for K=2, with each vertical bar representing an individual.

4.3.1 Genomic analysis

Haplotype network and phylogeny

Our 77 sampled giant root-rat individuals comprised 48 haplotypes, with no haplotypes shared among localities (Figure 2A). The haplotype network and phylogeny of the mitogenomes revealed two geographically separated and well-supported groups; one group comprising all samples collected in the north, with the inclusion of individuals WM07 and GG01 from the south, and one group comprising all other samples from the south (supporting information Figure S1). In the network, we identified 574 segregating sites among individuals, and the northern and southern haplogroups were separated by 334 segregating sites (Figure 2A). The north contained 21 haplotypes (32 individuals) and the south contained 27 haplotypes (45 individuals). Within the north, we identified two distinct, well-supported genetic clades, N_A and N_B (supporting information Figure S1). Clade N_A comprised six individuals (five haplotypes) from localities N1-N3. Individual GG01 from locality S6 was basal to the clade. Clade N_B comprised the remaining individuals from the north with individual WM07 from the south at basal position. We did not identify any spatial genetic structuring in the south.

The AMOVA yielded a high level of between-region variation when the eight localities (omitting S4 with n=1) were grouped into north and south (89.50 %, $p < 0.01$). Within each region, the variation was higher within localities (9.27 %) than among localities (1.24 %).

Principal component analysis and admixture proportions

We identified two main groups in the nuclear data, in agreement with the mitochondrial findings (Figure 2). In the PCA, individuals from the north separated from the individuals from the south, with almost 10% of the variation explained on the first principal component. The southern group showed a slight separation on the second component, with the more central localities S1 and S2 segregating from the localities further southeast, with 1.4 % variation explained (Figure 2C). The division of the data into north and south was also evident in the admixture analysis of

K = 2 (Figure 2D). The admixture analysis did not converge with K = 3, suggesting K = 3 did not reliably fit the data.

Gene flow

To investigate the origin of the mitochondrial lineages, present in individuals WW07 and GG01, which were more closely related to the northern haplogroup than the south (Figure 2A), we tested for ancient gene flow using the nuclear data. Using the topology [[WM07, south], north], we found most comparisons to have a D-score around 0 and a Z-score<|3|, indicating that WM07 and all individuals from the south were equally related to the northern individuals (Figure 3). We found positive D-scores (Z-score>3) when using the topology [[WM07, north], north], demonstrating a closer relationship between individuals from the north with each other than with WM07, which agrees with their more recent common ancestry and the basal position of WM07 in the phylogenetic tree (supporting information Figure S1). We found qualitatively the same results when we investigated the relationship of GG01 (sampled in locality S6) with individuals from the north and south (Figure 3). Hence our analysis did not support that the mitochondrial lineages in WM07 and GG01 were the result of recent gene flow between north and south.
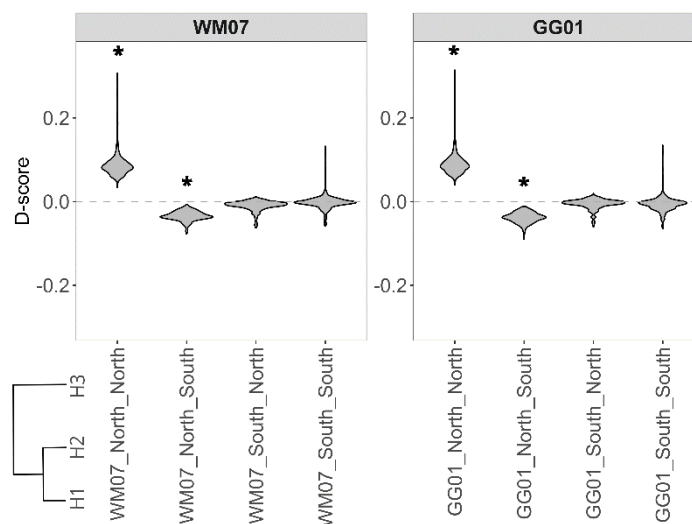
Figure 3: Analysis of signals of gene flow between individuals WM07 from locality S1 and GG01 from locality S6 and their source group in the south, using D-statistics. Negative D-scores suggest gene flow or recent common ancestry between H1 and H3 relative to H2 and H3, while positive D-scores suggest gene flow or recent common ancestry between H2 and H2 relative to H1 and H3. Statistical significance is indicated by asterisks (*) next to scores, when |Z| greater than 3 (supporting information Figure S2), determined by a one-sample Wilcoxon signed rank test.

Genetic differentiation among localities

Investigating pairwise genetic differentiation between localities, we found that F_{ST} - estimates were higher between regions than within regions, at both the mitogenome and nuclear level (Figure 4). For the mitogenomes, pairwise differences between localities of different regions ranged from 0.82 to 0.97 and were much higher than within regions, where values ranged from 0.09 to 0.29.

For the nuclear data, pairwise F_{ST} - estimates between localities from different regions ranged from 0.04 to 0.06 and were higher than values between localities within regions, which ranged from 0.01 to 0.02 (Figure 4).
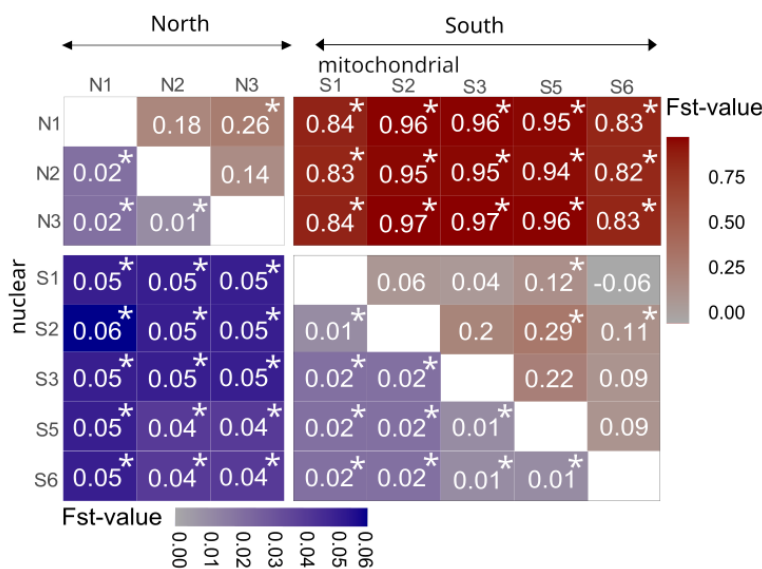
Figure 4: **Levels of genetic differentiation between the sampled giant root-rat localities from the north and south of Bale Mountains National Park**. Mitochondrial (red, above diagonal) and nuclear (blue, below diagonal) F_{ST}-estimates. * in cells indicates significant differences (*p*-values < 0.05), derived by permuting haplotypes between localities for mitochondrial data and by applying a one-sample t-test on F_{ST} -values for the nuclear data.

Diversity

We estimated levels of diversity for each region, and for each locality (omitting S4 as n=1). For the mitogenomes, diversity in the south ($\pi = 0.003 \pm 0.0002$) was significantly higher than in the north ($\pi = 0.001 \pm 0.001$, p < 0.05; Figure 2B), which reflected the presence of the divergent mitochondrial lineages in individuals WM07 and GG01 from localities S1 and S6 (Figure 2A). Thus, this was also apparent in localities S1 and S6 having the highest diversity levels, with S6 showing significantly differentiated levels of diversity (p < 0.05) and S1 showing marginal significant differentiation (p > 0.05 < 0.1, supporting information Table S3) to the remaining localities in the south.

Based on the nuclear data, we also observed significantly higher diversity in the south (π = 0.257 ± 0.0364) than in the north (π = 0.249 ± 0.0357, $p < 0.05$; Figure 2B). Among localities in the south, the two central localities S1 and S2 had lower diversity levels than the localities sampled further to the southeast (S3, S5, S6). All localities had significantly differentiated levels of diversity ($p < 0.05$, supporting information Table S3).

4.3.2 Landscape genetics

We used a reciprocal causal modelling approach with partial Mantel tests to relate genetic differentiation to the environmental distance matrices of the selected variables (vegetation index, soil moisture index, slope and elevation). Analysing levels of differentiation estimated for each region we found that elevation was the strongest model. Elevation was significantly related to genetic differentiation in all partial Mantel tests, regardless of the second environmental distance matrix controlling elevation (supporting information Table S4 A). Further, elevation showed the strongest relative support; all relative correlation values were positive, after the effect of the other environmental models were removed (supporting information Table S4 B). Geographic distance showed a significant relation with genetic differentiation when controlled by vegetation index, soil moisture index or slope, but was non-significant and the relative correlation value was negative, when controlled by elevation. We could not find significant effects of vegetation, soil moisture or slope on genetic differentiation; all variables had non-significant Mantel correlation values, showing the least support in the reciprocal causal modelling matrix (supporting information Table S4).

The raster layer optimization approach revealed that slope and elevation were the best-fitting models for explaining genetic differentiation. Slope was selected as top model in 71%, and elevation in 29% of the times across 10,000 bootstrap iterations (Table 1). The average weight from the bootstrap analyses supported geographic distance as a driver for genetic differentiation, while the parameters rank, AIC, maximum likelihood and R^2 suggested slope and elevation as the best models (Table 1). The the response curve of the optimised resistance surface showed that the resistance costs increased with increasing slope (supporting information Figure S3 C). As in the partial Mantel tests, we could not identify a contribution of the vegetation index or soil moisture index to genetic differentiation (Table 1).

Table 1: Model selection results for linear mixed-effect models, testing the effect of resistance distances (dispersal costs based on environmental condition) on levels of mitochondrial genetic differentiation (F_{ST}) in the giant root-rat. The parameters were calculated based on 10,000 bootstrap iterations using a random resampling of 75% of the sampled populations. Frequency top-model percentage, higher average weight and log-likelihood (LL), and lower average rank indicate the best supported models.

Resistance distance matrix	Average AIC	Average R^2m	Average LL	Average weight	Average rank	Frequency top model (%)
Slope	-16.61	0.92	12.31	4.8E-05	1.36	70.87
Elevation	-10.29	0.86	9.15	0.004	2.88	29.13
Vegetation	-7.16	0.78	7.58	4.0E-07	3.19	0
Soil moisture	-6.26	0.78	7.13	1.2E-06	3.57	0
Distance	-4.20	0.65	4.10	0.990	4.00	0

4.4. Discussion

Using complete mitochondrial genomes and low-coverage nuclear genomes from 77 giant root-rat individuals, we uncovered a clear subdivision of localities in the north and the south of the species range in the Bale Mountains, Ethiopia. Landscape genetic analysis identified topographic barriers such as the steep slopes and elevation differences between the two regions as the main drivers of population subdivision. Within regions, we did not identify any clear spatial structuring, suggesting a high level of gene flow when topographic barriers are absent.

Genetic subdivision between regions

The significant north and south geographic subdivision in the mitochondrial and nuclear genomes, was evidenced, for instance, by a high number of substitutions separating the divergent mitochondrial lineages present in each region, or by the nuclear PCA analysis (Figure 2, supporting information Figure S1). However, two giant root-rat individuals sampled in the south were mitochondrially more closely related to their northern counterparts than their source region, which may indicate ancient gene flow. Despite their closer relationship, both had a large number of substitutions distinguishing them from the rest of the northern individuals, suggesting that ancestral mitochondrial lineages may be retained in those two individuals that are also present in the north - a remnant of their shared evolutionary history. The phylogeny indicated these two southern individuals as basal to each of two distinct haplogroups found in the north, suggesting the lineages were derived from two distinct divergence events. Ancient lineage retention in the south was supported by our nuclear analysis, which found no evidence of recent or past gene flow between north and south (Figures 2D, 3).

The presence of genetically distinct subpopulations may be attributed to long-lasting extrinsic barriers, which prevent genetic exchange between them (Avise 2000; Bryja et al. 2010). Slope and elevation were identified as the primary drivers of genetic differentiation in our landscape analysis, and in combination they presumably cause the genetic subdivision between regions (Table 1, supporting information Table S4), similar to what has been observed in other fossorial rodents such as the Brazilian tuco tuco of the dunes (*Ctenomys flamarioni*), or the common water vole (*Arvicola terrestris*) (Berthier et al. 2005; Fernández-Stolz, Stolz, and De Freitas 2007). The south comprises the Sanetti Plateau, which is ~300 – 500 m higher in altitude than the northern region (Figure 1C) and the plateau margins northwards are characterised by broad valleys with steep slopes covered by dense *Erica* thickets. In addition to the slopes which themselves act as a barrier, the *Erica* thickets may further limit the dispersal of the species (Miehe and Miehe 1994; Yalden 1985). Giant root-rats are adapted to open grasslands with low vegetation and avoid dense shrubs such as *Erica*, likely due to the difficulties of burrowing in woody ground and the absence of food-plants. Additionally, the plateau is bounded by congealed lava flows of unknown age to the northwest. These barriers to dispersal and the fossorial lifestyle of the giant root-rat limiting the species' ability to traverse pronounced topographic structures, presumably caused the strong genetic subdivision of the species. Our landscape genetic result is in agreement with recent satellite-based mapping of the giant-root rat's distribution, which found that the texture of the landscape is the most critical factor in explaining the species' range (Wraase et al. 2022).

In addition to slope and elevation, the pronounced subdivision observed in giant root-rats may also have been reinforced by glacial extents during the Late Pleistocene. The Bale Mountains are currently ice-free, but the Sanetti Plateau, the south region, was glaciated between ~42,000 to 16,000 years ago (kya) (Figure 1C; Groos et al. 2021; Ossendorf et al. 2019). Except for this last glacial extent, exposure ages of moraines in the valleys in the northwestern part of the plateau (up to ~100 kya), and stone stripes close the mountain Tullu Dimtu (up to ~360 kya) could be interpreted in favour of earlier glacial periods (Groos et al. 2021). Possibly, giant root-rat individuals in the south were pushed towards the outer margins of the plateau by the glaciers, which increased the separation to the individuals in the north. As the glaciers retreated, colonisation of the central plateau from a more southern Late Pleistocene refugium may explain the significantly lower diversity in the central localities (S1 and S2) in comparison to the south eastern ones (S3, S5, S6, supporting information Table S3). This would be in agreement with the often-proposed hypothesis that populations of mammals exhibit reduced genetic diversity on recently deglaciated land (e.g. Hewitt, 1996, 2004). The glacial extent in the north and

northwestern valleys of the plateau margins persisted until ~16,000 years ago, while the ice shield on the plateau around Tullu Dimtu was smaller in extent already ~20,000 years ago (Groos et al. 2021).

Although vegetation and soil moisture were previously identified as essential factors influencing the local abundance of giant root-rats (Asefa et al. 2022; Šklíba et al. 2017), our study did not indicate any effect on genetic differentiation (Table 1), suggesting these factors play less of a role in hindering gene flow at the range-wide scale. However, the spatially coarse vegetation and soil moisture indices used in our analysis may not fully capture the highly specific food and soil requirements of the giant root-rat. Their primary food resource is *Alchemilla* (Yaba et al. 2011). The vegetation index, which is based on remotely-derived satellite data, may not distinguish its spectral signal from other non-preferred plants (Wraase et al. 2022). Additionally, the giant root-rat requires soil layers of approximately 50 cm in depth to engineer burrow systems and for thermoregulation (Sillero-Zubiri et al. 1995; Šumbera et al. 2020), and while soil depth and moisture are likely correlated (deeper soil can store more water, Tromp-van Meerveld and McDonnell 2006), soil moisture as a proxy for soil availability may not capture areas of sufficient soil depth. The vegetation and soil moisture indices were derived from a Sentinel-2 scene captured in December, just after the rainy season. During this period, vegetation is still lush and green and the soil is moist across large parts in the Bale Mountains National Park, and this thus might not fully reveal the specific habitat requirements (related to its preference for moorlands and wet grasslands with good soil depth) of the giant root-rat at that time of the year.

Gene flow within regions

We observed a lack of structuring among localities within both regions. Levels of differentiation were low, with nuclear F_{ST} - estimates of 0.01-0.02 within regions, which is considered as weak differentiation for nuclear data (Figure 4; Weir and Cockerham 1984; Wright 1978). This indicates high level of dispersal and gene flow across distances of at least 16 km, which was the maximum distance between two sampling localities within regions. The ability of giant root-rats to disperse across such relatively large distances was in contrast to our expectations; giant root-rats are fossorial, solitary and territorial. We had expected this, in combination with the heterogeneity in soil structure and food availability across its range, would lead to stronger genetic structuring at small spatial scales, similar to what has been observed in other fossorial rodents (Mapelli et al. 2012; Schweizer et al. 2007). Although direct observations for this are

71

still lacking, the limited substructuring within regions and the large dispersal distances suggest that giant root-rats can disperse aboveground and for relatively large distances. In fact, giant root-rats show morphological adaptations to surface activity, in that their eyes are situated dorsally on the head, which allows them to detect predators in open habitats (Yalden 1985). In support of our findings, radio tracking has evidenced the dispersal of a giant root-rat individual over a distance of up to 270 m within a span of two days; the tracked individual traversed across damp soil, suggesting it did not disperse underground (Šklíba et al. 2020). Aboveground dispersal has also been documented in other fossorial, solitary rodent species, such as blind mole-rats (*Spalax microphthalmus*; Zagorodniuk et al. 2018) and Tibetian plateau zokors (*Eospalax fontanieri*; Chu et al. 2021). Even in strictly subterranean African mole-rats, long-distance dispersal is not precluded (*Fukomys damarensis*, Bathyergidae; Finn et al. 2022). For giant root-rats, aboveground dispersal attempts could be triggered by decreasing food supply, the absence of sexual partners, or the presence of competitors (Šklíba et al. 2020; Zagorodniuk et al. 2018). Also, the behaviour may circumvent the patchy availability of suitable habitats and small home-ranges, maintaining gene flow and limiting genetic structuring across small spatial scales.

Dispersal events in the giant root-rat may be male-dominated, as it has been observed in tuco tucos (*Ctenomys talarum* and *C. australis*; Cutrera, Lacey, and Busch 2005; Mora et al. 2010), Chinese zokor (*Eospalax fontanierii*, Zhang 2007), giant mole-rats (*F. mechowii*; Kawalika and Burda 2007), and arvicoline rodents (Le Galliard et al. 2012). While sex-specific dispersal has not been studied in the giant root-rat yet, the observation of males being more frequently involved in dispersal attempts compared to females (Šklíba et al. 2020) and that microsatellite analysis also indicate that males disperse for longer distances (Dovičicová et al. in prep.) suggests that this type of dispersal may be prevalent in the species.

Our nuclear data did suggest slight subdivision in the south, with localities in the central part of the plateau (S1, S2) being more differentiated from localities in the southeast (S3-S6; Figure 1C). This was evidenced by increased F_{ST} in their pairwise comparisons and their segregation on the second principal component on the PCA (Figure 2C, D). Although overall differentiation among localities in the south were low, this pattern may reflect topographic features; the mountain Tullu Dimtu, the highest peak in the Bale Mountains National Park with 4,377 m a.s.l., is located close to localities S3 and S4, and may hinder gene flow (Figure 1C).

Conservation implications

Through landscape genetic analysis, we identified the drivers of population subdivision between north and south to be topographic barriers in the form of slope and elevation. While the species is capable of dispersing locally, our findings suggest that giant root-rats in the north and south must be considered separately when developing conservation strategies, as there is no opportunity for dispersal and gene flow between them. Giant root-rat impact their surrounding environment as ecosystem engineers and primary prey for the endangered Ethiopian wolf, which underscores the importance of their persistence (Sillero-Zubiri and Gottelli 1995; Šklíba et al. 2017). Already, the giant root-rat is believed to have a small census size due to its limited distribution range (although no census estimate is available), and is listed as endangered by the IUCN (Lavrenchenko and Kennerley 2016). The potential for reduction of the species' distribution range due to increasing human activities in the form of expanding livestock grazing and human settlements in the Bale Mountains, could harm the species' persistence with negative consequences for the overall ecological balance in the region (Gashaw 2015; Mekonen 2020; Stephens et al. 2001). Our study yields some key insights for planning future conservation strategies for the species and highlights the value of genomic data in expanding our understanding of the population dynamics and environmental features that drive the structuring of range-limited fossorial species. With ongoing environmental changes, it is crucial to utilize this knowledge to safeguard mountain biodiversity and ecosystem functioning.

Data accessibility and benefit-sharing statement

Data accessibility: The mitochondrial genome data that support the findings of this study will be openly available in GenBank of NCBI at https://www.ncbi.nlm.nih.gov under accession no. OQ207545-OQ207620 and MW751806, upon acceptance of this paper. The raw sequencing reads will be available in the associated BioProject PRJNA940645.

Benefit sharing: This project was designed as a joint Ethio-European research collaboration and developed with scientists from Ethiopia that provided the genetic samples. Our project is committed to international scientific partnerships and our collaborators are included as co-authors. The research addresses a priority concern, in this case the conservation of the studied organism.

Supplementary material

Supplementary material to this chapter can be found in Supplementary material Chapter IV.

Evolutionary history of fossorial rodent species reveals insights into Middle Stone Age foragers' resource-use and high-altitude residency in times of Late Pleistocene climate change

by

Victoria M. Reuber, Alba Rey-Iglesia, Michael V. Westbury, Mona Schreiber, Addisu Asefa, Nina Farwig, Alexander Groos, Georg Miehe, Götz Ossendorf, Dana G. Schabo, Paul Szpak, Luise Wraase, Tilaye Wube, Lars Opgenoorth* and Eline D. Lorenzen*

* These authors contributed equally to this study

Not published

ABSTRACT

Ancient biomolecular methods applied to subfossil remains allow for a robust exploration of the ecological and evolutionary history of terrestrial mammals, considering both human impacts and palaeoenvironmental conditions. We introduce the first complete ancient faunal mitochondrial genomes from Late Pleistocene Africa, focusing on the giant root-rat (*Tachyoryctes macrocephalus*), an endemic fossorial rodent found in the Bale Mountains of southern Ethiopia. We aim to explore the species' temporal patterns in phylogeny, diversity, and demographic history in relation to resource utilisation and high-altitude residency of Middle Stone Age foragers, and Late Pleistocene climatic change. Subfossil remains of the giant root-rat revealed its significance as a key food resource for Middle Stone Age foragers, who repeatedly occupied the glaciated Bale Mountains between 47,000 to 31,000 years ago. We retrieved 18 complete mitochondrial genomes of subfossil giant root-rats from the Fincha Habera archaeological site. Based on radiocarbon and molecular dating, the remains were aged ~ 44,000 to 32,000 years before present, and evidenced an almost continuous occupation of the site by Middle Stone Age foragers. Demographic reconstruction indicated a population decline of the northern giant root-rat population during occupation of Fincha Habera, presumably due to human hunting. Our analyses show giant root-rats diverged into the northern and a southern population approximately ~220,000 years ago. Phylogenetic and demographic analysis indicated climate-driven lineage divergence, and a population decline of the southern population during the Late Pleistocene glaciation due to reduced habitat availability. Additionally, ancient and contemporary carbon and nitrogen stable isotopes indicated limited water availability during Bale Mountain glaciation. Our findings emphasise the significance of using combined ancient biomolecular techniques to gain comprehensive understanding of the intricate interplay between human activities and faunal dynamics, alongside environmental shifts.

5.1. Introduction

The Bale Mountains in southern Ethiopia span 1,980 km^2 and comprise the largest afro-alpine and subalpine ecosystem above 3,000 m on the African continent (Groos et al. 2021; Miehe and Miehe 1994). The region is known for its high level of species endemism, and is characterised as a biodiversity hotspot (Hillman 1986). One of the defining characteristics of the Bale Mountains is the Sanetti Plateau, which ranges from 3,800 m to 4,377 m above sea level (a.s.l.)

76

(Figure 1). Exposure ages of moraine boulders and periglacial features have revealed the Sanetti Plateau and adjacent valleys were covered by ice shields during the Late Pleistocene (129-11.7 thousand of years before present, [kyr BP], Cohen et al. 2013), with a large glacial expansion 42-16 kyr BP (Groos et al. 2021). Notably, the Fincha Habera rock shelter, an archaeological site in the Web Valley in the northern part of the Bale Mountains, was repeatedly occupied by Middle Stone Age foragers during the last local glacial maximum, 47-31 kyr BP (Figure 1, Ossendorf et al. 2019).

Fincha Habera is recognised as the world's earliest known human high-altitude residential site (Ossendorf et al. 2019). Located ~ 500 m lower than the glaciers of the Sanetti Plateau, the site was exposed to a more moderate climate and possibly year-round water availability from the melting glaciers during the occupation of Middle Stone Age foragers (Ossendorf et al. 2019). Although the Late Pleistocene glacial extent never reached Fincha Habera during the period of human occupation, valley glaciers did come within 7 km of the site (Ossendorf et al. 2019). Radiocarbon dating of material from the Fincha Habera rock shelter revealed Middle Stone Age foragers occupied the site for three prolonged phases, presumably in an annual or seasonal circuit (Ossendorf et al. 2023).

Archaeological findings evidence the presence of the giant root-rat (*Tachyoryctes macrocephalus*) played a critical role in the site's occupation. The giant root-rat is a fossorial rodent species endemic to the afro-alpine ecosystem of the Bale Mountains (Yalden 1975), and massive accumulation of burnt giant root-rat bones have been identified in fire pits at Fincha Habera, revealing the species as a vital food resource. This likely facilitated human high-altitude habitation in the Bale Mountains, with Fincha Habera serving as a "base camp" in a transition area between the Afro-alpine and the Ericaceous ecosystems an ecotonal setting (Ossendorf et al. 2019). In addition to their importance for past human occupation of Fincha Habera, giant root-rats also play a broad ecological role in shaping the afro-alpine ecosystem, through the combined effect of soil perturbation and herbivory. At the same time, the species has strict habitat requirements; it is restricted by the extent of the Ericaceous Belt, a woody formation of dense *Erica* shrubs. Additionally, the giant root-rat is a key prey species for the endangered Ethiopian wolf (*Canis simensis*), at least in the Bale Mountains (Sillero-Zubiri and Gottelli 1995; Yalden 1985).

Ancient biomolecular analysis of subfossil faunal remains is a powerful approach to elucidating the evolutionary and ecological history of past populations (reviewed in Rosengren et al. 2021; Swift et al. 2019). Ancient DNA analysis of radiocarbon dated faunal remains may be used to

reconstruct species demographic histories, and to elucidate the timing and magnitude of response to external factors, such as humans and climate (Baca, Popović, Lemanik, et al. 2023; Campos et al. 2010; Hempel et al. 2022; Palkopoulou et al. 2013). In addition, stable carbon (δ^{13}C) and nitrogen (δ^{15}N) isotope analysis of the same individuals provide valuable insights into the paleoenvironmental conditions encountered during their lifetimes (e.g. Lehmann et al. 2016; Lüdecke et al. 2016; Rey-Iglesia et al. 2021).

Most ancient DNA studies have focused on megafauna in northern Eurasia and North America (Ersmark et al. 2019; Fellows Yates et al. 2017; Lorenzen et al. 2011). Investigations from warm and humid climates are still relatively rare, due to their detrimental effects on DNA preservation (Bollongino, Tresset, and Vigne 2008; Hofreiter et al. 2015). To date, ancient DNA studies in Africa have predominantly investigated human remains (e.g. Gallego Llorente et al. 2015; Skoglund et al. 2017; Vicente and Schlebusch 2020), with only a few exploring past populations of other fauna (e.g. Hempel et al. 2022; Kimura et al. 2011). In eastern Africa, well-preserved faunal remains have been discovered at archaeological sites that, in combination with charcoal from cultural layers of sediment deposits, have been used to understand settlement and resource use of Middle Stone Age foragers (Brandt et al. 2017; Prendergast et al. 2023). However, there is still a lack of ancient DNA studies on faunal remains in this context. The subfossil giant root-rat remains from Fincha Habera provide an ideal opportunity for integrating biomolecular analysis, as the colder temperatures at high altitudes and the shielding from UV radiation by the rock shelter, might facilitate better DNA preservation (Hofreiter et al. 2015). Regular exploitation by Middle Stone Age foragers of giant root-rats across 16,000 years, and the extensive glaciation of the Bale Mountains provides a unique setting for a joint investigation. This encompasses Late Pleistocene human presence in high altitudes, environmental change and the evolutionary and ecological history of past giant root-rat populations.

In this study, we aim to shed further light on the past resource use of and high-altitude residency of the Middle Stone Age foragers at Fincha Habera, through the prism of faunal giant root rat remains excavated at the site. In addition, we investigated the temporal patterns of phylogeny, diversity, and demographic history of the giant root-rat at a millennial time scale, to understand the species' response to human presence and Late Pleistocene climatic change. We used a complementary biomolecular approach combining radiocarbon dating, ancient DNA, and stable carbon (δ^{13}C) and nitrogen (δ^{15}N) isotope analysis of a sequence of giant-root rat subfossils excavated from the Fincha Habera site. We aimed to refine the occupation phases of the Fincha

Habera site, and to infer the temporal context of the faunal specimens. Therefore, we AMS radiocarbon dated seven giant root-rat subfossils and analysed those in combination with fifteen published faunal and charcoal dates from the site. We expect our new giant root-rat radiocarbon dates fall within the previously identified phases of Middle Stone Age occupation at the site. We investigated the phylogeography, diversity, and demographic history of giant root-rats using complete mitochondrial genomes (mitogenomes) from 13 Fincha Habera specimens, and 77 available mitogenomes from contemporary populations. A recent study revealed a deep divergence of contemporary giant root-rats into two genetically distinct populations in the north and south of the species range (Reuber et al. 2023, preprint). We expect population declines in both the northern and southern population, due to exploitation of the species by Middle Stone Age foragers and the extensive Late Pleistocene glaciation of the region, respectively. To investigate environmental shifts and changes in foraging ecology between the Late Pleistocene and contemporary root rats, we analysed bone collagen stable carbon ($\delta^{13}C$) and nitrogen ($\delta^{15}N$) isotopes from past and present specimens.
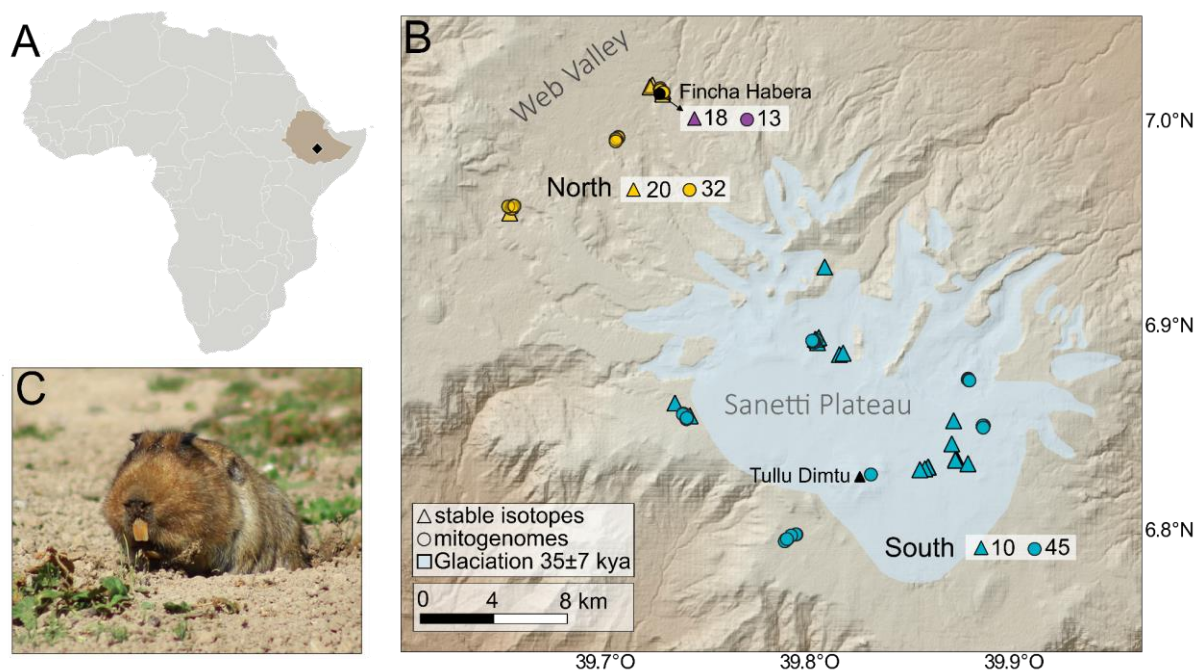
Figure 1: Sampling localities and radiocarbon ages of giant root-rats from the Bale Mountains National Park, Ethiopia. A) Map of Africa showing Ethiopia in brown and indicating location of Bale Mountains National Park; B) Sampling localities of subfossil Fincha Habera specimens (purple) and contemporary samples, which are grouped into genetically distinct clusters in the north (yellow) and south (turquoise; Reuber et al., 2023, preprint). Sample sizes for each data type (stable isotopes, mitogenomes) are indicated; light blue shading on map refers to Last Pleistocene glaciation stage I (local maximum; 42-28 kyr BP; Groos et al. 2021); C) Burrowing giant root-rat, photography by Philipp Kurt.

5.2. Material and methods

5.2.1 Samples and site

Our analysis included 18 Late Pleistocene subfossil giant root-rat specimens from the Fincha Habera site in Ethiopia, which were analysed using mitochondrial genomes (mitogenomes) and carbon and nitrogen stable isotopes (Figure 1A-C). The Fincha Habera rock shelter (3,469 m a.s.l.) is an archaeological site located in the eastern part of the Web Valley in the northern region of the Bale Mountain National Park (7.014577° N, 39.720068° E, Figure 1B). Two excavation campaigns were carried out at the site in 2017 and 2020, where approximately 10,000 faunal remains from five excavation squares of 1 m^2 dimensions were recovered, with the depths of the Middle Stone Age deposits varying between 30 and 110 cm (Ossendorf et al. 2023). The remains were derived from two soil layers (FHL-08 and FHL-09). The remains of giant root-rats were the most abundant in the analysed subsample (n=2305) of the faunal assemblage (FHL-08: 94.2%, FHL-09: 99.0%) and a majority of those showed indications for roasting giant root-rats on the open flame as humans' preferred method of preparation suggesting human processing (Ossendorf et al. 2019, 2023). Radiocarbon dates of two giant root-rat samples, on black carbon sample, nine charcoal, and three hyena coprolites unearthed from the two sediment layers, indicate three human occupation phases at the Fincha Habera site from approximately 45.6-42.9 kyr BP (n = 4, FHL-09), 38.9-34.9 kyr BP (n = 7; FHL - 08 lower) and 32.1-31.2 kyr BP (n = 3, FHL - 08, upper) (Supplementary Table S1, Ossendorf et al. 2019, 2023). The identified Middle Stone Age phases rest on sedimentary changes in the Middle Stone Age deposits as well as concomitant cultural (lithic technological) changes. Out of all subfossil giant root-rat remains, 18 lower-jaw bones excavated from two excavation squares (F13 and F15) during the second campaign, were used in this study (Supplementary Table S2).

The 18 subfossil Fincha Habera specimens were also used for stable isotope analyses in this study. To contextualise the data, we generated δ^{13}C and δ^{15}N records for 30 contemporary giant root-rats. Contemporary bone samples were collected from giant root-rat carcasses discovered opportunistically during field surveys in the Bale Mountains National Park in 2021 (Figure 1B, Supplementary Table S3). If possible, we always collected the left lower jaw to avoid double sampling of the same individual, otherwise the right lower jaw was collected.

Our analysis included 77 available giant root-rat mitogenomes, sampled from the north and southern part of the species range (Figure 1B) (Reuber et al. 2023, preprint). The mitogenomes

are from GenBank, NCBI, at https://www.ncbi.nlm.nih.gov under accession no. OQ207545-OQ207620 and MW751806.

5.2.2 Radiocarbon dating

Seven new Fincha Habera specimens were radiocarbon dated at the Keck Carbon Cycle AMS Facility (UCIAMS, Earth System Science Department, UC Irvine; Figure 2B). Collagen was extracted at Trent University Water Quality Center Lab following the protocol for bone collagen extraction recommended by UCIAMS. We calibrated the radiocarbon dates using OxCal v.4.4 (Bronk Ramsey 2009) online version (https://c14.arch.ox.ac.uk/oxcal/OxCal.html), with the IntCal20 (Reimer et al. 2020) calibration curve (Supplementary Table S1). Unless otherwise stated, specimen ages are discussed in calibrated mean radiocarbon dates (cal yr BP). We analysed our seven radiocarbon dates with fifteen radiocarbon dates available for samples from the Fincha Habera site: two giant root-rat, one black carbon, nine charcoal samples and three coprolites. We recalibrated those in OxCal v.4.4 with the IntCal20 calibration curve (Supplementary Table S1, Ossendorf et al. 2019, 2023). For our analyses, only samples of Middle Stone Age artefact-bearing layers from FHL-08 and FHL-09 were included, while results of the youngest deposits (COL5196.1.1, COL5195.1.1, COL6822.1.1, Beta-507233, COL6820.1.1, COL5198.1.1, COL6821.1.1) are not relevant for the Late Pleistocene occupation by Middle Stone Age foragers. We also omitted previously published radiocarbon dating results indicative of the mixing of sediments and their contents. This firstly refers to those identified as introgressions of recent charcoal (n = 5, COL5197.1.1, Beta-486378, COL5199.1.1, Beta-486376, Beta-486375) which entered the Middle Stone Age deposits by disturbances caused by humans. Secondly, results from bulk dating of black carbon from sediments (n = 3, Beta-507234, Beta-503927, Beta-507235) were omitted as these were used to infer the degree of internal mixing of Middle Stone Age layers, caused by hyenas and/or regular flooding by overbank deposits. Finally, two dates on coprolites were excluded due to their low C:N ratio (Beta-506526, D-AMS 037006) (Supplementary Table S1, Ossendorf et al. 2019, 2023).

We used OxCal 4.4 (Bronk Ramsey 2009) and the 'Boundary' function to refine start and end points of discrete temporal phases of Fincha Habera occupation, based on the new seven radiocarbon dates, and the fifteen dates already available for the site. We grouped our seven new dates with the fifteen available radiocarbon dates from the Middle Stone Age deposits (Supplementary Table S1, Ossendorf et al. 2019, 2023) of the site into three temporal groups

that were identified by Ossendorf et al. (2023) as phases of human activity, to refine start and end age ranges (94.5 % of samples will fall in that range) of each phase. The function assumes that a group of events is randomly sampled from a uniform distribution between the start and end boundaries of that phase.

5.2.3 Ancient DNA extraction, sequencing and data processing

We drilled 50-70 mg of bone powder from each of the 18 Fincha Habera specimens. The outer layer of each specimen was cleaned using a drill bit and excluded from the sampling to minimise environmental contaminants. The DNA extraction was carried out following the protocol from Allentoft et al. (2015), with some modifications. Bone powder was incubated overnight at 37 °C with constant rotation in 1 mL of extraction buffer. The extraction buffer was prepared in bulk for eight specimens and consisted of 8.1 mL 0.5M EDTA-solution, 225 μL of 10 mg/mL Proteinase K solution and 675 μL of sterile H_2O. Post-incubation, the supernatant was added to a 30 KDa Amicon® Ultra-4. The sample was spun down at 4,000 rpm, until the supernatant was concentrated down to 70 μl. The concentrate was combined with a 13x modified Qiagen PB buffer as described in Allentoft et al. (2015) and purified using Monarch columns (NEB). After binding, we performed two washes with Qiagen PE. DNA elution was performed in two steps; for every step, we added 25 μl of Qiagen EB buffer to the Monarch column, incubated for 5 min at room temperature, and centrifuged at 13,000 rpm (max speed) for 1 min.

Prior to library build, DNA extracts were treated with Thermolabile USER II enzyme (NEB). For each sample, the USER reaction was performed in 16 μl, with 2.4 μl of the Thermolabile USER II enzyme and 13.6 μl of each extract, and incubation time of 3 h at 37 °C. USER treated DNA extracts were purified using Monarch columns as described above; however, only one PE wash was used and DNA was eluted in 20 μl of EB.

DNA extracts were transformed into single-stranded DNA (ssDNA) sequencing libraries as in Kapp et al. (2021) and double-indexed using KAPA HiFi uracil+ premix (KAPA Biosystems). The number of cycles for the index PCR was determined from qPCR analysis. The resulting indexed libraries were quantified on a Qubit[TM] dsDNA HS (Invitrogen), and quality checked in either Agilent 2100 Bioanalyser or Agilent Fragment Analyzer™. All laboratory work was carried out in the designated clean lab facilities at Globe Institute, University of Copenhagen.

Indexed libraries were shotgun sequenced on an Illumina HiSeq 4000 SR 80 base pairs (bp). Shotgun sequencing revealed a limited number of endogenous sequences; to increase the

number of retrieved endogenous mitochondrial sequences, we performed target-enrichment by hybridization capture (Supplementary Table S3). The hybridization capture was performed using myBaits Mito (Arbor Biosciences) with RNA baits designed to target the reference mitogenome of the giant root-rat (MW751806). The capture procedure was carried out as described in the myBaits manual v.4.01, with a hybridization step at 55 °C for 24 h. After capture, 15 μl of the libraries were re-amplified KAPA HiFi uracil+ premix (KAPA Biosystems) following the myBaits manual. Re-amplified libraries were quantified and quality checked as described above. Sequencing was carried out in NovaSeq 6000 150 PE.

We used the Paleomix v1.2.13.1 pipeline to remove low-quality reads, trim adapters, mapping, duplicate removal, and damage analyses (Schubert et al. 2014). Adapter and quality trimming were conducted with AdapterRemoval v2.2.2 (Schubert, Lindgreen, and Orlando 2016), removal of duplicated reads with MarkDuplicates, mapping of the reads with the BWA algorithm 0.7.15 (read alignment), and damage analyses with mapDamage v2.0.6 (Jónsson et al. 2013). Reads with less than 25 bp were excluded during adapter trimming. We required a minimum mapping quality of 20. Reads were mapped against the giant root-rat mitogenome reference (Genbank accession: MW751806; Reuber et al. 2021). We generated mitochondrial consensus sequences from the BAM files with unique reads using ANGSD v0.919 requiring a minimum base quality score of 25 and at least 5x coverage (Korneliussen et al. 2014).

5.2.3 Haplotype network and phylogeny

Haplotype network

We generated a median-joining network of the Fincha Habera specimens and contemporary giant root-rat samples, using PopArt v.1.7 (Leigh and Bryant 2015). We aligned the Fincha Habera mitogenomes with a minimum depth of coverage of 10 x (n=13) with the 77 publicly available contemporary mitogenomes using Mafft v.7.490 (Katoh and Standley 2013).

Phylogeny and molecular dating

We conducted several phylogenetic analyses using the software Beast v1.10.4 (Suchard et al. 2018), to (i) estimate the age of the undated giant root-rat Fincha Habera specimens from which we had > 10x coverage mitochondrial sequences (n = 6), (ii) estimate divergence times within the giant root-rat phylogeny, and (iii) reconstruct the species demographic history. For each of

these analyses, we used a different alignment including a different number of sequences. We used PartitionFinder v2.1.1 (Lanfear et al. 2017) to identify a partition scheme for each sequence alignment, and the best model of substitution for each partition. For each analysis, based on PartitionFinder results, the alignments were partitioned into four subsets, i) tRNAs, rRNAs, first codon position, ii) second and iii) third codon position, and iv) control region. For each subset, we set the HKY + I + X, HKY + X, TRN + X and the HKY + I +G + X as optimal models of substitution, respectively. The final length of the partitioned alignments was 16,499 bp.

We used a tip dating approach in Beast to molecularly estimate the age of the undated specimens. This analysis was done individually for six Fincha Habera specimens that lacked radiocarbon dates (minimum 10x coverage). For each undated specimen, we built a phylogenetic tree using the radiocarbon dated Fincha Habera (n = 7) specimens, all contemporary haplotypes obtained in the network analyses, and one undated specimen. We fixed the ages of the dated subfossil and used the mean age and standard deviation of the radiocarbon dated specimens (mean ± sd = 40,591±4,086) as prior values for the undated specimens, applying a lognormal distribution. The molecular estimated ages of respective sequences were retrieved using Tracer v1.7.2 (Rambaut et al. 2018).

We manually assigned the molecular-dated specimens in accordance with their estimated ages to the temporal phases identified in OxCal using our seven radiocarbon dated specimens, in combination with the available radiocarbon dates from the site. For dating the phylogenetic tree, we used the radiocarbon and molecularly dated Fincha Habera mitogenomes (minimum 10x coverage, n = 13), and the contemporary haplotypes. We built the intraspecific phylogeny using the tip dating approach, fixing the seven calibrated radiocarbon dates and the six molecular estimated ages of the subfossils. We applied a single species, coalescent constant population model. We linked trees and clock rate and applied a strict clock as we assumed little heterogeneity in clock rate within giant root-rats.

We applied a cross-validation method for our tip dating approach, estimating the age of the seven Fincha Habera specimens with radiocarbon dates to evaluate if similar ages were estimated using our calibrated phylogeny. To validate that there is a temporal signal in our data set, we performed a date-randomization test with the TipDating package v.1.1-0 in R (Rieux and Khatchikian 2017). The seven calibrated and six molecular estimated dates of the Fincha Habera specimens were shuffled 10 times and date-randomised BEAST xml files were

generated. The estimated parameters were subsequently compared to the original dates. The test passed, hence a temporal signal was present in our data set (Supplementary Figure S1).

For all Beast analyses, we ran two independent MCMC chains of 50,000,000 generations, logged every 5,000 generations. We combined the log and the tree files of both runs using logCombiner v.1.10 with a burning of 10% and subsequently inspected convergence and stationarity (ESS > 200) using Tracer v1.7.2 (Rambaut et al. 2018). We created a tree with maximum clade credibility and a probability limit of 0.8 using the combined trees, with Tree Annotator. The resulting phylogeny with mean node ages of clades and 95% HPD intervals was visualised using FigTree v1.4.4 (http://tree.bio.ed.ac.uk/software/figtree/).

5.2.4 Demographic reconstruction

For demographic reconstruction, we conducted a Bayesian Skyline plot analysis in Beast v1.10.4 (Drummond et al. 2005; Suchard et al. 2018), using the radiocarbon and molecular dated specimens (minimum 10x coverage, n = 13) and all but two available contemporary mitogenomes (n = 75, excluding GG01 and WM07). We excluded the southern contemporary samples GG01 and WM07 from the analysis, as they clustered with the northern samples with high divergence (69 and 38 segregation sites, respectively) due to incomplete lineage sorting and not recent or ancestral gene flow (Reuber et al. 2023, preprint). Bayesian skyline estimates are affected by incomplete lineage sorting and population structure, leading to false population increase or decline (Heller, Chikhi, and Siegismund 2013). Hence, the inclusion of GG01 and WM07 may bias the demographic estimations, and were subsequently excluded from these analyses. Except for those two individuals, the phylogeny showed two distinct groups of mitogenomes based on the individuals' sampling region north and south, therefore we conducted separate runs for each group. The subfossil Fincha Habera specimens were included in either of the groups, based on their position in the phylogeny (north n = 12, specimens: ID 559, 650, 1026, 1064, 1004, 680, 677, 964, 681, 989, 966, 678; south n = 1, specimen: 689)

We used the same parameter settings as in the molecular-dated phylogeny but ran the Coalescent Bayesian Skyline model instead. Further, for both clades, we calibrated the age of the root, which is the mean and the 95 % highest posterior density (HPD) of the oldest giant root-rat divergence date estimated with the phylogeny. We applied a log-normal distribution to the root and truncated the lower limit of the root to the oldest Fincha Habera specimen in the respective run (north: 43,754 years, specimen ID 681; south 40,594 years, specimen ID 689).

We ran two independent MCMC chains of 50,000,000 generations and logged every 5,000 generations. The log files were visually inspected in Tracer v1.7.2 (Rambaut et al. 2018) for convergence and stationarity, and parameters showed ESS values > 200.

5.2.5 Diversity

We estimated the nucleotide diversity for the Fincha Habera specimens (coverage > 10x, n = 13) and for the contemporary data in the north (n = 32) and south (n = 45), following the finding of population subdivision between these two contemporary populations by Reuber et al. (2023, preprint). Since the number of sequences varied per group and phases, we randomly subsampled the data taking two samples iteratively 1000 times in a bootstrap approach with replacement, excluding missing gaps in sequences. We estimated nucleotide diversity for each random sample, and summarised standard deviation for each group and phase. The analyses were conducted in R (R Core Team 2021), using the pegas v.1.1. package (Paradis and Barrett 2010).

5.2.6 Stable isotope analysis

For stable carbon (δ^{13}C) and nitrogen (δ^{15}N) isotope measurements of the 18 Fincha Habera specimens and the 30 contemporary giant root-rat samples (north = 20, south n = 10), we cut a bone fragment of 100-300 mg from each sample using an Ultimate XL-D micromotor. Each fragment was crushed into smaller pieces using Plattner mortar and pestle. The crushed fragments were immersed in 9 mL of 0.5 M hydrochloric (HCl) acid at room temperature for demineralization. Throughout the demineralization treatment, the samples were agitated on an orbital shaker. Samples remained in acid between 17-30 h and were removed from the demineralization solution when the fragment was soft and/or floating in solution. Immediately upon removal from the demineralization solution, each sample was rinsed four times in 10 mL of Type I water (resistivity >18.2 MΩ cm). Following demineralization, the specimens were solubilized in 3.5 mL of 0.01 M HCl at 75 °C for 36 h. The samples were centrifuged to precipitate the insoluble material, and the collagen suspended in solution was transferred into a glass vial and frozen for 24 h. Once frozen, the collagen samples were lyophilized for 48 h. Dried collagen weighing between 0.5-0.6 mg was transferred into tin capsules for stable isotope and elemental analysis. These analyses were performed at the Trent University Water Quality Center using a Nu Horizon continuous flow isotope ratio mass spectrometer paired with a Euro Vector EA 300 elemental analyser. The stable isotope results were calibrated using Vienna Pee

Dee Belemnite (VPDB) for δ^{13}C and atmospheric nitrogen for δ^{15}N. International reference standards USGS40 and USGS66 were used to perform these calibrations. In-house laboratory standards SRM-1 (caribou bone collagen), SRM-2 (walrus bone collagen), and SRM-14 (polar bear bone collagen) were used to monitor analytical accuracy and precision of the analyses. For the δ^{13}C values of the contemporary samples, we corrected for the Suess effect by adding 2.04 to each value, following the correction curve from Dombrosky (Dombrosky 2020).

We analysed the stable isotope records as three groups: Fincha Habera, north, and south. We combined the 18 Fincha Habera records in one group to provide a sufficiently large sample size. To statistically test for differences of δ^{13}C and δ^{15}N values between groups, we used a Wilcoxon test, which accounts for unequal sample size and non-normality of the variables δ^{13}C and δ^{15}N, which have been visually investigated via diagnostic plots.

5.3. Results

5.3.1 Radiocarbon and molecular dates of subfossils

We radiocarbon dated seven Fincha Habera specimens and gained dates between 27,940 and 39,900 ^{14}C years before the present (Supplementary Table S2). The seven dates were calibrated using the IntCal 20 curve, which yielded mean ages spanning approximately 12,000 years, between 43,982 and 32,090 calibrated years before the present (cal yr BP, Figure 2B).

The ages of the molecular-dated specimens ranged between 32,174 and 43,576 yr BP and fell within the age range of the radiocarbon dated specimens (Figure 4B).
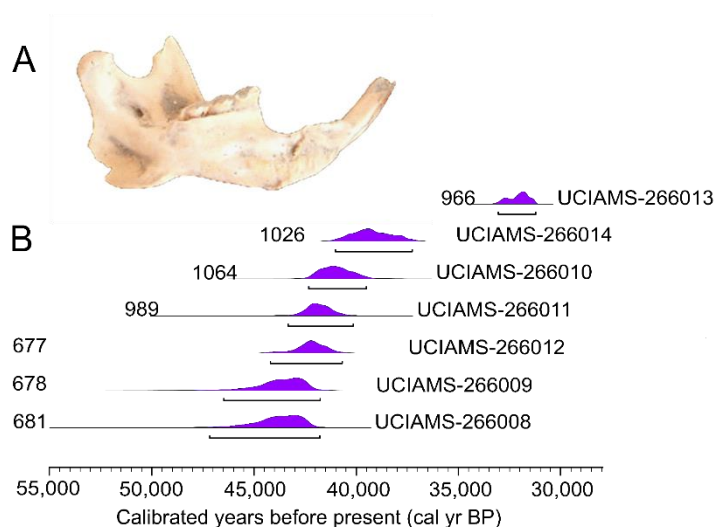
Figure 2: Radiocarbon ages of giant root-rats. A) One of the subfossil specimens analysed; Photography by Götz Ossendorf; B) Calendar median year calibration of the seven radiocarbon dated subfossils, estimated in OxCal (Bronk Ramsey 2009). To the left: specimen ID; to the right: ^{14}C Lab ID

Activity phases

We statistically combined our seven radiocarbon dates of the Fincha Habera specimens with the fifteen published radiocarbon dates from the site to identify temporal boundaries of human activity phases. Based on 10 radiocarbon dates, boundary ages of Phase 1 were identified from 46.3-43.6 to 42.4-40.2 (mean±sigma; 45.1±0.6 to 41.4±0.6; Figure 3, Supplementary Table S5) cal kyr BP. Phase 2, supported by seven radiocarbon dates, ranged between 41.4-39.3 to 34.3-32.4 (40.2± 0.6 to 33.5±0.5) cal kyr BP. The mean age of specimen 1064 (40,983 cal yr BP) fell between Phase 1 and 2, wherefore we ran the analyses twice with grouping this specimen once in Phase 1 and once in Phase 2. The Agreement index for this specimen (A) was higher in Phase 3, thus we placed it in that phase (Supplementary Table S5). Boundaries of Phase 3 were from 33.2-31.8 to 31.6-30.4 (32.4±0.4 to 31.1±0.4) cal kyr BP, derived with five dates (Figure 3, Table S5).

After the identification of the three temporal phases, we assigned the six molecular dates based on their mean value falling within the temporal boundaries (mean±sigma) of each phase; three molecular dates grouped in Phase 1 (ID 989, 680, 1004), two molecular date (ID 650, 689) grouped in Phase 2. One molecular dated specimen grouped into the third phase (ID 559) (Figure 4B, Supplementary Table S2).
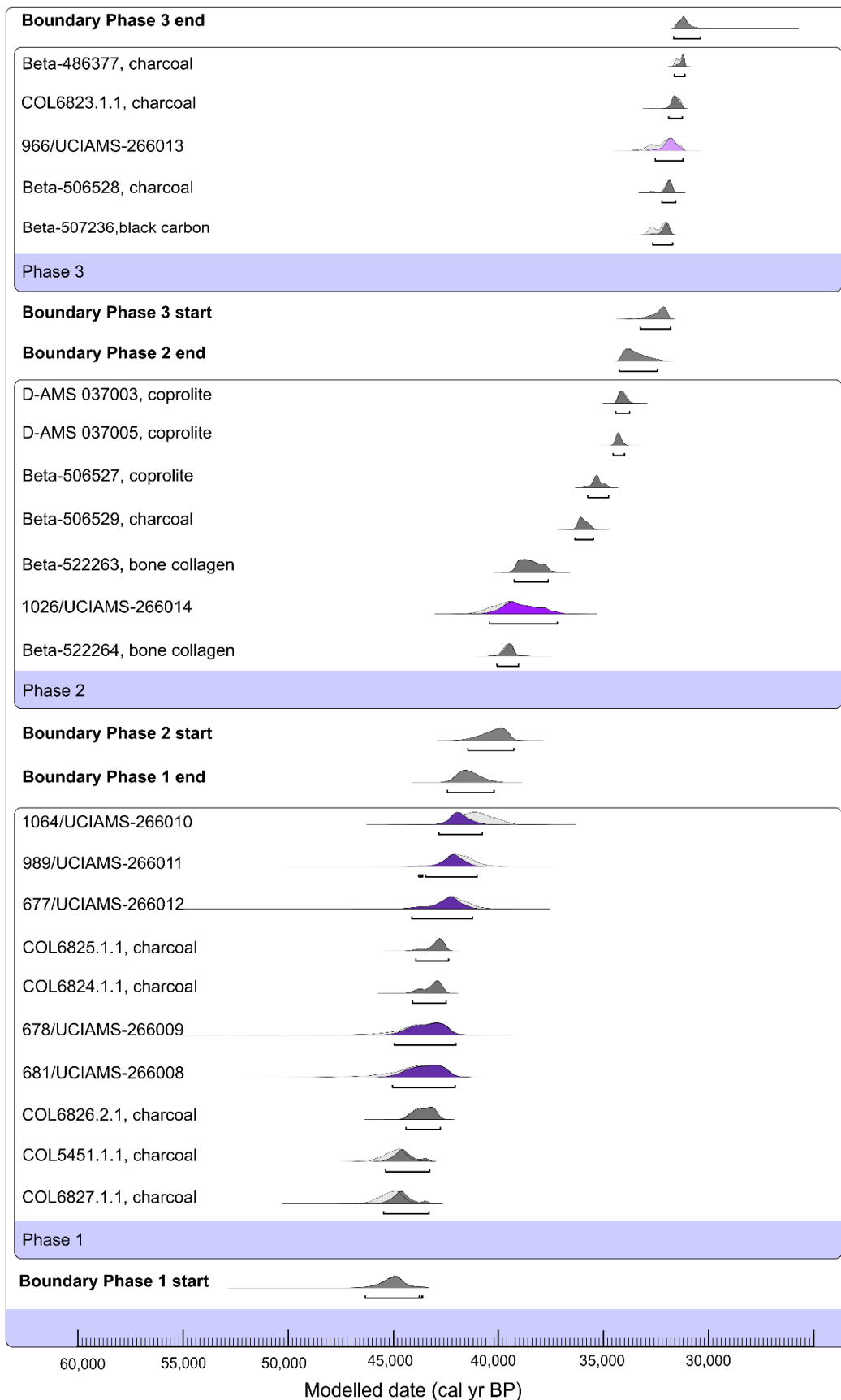
Figure 3: Three temporal phases of human activity at the Fincha Habera archaeological site indicated by modelled radiocarbon dates. New (purple) and published (grey) radiocarbon dates (Ossendorf et al. 2019, 2023) from the site. We used the 'Boundary' function in OxCal to determine start and end boundary ages of human activity with 94.5 % certainty.

5.3.2 Haplotype network and phylogeny
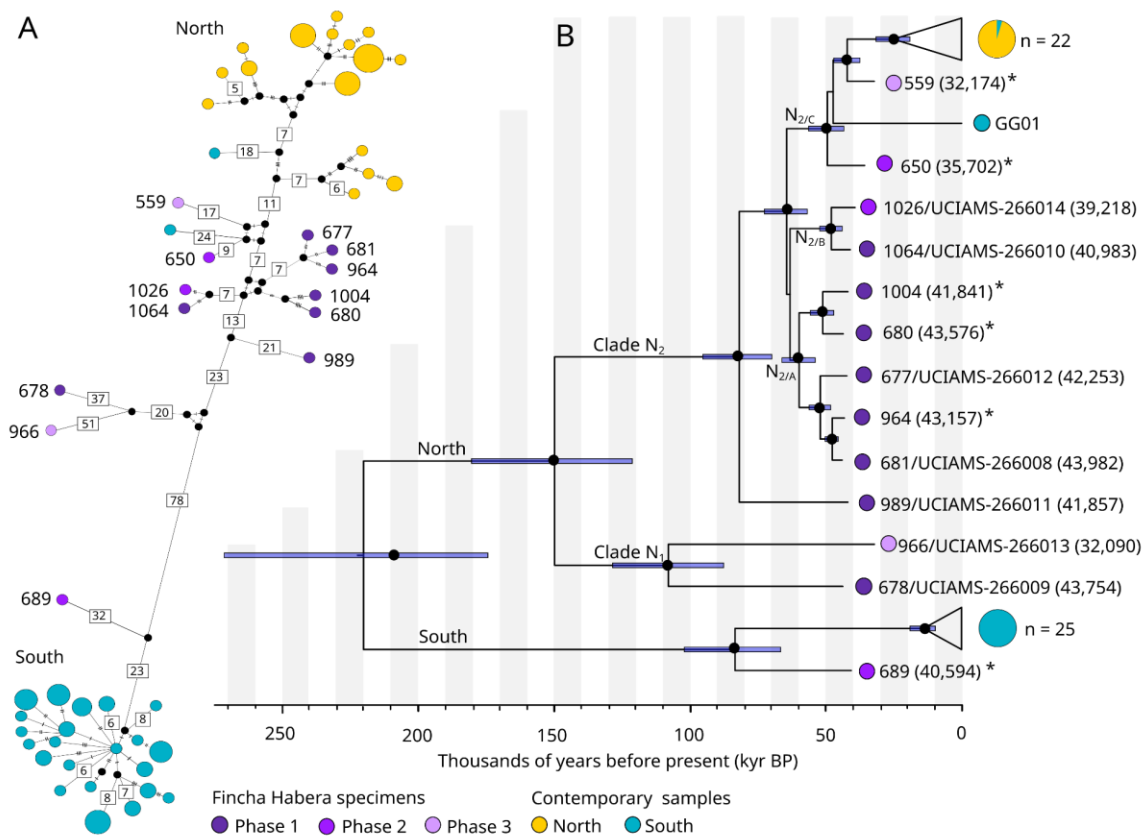
Figure 4: Evolutionary relationships among giant root-rat mitochondrial genomes. (A) Haplotype network of the 61 haplotypes present among the 90 mitogenome sequences with coverage > 10 x, comprising 13 Fincha Habera specimens and 77 contemporary samples. Dashes between haplotypes indicate number of substitutions and are shown by number when > 5. Circle size indicates the relative number of specimens with each haplotype. Black dots indicate haplotypes not present in the data. Of note, distances between haplotypes are not to scale. (B) Dated phylogeny of the 61 haplotypes. The mitogenomes are labelled with their specimen ID. For the seven samples with radiocarbon ages, the mean calibrated sample age is shown in brackets. Six samples were molecularly dated, indicated by an asterisk. Black circles at nodes depict bootstrap support values >0.8; 95% HPD intervals of divergence dates of the internal nodes are displayed in horizontal blue bars. To ease the readability of the phylogenetic tree, clades comprising contemporary samples collected in the north (yellow) and south (turquoise) of the species range have been collapsed, with sample size indicated.

We generated complete mitogenomes from 18 Fincha Habera specimens with coverages ranging between 0.24x and 124.29x (Supplementary Table S4). We omitted the five sequences with < 10x coverage from further analysis. The remaining 13 Fincha Habera sequences (seven radiocarbon dated, six molecularly dated) were combined with 77 available contemporary mitogenomes (Fig 1A). Among the 90 sequences, we identified 61 haplotypes.

In the haplotype network and the phylogeny, 12 Fincha Habera specimens grouped with the contemporary clade in the north, and one specimen grouped with the contemporary clade in the south. In the network, we identified that the northern clade was separated from the southern

clade by at least 78 segregating sites (Figure 4A). The divergence of the northern and southern clade was estimated at 220.2 (95 % HPD: 174.4–271.5, Figure 4B) kyr BP.

We identified two distinct genetic clades in the north (N_1 and N_2) that diverged ~148.5 (95 % HPD: 121.3–180.4) kyr BP (Figure 4B). Clade N_1 comprised two Fincha Habera specimens (ID 966, 678), which were separated by 88 mutations in the haplotype network and differed in age by almost 12,000 years. Their estimated divergence was ~110 kyr BP. Clade N_2 included ten subfossil specimens with ages spanning all three temporal phases, in addition to all contemporary samples from the north. Fincha Habera specimen 989 diverged from clade N_2 81.8 (95 % HPD: 69.9-95.3) kyr BP. The remaining mitogenome lineages revealed a temporal pattern. Five Phase 1 Fincha Habera specimens grouped in clade $N_{2/A}$; one Phase 1 and one Phase 2 specimen in clade $N_{2/B}$; one Phase 2 and one Phase 3 specimens in clade $N_{2/C}$. The latter specimens, which were the youngest subfossils, were phylogenetically the closest to the contemporary samples. The divergences of contemporary samples started at 25.1 (95 % HPD: 19.0-31.5, Supplementary Figure S2) kyr BP.

One Fincha Habera specimen grouped with the southern clade. However, the sequence was relatively distinct, with a divergence time from the contemporary clade of ~83.4 (95% HPD: 66.6-102.1) kyr BP, and 55 segregating sites separation (Figure 4). Divergence within the contemporary southern clade started 14.0 (95% HPD: 9.7-19.0, Supplementary Figure S2) kyr BP, with a star-like topology of the sequences in the network.

5.3.3 Demographic reconstruction

Mitogenome demographic reconstruction showed a gradual decline in female effective population size in the north around ~60 kyr BP until approximately 5 kyr BP, with a cumulative decrease of ~80 % in female effective population size (N_e) (Figure 5A). Between ~42-37 kyr BP, there was an increase in the median rate of decline, followed by a time of rather stable population size until ~27 kyr BP. From this time onwards, the population continuously decreased until ~5 kyr BP.

The southern group showed a gradual minor decline in N_e starting ~50 kyr BP, with an increase in the median rate of decline starting ~40 kyr BP. The population size decreased by one third, reaching its minimum ~28 kyr BP, which lasted until ~15 kyr BP (Figure 5B). From ~15 kyr BP, the giant root-rat N_e increased 3-fold until ~3 kyr BP.

91
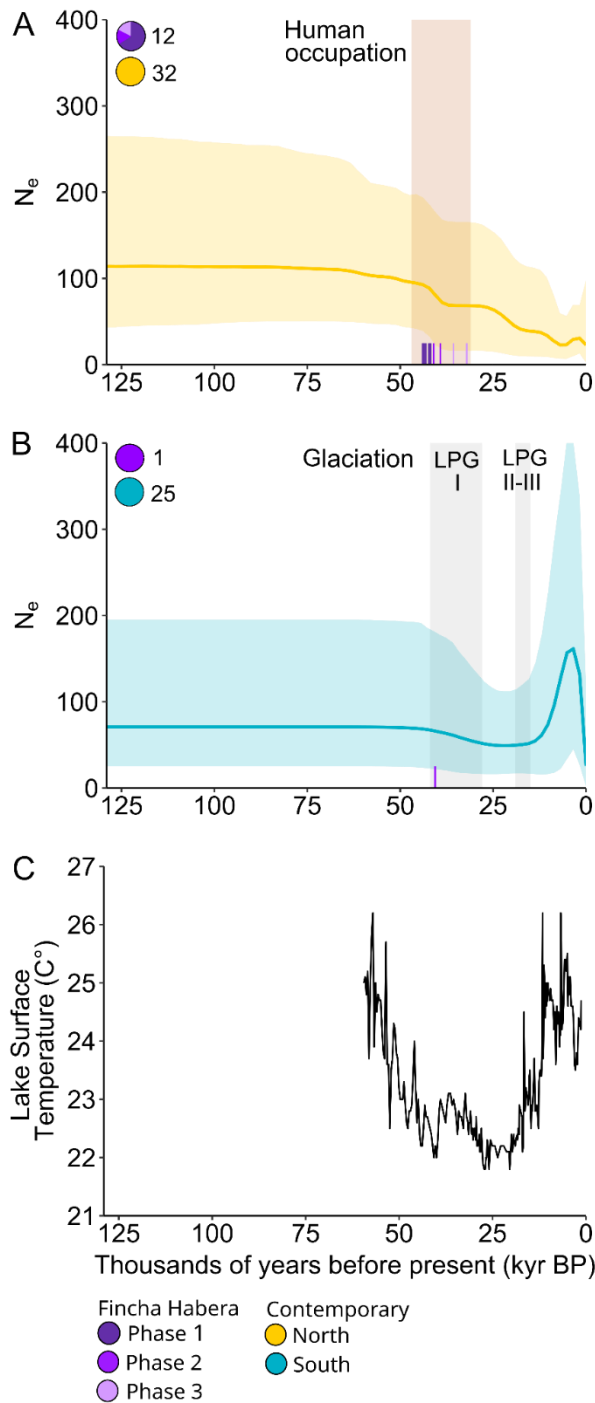
Figure 5: Demographic reconstruction of giant root-rat populations. Bayesian skyline plots estimated for (A) the northern (yellow) and (B) southern (turquoise) population. Sample sizes used for each analysis are indicated with the circles and colours. Ages of the Fincha Habera (purple) specimens included in each analysis are indicated along each x-axis (see Figure 4B); LPG = Last Pleistocene glaciation stage I (local maximum, 42-28 kyr BP), II (19-17 kyr BP) and III (17-15 kyr BP; Groos et al. 2021), N_e = female effective population size. (C) Lake surface temperature curve for Lake Tanganyika for the past 60,000 years ((Tierney et al. 2008).

5.3.4 Diversity

We found higher nucleotide diversity in Fincha Habera specimens ($\pi = 0.007\pm0.001$) compared to both contemporary populations (north: $\pi = 0.001\pm0.0003$, south: $\pi = 0.003\pm0.002$; Supplementary Figure S3).

92

5.3.5 Stable isotope analysis

To investigate environmental changes between the Late Pleistocene and the present, we investigated the temporal and spatial variation in stable isotopic compositions of giant root-rats between the Fincha Habera specimens and the contemporary samples. Subfossil 559 was omitted from the analysis as the C:N atomic value was outside the recommended range of 2.9-3.6 (Supplementary Table S5). Across time, δ^{13}C values ranged between -16.50 ‰ and -21.90 ‰, and δ^{15}N values ranged between 2.41 ‰ and 9.23 ‰ (Supplementary Table S6).
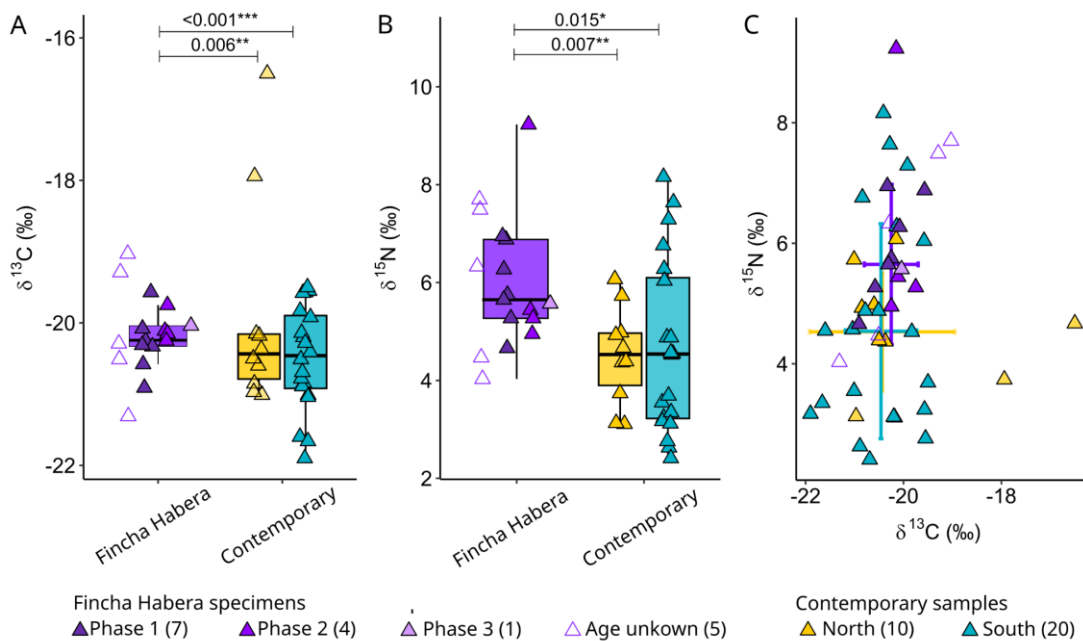
Figure 6: **Bone collagen stable carbon and nitrogen isotopic analysis of available giant root-rats**. (A) δ^{13}C and (B) δ^{15}N values by group, including the temporal phases of Fincha Habera, and the contemporary populations in north and south, with sample sizes indicated in brackets. Significance of each pairwise comparison is indicated; differences between groups are shown by an asterisk next to the *p*-values; with significance levels * = p <0.05, **p = <0.01, ***p = <0.001; ns = not significant. (C) Bivariate plot of δ^{13}C and δ^{15}N ranges, crosses represent median values ± sd for each group.

We identified significantly higher average δ^{13}C values in the Fincha Habera specimens, compared to either of the contemporary groups north or south (Figure 6A). Within the subfossil specimens, there was no clear trend in the temporal variation across their time span of 12,000 years visible in δ^{13}C values. The bivariate plots showed higher median δ^{13}C values for the Fincha Habera specimens than for the contemporary groups. (Figure 6C).

We found significantly higher average δ^{15}N values in the group of Fincha Habera specimens compared to both contemporary groups north and south. There was no clear trend in δ^{15}N within the Fincha Habera specimens across their age range (Figure 6B). We further explored

differences in δ^{15}N between the Late Pleistocene and today using bivariate plots and found elevated average δ^{15}N in the Fincha Habera specimens (Figure 6C).

5.4. Discussion

To explore temporal patterns in the phylogeny, diversity, and demographic history of the giant root-rat in relation to resource utilisation and high-altitude residency of Middle Stone Age foragers, alongside responses to Late Pleistocene climatic change, we used a combined biomolecular approach. We used ancient DNA, radiocarbon dating, and stable carbon and nitrogen isotope analysis on 18 subfossil giant root-rat specimens from the Fincha Habera archaeological site in the afro-alpine regions of the Bale Mountains, Ethiopia. Phylogenetic and radiocarbon dating placed the Fincha Habera specimens between ~44-32 kyr BP and helped to refine the time of occupation of the Fincha Habera rock shelter by Middle Stone Age foragers. Our analyses of the first Late Pleistocene faunal mitochondrial genomes from the African continent disclose Middle Stone Age resource use of the giant root-rat and a demographic decline of the species during occupation of the Fincha Habera site. Further, we found phylogenetic lineage divergence and demographic changes driven by Late Pleistocene climatic change.

Phases of human activity at the Fincha Habera rock shelter

Human occupation of Fincha Habera has been estimated in two recent studies, and bracketed 47-31 kyr BP, with relatively large, unoccupied intervals in between. In tandem with stratigraphic observations and cultural change, the dating of nine charcoal, two giant root-rat bones and three hyena coprolites to identify the coeval presence of humans and carnivores, led to the identification of three distinct phases of human activity: Phase 1 45.6-42.9 kyr BP; Phase 2 38.9-34.9 kyr BP; Phase 3 32.1-31.2 kyr BP (Ossendorf et al. 2019, 2023).

The seven new radiocarbon dates of giant root-rats presented in this study were used to refine this chronology of human activity at Fincha Habera. Based on the combined data of 22 dates, we too identified three temporal phases between 46-31 kyr BP. However, our findings suggest an extended duration of human activity during Phase 1 and Phase 2 relative to previous estimates, narrowing the gaps between phases. Specifically, our Phase 1 estimate ranged from 45.1±0.6 to 41.4±0.6 cal kyr BP (n = 10, Figure 3), relative to 45.6±1.4 to 42.9±0.4 kyr BP in the Ossendorf et al. (2023) study. Three of our molecular dates also fell within this early time

frame; they were phylogenetically closely related to two directly dated specimens (Figure 4B). The new estimated boundaries of Phase 2 were 40.2±0.6 to 33.5±0.5 cal kyr BP (Figure 3) compared to 38.9±0.6 to 34.9±0.4 kyr BP (Ossendorf et al. 2023). Two molecularly estimated dates also fell within Phase 2. It should be noted that the two youngest age estimates of this phase were derived from hyena coprolite samples. Since coprolites were consistently found in direct association with human cultural remains within the Middle Stone Age deposits, they are interpreted as indicative for non-simultaneous cohabitation of humans and hyenas at Fincha Habera. Hence, humans and hyenas were never in the shelter simultaneously. Only when humans had left the site, even for a short time, hyenas explored the various human legacies, a behaviour that is well documented at several prehistoric sites (Campmas, Stoetzel, and Denys 2018). However, although unlikely, the absence of humans during the end of Phase 2 cannot be entirely ruled out. The youngest Phase 3, which also included 2 molecular dates, stayed essentially the same, spanning 32.4±0.4 to 31.1±0.4 kyr BP compared to 32.1±0.2 to 31.2±0.5 kyr BP (Ossendorf et al. 2023). Thus, the remaining gaps now only amount to 1,200 years and to 1,100 years, respectively, indicating longer Middle Stone Age forager activity at the site for Phase 1 and Phase 2 than initially assumed, and thus substantially shortening the hiatus between phases (Supplementary Table S5). This indicates a more regular and repeated occupation of Middle Stone Age foragers' annual or seasonal subsistence circuit, supporting previous inferences (Ossendorf et al. 2023). It is possible the high-altitude Bale Mountains have formed an integral part of prehistoric land use systems throughout the entire period of ~46-31 kyr BP.

Although the radiocarbon dates presented in this study improved our previous understanding of Middle Stone Age forager activity at the site, the dates of three new Fincha Habera giant root-rats was not in accordance to their expected date based on their position in sediment layers. Specimen 989 was excavated from the upper FHL-08 layer (Phase 2 38.9 to 34.9±0.4 kyr BP, Ossendorf et al., 2023) and specimens 681, 677 from the lower FHL-08 layer (Phase 3 32.1-31.2 kyr BP, Supplementary Table S1, Ossendorf et al. 2023). However, radiocarbon dates of these three Fincha Habera giant root-rats ranged between 41.2-44.5 cal kyr BP (Figure 2B). This suggests post-depositional processes, such as bioturbation, relocated giant root-rat samples into deeper soil layers. The coeval presence of hyenas and humans was suggested before for the site, and might explain the mixing of layers (Ossendorf et al. 2019, 2023).

Giant-root rats inform past human resource use

Nuclear genome analyses of contemporary giant root-rat individuals revealed a deep divergence of individuals in a northern and southern population (Reuber et al. 2023, preprint). All but one of the subfossil giant root-rats grouped with the northern contemporary population (Figure 4). This finding suggests the Middle Stone Age foragers limited their food provisioning activities predominantly to the northern region of the Bale Mountains and did not venture around the glacier to the south. It is rather unlikely that the hunter-gatherers were not able to cope with the harsh and glaciated environments in the south. Although the glaciers never reached Fincha Habera, geochemical studies on obsidian lithic tools recovered at Fincha Habera have shown that the Middle Stone Age foragers carried out logistical forays to extract volcanic material (obsidian) from an ice-free ridge within the glaciated regions. This suggests they were familiar with the harsh and glaciated environments (Groos et al. 2021; Ossendorf et al. 2019).

Demographic reconstruction of the northern giant root-rat population showed an increase in the rate of population decline 42-37 kyr BP (Figure 5A). Although confidence intervals remain large during this period, the decline may reflect the impact of human hunting on giant root-rat populations, supporting the hypothesis of root-rats serving as pivotal food resources for Middle Stone Age foragers occupying the Fincha Habera rock shelter 47-31 kyr BP (Ossendorf et al. 2019). Indeed, this demographic decline was not observed in the southern population, supporting our interpretation that Middle Stone Age foragers did not venture to the south for giant root-rat hunting. The decrease of the giant root-rat population could also have been influenced by its main predator, the Ethiopian wolf (Sillero-Zubiri and Gottelli 1995; Yalden 1985). However, high-coverage nuclear genome analyses revealed a population bottleneck of the Ethiopian wolf ~40-27 kyr BP (Mooney et al. 2023), wherefore we suggest that rather human presence played a significant role in the reduction of the giant root-rat population.

The high numbers of giant root-rat remains found at the Fincha Habera site indicate a sustained exploitation of the species during the time of occupation. Five 1 m^2 sections sustained approximately 10,000 faunal remains with 94-99% being giant root-rats, the majority of them showing burn marks. Given an even vertical and horizontal distribution of giant root-rat remains within the excavated sections, and the fact that the excavated area comprised approximately 2.5% of the total area, one might expect that only at the Fincha Habera rock shelter, at least 400,000 giant root-rat remains are buried in total (Ossendorf et al. 2023, Pers. comm). The consumption of rodent species is well known for other parts of the globe; subfossil remains from archaeological sites evidence for instance the use of small rodents in the eastern Andes,

in central Chile, and for the cape mole-rat in South Africa (Andrade and Fernández 2017; Fiedler 1990; Henshilwood 1997; Simonetti and Cornejo 1991), and even in recent times (Fiedler 1990).

Climate-driven demographic shifts in the south and lineage divergence

Our phylogenetic analysis revealed that the northern and southern mitochondrial lineages of giant root-rats diverged ~220 kyr BP. Landscape genetic analyses of contemporary giant root-rat mitogenomes revealed that topographic features, namely steep slopes and elevation, played a crucial role in shaping the genetic division of these clades (Reuber et al., 2023, preprint). Additionally, petrified lava streams along the northern boundaries of the Sanetti Plateau (Fig 1B) might act as physical barriers, impeding gene flow between the northern and southern populations. Moreover, the Late Pleistocene climate changes in eastern Africa, including 20-30% more precipitation than today, warm temperatures and regional vegetation changes during 200-125 kyr BP, (Schaebitz et al. 2021), may have played a role in promoting lineage divergence. This is because in warm interglacial period in the Late Pleistocene, mountainous forests and ericaceous vegetation spread which might have caused a reduction of open grasslands habitats for giant root-rats (Dupont 2011). This inference is supported by the similar timing of mitochondrial lineage divergences of other small mammals also adapted to open grassland habitats. For instance, narrow-headed voles (*Stenocranius spp.)* diverged into three main lineages, and collared lemmings into two main lineages (*Dicrostonyx spp.*), suggesting concomitant responses of species with similar habitat requirements (open grasslands) in interglacial environments (Baca, Popović, Agadzhanyan, et al. 2023; Baca, Popović, Lemanik, et al. 2023; Lord et al. 2022).

The timing of deep divergence events in our phylogeny in clades N_1 and N_2 in the north, (Figure 4B) is contemporaneous at or after the tapering off of warm and humid conditions ~120 kyr BP, transitioning towards greater aridity and colder temperatures in eastern Africa (Schaebitz et al. 2021), This suggests an environmental driver of lineage divergence. Notably, one Fincha Habera specimen clustered with the southern population but had a large number of substitutions separating it from the rest of the population. It diverged from the contemporary individuals around 80 kyr BP, which coincides with the onset of cold and arid conditions at the end of marine isotope stage 5 (Schaebitz et al. 2021). This high number of substitutions may indicate incomplete lineage sorting. Similar early glacial divergences have been observed for other cold-adapted species, such as Eurasian collared lemmings (*Dicrostonyx torquatus*) or narrow-headed

common voles (*Stenocranius anglicus; S. gregalis*) (Baca, Popović, Agadzhanyan, et al. 2023; Baca, Popović, Lemanik, et al. 2023; Lord et al. 2022).

The onset of the last glacial period ~120 kyr BP (after MIS5e) in eastern Africa brought a cooling of climate and increasing aridity resulting in the expansion of the afro-alpine habitat (Schaebitz et al. 2021). During the peak glaciation, ~42-28 kyr BP, the afro-alpine vegetation in the Bale Mountains was approximately 700 m a.s.l. lower in elevation than today and the *Erica* thickets were reduced in size (Figure 1B; Groos et al. 2021; Ossendorf et al. 2019). Our phylogeny suggests that the northern giant-root rat population expanded before the glaciation (70-50 kyr BP), as indicated by many divergences among the Fincha Habera specimens during that time (Figure 4B). The local last glacial maximum (42-28 kyr BP) aligns with a 30% population decrease in the south (Figure 5B; Groos et al. 2021). During glaciation, giant root-rats in the south likely shifted their range to ice-free refugia, either towards the margins of the Sanetti Plateau or downhill which would have been feasible due to the lower afro-alpine vegetation (Casas-Gallego et al. 2023; Groos et al. 2021). Although speculative, this population decline may have had adverse effects on the Ethiopian wolf, which experienced a population bottleneck ~40-27 kyr BP (Mooney et al. 2023), potentially in response to the decline in giant root-rats as a primary food resource.

The demographic reconstruction of the southern population indicated a post-glacial population expansion ~15 kyr BP (Figure 5B), coinciding with several coalescent events within the contemporary southern individuals (~14 kyr BP) (Figure S2), and their star-like topology in the haplotype network (Figure 4A). As the glaciers melted and permafrost thawed (~16 kyr BP, Groos et al. 2021), giant root-rats were able to recolonise the plateau with lower genetic diversity of contemporary samples from the more central part of the plateau region supporting recolonization from southern refugia (Reuber et al. 2023, preprint). This population expansion might have been supported by the increase in human presence across the Bale Mountains 4.5-1.7 kyr BP. According to Tariku (2021, MA thesis), the functionality of rock shelters in the area underwent changes during this period, characterised by the presence of charcoal-rich deposits, increased faunal remains, especially small bovids, hares and hyraxes, and distinct lithic assemblages, suggesting larger groups of humans, longer occupation durations, and potentially more intensive settlement activities (Tariku 2021, MA thesis). The expanding human presence likely led to landscape clearance by burning the *Erica trimera* thickets, creating a more suitable habitat for the giant root-rats, which thrive in areas dwarf afro-alpine shrublands and grasslands (Miehe and Miehe 1994; Sillero-Zubiri et al. 1995; Šklíba et al. 2017). This suggestion finds

support in recent autecological studies of the species, which revealed increasing giant root-rat activity with increasing livestock (Asefa et al. 2022).

The demographic reconstruction of the northern population showed a different pattern (Figure 5A), supporting inferences of an absence of gene flow between north and south concluded from nuclear analysis of contemporary individuals (Reuber et al. 2023, preprint). After the initial 30% decline ~42-37 kyr BP, which we hypothesise was associated with human offtake, we observed a stable population size until ~27 kyr BP. The subsequent continuous population decline until 5 kyr BP coincides with the mitochondrial lineage divergences of the contemporary individuals starting ~25 kyr BP (Figure S2). The northern population continuously decreased until ~5 kyr BP, losing almost 80% of its pre-glacial size, which is also indicated in the lower mitochondrial nucleotide diversity of the northern contemporary samples (Supplementary Figure S3).

We suggest that the population decline in the north might be environmentally driven. For the Bale Mountains, analyses of lacustrine sediments suggest an abrupt onset of the African humid period 15 kyr BP (Mekonnen et al. 2022). Pollen analysis indicated an expansion of the Ericaceous Belt on parts of the Sanetti Plateau and a decrease of afro-alpine vegetation during the early to mid-Holocene, as a consequence of the warm and humid climate (Gil-Romera et al. 2019; Umer et al. 2007). While the climatic conditions might have been too severe (above 3,800 m a.s.l.) for a full coverage of *Erica* on the plateau (Mekonnen et al. 2022), the generally milder conditions in the less-elevated northern part could have favoured the spread of *Erica* thickets or forests in close vicinity to Fincha Habera. Generally, the afro-alpine vegetation decreased after the last glacial period until today in the Ethiopian mountain ecosystem (Casas-Gallego et al. 2023) which likely led to a reduction of the root-rats natural habitat and thereby causing the population decline.

Temporal variation in isotopic signatures

The δ^{13}C values obtained from both Fincha Habera specimens and contemporary samples showed an average of -21.55 (‰) which is consistent with the expected values for a herbivorous species inhabiting cold climates with a predominant diet of herbaceous C_3-plants, i.e. mainly *Alchemilla abyssinica* followed by *Festuca* (grasses) and *Trifolium* species (Supplementary Table S6; Bocherens 2003; Šklíba et al. 2017; Yaba et al. 2011; Yalden 1975). Interestingly, our dataset revealed elevated bone collagen δ^{13}C values in the Fincha Habera specimens relative

to the contemporary samples (Figure 6A). As Fincha Habera specimens originate from the last glacial period within the Bale Mountains (Ossendorf et al. 2019), differences in isotopic composition may either indicate shifts in food resources and diets, or environmental disparities between the Late Pleistocene period and the present. We propose that the elevated δ^{13}C values in the Fincha Habera specimens were influenced by the environmental conditions during that time, as water stress can increase δ^{13}C values (Rey-Iglesia et al. 2021; Stewart et al. 1995). Although glaciers did not extend to the Fincha Habera rock shelter, a significant portion of water during this period was stored in the valley glaciers and in the ice cap on the Sanetti Plateau, leading to limited water availability in the region (Ossendorf et al. 2019), which might have increased δ^{13}C values within the collagen of the herbivorous giant root-rat.

We ruled out differences in food choices as factors causing the different carbon isotopic signatures, as we observe no difference in δ^{13}C between contemporary individuals from the north and south, which suggests similar foraging ecology in both populations.

In addition to δ^{13}C, we observed elevated δ^{15}N in the Fincha Habera specimens relative to the contemporary individuals (Figure 6B), which, similar to carbon stable isotopes, might be attributed to limited water availability during the Late Pleistocene in the Bale Mountains (Ossendorf et al. 2019). A decrease in nitrogen levels from the last glacial period to the present has also been reported for other herbivorous species such as for the European reindeer (Stevens et al. 2008).

Regarding the contemporary samples, we noticed larger variation in carbon and nitrogen stable isotopes for the southern population, possibly due to the larger spatial scale on which southern bone samples were collected, leading to more variable climatic conditions that presumably affect food resource availability (Figure 6). Although giant root-rats feed on the same plant species across their distribution range, the composition of *Alchemilla* and *Festuca* species might vary according to their availability, influenced by the local climatic conditions (Yaba et al. 2011).

5.5. Conclusion

In conclusion, the ecological and evolutionary history of the giant root-rat provides new insights into the archaeological context of the Middle Stone Age foragers resource utilisation and high-altitude residency during the Late Pleistocene, and reveals the species responses to human influences and environmental change. Integrating ancient DNA and radiocarbon dating, we

revealed prolonged human activity with narrow temporal gaps between phases at the Fincha Habera archaeological site. This is indicative of relatively regular seasonal habitation at the oldest human high-mountain residential site. The Middle Stone Age foragers' reliance on giant root-rat as food resources was reflected in the species' demographic decline during the occupation. Further, Late Pleistocene climate change shaped lineage divergence and demographic shifts of the giant root-rat, demonstrating the close interaction between the species and its environment over long temporal scales. Reduced genetic diversity of contemporary populations in comparison to subfossil specimens reflects the severe impact of habitat and associated population reduction on a species genetic variation, which is fundamental for a species resilience. Our study shows that ancient DNA from subfossil specimens from Africa opens up new research possibilities not only to understand Middle Stone Age human dispersal and resource exploitation strategies, but concomitantly demonstrates the tight interaction between the ecological and evolutionary history of a species in relation to human impacts and environmental change.

Supplementary material

Supplementary material to this chapter can be found in Supplementary material Chapter V.

Chapter VI — Synthesis

Species-environment interactions build the backbone of biodiversity and ecosystems. Understanding how species are affected and structured by the environment across spatial scales and over time, and how they are disrupted by human activities is important to predict and reverse the ongoing decline in biodiversity worldwide. In this thesis, I examined how the giant root-rat, a range-limited, fossorial rodent species endemic to the bale Mountains in southern Ethiopia, is shaped by its environment and human activities. These investigations spanned from present, local environmental conditions to the species' entire distribution range, and to past environmental conditions and their effect on the genetic structure and population dynamics of the species.

6.1. Environmental conditions and human activities drive activity of giant root-rat at local scales

Ecosystem engineers, such as many fossorial rodents, possess the ability to shape landscapes through soil perturbation and herbivory (Huntly and Reichman 1994; Jones et al. 1994; Kraus et al. 2022; Reichman and Seabloom 2002). Concurrently, their activity is influenced by environmental conditions (Eldridge and Whitford 2014; Reichman 1975; Vlasatá et al. 2017). In the context of Chapter II, Addisu Asefa and I aimed to examine the ecosystem engineering role of the giant root-rat and its intricate relationships with environmental conditions and human land-use in the Bale Mountains. To this end, we conducted an ecological field study, collecting data on 25 x 25 m plot level on burrow density (as a proxy for giant root-rat activity), vegetation cover, plant species richness, soil moisture, temperature, and number of cow dung (as proxy for livestock grazing intensity) on 62 plots, and analysed their interrelation using reciprocal path analyses.

Through the path analysis, we found that increasing giant root-rat activity reduced vegetation cover, presumably due to soil perturbation and herbivory of the species. During the excavation of burrow systems, freshly perturbated soil covers short vegetation, while the species' herbivory actively reduces the vegetation cover (Hausmann, 2017, Wu et al. 2015, Skliba et al. 2017). In the reciprocal path model, giant root-rat activity increased with decreasing vegetation cover and elevated livestock grazing intensity, which indicates the preference of the species for open habitats (Sillero-Zubiri et al. 1995; Yalden 1975). The fact that giant root-rat activity increased with livestock grazing contradicts our initial hypothesis and may suggest that giant root-rats

predominantly feed on below-ground vegetation organs in areas with livestock presence, thus avoiding negative influences from livestock. Furthermore, we observed that giant root-rat activity increased with species richness, which might be a by-product of the species' habitat preference for wet soils (Sillero-Zubiri et al. 1995; Šklíba et al. 2020; Yalden 1975). Our analysis revealed that giant root-rat activity increased with soil moisture, possibly because wetlands exhibit easy to dig soils (Sillero-Zubiri et al. 1995). Our findings illuminate the tight, complex interaction between the species, local environmental conditions and human activity.

6.2. Texture metrics define the giant root-rats' distribution range at landscape scale

While ecological field studies are useful to examine local species-environment interactions, remote sensing allows us to extend these analyses to the landscape scale. The distribution of animal species is often linked to above-ground features such as plant species composition or landscape structure (Culbert et al. 2012; Estes et al. 2010; Grigusova et al. 2021). Therefore, satellite-based remote sensing approaches can be used to predict the distribution of fossorial species that leave distinct landscape marks above ground (Koshkina et al. 2020). In my third chapter, Luise Wraase and I aimed to predict the range-wide distribution of the giant root-rat across the landscape in the Bale Mountains. We used a combination plant species composition data from giant root-rat presence and absence areas (47 plots each) collected in the field, and remotely derived satellite data. With this approach, we upscaled the species-environment interaction from the local scale to the landscape scale and thereby identified the factors shaping the overall species' distribution. We compared three machine learning-based modelling strategies that included no, some and extensive fieldwork data to test how such data improves prediction quality, in comparison to remote sensing data.

The model which included no field work data was based on visually selected training areas (data points) of giant root-rat presence on a Google Earth image, and showed the best species distribution prediction. This was likely due to the spatial coverage of the training areas covering the species' distribution range (Berhane et al. 2019; Hengl 2007; Warren et al. 2014). The main factors for the prediction of the species' distribution range were texture metrics, i.e. remotely derived indices that described for instance topographic differences across the landscape. The model using plant species composition data from giant root-rat presence and absence areas as training data, showed the lowest accuracy despite the well-known impact of giant root-rats on vegetation (Miehe and Miehe 1994; Sillero-Zubiri et al. 1995; Šklíba et al. 2017; Yalden 1975).

One explanation might be that the spectral difference of plant species between areas with and without giant root-rat activity was not pronounced enough to reliably indicate their presence or absence. In fact, the most abundant plant species in presence and absence areas was *Alchemilla abyssinica*. Thus, the spectral differences between both areas was presumably not strong enough to predict either giant root-rat presence or absence. Our findings suggest that impacts of the species on its biotic environment, like plant species composition is not a reliable predictor for species distribution in a homogenous environment. Nevertheless, in arid ecosystems with sparse vegetation, remote sensing data enables accurate species distribution predictions by tracing above-ground landscape marks created by the species, which is especially useful in remote areas.

6.3. Topographic barriers drive genetic subdivision

Ecological and remote sensing studies assess the present species-environment interaction but lack a temporal scale. By utilizing genetic data, I aimed to integrate the temporal perspective on species-environment interaction, as the long-term impact of the environment is reflected in the species' genetic population structure and diversity. Fossorial species with predominantly below-ground activity often exhibit limited dispersal ability and a localized distribution. This leads to small and isolated groups of individuals with low genetic variation and increased population subdivision across relatively small spatial scales (Mirol et al. 2010; Nevo 1999; Schweizer et al. 2007; Šklíba et al. 2020; Tucker et al. 2014). Such patterns may be exacerbated in harsh mountain ecosystems, where landscape geomorphology additionally limits species' dispersal ability (Badgley et al. 2017; Rahbek, Borregaard, Colwell, et al. 2019). In my fourth chapter, I analysed the spatial genetic subdivision and diversity of the giant root-rat across its distribution range. I further utilized landscape genetic analysis to elucidate the long-term influence of the environment on the species (Avise 2000; Berthier et al. 2005; Manel et al. 2003).

I generated complete mitochondrial and low-coverage nuclear genomes from tissue samples of 77 giant root-rat individuals sampled in the Web valley (north) and the Sanetti plateau (south) of the Bale Mountains (Figure 1.1). I found a distinct division of the giant root-rat individuals into a northern and a southern population, with no signs of gene flow between them on the nuclear level. Two mitochondrial genomes from individuals sampled in the south clustered with the northern population, but nuclear genome analyses revealed that this pattern was caused by incomplete lineage sorting, and not recent or ancient gene flow between the populations.

Landscape genetic analyses of the mitochondrial genomes indicated that the pronounced division between populations was driven by topographic barriers, specifically steep slopes and elevation differences between the north and south. Despite this pronounced subdivision observed at the range-wide landscape scale, I found only weak geographic structuring of sampling localities within populations on the local scale. This contradicted our initial hypothesis, as we expected strong genetic subdivision on small spatial scales. In fact, in combination with the low genetic differentiation within populations, my results indicated gene flow across distances of at least 13 km. This suggests above-ground dispersal and high mobility for relatively long distances for the giant root-rat. Consequently, and confirmed by the landscape genetic analysis, vegetation and soil moisture, played less of a role in hindering gene flow at the range-wide landscape scale, although these factors have been identified as essential factors influencing the local abundance of giant root-rats (Asefa et al. 2022; Sillero-Zubiri et al. 1995; Šklíba et al. 2020). Despite their relatively high local dispersal ability, my findings demonstrate that the northern and southern population must be considered separately when developing conservation strategies as there is no opportunity for dispersal and gene flow between them.

6.4. Late Pleistocene climatic change and human activity shaped species' evolutionary history

By analysing ancient DNA, I included another temporal scale variable, examining species-environment interactions over millennia. Ancient DNA research on terrestrial mammals has revealed the impact of environmental changes and human activities during the Late Pleistocene on species' populations structure and demography (Baca, Popović, Lemanik, et al. 2023; Campos et al. 2010; Graham et al. 1996). In turn, for instance species demography can reveal insights into early human presence and resource utilization (e.g. Yu et al. 2022). Such inquiries deepen the understanding of how species respond to environmental changes and humans, which is a precondition to protect species in the future. Thus, in Chapter V, I explored the phylogenetic divergences and demographic history of the giant root-rat during the Late Pleistocene climatic change in Africa, in the context of human high-altitude residency and human resource use of the giant root-rat. I used biomolecular approaches of ancient DNA, radiocarbon dating, and stable isotope analysis (carbon and nitrogen) on 18 subfossil giant root-rat specimens from the Late Pleistocene, which were discovered at the Fincha Habera rock shelter in the Bale Mountains. Middle Stone Age foragers repeatedly occupied the rock shelter around 47,000 to

31,000 years ago used giant root-rats as main food resource, indicating that species was shaped by humans across millennia (Ossendorf et al. 2019).

I radiocarbon dated seven subfossils and applied phase models to all published, radiocarbon dated material from the site. Radiocarbon and molecular dating placed the giant root-rat Fincha Habera specimens between ~44,000 to 32,000 years ago and revealed an almost continuous occupation of the site by Middle Stone Age foragers. With the demographic reconstructions using 13 ancient and 77 contemporary mitochondrial genomes, I found that the northern population experienced a decline during the period of human occupation, possibly due to intensive hunting. Further, the phylogenetic analysis uncovered that the giant root-rat species diverged into the northern and southern populations approximately ~220,000 years ago. I found a demographic decline in the southern population during the Late Pleistocene glaciation of the Sanetti Plateau (42,000-16,000 years ago, Figure 1.1; Groos et al. 2021; Ossendorf et al. 2019), followed by an increase after the deglaciation period. The northern population showed a decline since the African Humid period (~ 15,000 years ago), which correlates with the reduction of afro-alpine vegetation since the end of the last glacial (Chapter V) (Casas-Gallego et al. 2023; Gil-Romera et al. 2019; Mekonnen et al. 2022). Importantly, this continuous decline may explain the lower mitochondrial genetic diversity found in contemporary individuals compared to ancient individuals. The stable isotope analysis of ancient and contemporary bone samples might indicate less water availability during the Late Pleistocene than today (Bocherens 2003; Stevens et al. 2008), presumably because most of the water during that time was stored in the glaciers on the Sanetti plateau and adjacent valleys (Ossendorf et al. 2019).

6.5. General conclusion

All presented studies in this thesis showed the complex and strong interplay between the giant root-rat, environmental conditions and human activities in the Bale Mountains ecosystem. My studies showed that the interplay varies from local (Chapter II) to landscape scale (Chapter III) and is highly dynamic over time (Chapter IV and V). I can derive three main implications from my chapters, which relate to species' persistence and functionality of mountain ecosystems which they inhabit.

Species-environment interaction is scale dependent

Firstly, by employing a combination of methods, I found that the interaction of the giant root-rat with its environment is scale dependent. The environmental conditions shaping the species' local activity, differ from those determining the species' distribution range. Thereby, my findings emphasize that species engage with their environment through diverse mechanisms, and that the interaction depend on either the scale at which the species experience their environment, or the scale at which extrinsic processes generate heterogeneity.

The ecological field study showed that vegetation cover and soil moisture determined giant root-rat activity at the local scale, underscoring the strong short-term impact of these factors on a species with limited rather dispersal ability (Chapter II). In contrast, those factors played a subordinate role considering the range-wide distribution of the species. The remote sensing (Chapter IV) and landscape genetic analyses (Chapter II) revealed that on the landscape scale, topographic barriers determined giant root-rat distribution and dispersal. Hence, my findings suggest that giant root-rats are unable to traverse topographic barriers due to their predominant below-ground activity, which exerts a lasting impact on their overall distribution. Taken together, this highlight that species with limited dispersal might be particularly vulnerable to environmental changes (Crawford et al. 1993; Eldridge and Whitford 2014; Reichman 1975; Vlasatá et al. 2017). While species in more homogenous environments or those with greater dispersal abilities can relocate to suitable habitats, this may not be feasible for fossorial species in mountain ecosystems due to landscape geomorphology (Hoffmann et al. 2017).

Giant root-rats are shaped by environmental conditions over time

Secondly, apart from the influences of local environmental conditions on the species, I could show historical influences of the environment on giant root-rats by analysing their genetic structure and demography (Chapter IV, V). Elevation and slope likely caused a pronounced lineage divergence ~220,000 years ago which presumably led to the subdivision into two populations. Importantly, I found that the northern population declined since the African Humid period, which correlates with the reduction of afro-alpine vegetation since the end of the last glacial, and might have caused lower nucleotide diversity in contemporary individuals (Chapter V) (Casas-Gallego et al. 2023; Gil-Romera et al. 2019; Mekonnen et al. 2022). This assumption is supported by our finding, that giant root-rat activity decreased with vegetation cover as observed in the ecological field study.

Combining the findings of the ecological field study with the demographic reconstructions of the giant root-rat, helps to infer future scenarios for the giant root-rat and other fossorial rodent species in high altitude ecosystems. Demographic declines as a consequence of habitat reduction and associated loss in genetic diversity, suggest that future climatic or environmental changes may potentially threaten the persistence of fossorial species that are adapted to open grasslands. Mountain ecosystems are experiencing some of the highest rates of warming under anthropogenic climate change and which alters vegetation compositions (Lamprecht et al. 2018; Lenoir et al. 2008; Rangwala and Miller 2012; Steinbauer et al. 2018). Increasing temperatures have been observed for instance in the Tibetan highlands or the Andes (Rangwala and Miller 2012; Yang et al. 2012). Also in Ethiopia, temperature increases have been recorded over the last decades and analyses suggest, that the southern highlands of Ethiopia will continue to experience elevated temperatures and decreasing precipitation (Gebrechorkos, Hülsmann, and Bernhofer 2019; Jury and Funk 2013). As a consequence, for the Bale Mountains ericaceous vegetation is expected to shift upwards mountain slopes and may potentially outcompete typical afro-alpine vegetation (Casas-Gallego et al. 2023; Kidane et al. 2022). Reduced afro-alpine vegetation and increasing aridity limits habitat availability for species adapted to open grasslands. For the giant root-rat this may lead to further population declines and loss of genetic diversity. In addition to their lower dispersal, the typically strong genetic subdivision and small population sizes likely makes fossorial species especially vulnerable to environmental change (Hoffmann et al. 2017; Lande 1988; Willi et al. 2006).

Human activities shape giant root-rats

Third, I found that giant root-rats are shaped by present and past human activities, which may have strong implications for future ecosystem processes in the Bale Mountains. We found that giant root-rats are positively influenced by livestock grazing (Chapter II) while another study of our research consortium found that giant root-rat activity increases in the proximity to permanent settlements (Asefa et al. 2023). Over the past few decades human settlements and livestock grazing intensified within the borders of the Bale Mountain National Park which likely enhanced clearance of the landscape (Gashaw 2015; Mekonen 2020; Stephens et al. 2001) and thereby to elevated habitat availability for giant root-rats. Similar scenarios have been observed in other mountain ecosystems with consequences for ecosystem functionality (Chen, Yi, and Qin 2017; Feng et al. 2020).

Many mountain ecosystems experience grassland degradation due to livestock grazing and climatic change (Gao et al. 2010; Gibbs and Salmon 2015; Miehe et al. 2008; Payne et al. 2017), which can promote the activity of fossorial rodent species (Feng et al. 2020). At the same time, mountain ecosystems provide disproportionally high biodiversity and contribute to many ecosystem functions including water conservation and carbon storage (DeLuca and Aplet 2008; Padilla et al. 2010; Ruiz et al. 2008). Elevated burrowing activity of fossorial rodent can reduce soil moisture and hardness. This, in turn can lead to enhanced soil erosion, limited vegetation restoration, and negatively impact water conservation, as observed for instance for plateau pikas (*Ochotona curzoniae*) on the Tibetan highlands (Chen et al. 2017; Feng et al. 2020). Consequently, increasing populations of fossorial species due to human habitat degradation, may contribute to desertification and disrupt ecosystem functionality. This effect could be intensified, if fossorial species become more abundant in the future with rising temperatures in mountain ecosystems, which is for instance predicted for the northern pocket gopher *Thomomys talpoides,* in Colorado (USA) (Lynn et al. 2018).

The positive effect of livestock grazing on the giant root-rat was unexpected, as it is postulated that one of the major threats for the species is habitat degradation (Lavrenchenko and Kennerley 2016). Thus, alternatively, more settlements and livestock grazing could also pose problems for the giant root-rat when resources are overexploited. Additionally, hunting of the species, as revealed by the ancient DNA study, has historically decreased its population size, at least in northern region of the Bale Mountains (Chapter V). Decreasing activity of fossorial species may disrupt the natural regeneration of the ecosystem adapted to bioturbating activity, as they contribute to ecosystem functionality by altering soil environments, promote plant community diversity, and create habitats for other species (Jones et al. 1997; Reichman and Seabloom 2002; Yoshihara et al. 2009; Zhang 2007; Zhang et al. 2003). In fact, fossorial rodents may also contribute to the regeneration of degraded grasslands, as for instance suggested for Mongolian grasslands (Yoshihara et al. 2009). In conclusion, both scenarios, thus unregulated increase or drastic population declines of the giant root-rat, may potentially threaten ecosystem functionality and thus should be given due consideration in conservation management efforts, due to their role as ecosystem engineers.

Final remarks

With the giant root-rat as a prime example, this thesis underscored the intricate and multifaceted relationship between an endemic species, its environment, and human activities, as they evolve across time. The inferences drawn from this study shed light on the inherent vulnerability of species within mountain ecosystems. The Bale Mountains and many other high-altitude ecosystems, stand out as biodiversity hotspots (Myers et al. 2000; Rahbek, Borregaard, Colwell, et al. 2019). Geomorphological attributes and harsh environmental conditions have been pivotal in driving the emergence of endemic flora and fauna in mountain ecosystems, and likely play a role in maintaining biodiversity. Approximately 87% of amphibians, birds and mammals inhabit mountain regions, and large numbers of these are endemic to mountain ecosystems (Myers et al. 2000; Rahbek, Borregaard, Antonelli, et al. 2019; Rahbek, Borregaard, Colwell, et al. 2019). However, habitat modification and climatic changes evoke environmental changes which, as demonstrated in the case of the giant root-rat, may imperil many of these species with limited dispersal abilities, warranting careful consideration in the formulation of conservation strategies (Hoffmann et al. 2017; Lande 1988; Willi et al. 2006). In regard to the Bale Mountains, traditional housing currently seems not to pose a threat to the giant root-rat, however, the construction of more distinct barriers would presumably further limit gene flow subdividing populations. In fact, because an expansion of human settlement leading to more habitat encroachment is expected and climatic change is ongoing, plans exist for relocation of some individuals to nearby Arsi mountains to create reserve population in case the Bale giant root-rats are in the risk of extinction (Kasso M. and Lavrenchenko L. personal communication). Hence, clearly habitat protection would be advisable for the protection of the giant root-rat and other mountain species. Understanding the interplay among environmental conditions, humans and species is crucial for effectively managing and conserving the afro-alpine ecosystem functionality and biodiversity, and other similar environments where species and their habitats are closely intertwined.

Chapter VII — Perspectives

Throughout the chapters of my thesis, I have explored the interactions between the giant root-rat and the afro-alpine ecosystem of the Bale Mountains across different spatial scales and over time. While this study has provided valuable insights, it has also given rise to several intriguing questions that remain unanswered. In this final chapter, I aim at emphasizing some of these open questions and outline promising directions for future research.

In chapter II, we found that giant root-rat activity increased with livestock grazing, but this relation and the consequences for the Bale Mountain ecosystem are not entirely clear yet. In regard to this finding, two future questions should be tackled. Firstly, comprehensive field-research should be conducted spanning both the dry, and wet seasons of the Bale Mountains over several years. This effort aims to elucidate if livestock grazing adversely impacts fossorial rodent species over the long term. Secondly, if livestock grazing indeed is promoting giant root-rat activity, it should be investigated if intensified burrowing activity of the species leads to accelerated desertification of the ecosystem. Thereby, grassland degradation can further be intensified, analogous to the observed scenario with plateau pikas (Chen et al. 2017; Feng et al. 2020). Since mountain ecosystems provide disproportionally high biodiversity (Rahbek, Borregaard, Antonelli, et al. 2019; Rahbek, Borregaard, Colwell, et al. 2019) and contribute to many ecosystem functions including water conservation and carbon storage, it is necessary to clarify cascading effects of habitat degradation on biotic and abiotic conditions. Field studies investigating fossorial species and their interaction with the environment, should therefore measure soil moisture, soil hardness and soil texture composition in areas with and without fossorial activity. Soil moisture and soil hardness could be directly measured *in-situ*, while soil cores could be collected to assess topsoil gravel content in the laboratory (Chen et al. 2017; Feng et al. 2020).

The complex relationship between giant root-rat activity and livestock grazing highlights the importance to further develop methods that allow to observe fossorial animal species quickly and with little effort across large spatial extends. This is another research gap that I did not entirely filled in the course of my thesis. In chapter III, Luise Wraase and I developed a remote sensing approach to effectively observe the giant root-rat across its distribution range. However, we did not test if our method is applicable to other ecosystems or species. For instance, the sister species of the giant root-rat (*T. splendens*) has a widespread distribution throughout East Africa and inhabits a variety of habitats, ranging from tropical moist forest and open woodland

to savanna habitats, grasslands and agricultural areas, including coffee plantations and pasture areas (Jarvis 2013; Monadjem et al. 2015). Many fossorial species are distributed across much larger ranges than the giant root-rat and are there more difficult to observe, such as *Ochotona curzoniae*, *Marmota caudata* or *Microtus arvalis* (Krystufek and Vohralik 2013; Shenbrot and Krasnov 2005; Smith et al. 1990). Hence, their distribution range is more heterogenous, wherefore the landscape marks the species leave above ground may be more difficult to detect remotely. Especially the body size of the fossorial species may play a role here, as smaller burrowing species excavate less amount of soil (e.g Kraus et al., 2022). Testing our remote sensing approach to varying ecosystems and species thus would broaden its applicability to a wider range of the research community and help to detect changes in ecosystem functionality related to fossorial species.

The increasing threats imposed on species under present environmental and climate change lead to my next suggestion for future research. In chapter IV, I assessed genetic diversity for the giant root-rat. However, I did not analyse genetic diversity in comparison to other fossorial rodent species which may help to identify species threatened by genetic depletion. Large genetic variation means a great variability in phenotypes to cope with or adapt to new climates (Frankham et al. 2002), and further gives insights into the evolutionary history of the species. To start with, future studies could concentrate on the members of Spalacidae family, which predominantly follow a subterranean lifestyle and have their main distribution in East Asia and Africa (Begall et al. 2007). To do so, sequences from individuals should be chosen who have been collected within a similar range as the giant root-rat individuals, as genetic distance usually increases with geographic distance (e.g. Berthier et al. 2005), potentially leading to distorted results.

In chapter IV, I also utilized landscape genetic analyses with remotely derived data to explain genetic differentiation and to identify potential gene-flow barriers of the giant root-rat. However, I did not explore, how future climate change might reduce the species' range and thereby influence the genetic structure or diversity, although genetic diversity is one of the main components for a species' resilience in a changing environment (Frankham et al. 2002; Parmesan 2006). The reduction of geographic range can spiral into a feedback loop, where genetic diversity loss further increases the risk of species extinction. Building on this knowledge, two potential steps could follow.

First, by modelling habitat changes under future climatic scenarios, regions where populations might become isolated or restricted in their distribution could be identified, for instance using a classic climate change scenario of the Intergovernmental Panel on Climate Change (e.g. "business-as-usual" scenario 2080; IPCC, 2023). A reduction in habitat usually leads to a intraspecific loss of genetic diversity, as certain haplotypes of a species could vanish (Exposito-Alonso et al. 2022; Parmesan 2006). For illustration of how genetic diversity can reduce if the population size decreases, I applied a simple scenario for the giant root-rat. I calculated nucleotide diversity using the complete mitochondrial genomes of contemporary individuals (Chapter IV). I assumed that individuals
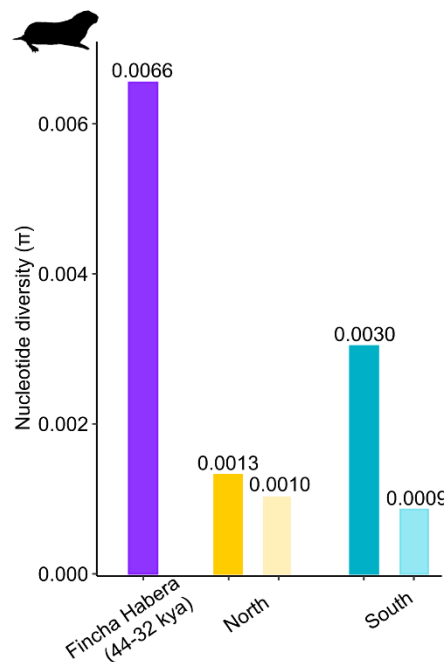
Figure 5.1: Nucleotide diversity estimates for ancient (Fincha Habera) and contemporary giant root-rat populations north and south. Light yellow and light turquois bars represent reduction of either population by individuals of lowest elevation locality.

from the lowest elevation localities in the north and south (localities N1 and S3, Figure 1C, Chapter IV) disappear due to climate-driven upslope movement of ericaceous vegetation (Casas-Gallego et al. 2023; Kidane et al. 2022). In such simple scenario, nucleotide diversity is reduced by 24% in the northern population and by 70% in the southern population (Figure 6.1). Similarly, nucleotide diversity of Late Pleistocene Fincha Habera specimen was five times higher compared to contemporary individuals from the north, highlighting the loss of genetic diversity with decreasing population size. Indeed, demographic analyses indicated that northern giant root-rat population size has decreased by approximately 80% since the Late Pleistocene until today (Chapter V). Thus, a comparable approach applied to other fossorial species living in similar environments, could help to identify species with particularly low genetic diversity which can be used to inform conservation practitioners.

Second, looking at past climatic stability across a species' range can give information about genetic variability of a species and certainly delivers information about a species' resilience (Pauls et al. 2013). Genetic diversity is supposed to be higher for species which have experienced climatic stability in the past (Yannic et al. 2013). This has been evaluated for instance for the Caribou, for which researchers identified that the two existing lineages of the species experienced varying climatic changes, and that the lineage which experienced less instability showed a higher genetic diversity (Yannic et al. 2013). Further, genetic diversity is

supposed to be higher in regions with future climate stability (Yannic et al. 2013). Hence, studies could assess climatic stability for the past and the future of certain mountain ecosystems, to gain valuable insights into evolutionary history and adaptive potential of fossorial species inhabiting those. In the case of giant root-rats, this would also inform conservation practitioners in regard to the persistence of the highly endangered Ethiopian wolf. This iconic canid species of the African continent exhibits extremely low population sizes (Martínez-Navarro et al. 2023). In the Bale Mountains, its main prey is the giant root-rat, wherefore the rodent species is crucial for its persistence (Sillero-Zubiri and Gottelli 1995). Already, future climatic scenarios indicate drastic habitat shrinkage, posing a severe threat to the wolf's survival by potentially bringing it close to extinction by 2100 (Martínez-Navarro et al. 2023).

Generally, the interaction between the Ethiopian wolf and the giant root-rat should further be examined. The recent discovery of an Ethiopian wolf fossil, suggests a minimum of 1.6 - 1.4 million years for the species' presence in Africa. According to Šumbera et al., 2018, giant root-rats diverged from its sister species ~1.3 million years ago, while the entire genus *Tachyoryctes* diversified ~ 2.1 million years ago, which could indicate some sort of co-evolution between root-rats (*Tachyoryctes sp.*) and Ethiopian wolves. Interestingly, Mooney et al. (2023) found evidence of a bottleneck event for the wolf population between 40,000 and 27,000 years ago, which coincides with the population decline of the norther giant root-rat population (Chapter V) (Mooney et al. 2023). This suggests a possible dependence of the predator on the giant root-rat, at least in the Bale Mountains. In turn, the dorsally located eyes located on the top of giant root-rat heads indicate their morphological adaptation to spot predators in the open landscape (Šumbera et al. 2018). These adaptations raise questions about the high-altitude adaptations of both species, warranting further research in this area.

Acknowledgments

Nach fast vier Jahren Doktorarbeit wird es nun dringlichst Zeit all den Personen zu danken, die mich auf meiner Riesenmaulwurfsratten-Reise begleitet haben und überhaupt, mir die Möglichkeit gegeben haben in diesem einzigartigen Projekt mit zu wirken.

Zuallererst möchte ich mich bei dir bedanken, liebe Dana, für all deine Unterstützung über die letzten Jahre! Was mit der gemeinsamen Feldarbeit in Bale begann, bei minus Temperaturen und stundenlangem Warten vor Maulwurfrattenbauten, und weiter ging über stete Unterstützung auf statistischer oder emotionaler Ebene. Vielen Dank für dein Verständnis und dein Vertrauen in meine Arbeit, für deine offene und lockere Art und dass du mir das Gefühl vermittelt hast, keine Frage ist zu dumm um sie zu stellen. Ich hatte eine gute Zeit und war stets froh von dir betreut zu werden.

Einen herzlichen Dank geht auch an die anderen Mitglieder der Prüfungskommission. Ein besonderer Dank an dich Nina, deine Zuverlässigkeit, und Fähigkeit, für alle Probleme eine Lösung zu finden. Ich danke dir das du mir die Möglichkeit gegeben hast, in dieser wunderbaren AG meine Dissertation durchführen zu können. Vielen lieben Dank Lars, für deine kritischen Fragen und guten Ideen, dich mich auf jeden Fall dazu gebracht haben über den Tellerrand zu blicken, und generell für das Bale Projekt und für die Möglichkeit darin mitzuwirken. Many thanks also to you Eline. I am very grateful that you gave me the opportunity to work in your lab, for opening up the world of genetics to me and for guiding my way through scientific writing. I am sincerely grateful for your expertise and the excellent discussions.

Special thanks to Alba and Mick. Alba, thank you so much for showing me the way through the lab and for countless zoom-talks. Your support was truly invaluable. Many thanks also to you Mick and for your great support throughout this entire project.

Many thanks to my project partners and field buddies Addisu, Mohammed and Luise. Addisu, it was great working with you over the last years, thanks a lot for all your support and guidance in the field. Liebe Luise, ob bei der Feldarbeit, beim Schreiben von Manuskripten, analytischen Support, Remote Rensing Erklärungen oder das Teilen des Disney-Plus Channels, auf dich kann man sich verlassen und stets ein gutes Pläuschchen halten. Vielen Dank für den gemeinsamen Weg über die letzten vier Jahre. Lieber Georg, vielen Dank für deinen Enthusiasmus das Rätsel der Mole-rats und der Menschen zu lösen!

Insbesondere möchte ich auch meinen (ehemaligen) Mitstreiter*innen aus der AG Naturschutz danken! Julia, vor allem für deinen Support in den letzten Tagen, Diana, für die vielen tollen Bürogespräche, Kim, Finja, Nadja, Annemarie, Eva, Finn und Marcel! Vielen Dank für die teilweise therapeutischen Mittagspausen, für die offenen Ohren und dir kreativen Ideen.

Ein gesonderter Dank and Kati und Stefan fürs Korrektur lesen der Arbeit!

Des Weiteren möchte ich meinen Freund*innen Nici, Gerrit und Janina, Nanni und Caro danken!! Ihr seid alle nun schon so lange an meiner Seite, ich hoffe es geht noch lange so weiter. Vielen Dank für euren Unterstützung, die gemeinsame Zeit, das zusammen Lachen und eure Liebe! Ich freue mich auf unsere nächsten Jahre. Und natürlich danke ich meinen Hummeln aus Mainz und den Grassenbergis, für all die Wunderbaren Abende und das schöne gemeinsame (WG-) Leben.

Schließlich kann ich meiner Familie nicht genug danken, ohne die ich nicht die Person wäre, die ich heut bin. Mama, du bist die Beste! Danke, dass du mich immer unterstützt, mir immer Mut und einfach immer da bist. Tausend Dank an meine wunderbaren Geschwister Kati, Nico, Isa und Consti, für euer Dasein und unseren Zusammenhalt, der uns auch schon durch die schwersten Zeiten gebracht hat. Vielen Dank an die kleinen Nika, Moritz und Lillie, ich hab euch sehr lieb <3.
Papa, wir vermissen dich sehr! Ich wünschte du könntest dies lesen. Im Herzen bist du bei mir und diese Arbeit ist in Erinnerung an dich geschrieben.

Und nun zuletzt zu dir, lieber Lucas. So lange kennen wir uns nun schon und fast ebenso lang bist an meiner Seite! Danke für deine Liebe, deine Unterstützung und Geduld, dass du mich zu zum Lachen bringst und in den Wahnsinn treibst, für mich kochst und du immer für mich da bist. Danke für die gemeinsame Zeit und die wunderbare Zukunftsperspektive mit dir.

Supplementary material

Complete mitochondrial genome of the giant root-rat (*Tachyoryctes macrocephalus*)

by

Victoria M. Reuber, Alba Rey-Iglesia, Michael V. Westbury, Andrea A. Cabrera, Nina Farwig, Mikkel Skovrind, Radim Šumbera, Tilaye Wube, Lars Opgenoorth, Dana G. Schabo, Eline D. Lorenzen

ABSTRACT

The endangered giant root-rat (*Tachyoryctes macrocephalus*, also known as giant mole rat) is a fossorial rodent endemic to the afro-alpine grasslands of the Bale Mountains in Ethiopia. The species is an important ecosystem engineer with the majority of the global population found within 1,000 km^2. Here, we present the first complete mitochondrial genome of the giant root-rat and the genus *Tachyoryctes*, recovered using shotgun sequencing and iterative mapping. A phylogenetic analysis including 15 other representatives of the family Spalacidae placed *Tachyoryctes* as sister genus to *Rhizomys* with high support. This position is in accordance with a recent study revealing the topology of the Spalacidae family. The full mitochondrial genome of the giant root-rat presents an important resource for further population genetic studies.

Main text

The giant root-rat (*Tachyoryctes macrocephalus*, Rüppell, 1842), also known as giant mole rat and big-headed African mole rat, is a fossorial rodent and ecosystem engineer endemic to the Bale Mountains of south-east Ethiopia. The species is naturally confined to afro-alpine grasslands, where it constructs large underground burrow systems (Yalden 1985). Giant root-

118

rats substantially impact their surroundings through a combined effect of soil perturbation and above-ground herbivory, with consequences for vegetation patterns, soil formation, and nutrient availability (Šklíba et al. 2017). In addition to their ecological importance, they are the most important prey of the endangered Ethiopian wolf (*Canis simensis;* Sillero-Zubiri & Gottelli, 1995) in the Bale Mountains. Giant root-rats have a limited distribution range across the Bale Mountain massif at elevations ranging between 3,000 and 4,150 m above sea level, with the majority of the population occurring within 1,000 km^2 (Sillero-Zubiri et al., 1995). The species is prone to human-induced habitat degradation and is currently listed as endangered by the IUCN (Lavrenchenko and Kennerley 2016).

A recent study revealed that giant root-rats were the key food resource of prehistoric hunter gatherers inhabiting rock shelters in the Bale Mountains 47,000-31,000 years ago. The consumption of the species facilitated the occupation of the world's earliest known high-altitude residential site (Ossendorf et al. 2019), and suggests that the giant root-rat population has been shaped by human activities across millennia.

To date, genetic studies on the giant root-rat are limited. However, one study presented a phylogeny of *Tachyoryctes* based on two mitochondrial genes (cytochrome b and cytochrome oxidase subunit I) and three nuclear genes (NAD synthetase 1, wntless, and recombination activating gene 1) (Šumbera et al., 2018). The analysis revealed a split between the giant root-rat and one lineage of the African root-rat (*T. splendens 1* sensu, Šumbera et al., 2018), about 1.3 million years ago. Another recent study revealed the topology of the entire Spalacidae family (He et al. 2020). Complete mitochondrial genomes are still lacking for the *Tachyoryctes* genus.

We collected a tissue sample from a live giant root-rat individual in February 2020, from the eastern part of the Sanetti Plateau of the Bale Mountain National Park (6°52'24.5 N, 39°52'25.4 E), under permits from the Ethiopian Wildlife Conservation Association. The voucher tissue sample of *T. macrocephalus* was deposited at the Conservation Ecology group, University of Marburg (www.uni-marburg.de, Dana G. Schabo, dana.schabo@staff.uni-marburg.de) and DNA extracts at the GLOBE institute, University of Copenhagen (Denmark; voucher number: CGG_1_024459). The DNA was extracted using the Qiagen DNeasy® Blood and Tissue Kit and sheared to approximately 400 bp using the Covaris M220 Focused-ultrasonicator. DNA fragments were built into an Illumina library following the protocol from Carøe et al. (2018), and sequenced on an Illumina HiSeq 4000. We trimmed the adapter sequences from the raw reads using Skewer v0.2.2 (Jiang et al. 2014), and removed PCR

duplicates of 100% identity using Prinseq-lite v0.20.4 (Schmieder and Edwards 2011). For the assembly of the complete mitochondrial genome, we followed an iterative approach using MITObim v1.8 (Hahn, Bachmann, and Chevreux 2013) with default parameters, 51 k -bait and a mismatch value of 3. We repeated this analysis five times independently using one of five available Spalacidae mitochondrial genomes as reference sequences (GenBank accession KC789518.1, NC_020756.1, JN540033.1, JX014234.1 and JN571130.1). We imported the resultant alignment files into Geneious Prime 2021 and created five consensus sequences (one for each reference) with a minimum read depth of 20x and a 75% consensus base call threshold. All five consensus sequences were aligned using MAFFT v7.392 (Katoh and Standley 2013) and were manually inspected for mismatches and to find point of circularity. All consensus sequences were near identical, regardless of mapping reference with the exception of some insertions/deletions (indels). As indels were not shared between multiple reference sequences, they were excluded them from the final consensus sequence.

We obtained a 16,646 bp sequence length (GenBank accession MW751806) and conducted an annotation using MITOS (Bernt et al. 2013), which uncovered all protein-coding genes, tRNAs and rRNAs typical for vertebrate mitochondrial genomes. We compiled a Maximum-likelihood phylogenetic tree with 15 mitochondrial genomes available for the Spalacidae family, and specified *Nannospalax galili* as outgroup. The analysis was conducted using RaxML-HPC2 on XSEDE v8.2.12 (Stamatakis 2014) on the Cipres server (Miller, Pfeiffer, and Schwartz 2010), and run with default parameters.

Our phylogenetic tree places the giant root-rat as sister clade to the genus *Rhizomys* - which are also fossorial rodents (Wilson and Reeder 2005) - with high support, in accordance with a phylogenetic analysis based on mitochondrial and nuclear genes (Figure 1; Šumbera et al., 2018). Furthermore, our retrieved topology of the Spalacidae family is consistent with the phylogeny recently presented in He et al., (2020). The full mitochondrial genome of the giant root-rat is a vital resource for future population genetic studies of the species.
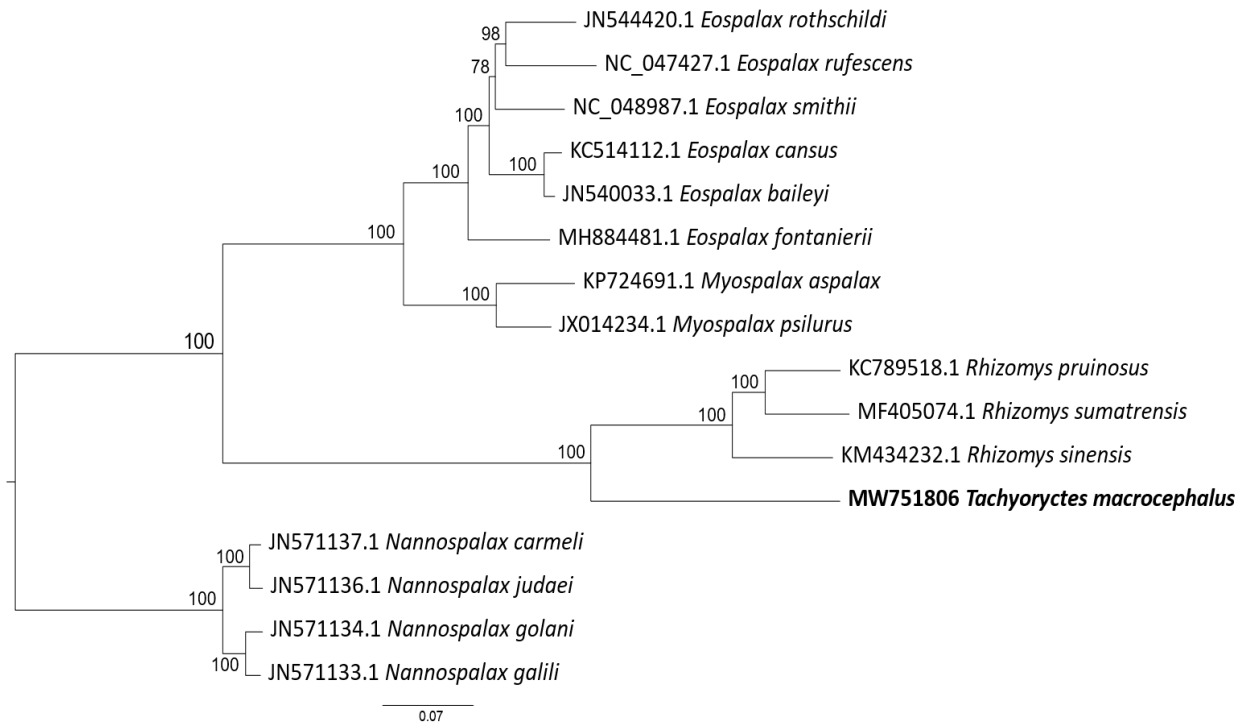
Figure 6. Maximum-likelihood phylogenetic tree showing the relationship between the giant root-rat (*Tachyoryctes macrocephalus*, in bold) and other representatives of the Spalacidae family. The numbers on branches display bootstrap support.

Disclosure statement

We would like to report no potential conflicts of interest.

Data availability

The data that support the findings of this study are openly available in GenBank of NCBI at https://www.ncbi.nlm.nih.gov under the accession no. MW751806. The associated BioProject, SRA, and Bio-Sample numbers are PRJNA735606, SRX11080558, and SAMN19589957, respectively.

Supplementary material Chapter II

Appendix A. Supplementary data

Appendix A Table 1. Spearman's correlation coefficients between (a) GRR old and fresh burrow densities measured at 10x10m (below diagonal), at 25 x 25m plots (above diagonal), and each variable between 10 x10m vs 25x25m plots (diagonal); (b) between species richness and Shannon diversity measure at each plot scale, and within a variable measured at the two scales.

a) GRR activity

	Fresh burrow	Old burrow	% Mound Soil
Fresh burrow	**0.97**	0.67	0.96
Old burrow	0.53	**0.90**	0.67
% Mound Soil	0.57	0.94	**0.94**
(b) Plant richness vs diversity			
	Shannon (10 x10 m)	Richness (25 x25 m)	
Richness (10 x10 m)	0.72	0.83	
Shannon (25 x25m)	0.84	0.75	

Appendix A Table 2. Spearman's correlation coefficients between each pairs of variables analysed.

Variables	GRR burrow density	Temperature	No. cow dung	Habitat wetness	Vegetation cover
Temperature	0.04				
No. cow dung	0.36*	0.48*			
Habitat wetness	0.50*	0.08	0.27*		
Vegetation cover	0.29*	0.07	0.01	-0.11	
Plant species richness	0.07	0.04	0.09	0.17	0.18

*statistically significant correlation

Appendix A Table 3. Direct, indirect and total effects and relative effect size (RE; given as the ratio of the indirect effect to the direct effect) of temperature, habitat wetness, livestock grazing and GRR burrow density on plant species richness and vegetation cover. The direct effects are the standardized path coefficients provided in Table 1 and 3, while the standardized indirect effects were calculated as described in the methods section. Total effects were the sum of the direct and indirect effects. Values of direct and indirect effects indicated by with asterisk (*) denote significant effects at P < 0.05 significance levels.

Predictors	Direct	Indirect	ER	Predictors	Direct	Indirect	ER
(a) Effects on species richness via GRR				(c) Effects on GRR via species richness			
Habitat wetness	0.332*	-0.007	0	Habitat wetness	0.013	0.008	0.6
Temperature	0.163	-0.005	0	Temperature	0.002	0.006	3.0
Livestock grazing	-0.036	-0.041	1.1	Livestock grazing	**0.185**	-0.003	0.0
(b) Effects on vegetation cover via GRR				(d) Effects on GRR via vegetation cover			
Habitat wetness	0.09	-0.014*	0.2	Habitat wetness	**0.05**	0.006	0.1
Temperature	0.074	-0.009	0.1	Temperature	-0.021	-0.025	1.2
Livestock grazing	0.023	-0.077*	3.3	Livestock grazing	**0.062**	0.021	0.3

Supplementary material Chapter III

Supplementary Method 1: Landsat-8 and ASTER DEM based air temperature predictions for the vegetation composition analysis

To conduct a constraint correspondence analysis (CCA) of the recorded plant species composition with temperature as constraining variable, averaged temperature information for the given field survey locations was derived from a machine learning model that predicts monthly mean air temperatures based on station observations at 2 m height, Landsat-8 images and solar irradiation data. The automatic weather stations were installed in early February 2017 (see Fig. 1b for the locations) and monthly mean air temperatures were derived for each month. Landsat-8 observations were retrieved from the USGS Earth Explorer (www.earthexplorer.com) on a two weekly basis and atmospherically corrected using the R-packages satellite and RStoolbox (Leutner et al. 2017). The bi-weekly and 30 m resolution solar and thermal Landsat-8 observations were averaged within each month to match the temporal resolution of the averaged station records. In addition, a digital elevation model (DEM) derived from 30 m resolution ASTER and also provided by the USGS Earthexplorer was included in the model. Since machine learning models are considerably biased when static input datasets are used to predict temporal dynamic target variables like air temperature (Meyer et al. 2018), the static DEM values were replaced by dynamized monthly clear sky solar irradiation information that was computed using RSAGA, 2021 CRAN and (Conrad et al. 2015). The mean monthly temperature was finally modelled using a forward feature selection (Meyer et al. 2018) approach together with a partial-least squares model with the Landsat-8 and solar irradiation data as independent variables and the locally recorded air temperature as dependent variable. The final model was applied to the area-wide Landsat-8 and solar irradiation datasets and monthly air temperature predictions were extracted from the resulting maps for the vegetation survey locations.

Supplementary Method 2: Analysis of GRR presence by MaxEnt modelling and comparison to the three random forest-based approaches M1-M3

Model description

To compare the random forest-based models to a Maximum Entropy (MaxEnt) based modelling approach we used the R-package *dismo* with Maxent 3.4.3 (Hijmans et al. 2017; R Core Team 2021). MaxEnt is a machine learning approach using presence-only data (Phillips et al. 2006)

and is particularly robust for small numbers of presence data sets. For the MaxEnt modeling approach, we used the same in-situ collected presence data points as for the models M2 and M3 (see method section 2.1 Field survey). Absence data or "background" points are generated by a function, taking a self-set number of random points, (47 as in M1, M2 and M3), from within the whole given research area. To achieve the best comparability between the MaxEnt and the random forest models, all settings were matched, i.e. the 10-fold cross validation, the split of the data into 70% training and 30 % testing data and the predictor variables including the modelled CA1/CA2 scores.

Model Tuning

In recent time, studies using MaxEnt modelling have been critiqued that those often focus only on the default setting (Merow, Smith, and Silander 2013; Morales, Fernández, and Baca-González 2017). To ensure that not only the default settings were computed, several model and variable settings and configurations were tested with the help of the R-package *Maxent Variable Selection* (Jueterbock et al. 2016). Altogether 1280 combinations with 32 different feature class combinations and regularisation multipliers have been compared. The final regularization parameter Beta Multiplier was used in sequence beginning at 0.5 up to 4 in steps of 0.5. The best model and the best variable parameters have been found in comparison by using AUC (area under the curve) and AIC (Akaike information criterion) (Akaike 1974) respectively. The script structure was followed as published in Gottwald et Al. 2017 (Gottwald et al. 2017) and Höfs et al. 2021 before (Hoefs et al. 2021).

Model evaluation, variable contribution and comparison

MaxEnt was performing slightly better with an AUC of 0.894, then the best random forest model M1 with an AUC of 0.849 (Figure S6). However, the MaxEnt approach also relied on the texture metrics GLCM as in M1. In contrast, MaxEnt only selected two instead of eight predictors compared to M1 (Figure S7). Excluding the predictor GLCM homogeneity W11 G32 indices stack the other variable has been observed to be chosen before in M1 and M2 (Figure 4). Interestingly, the MaxEnt model did not select either of the two CA variables in its final model, strengthening the result that for predicting GRR distribution with remote sensing data, vegetation composition is less relevant. Instead, the use of texture metrics is useful for covering the different patterns and contrasts of the landscape that vegetation indices alone cannot highlight. Those final model similarities between random forest model M1 or Maximum

Entropy suggest that choosing either one, does not greatly affect the final result for modelling the GRR distribution.

Supplementary Tables

Table S1: List of predictors used in the regression and classification modelling processes

Index	Name	Formula description
NDVI	Normalized Difference Vegetation Index	NIR-RED/NIR+RED
VVI	Visible Vegetation Index	1-RED-30/RED+30*1-GREEN-50/GREEN+50 *1-BLUE-1/BLUE+1
NDTI	Normalized Difference Turbidity Index	RED-GREEN/RED+GREEN
GLI	Green Leaf Index	2*GREEN - RED - BLUE/2*GREEN + RED + BLUE
RI	Redness Index	RED*2/BLUE*GREEN*3
ARI	Anthocyanin Reflectance Index	1/GREEN-1/REDEDGE
LSWI	Land Surface Water Index	NIR-SWIR/NIR+SWIR
Sentinel-2 band 2	Blue	
Sentinel-2 band 3	Green	
Sentinel-2 band 4	Red	
Sentinel-2 band 5	Red Edge	
Sentinel-2 band 8	Near Infrared (NIR)	
Sentinel-2 band 11	Short Wave Infrared (SWIR)	
KMDC Sentinel-2 band stack	k-Means Distance from Centroid	Band stack consist of red, green, blue, red edge, near-infrared and shortwave infrared
KMDC indices stack	k-Means Distance from Centroid	Indices stack consist of: NDVI, VVI, NDTI, GLI, SAT, RI, ARI, LSWI, SI
GLCM W03 G32 entropy Sentinel-2 band stack	Grey level co-occurrence matrix, window size 3, grey level 32, feature type entropy	Calculated on the results of KMDC for Sentinel-2 band stack (red, green, blue, red edge, near-infrared and shortwave infrared)
GLCM W03 G32 homogeneity Sentinel-2 band stack	Grey level co-occurrence matrix, window size 3, grey level 32, feature type homogeneity	Calculated on the results of KMDC for Sentinel-2 band stack (red, green, blue, red edge, near-infrared and shortwave infrared)
GLCM W03 G32 second moment Sentinel-2 band stack	Grey level co-occurrence matrix, window size 3, grey level 32, feature type second moment	Calculated on the results of KMDC for Sentinel-2 band stack (red, green, blue, red edge, near-infrared and shortwave infrared)
GLCM W11 G32 entropy Sentinel-2 band stack	Grey level co-occurrence matrix, window size 11, grey level 32, feature type entropy	Calculated on the results of KMDC for Sentinel-2 band stack (red, green, blue, red edge, near-infrared and shortwave infrared)

GLCM W11 G32 homogeneity Sentinel-2 band stack	Grey level co-occurrence matrix, window size 11, grey level 32, feature type homogeneity	Calculated on the results of KMDC for Sentinel-2 band stack (red, green, blue, red edge, near-infrared and shortwave infrared)
GLCM W11 G32 second moment Sentinel-2 band stack	Grey level co-occurrence matrix, window size 11, grey level 32, feature type second moment	Calculated on the results of KMDC for Sentinel-2 band stack (red, green, blue, red edge, near-infrared and shortwave infrared)
GLCM W31 G32 entropy Sentinel-2 band stack	Grey level co-occurrence matrix, window size 31, grey level 32, feature type entropy	Calculated on the results of KMDC for Sentinel-2 band stack (red, green, blue, red edge, near-infrared and shortwave infrared)
GLCM W31 G32 homogeneity Sentinel-2 band stack	Grey level co-occurrence matrix, window size 31, grey level 32, feature type homogeneity	Calculated on the results of KMDC for Sentinel-2 band stack (red, green, blue, red edge, near-infrared and shortwave infrared)
GLCM W31 G32 second moment Sentinel-2 band stack	Grey level co-occurrence matrix, window size 31, grey level 32, feature type second moment	Calculated on the results of KMDC for Sentinel-2 band stack (red, green, blue, red edge, near-infrared and shortwave infrared)
GLCM W03 G32 entropy Indices stack	Grey level co-occurrence matrix, window size 3, grey level 32, feature type entropy	Calculated on the results of KMDC for Indices stack (NDVI, VVI, NDTI, GLI, SAT, RI, ARI, LSWI, SI)
GLCM W03 G32 homogeneity Indices stack	Grey level co-occurrence matrix, window size 3, grey level 32, feature type homogeneity	Calculated on the results of KMDC for Indices stack (NDVI, VVI, NDTI, GLI, SAT, RI, ARI, LSWI, SI)
GLCM W03 G32 second moment Indices stack	Grey level co-occurrence matrix, window size 3, grey level 32, feature type second moment	Calculated on the results of KMDC for Indices stack (NDVI, VVI, NDTI, GLI, SAT, RI, ARI, LSWI, SI)
GLCM W11 G32 entropy Indices stack	Grey level co-occurrence matrix, window size 11, grey level 32, feature type entropy	Calculated on the results of KMDC for indices stack (NDVI, VVI, NDTI, GLI, SAT, RI, ARI, LSWI, SI)
GLCM W11 G32 homogeneity Indices stack	Grey level co-occurrence matrix, window size 11, grey level 32, feature type homogeneity	Calculated on the results of KMDC for indices stack (NDVI, VVI, NDTI, GLI, SAT, RI, ARI, LSWI, SI)
GLCM W11 G32 second moment Indices stack	Grey level co-occurrence matrix, window size 11, grey level 32, feature type second moment	Calculated on the results of KMDC for indices stack (NDVI, VVI, NDTI, GLI, SAT, RI, ARI, LSWI, SI)
GLCM W31 G32 entropy Indices stack	Grey level co-occurrence matrix, window size 31, grey level 32, feature type entropy	Calculated on the results of KMDC for indices stack (NDVI, VVI, NDTI, GLI, SAT, RI, ARI, LSWI, SI)
GLCM W31 G32 homogeneity Indices stack	Grey level co-occurrence matrix, window size 31, grey level 32, feature type homogeneity	Calculated on the results of KMDC for indices stack (NDVI, VVI, NDTI, GLI, SAT, RI, ARI, LSWI, SI)
GLCM W31 G32 second moment Indices stack	Grey level co-occurrence matrix, window size 31, grey level 32, feature type second moment	Calculated on the results of KMDC for Indices stack (NDVI, VVI, NDTI, GLI, SAT, RI, ARI, LSWI, SI)
RAO`s Q Sentinel-2 band stack	Rao`s Q Diversity Index	Band stack consist of red, green, blue, red edge, near-infrared and shortwave infrared

RAO`s Q Indices stack	Rao`s Q Diversity Index	Indices stack consist of: NDVI, VVI, NDTI, GLI, SAT, RI, ARI, LSWI, SI
RAO`s Q KMDC Sentinel-2 band stack	Rao`s Q Diversity Index	Band stack consist of red, green, blue, red edge, near-infrared and shortwave infrared
RAO`s Q KMDC Indices stack	Rao`s Q Diversity Index	Indices stack consist of: NDVI, VVI, NDTI, GLI, SAT, RI, ARI, LSWI, SI

Table S2: Overview of the three model specifications

	M1	**M2**	**M3**
Predictors	Individual satellite bands (Sentinel-2) Individual spectral indices, texture metrics (KMDC, GLCM, Rao'sQ)	Individual satellite bands (Sentinel-2) Individual spectral indices, texture metrics (KMDC, GLCM, Rao'sQ)	Individual satellite bands (Sentinel-2) Individual spectral indices, texture metrics (KMDC, GLCM, Raos'Q) + CA1 and CA2
Response	GRR presence/absence	GRR presence/absence	GRR presence/absence
Training areas	Visually chosen via Google Earth images	GPS points sampled in field	GPS points sampled in field
Prediction in space	Sentinel-2 image	Sentinel-2 image	Sentinel-2 image

Table S3: Selected predictors for classifications of model strategies M1, M2, M3 and for regression models of CA score predictions.

M1	**M2**	**M3**	**CA1**	**CA2**
KMDC Indices stack	GLCM W03 G32 homogeneity Indices stack	CA2 predicted	NDVI	Sentinel-2 band 2
RAO`s Q KMDC Indices stack	VVI	RAO`s Q KMDC Sentinel-2 band stack	LSWI	GLI
GLCM W31 G32 entropy Sentinel-2 stack	Sentinel- 2band 3		GLCM W31 G32 homogeneity Sentinel-2 band stack	RAO`S Q Sentinel-2 band stack
GLCM W11 G32 2nd moment Indices stack	GLCM W03 G32 entropy Indices stack		RAO`S Q Sentinel-2 band stack	GLCM W03 G32 homogeneity Sentinel-2 band stack
GLCM W11 G32 entropy Indices stack	Sentinel-2 band 4		Sentinel- 2 band 3	GLCM W11 G32 entropy Sentinel-2 band stack

RAO`s Q Indices stack	Sentinel-2 band 2	RAO`S Q KMDC Indices stack	GLCM W31 G32 2nd moment Sentinel-2 band stack
GLCM W03 G32 homogeneity Indices stack	Sentinel-2 band 11		GLCM W31 G32 entropy Sentinel-2 band stack
			GLCM W31 G32 homogeneity Sentinel-2 band stack

Supplementary Figures
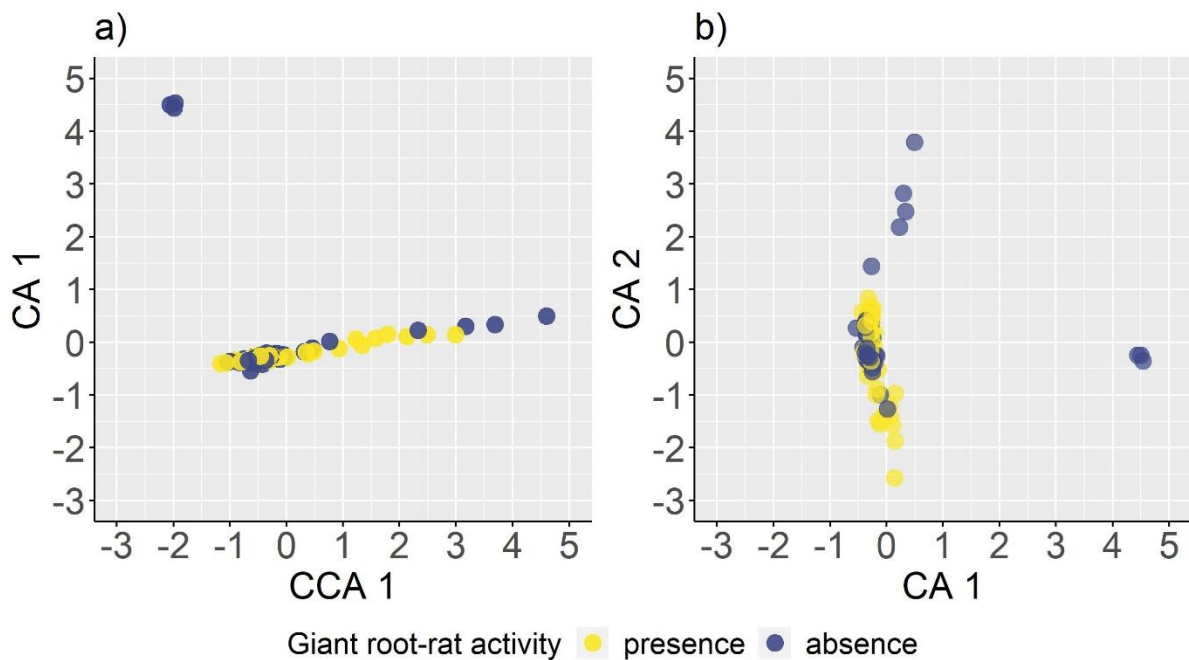
Figure S1: Constrained correspondence analysis with temperature as constraining variable (CCA1), based on the correlation matrix of 79 plant species recorded on plots with a) presence and absence of GRR activity and b) unconstrained axes (CA1 and CA2) for presence and absence of GRR activity.
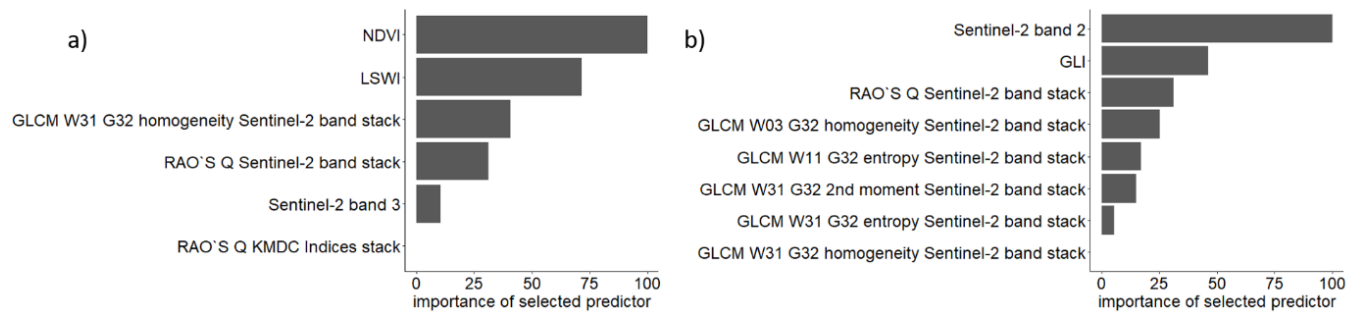
Figure S2: Selected variables and their importance (in %) in the final regression model for CA1 (a) and CA2 (b).
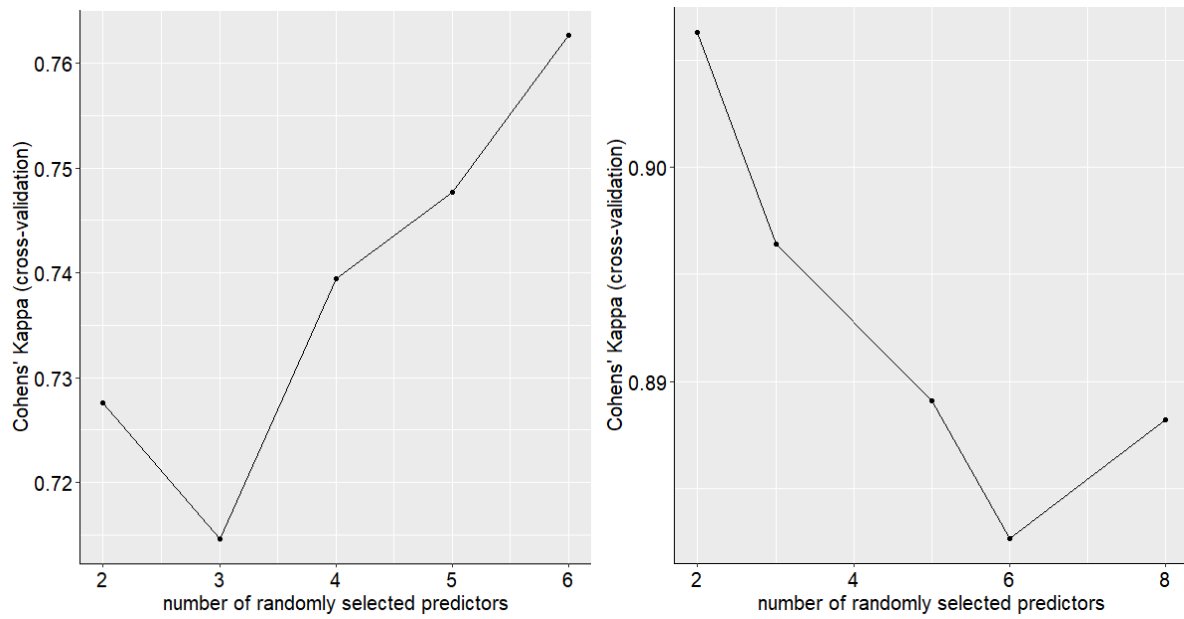
Figure S3: Root mean square error (RMSE) values from the internal model iterations and number of randomly selected predictors. The response variable CA1 (left) and CA2 (right).
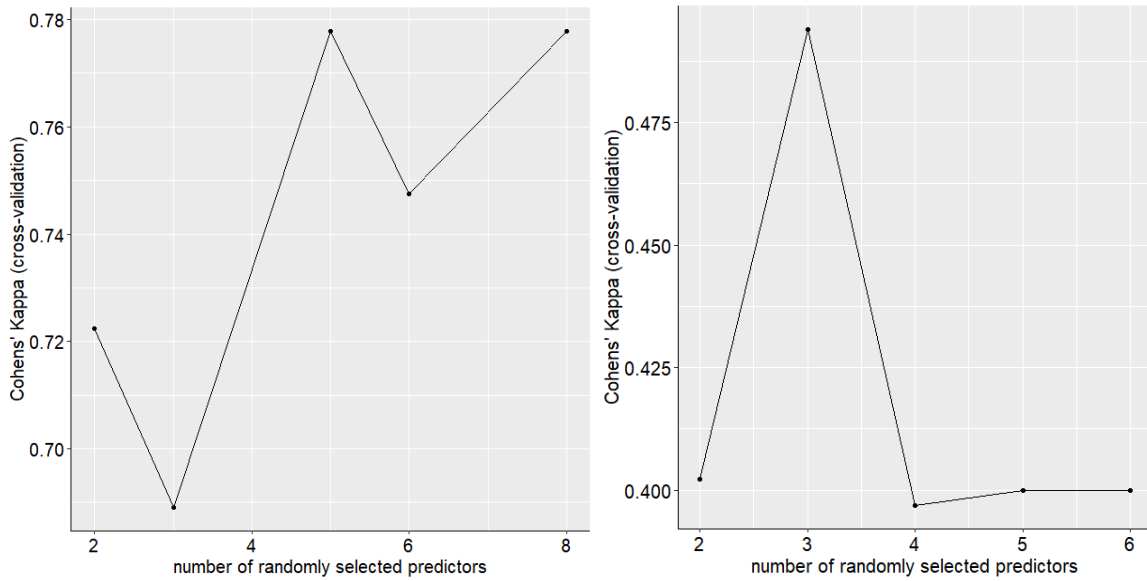
Figure S4: Root mean square error (RMSE) values from the internal model iterations and number of randomly selected predictors for the classification models M1 (left) and M2 (right), training areas based on Google Earth (M1), local GPS records (M2).
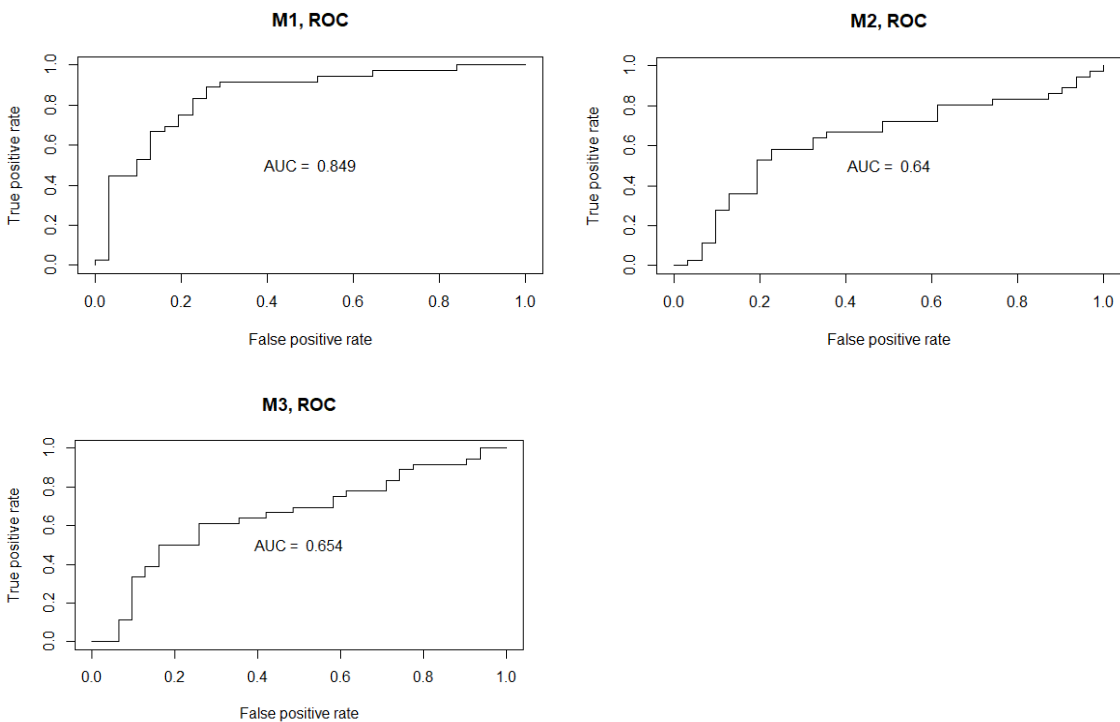
Figure S5: ROC curves and calculated AUC values for all three methods training areas based on Google Earth (M1), local GPS records (M2 and M2) and M3 including CA scores.
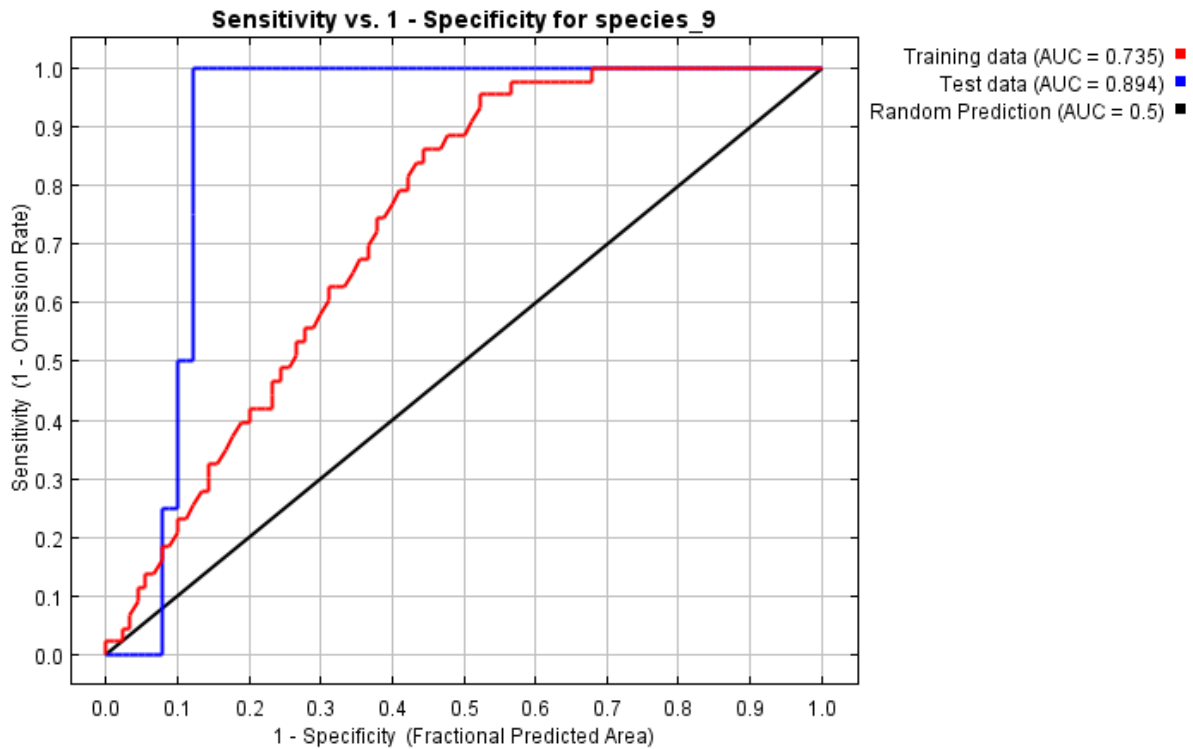
Figure S6: ROC curves and calculated AUC values for the MaxEnt model training areas based on local GPS records for presence data and random background point data.
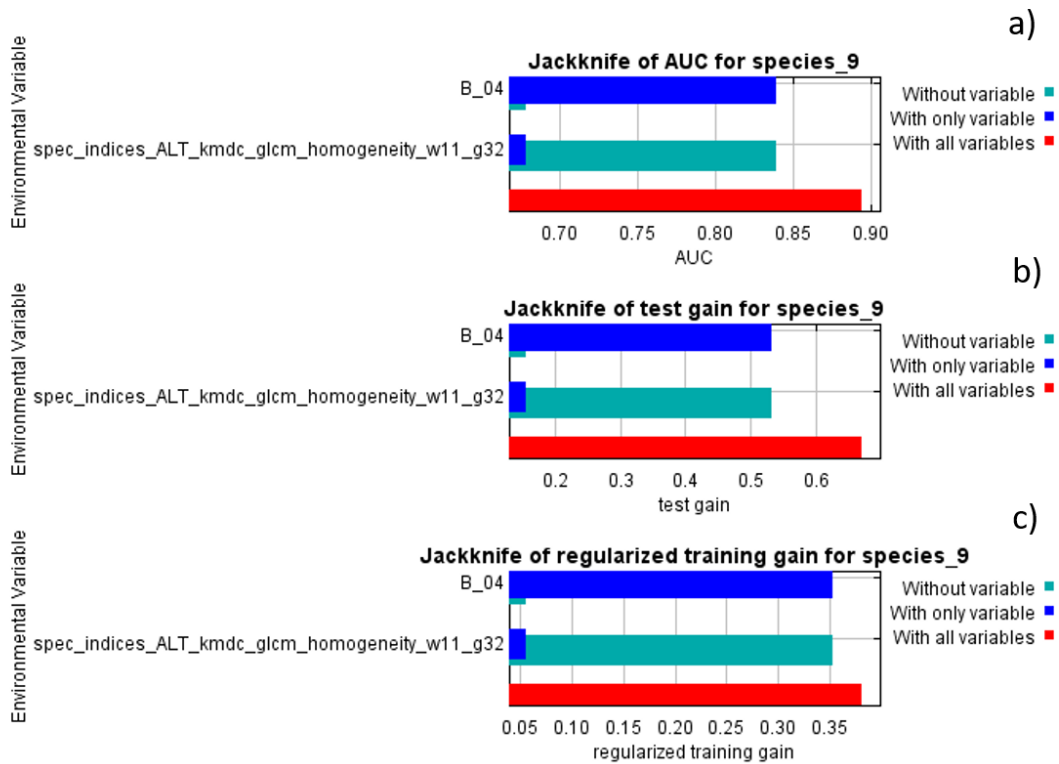
Figure S7: Jacknife tests of AUC a), of test gain b) and training gain c) for the final MaxEnt model's variables.
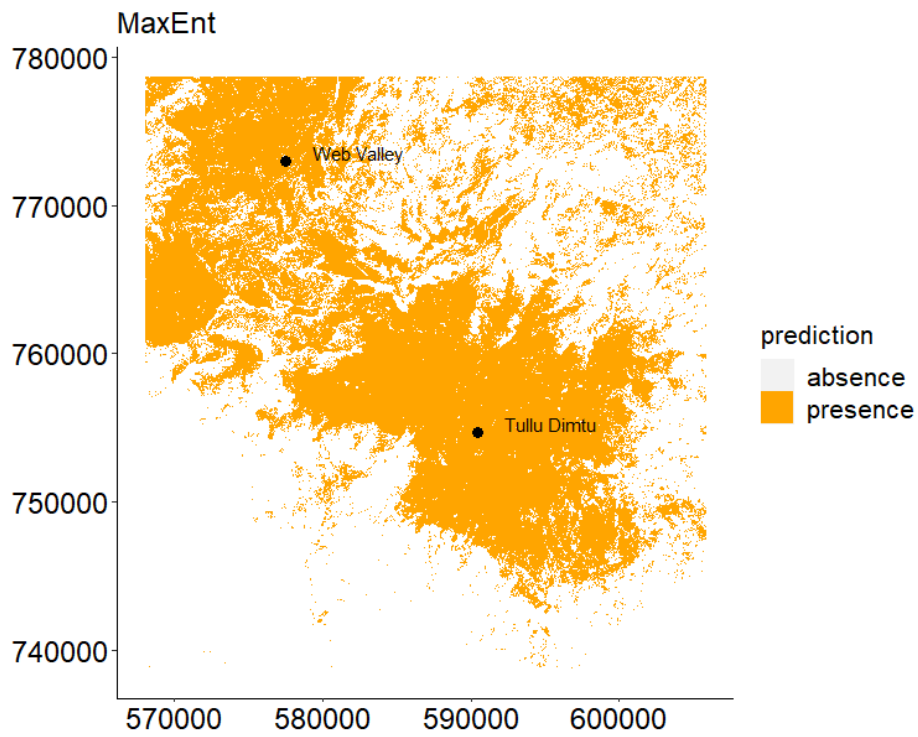
Figure S8: Spatial predictions of giant root-rat (GRR) presence across the Bale plateau. The map depicts the distribution of the GRR with a MaxEnt model strategy. The prediction layer of GRR distribution shows presence in orange and absence in white. This is based on the best fitting threshold from the MaxEnt model strategy defined by a receiver operating characteristic (ROC) curve analysis (see Figure S6 for plotted ROC curve).

Supplementary material Chapter IV

Supporting figures
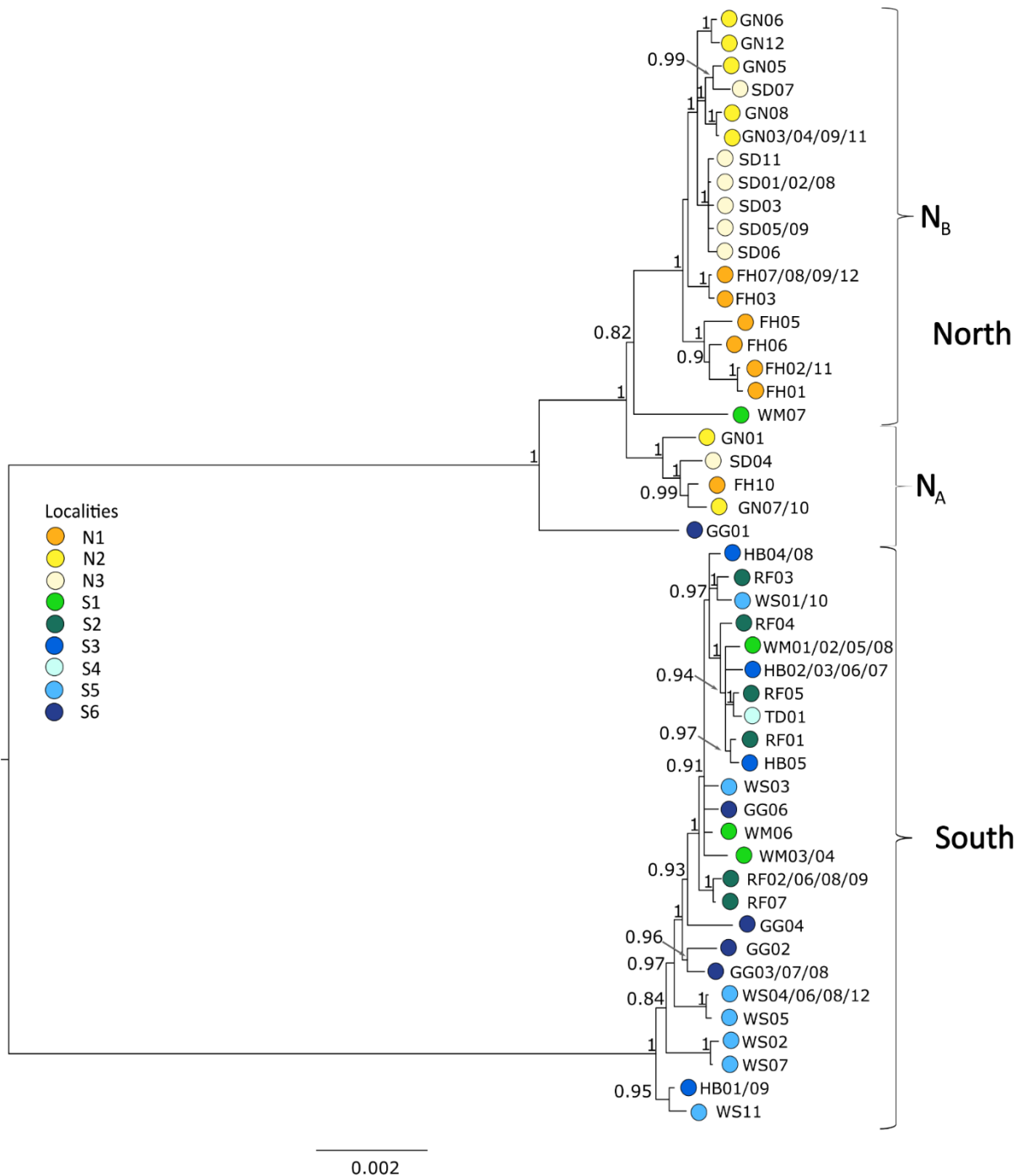
Figure S1: MrBayes phylogenetic tree of 48 unique mitochondrial haplotypes of the giant root-rat. Colours of dots show source sampling localities of individuals, see map Figure 1A; more than one sample identifier indicates shared haplotype sequences among individuals. Genetic groups discussed in the main text are indicated. Bootstrap support values > 0.8 are shown at nodes. Scale bar shows expected substitution per site.
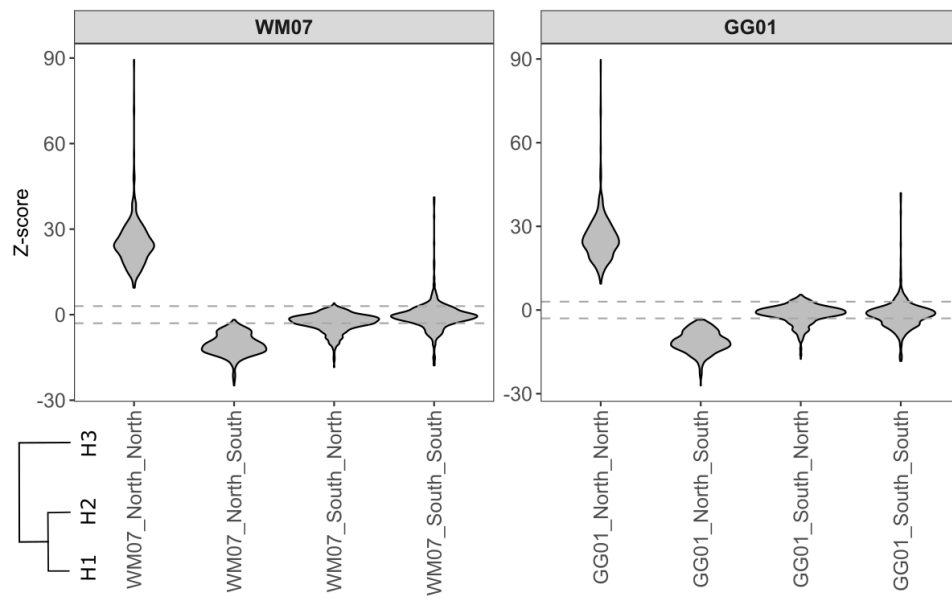
Figure S2: Z-scores of D-statistics test of gene flow analyses. Z-scores show the significance of D-scores (Figure 2, main text) from 0. |Z|>3 (shown by the dotted lines) represents a significant difference from 0, determined by a one-sample Wilcoxon signed rank test
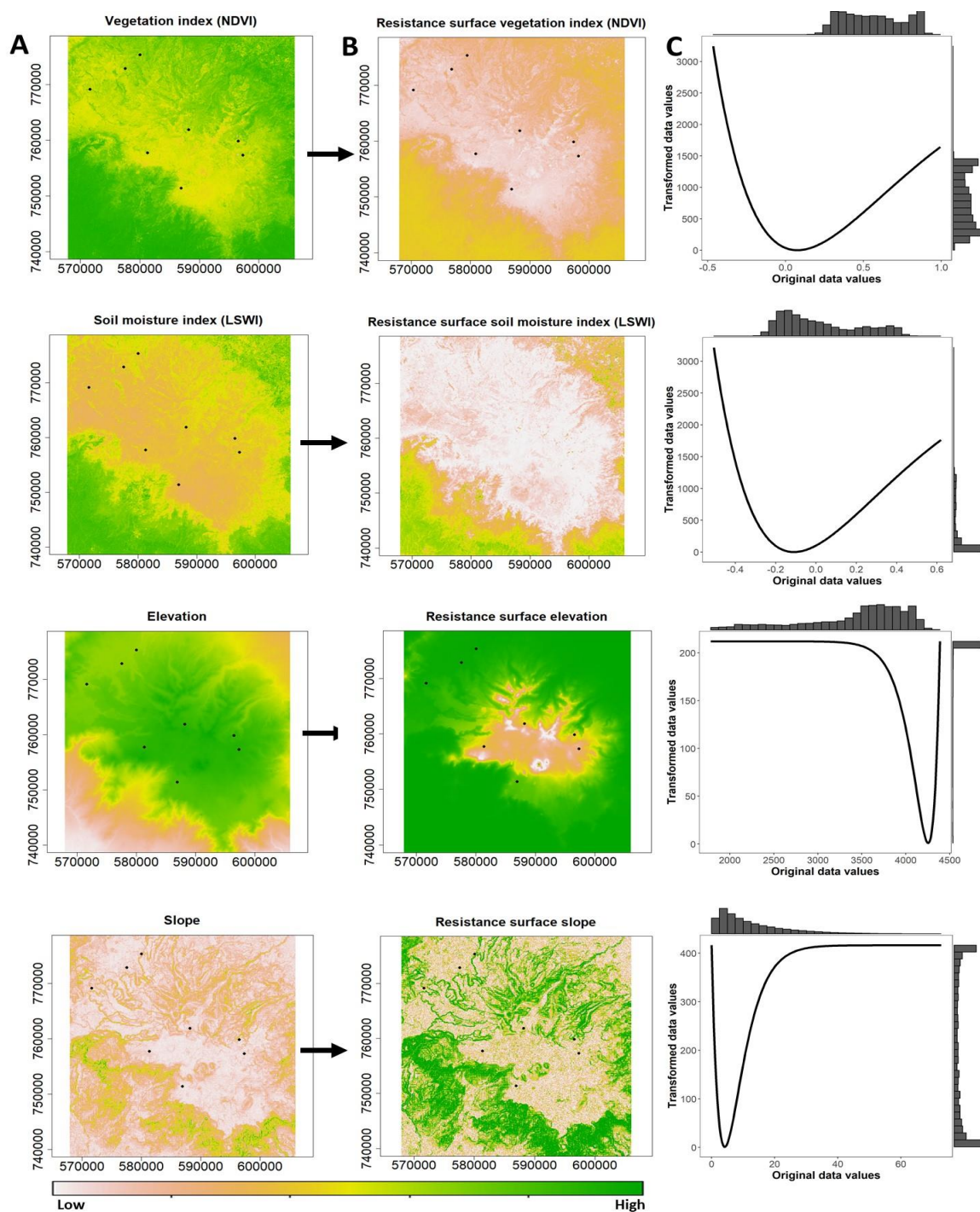
Figure S3: Raster layers of environmental variables and resistance surfaces after raster layer optimization. A) Raster layers of the Normalised Vegetation Differentiation Index (NDVI, referred to as vegetation index in main text), Land Surface Water Index (LSWI, soil moisture index), elevation, and slope. The layers were derived from a Sentinel-2 scene (www.earthexplorer.usgs.gov) (B) Resistance surfaces after the single surface optimization with ResistanceGA. The resistance costs are indicated by the colour of the bar. C) Response curves for the environmental variables, showing the resistance cost values obtained after the optimization procedure. Histogram bars indicate the frequency of each resistance value of the environmental variable.

136

Supporting tables

Table S1: Sample information of the 77 giant root-rat individuals analysed, including NCBI GenBank accession number, sampling region and locality, elevation and putative sex as observed during sampling in the field.

GenBank Accession nr.	Sample ID	Area	Locality	Longitude	Latitude	Elevation [m]	Sex
OQ207553	WM01	South	C1	39.7993786	6.89272543	4067	male
OQ207554	WM02	South	C1	39.7979935	6.89250161	4052	female
OQ207555	WM03	South	C1	39.7984543	6.89203954	4066	female
OQ207556	WM04	South	C1	39.7984361	6.8919853	4074	male
OQ207557	WM05	South	C1	39.7984264	6.89159638	4077	male
OQ207558	WM06	South	C1	39.7982458	6.89185899	4069	female
OQ207559	WM07	South	C1	39.797776	6.8923663	4061	female
OQ207560	WM08	South	C1	39.7973869	6.89243931	4059	male
OQ207561	RF01	South	S2	39.7341839	6.85683888	4060	female
OQ207545	RF02	South	S2	39.7361359	6.85497257	4077	female
OQ207546	RF03	South	S2	39.7353867	6.85627624	4068	female
OQ207547	RF04	South	S2	39.7340746	6.85637774	4045	male
OQ207548	RF05	South	S2	39.7359542	6.85453867	4079	male
OQ207549	RF06	South	S2	39.7360538	6.85455661	4082	female
OQ207550	RF07	South	S2	39.7360626	6.85434855	4085	female
OQ207551	RF08	South	S2	39.7357906	6.85404143	4086	female
OQ207552	RF09	South	S2	39.7359544	6.85463817	4074	male
OQ207565	FH01	North	N1	39.722694	7.01545104	3432	female
OQ207566	FH02	North	N1	39.723002	7.01585001	3450	male
OQ207567	FH03	North	N1	39.723049	7.01484603	3454	male
OQ207568	FH05	North	N1	39.724233	7.01355002	3460	male
OQ207569	FH06	North	N1	39.724517	7.01387499	3461	female
OQ207570	FH07	North	N1	39.724613	7.01381296	3463	female
OQ207571	FH08	North	N1	39.724612	7.01382796	3466	male
OQ207572	FH09	North	N1	39.724365	7.01379502	3462	NA
OQ207562	FH10	North	N1	39.724167	7.01372101	3460	NA
OQ207563	FH11	North	N1	39.72443	7.01378597	3461	male
OQ207564	FH12	North	N1	39.72443	7.01378597	3461	NA
OQ207573	GG01	South	S6	39.873655	6.87388103	3996	female
OQ207574	GG02	South	S6	39.873954	6.87302599	3932	female

OQ207575	GG03	South	S6	39.873791	6.87366704	4039	male
OQ207576	GG04	South	S6	39.873474	6.87347903	4045	female
MV751806	GG06	South	S6	39.873731	6.87346403	4039	female
OQ207577	GG07	South	S6	39.873964	6.873229	4039	female
OQ207578	GG08	South	S6	39.874289	6.87294401	4042	female
OQ207587	GN01	North	N2	39.649925	6.95700897	3330	male
OQ207588	GN03	North	N2	39.649347	6.95741398	3543	male
OQ207589	GN04	North	N2	39.648648	6.95798303	3546	female
OQ207579	GN05	North	N2	39.650556	6.958222	3446	male
OQ207580	GN06	North	N2	39.648671	6.95795302	3544	female
OQ207581	GN07	North	N2	39.651052	6.95835804	3546	female
OQ207582	GN08	North	N2	39.650912	6.95715699	3550	female
OQ207583	GN09	North	N2	39.650212	6.95687796	3550	male
OQ207584	GN10	North	N2	39.650925	6.95836902	3550	male
OQ207585	GN11	North	N2	39.648578	6.95802502	3548	female
OQ207586	GN12	North	N2	39.651665	6.95825301	3552	male
OQ207590	HB01	South	S2	39.7853	6.79550101	3623	female
OQ207591	HB02	South	S2	39.78964	6.79768098	3853	female
OQ207592	HB03	South	S2	39.784437	6.79520002	3850	male
OQ207593	HB04	South	S2	39.787152	6.79719399	3852	female
OQ207594	HB05	South	S2	39.789308	6.797743	3851	female
OQ207595	HB06	South	S2	39.78687	6.79702501	3850	female
OQ207596	HB07	South	S2	39.787018	6.79715199	3854	male
OQ207597	HB08	South	S2	39.783954	6.79434397	3849	female
OQ207598	HB09	South	S2	39.784998	6.79543303	3849	male
OQ207600	SD01	North	N3	39.702559	6.99164601	3509	male
OQ207601	SD02	North	N3	39.702437	6.99169002	3477	NA
OQ207602	SD03	North	N3	39.702509	6.99163897	3508	NA
OQ207603	SD04	North	N3	39.70244	6.99198204	3501	female
OQ207604	SD05	North	N3	39.701275	6.991054	3394	female
OQ207605	SD06	North	N3	39.702295	6.99160896	3507	male
OQ207606	SD07	North	N3	39.702515	6.99174198	3516	NA
OQ207607	SD08	North	N3	39.70168	6.99056902	3506	female
OQ207608	SD09	North	N3	39.701255	6.991054	3502	female
OQ207599	SD11	North	N3	39.701205	6.98984399	3503	male
OQ207609	TD1	South	S4	39.826091	6.82700104	4224	male
OQ207610	WS01	South	S5	39.88116	6.850291	4117	male

OQ207611	WS02	South	S5	39.881139	6.85024498	4114	female
OQ207612	WS03	South	S5	39.881217	6.850794	4100	female
OQ207613	WS04	South	S5	39.880863	6.850406	4111	female
OQ207614	WS05	South	S5	39.880683	6.85055603	4111	female
OQ207615	WS06	South	S5	39.880764	6.85039301	4114	male
OQ207616	WS07	South	S5	39.881243	6.85041497	4113	female
OQ207617	WS08	South	S5	39.88116	6.85078603	4111	NA
OQ207618	WS10	South	S5	39.881335	6.85093397	4112	NA
OQ207619	WS11	South	S5	39.880807	6.850924	4113	male
OQ207620	WS12	South	S5	39.881034	6.84992597	4116	male

Table S2: Mapping statistics of the 77 giant root-rat samples analysed. Raw sequencing reads were mapped against the hoary bamboo rat (*Rhizomys pruinosus*) nuclear genome (Genbank accession: VZQC00000000.1; Guo et al. 2021) combined with the giant root-rat mitogenome (Genbank accession: MW751806; Reuber et al. 2021). Bp = base pairs; Mitogenomes = mitochondrial genomes

Sample ID	# Raw read pairs	# Reads mapping	Nuclear coverage	Nuclear mapped bp	Mitogenome coverage	Mitogenome mapped bp
FH01	16,978,992	7,992,025	0.29	1,080,644,275	226.90	3,776,908
FH10	18,494,391	12,855,168	0.51	1,901,006,013	182.64	3,040,203
FH11	19,750,607	10,262,289	0.40	1,487,884,552	144.36	2,403,072
FH12	17,227,253	11,333,662	0.45	1,651,542,774	128.76	2,143,278
FH02	14,883,520	8,146,465	0.32	1,183,176,147	168.19	2,799,747
FH03	16,251,258	10,476,801	0.43	1,582,232,753	181.38	3,019,192
FH05	16,852,614	10,499,672	0.41	1,510,446,294	250.02	4,161,839
FH06	19,896,506	12,832,141	0.52	1,906,513,326	192.50	3,204,294
FH07	19,431,703	9,452,783	0.35	1,283,194,137	147.39	2,453,482
FH08	15,914,201	8,510,001	0.32	1,189,432,482	179.62	2,990,019
FH09	17,438,587	9,371,585	0.36	1,320,089,804	234.83	3,908,968
GG01	22,295,022	13,577,661	0.55	2,023,849,334	170.93	2,845,211
GG02	17,747,863	11,139,869	0.44	1,630,575,444	147.06	2,447,920
GG03	16,768,929	7,684,884	0.27	1,014,360,345	102.97	1,714,101
GG04	24,563,197	1,535,631	0.12	442,335,192	24.94	415,083
GG06	24,526,276	12,539,983	0.49	1,803,094,277	220.69	3,673,638
GG07	20,381,975	12,354,185	0.49	1,793,309,550	232.45	3,869,412
GG08	4,425,384	12,274,902	0.47	1,719,823,251	212.03	3,529,394
GN05	26,875,116	7,969,437	0.38	1,396,716,389	94.19	1,567,817
GN06	19,415,999	10,070,286	0.40	1,474,915,866	155.88	2,594,709
GN07	16,723,334	7,006,642	0.28	1,042,333,258	121.03	2,014,703
GN08	25,301,937	10,848,812	0.43	1,602,419,125	191.59	3,189,169

139

GN09	21,256,957	9,479,533	0.38	1,401,602,300	155.62	2,590,518
GN01	16,003,381	8,207,272	0.32	1,175,154,307	230.38	3,834,928
GN10	21,011,631	13,404,421	0.53	1,943,213,143	218.10	3,630,495
GN11	25,847,517	16,396,946	0.64	2,378,222,263	242.29	4,033,095
GN12	22,475,014	12,581,467	0.50	1,831,406,864	146.60	2,440,378
GN03	14,555,865	6,320,660	0.24	895,094,428	143.31	2,385,457
GN04	19,336,769	12,560,208	0.50	1,835,220,325	240.73	4,007,196
HB01	21,973,877	10,182,380	0.43	1,583,136,018	102.69	1,709,392
HB02	25,529,934	17,319,108	0.68	2,504,372,366	219.52	3,654,153
HB03	21,702,035	7,539,986	0.30	1,122,205,194	129.43	2,154,491
HB04	23,433,747	14,126,631	0.56	2,088,257,975	159.68	2,658,019
HB05	23,994,437	14,449,681	0.57	2,118,929,629	361.16	6,011,848
HB06	19,951,156	11,088,337	0.44	1,626,922,114	126.54	2,106,308
HB07	16,010,826	9,260,591	0.37	1,356,991,234	160.97	2,679,465
HB08	24,162,995	13,835,736	0.56	2,054,483,977	182.77	3,042,383
HB09	23,621,873	13,184,020	0.57	2,118,929,629	199.79	3,325,660
SD01	21,121,011	6,635,909	0.30	1,097,745,936	144.43	2,404,109
SD11	14,776,896	6,401,618	0.26	952,603,757	85.26	1,419,154
SD02	20,060,768	13,430,376	0.54	1,982,436,708	249.92	4,160,133
SD03	12,197,516	8,320,803	0.33	1,211,921,153	183.82	3,059,800
SD04	15,072,836	9,636,470	0.38	1,394,660,022	171.47	2,854,279
SD05	3,300,973	10,258,149	0.40	1,466,709,062	258.30	4,299,641
SD06	18,112,628	11,862,203	0.47	1,728,272,832	291.72	4,855,990
SD07	17,365,379	4,706,885	0.19	711,542,791	93.47	1,555,961
SD08	14,927,338	7,899,143	0.31	1,127,141,716	226.73	3,774,112
SD09	14,754,546	3,961,884	0.22	814,631,762	116.97	1,947,051
TD01	18,360,169	8,194,229	0.29	1,076,743,466	182.60	3,039,521
WS01	27,711,489	6,982,153	0.43	1,576,780,562	383.22	6,379,103
WS10	21,495,541	10,268,532	0.38	1,405,339,675	276.23	4,598,081
WS11	20,698,366	12,000,838	0.47	1,726,480,366	153.60	2,556,859
WS12	20,877,111	9,511,682	0.34	1,240,687,498	167.02	2,780,161
WS02	20,283,118	10,724,014	0.42	1,558,731,684	129.18	2,150,311
WS03	22,665,497	12,505,010	0.49	1,814,919,219	157.34	2,619,039
WS04	20,531,719	11,151,303	0.44	1,626,149,287	148.33	2,469,173
WS05	19,546,437	10,341,864	0.40	1,495,657,674	147.86	2,461,306
WS06	22,699,761	13,505,918	0.54	1,983,859,527	231.53	3,854,088
WS07	19,914,784	12,277,532	0.48	1,789,796,875	123.11	2,049,223
WS08	17,942,128	10,381,806	0.42	1,552,684,778	126.66	2,108,292
WM01	25,415,257	19,240,329	0.74	2,752,021,342	121.31	2,019,292
WM02	22,638,733	15,910,096	0.65	2,414,133,391	125.53	2,089,639

WM03	24,802,453	18,354,244	0.77	2,837,925,408	177.23	2,950,212
WM04	22,795,120	14,958,043	0.70	2,582,763,905	158.99	2,646,611
WM05	19,230,604	18,829,904	0.55	2,047,322,685	68.19	1,135,121
WM06	21,399,645	17,553,235	0.63	2,345,642,536	70.48	1,173,188
WM07	20,423,503	14,526,040	0.62	2,290,090,671	97.40	1,621,323
WM08	22,856,570	17,206,734	0.69	2,568,908,319	93.53	1,556,848
RF01	22,228,252	19,833,972	0.67	2,471,394,141	104.29	1,735,935
RF02	24,670,699	17,585,365	0.71	2,626,112,333	108.40	1,804,460
RF03	19,537,627	20,573,370	0.59	2,187,672,230	116.29	1,935,731
RF04	23,599,367	18,644,450	0.69	2,553,480,252	166.93	2,778,720
RF05	17,913,386	14,957,434	0.56	2,063,675,254	128.10	2,132,328
RF06	22,795,981	17,160,550	0.70	2,596,803,976	126.18	2,100,317
RF07	22,941,232	16,563,368	0.65	2,408,176,843	99.55	1,657,191
RF08	18,119,643	18,563,076	0.54	2,001,105,976	136.84	2,277,795
RF09	20,711,128	17,982,889	0.64	2,372,186,376	139.21	2,317,277

Table S3: *P*-Values of the test of significant differences in nucleotide diversity difference between localities for mitochondrial and nuclear genomes. For mitochondrial genomes (above diagonal) a permutation approach was conducted, where haplotypes were resampled (n=1000) across the entire giant root-rat population, in order to test whether the observed genetic diversity of each locality was equal or greater than the genetic diversity simulated in the permutation approach. For nuclear genomes (below diagonal), we used a Welch-test (unpaired t-test), accounting for unequal variance. *p*-values < 0.05 present significant nucleotide differences between localities (in italics)

	N1	N2	N3	S1	S2	S3	S5	S6
N1	--	0.804	0.725	0.069	0.672	0.759	0.979	*0.042*
N2	*<0.001*	--	0.599	0.072	0.576	0.648	0.782	0.056
N3	*<0.001*	*0.023*	--	0.064	0.897	0.987	0.746	*0.032*
S1	0.708	*0.002*	*<0.001*	--	0.065	0.078	0.052	0.613
S2	*0.001*	*<0.001*	*<0.001*	*0.003*	--	0.823	0.677	*0.030*
S3	*<0.001*	*<0.001*	*<0.001*	*<0.001*	*<0.001*	--	0.755	*0.042*
S5	*<0.001*	*<0.001*	*<0.001*	*<0.001*	*<0.001*	*0.003*	--	*0.043*
S6	*<0.001*	*<0.001*	*<0.001*	*<0.001*	*<0.001*	*<0.001*	*<0.001*	--

Table S4: a) Correlation matrix of partial Mantel test of column variables (focal model) controlled by the row variables (alternative model) for mitochondrial data. a) Shown is the correlation coefficient r, bold values indicate a significant correlation. b) Reciprocal causal modelling matrix, showing the relative support of the focal models in columns (e.g. elevation distance|geographic distance), compared to alternative models in rows (geographic distance|elevation distance). Values depict differences in r-values between focal and alternative model. Positive values support the focal, negative the alternative model.

	Focal model				
Alternative model	Geographic distance	Vegetation distance	Moisture distance	Elevation distance	Slope distance
A) Correlation matrix					
Geographic distance	0.00	0.11	-0.06	**0.42**	0.21
Vegetation distance	**0.56**	0.00	0.18	**0.65**	0.19
Moisture distance	**0.55**	0.18	0.00	**0.64**	**0.27**
Elevation distance	0.19	0.16	-0.09	0.00	0.17
Slope distance	**0.55**	-0.02	-0.19	**0.63**	0.00
B) Reciprocal causal modelling matrix					
Geographic distance	0.00	-0.44	-0.61	0.24	-0.34
Vegetation distance	0.44	0.00	0.00	0.49	0.21
Moisture distance	0.61	0.00	0.00	0.73	0.46
Elevation distance	-0.24	-0.49	-0.73	0.00	-0.47
Slope distance	0.34	-0.21	-0.46	0.47	0.00

Supplementary material Chapter V

Supplementary Figures
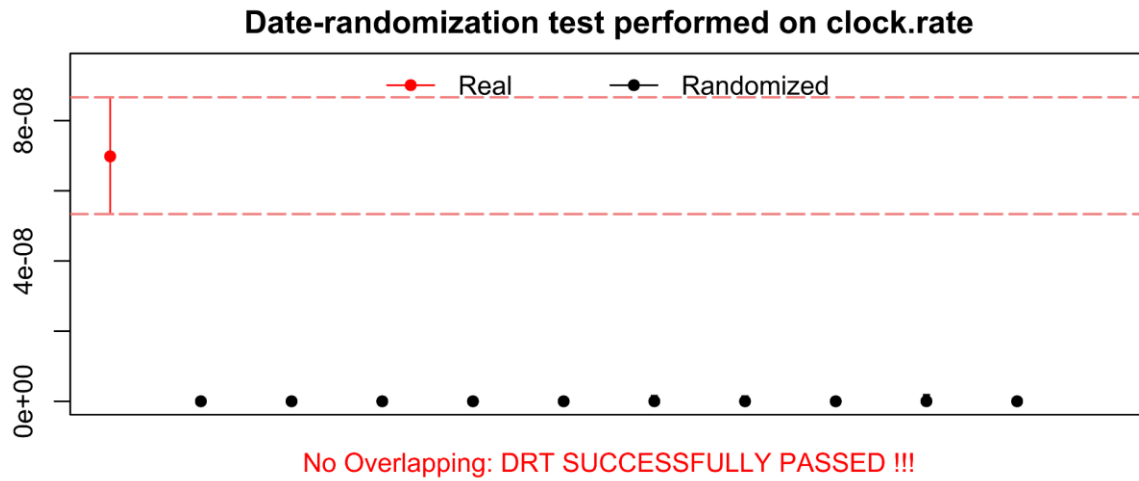
Figure S1: Comparison of the clock rates estimates using BEAST using both the real data and 10 date-randomised datasets from the date-randomization test (DRT).
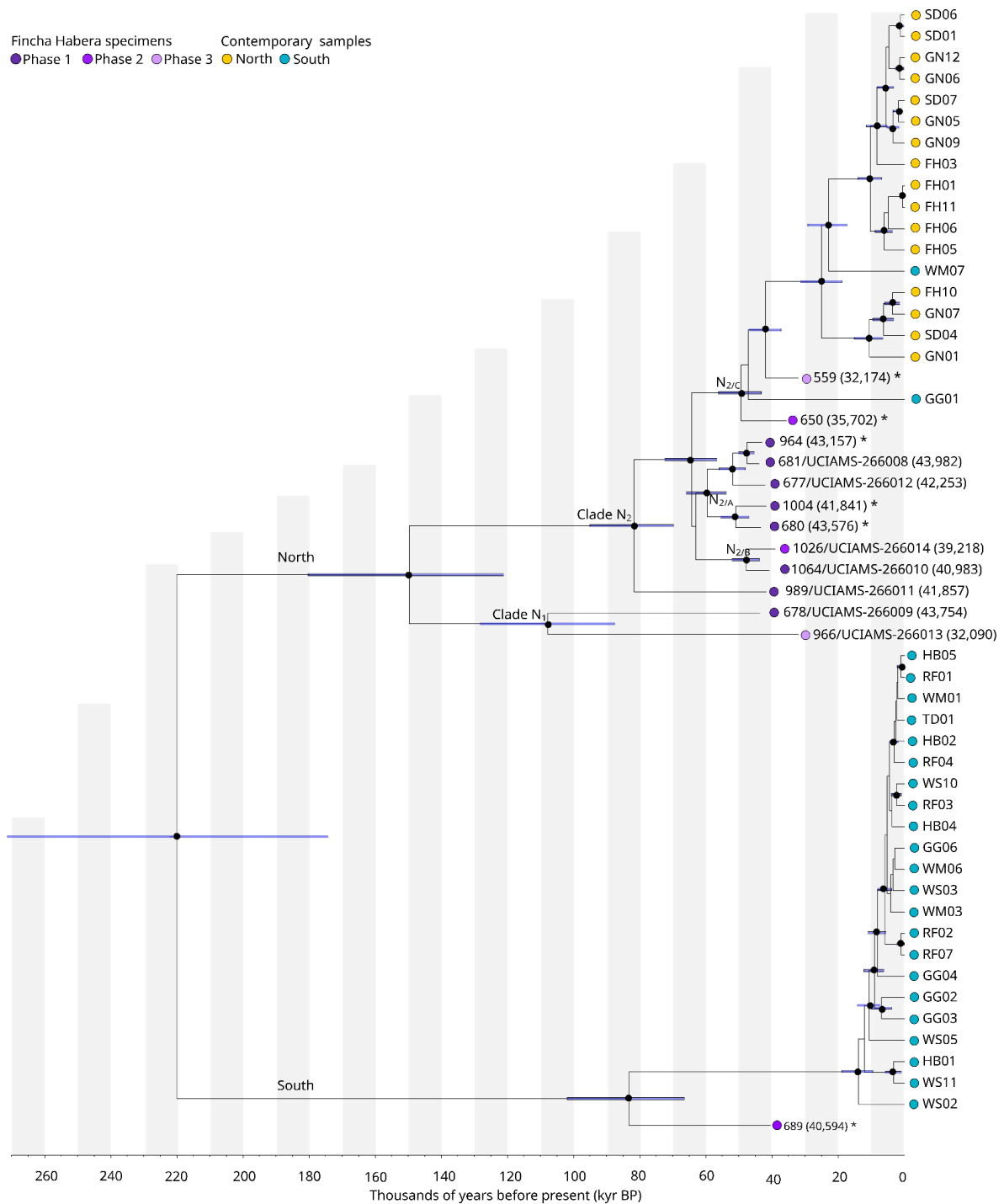
Figure S2: Dated phylogeny of the 61 giant root-rat haplotypes present among the 90 mitogenome sequences with coverage > 10 x, comprising 13 Fincha Habera specimens and 77 contemporary samples. The mitogenomes are labelled with their specimen ID and radiocarbon lab ID (if ¹⁴C dated, calibrated age). Numbers in brackets show the estimated mean sample age; six samples were molecularly dated, indicated by an asterisk. Black circles at nodes depict bootstrap support values >0.8; 95% HPD intervals of divergence dates of the internal nodes are displayed in horizontal blue bars.
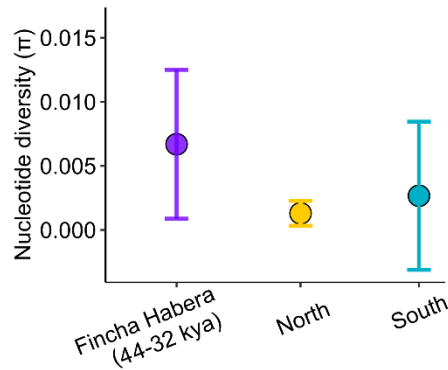
Figure S3: Average nucleotide diversity estimated for 13 Fincha Habera specimens and 77 contemporary giant root-rat samples. To accommodate for differences in sample size, diversity was estimated using a subsample of 13 randomly selected sequences for each group (as Fincha Habera specimen n = 13), 1000 times in an iterative approach with replacement. Mitogenomes from subfossils have a coverage of >10x. Bars represent standard deviation for the 1000 subsamples

Supplementary Tables

Table S1: Sampling information, ^{14}C and calibrated (cal.) age range (95.4% probability, 2σ) of radiocarbon dates of published and new available samples for the Fincha Habera site , including outliers and samples from non-MSA deposits. Non MSA deposits: COL5196.1.1, COL5195.1.1, COL6822.1.1, Beta-507233, COL6820.1.1, COL5198.1.1, COL6821.1.1; Outliers: unreliable bulk dating of black carbon mixed sediments Beta-507234, Beta-503927, Beta-507235; intrusions of younger charcoal into the MSA-layers COL5197.1.1, Beta-486378, COL5199.1.1, Beta-486376, Beta-486375; low C:N ratios Beta-506526, D-AMS 037006. Excav. unit = Excavation unit; Lith. unit = Lithostratigraphical unit

^{14}C Lab ID/ Specimen ID	Excav. unit	Lith. unit	Material	14C-date [BP]	Cal. age range (2σ) [cal BP]	References
COL5197.1.1	E8-NW-L6	FHL-07	Charcoal	143 ± 37	**281 - 0**	Ossendorf et al. (2019)
Beta-486378	E8-SW-L7	FHL-07	Charcoal	330 ± 30	**471 - 310**	Ossendorf et al. (2019)
COL5196.1.1	E8-SE-L3	FHL-04	Charcoal	533 ± 38	**633 - 505**	Ossendorf et al. (2019)
COL5195.1.1	E8-SW-L3	FHL-05	Charcoal	547 ± 36	**638 - 512**	Ossendorf et al. (2019)
COL5199.1.1	H11-SE-L8	FHL-08	Charcoal	558 ± 37	**645 - 516**	Ossendorf et al. (2019)
COL6822.1.1	F13-ID611-49.47	FHL-06	Charcoal	651 ± 34	**670 - 554**	Ossendorf et al. (2023)
Beta-486376	H11-SE-L7	FHL-08	Charcoal	660 ± 30	**672 - 556**	Ossendorf et al. (2019)
Beta-507233	E8-NW-P17	FHL-04/-05/-06	Black carbon	680 ± 30	**675 - 560**	Ossendorf et al. (2019)
COL6820.1.1	F13-ID441-49.68	FHL-07	Charcoal	704 ± 35	**689 - 560**	Ossendorf et al. (2023)
Beta-486375	H11-NW-L11	FHL-08	Charcoal	780 ± 30	**731 - 671**	Ossendorf et al. (2019)
COL5198.1.1	H11-SE-L5	FHL-07	Charcoal	770 ± 38	**738 - 655**	Ossendorf et al. (2019)
COL6821.1.1	F13-ID350-49.62	FHL-07	Charcoal	1.078 ± 35	**1.059 - 926**	Ossendorf et al. (2023)

145

Beta-507234	E8-NW-P25	FHL-07	Black carbon	9.710 ± 30	**11.221 - 10.890**	Ossendorf et al. (2019)
Beta-503927	E8-NW-P49	FHL-08/-09	Black carbon	14.930 ± 60	**18.597 - 18.139**	Ossendorf et al. (2019)
Beta-506526	H11-SE-L9	FHL-08	Coprolite	18.320 ± 60	**22.406 - 22.123**	Ossendorf et al. (2019)
D-AMS 037006	H11-SE-L6	FHL-08	Coprolite	20.531 ± 98	**25.030 - 24.318**	Ossendorf et al. (2023)
Beta-507235	E8-NW-P36	FHL-08	Black carbon	21.520 ± 80	**25.965 - 25.720**	Ossendorf et al. (2019)
Beta-486377	E8-NW-L11	FHL-08	Charcoal	27.240 ± 120	**31.558 - 31.091**	Ossendorf et al. (2019)
COL6823.1.1	F13-ID352-49.40	FHL-08	Charcoal	27.654 ± 168	**31.888 - 31.214**	Ossendorf et al. (2023)
UCIAMS-266013/966	F15-ID966-49.57	FHL-08	Bone collagen	27.940 ± 350	**33.051 - 31.221**	this paper
Beta-506528	H11-NE-L11	FHL-08	Charcoal	28.000 ± 140	**32.825 - 31.559**	Ossendorf et al. (2019)
Beta-507236	E8-NW-P43	FHL-08	Black carbon	28.220 ± 130	**32.925 - 31.814**	Ossendorf et al. (2019)
D-AMS 037003	H11-SE-L7	FHL-08	Coprolite	29.499 ± 164	**34.415 - 33.704**	Ossendorf et al. (2023)
D-AMS 037005	H11-SE-L6	FHL-08	Coprolite	29.736 ± 150	**34.541 - 33.976**	Ossendorf et al. (2023)
Beta-506527	H11-NE-L11	FHL-08	Coprolite	30.940 ± 170	**35.739 - 34.747**	Ossendorf et al. (2019)
Beta-506529	E8-SW-L10	FHL-08	Charcoal	31.640 ± 200	**36.361 - 35.480**	Ossendorf et al. (2019)
Beta-522263	H11-NW-L13	FHL-08	Bone collagen	33.600 ± 230	**39.245 - 37.625**	Ossendorf et al. (2019)
UCIAMS-266014/1026	F15-ID1026-49.38	FHL-08	Bone collagen	34.260 ± 770	**41.021 - 37.266**	this paper
Beta-522264	E8-NW-L12	FHL-08	Bone collagen	34.380 ± 250	**40.166 - 39.089**	Ossendorf et al. (2019)
UCIAMS-266010/1064	F15-ID1064-49.31	FHL-09	Bone collagen	36.040 ± 970	**42.318 - 39.501**	this paper
UCIAMS-266011/989	F13-ID989-49.45	FHL-08	Bone collagen	37.300 ± 1100	**43.328 - 40.144**	this paper
UCIAMS-266012/677	F13-ID677-49.49	FHL-08	Bone collagen	37.800 ± 1200	**44.191 - 40.689**	this paper
COL6825.1.1	F13-ID895-49.04	FHL-09	Charcoal	39.414 ± 544	**43.938 - 42.369**	Ossendorf et al. (2023)
COL6824.1.1	F13-ID866-49.27	FHL-09	Charcoal	39.675 ± 540	**44.084 - 42.475**	Ossendorf et al. (2023)
UCIAMS-266009/678	F13-ID678-49.21	FHL-09	Bone collagen	39.700 ± 1500	**46.479 - 41.757**	this paper
UCIAMS-266008/681	F15-ID681-49.01	FHL-08	Bone collagen	39.900 ± 1600	**47.166 - 41.781**	this paper
COL6826.2.1	F13-ID1010-48.87	FHL-09	Charcoal	40.286 ± 579	**44.413 - 42.751**	Ossendorf et al. (2023)

| COL5451.1.1 | H11-SW-L12 | FHL-09 | Charcoal | 42.086 ± 711 | **46.096 - 43.430** | Ossendorf et al. (2019) |
| COL6827.1.1 | F13-ID1019-48.82 | FHL-09 | Charcoal | 42.351 ± 736 | **46.535 - 43.999** | Ossendorf et al. (2023) |

Table S2: Sampling information of 18 giant root-rat Fincha specimens from this study, with ^{14}C and mean calibrated (cal.) radiocarbon dates of seven specimens, molecular estimated dates of six specimens and phase affiliation of specimen to human occupation phase at Fincha Habera, where applicable. Coordinate of all samples is - 7.014577 N, 39.720068 E.

Speci-men ID	[14]C Lab ID	Square	Layer	14C dates	Cal. dates (mean)	Estimated dates	Phase
1003	-	F15	FHL-08 lower	NA	NA	NA	NA
1004	-	F15	FHL-08 lower	NA	NA	41,841	1
1026	UCIAMS-266014	F15	FHL-08 lower	34,260 ± 770	39,218	NA	2
1064	UCIAMS-266010	F15	FHL-09	36,040 ± 970	41,857	NA	1
518	-	F13	FHL-08 upper	NA	NA	NA	NA
559	-	F13	FHL-08 lower	NA	NA	32,174	3
659	-	F13	FHL-08 upper	NA	NA	NA	NA
677	UCIAMS-266012	F13	FHL-08 lower	37,800 ± 1200	40,983	NA	1
678	UCIAMS-266009	F13	FHL-09	39,700 ± 1500	43,754	NA	1
680	-	F13	FHL-08 lower	NA	NA	43,576	1
681	UCIAMS-266008	F13	FHL-08 lower	39,900 ± 1600	43,982	NA	1
689	-	F13	FHL-08 lower	NA	NA	40,594	2
966	UCIAMS-266013	F15	FHL-08 upper	27,940 ± 350	32,090	NA	3
989	UCIAMS-266011	F15	FHL-08 upper	37,300 ± 1100	42,253	NA	1
650	-	F13	FHL-08 upper	NA	NA	35,702	2
964	-	F15	FHL-08 upper	NA	NA	43,157	1
619	-	F13	FHL-09	NA	NA	NA	NA
511	-	F15	FHL-08 upper	NA	NA	NA	NA

Table S3: Sampling information, carbon and stable isotope values for Fincha Habera specimens and contemporary bone samples, with calibrated (cal.) radiocarbon dates of seven specimens and molecular estimated age (est.) of six specimens. Phase describes to which Middle Stone Age foragers activity phase specimens were assigned, if applicable. Group describes placement of sample to either Fincha Habera specimen, or contemporary (cont.) population north (N) or south (S).

Speci-men ID	Coordinates	$\delta^{13}C_{VPDB}$	$\delta^{15}N_{AIR}$	wt% C	wt% N	C:N$_{Atomic}$	Group	Phase	Age (cal/est)
511	- 7.014577 N, 39.720068 E	-21.31	4.03	3.48	1.13	3.58	F. H.	NA	NA
518	- 7.014577 N, 39.720068 E	-19.03	7.7	35.41	12.95	3.19	F. H.	NA	NA
559	- 7.014577 N, 39.720068 E	-24.79	5.46	3.13	0.72	5.09	F. H.	3	32,174
619	- 7.014577 N, 39.720068 E	-19.29	7.49	28.1	10.29	3.19	F. H.	NA	NA
650	- 7.014577 N, 39.720068 E	-20.25	4.95	8.3	2.89	3.35	F. H.	2	35,703
659	- 7.014577 N, 39.720068 E	-20.29	6.33	21.6	7.9	3.19	F. H.	NA	NA
677	- 7.014577 N, 39.720068 E	-20.08	6.27	39.5	14.2	3.25	F. H.	1	42,253
678	- 7.014577 N, 39.720068 E	-20.91	4.66	38.2	13.8	3.22	F. H.	1	43,754
680	- 7.014577 N, 39.720068 E	-20.33	6.95	20.3	7.29	3.25	F. H.	1	43,576
681	- 7.014577 N, 39.720068 E	-20.25	5.75	42.1	15.2	3.23	F. H.	1	43,982
689	- 7.014577 N, 39.720068 E	-19.75	5.27	26.01	9.53	3.18	F. H.	2	40,594
964	- 7.014577 N, 39.720068 E	-20.58	5.27	27.34	9.97	3.2	F. H.	1	43,158
966	- 7.014577 N, 39.720068 E	-20.04	5.57	35	12.5	3.27	F. H.	3	32,090
989	- 7.014577 N, 39.720068 E	-20.31	5.65	36	13.2	3.19	F. H.	1	41,857
1003	- 7.014577 N, 39.720068 E	-20.51	4.47	3.72	1.23	3.52	F. H.	NA	NA
1004	- 7.014577 N, 39.720068 E	-19.57	6.88	24.51	8.89	3.22	F. H.	1	41,842
1026	- 7.014577 N, 39.720068 E	-20.15	9.23	34.7	12.3	3.3	F. H.	2	39,218
1064	- 7.014577 N, 39.720068 E	-20.11	5.44	38.6	14.1	3.2	F. H.	1	40,983
FH1	-7.0142328 N, 39.724306 E	-22.64	4.98	40.7	14.7	3.23	N	cont.	0
FH2	-7.0129304 N, 39.724177 E	-22.19	6.07	41.87	14.62	3.34	N	cont.	0

FH3	-7.0174698 N, 39.719187 E	-19.98	3.74	40.78	14.66	3.24	N	cont.	0
FH5	-7.0165128 N, 39.717999 E	-18.54	4.67	41.04	14.88	3.22	N	cont.	0
GN2	-6.9547875 N, 39.649325 E	-22.89	4.93	41.25	14.82	3.25	N	cont.	0
GN5	-6.9547875 N, 39.649325 E	-23.05	5.73	40.81	14.42	3.3	N	cont.	0
MB1	-6.9049405 N, 39.584557 E	-23.01	3.13	40.67	14.27	3.32	N	cont.	0
MB2	-6.9053754 N, 39.584033 E	-22.41	4.37	39.9	14.2	3.28	N	cont.	0
MB3	-6.9056105 N, 39.584087 E	-22.54	4.39	39.58	13.86	3.33	N	cont.	0
MB5	-6.9083602 N, 39.584172 E	-22.22	3.11	38.39	13.59	3.29	N	cont.	0
RF11	-6.8556849 N, 39.737585 E	-21.61	3.24	40.63	14.39	3.29	S	cont.	0
RF8	-6.8619646 N, 39.730173 E	-21.87	4.53	39.92	14.38	3.24	S	cont.	0
SNT4	-6.8344822 N, 39.868168 E	-21.54	3.69	41.81	14.74	3.31	S	cont.	0
SNT8	-6.8345104 N, 39.867552 E	-21.62	6.04	39.4	13.84	3.32	S	cont.	0
SNT10	-6.8340494 N, 39.867425 E	-22.73	2.41	40.61	14.59	3.25	S	cont.	0
SNT18	-6.8306268 N, 39.854224 E	-22.32	7.64	41.48	15.06	3.21	S	cont.	0
SNT19	-6.8306272 N, 39.854016 E	-22.18	6.28	41.14	14.96	3.21	S	cont.	0
SNT22	-6.8297615 N, 39.852494 E	-23.08	4.57	39.03	14.09	3.23	S	cont.	0
SNT24	-6.8293588 N, 39.850041 E	-22.82	4.88	40.44	14.66	3.22	S	cont.	0
SNT25	-6.8322926 N, 39.873566 E	-22.24	3.12	36.91	13.47	3.2	S	cont.	0
SNT27	-6.8419488 N, 39.865665 E	-21.59	2.76	40.34	14.43	3.26	S	cont.	0
SNT28	-6.8533077 N, 39.866582 E	-22.93	2.63	41.28	14.99	3.21	S	cont.	0
WM1	-6.885606 N, 39.810635 E	-22.45	8.16	41.78	14.73	3.31	S	cont.	0
WM2	-6.8863265 N, 39.812491 E	-23.7	3.35	41.3	14.59	3.3	S	cont.	0
WM5	-6.8926799 N, 39.799578 E	-21.96	7.29	39.99	14.31	3.26	S	cont.	0

WM6	-6.8927612 N, 39.799605 E	-23.64	4.55	39.85	13.99	3.32	S	cont.	0
WM7	-6.8914129 N, 39.799974 E	-23.94	3.17	43.02	15.28	3.28	S	cont.	0
WM9	-6.8939174 N, 39.800584 E	-22.55	4.88	40.65	14.7	3.22	S	cont.	0
WM12	-6.9284287 N, 39.803467 E	-22.88	6.76	39.93	14.58	3.19	S	cont.	0
WM13	-6.8931425 N, 39.7988 E	-23.05	3.55	39.64	14.49	3.19	S	cont.	0

Table S4: Mapping statistics of Fincha Habera specimens before and after capture approach. In column "Mapped BP" (base pairs), number of mapped BP in italics for specimens 650, 964, 619, 511 are averaged bp mapped.

| Speci-men ID | Before capture | After capture | | | | | |
	Mapped reads	Raw reads	Trimmed and merged reads	Mapped reads	Uniquely mapped reads	Cove-rage	Mapped BP
1003	1	760,269	739,558	1,307	98	0,24	4,035
1004	102	251,264	242,931	80,787	11,418	42,51	707,667
1026	42	863,817	849,730	37,983	13,872	58,20	968,817
1064	37	1,111,919	1,081,393	14,555	8,121	29,71	494,630
518	12	799,683	779,029	5,191	3,157	8,77	145,945
559	20	766,373	749,437	8,110	4,058	10,40	173,086
659	6	1,278,114	1,253,096	6,493	3,162	8,44	140,488
677	128	1,196,572	1,141,529	91,476	21,479	90,65	1,508,963
678	23	669,070	659,565	23,165	7,976	24,92	414,826
680	1016	1,032,020	1,009,373	594,660	29,187	124,29	2,068,958
681	446	1,291,839	1,264,363	215,595	25,229	102,42	1,704,805
689	389	1,166,011	1,127,121	170,915	25,322	94,98	1,580,973
966	84	1,793,081	1,752,902	43,689	15,589	72,27	1,202,981
989	207	736,955	716,411	153,127	23,448	104,21	1,734,708
650	13	405,009	386,519	11,516	3,662	10,87	*181085,9*
964	117	519,328	512,798	39,371	15,180	71,82	*1195576,8*
619	4	885,342	807,745	1,759	699	1,52	*25,218,522*
511	2	740,953	737,506	928	638	2,18	*36,246,056*

Table S5: New and published ¹⁴C dates and calibrated dates of Fincha Habera specimens, charcoal and faunal remains used in the OxCal phasing model, with 95.4 % certainty, and their modelled values within phases. New giant root-rat (GRR) radiocarbon dates from this study are indicated with an asterisk. Published outliers and non-Middle Stone Age deposits were removed before phase modelling (see Table S1).

	14C dates	Calibrated mean	Modelled BP Mean	Sigma	Median	From	To	Diagnostic criteria A	C	Material
Phase 3										
Boundary Phase 3 end			31,088	378	31,155	31,645	30,356			
Beta-486377	27,240 ± 120	31,272	31,357	152	31,332	31,635	31,120	74.2	99.9	Charcoal
COL6823.1.1	27,654 ± 168	31,557	31,578	170	31,584	31,893	31,240	102.2	99.9	Charcoal
966/UCIAMS-266013	27,940 ± 350	32,090	31,838	322	31,813	32,531	31,209	118.4	99.9	GRR *
Beta-506528	28,000 ± 140	31,977	31,894	182	31,875	32,220	31,555	110.6	99.9	Charcoal
Beta-507236	28,220 ± 130	32,328	32,074	231	32,029	32,656	31,705	106.7	99.9	Black carbon
Boundary Phase 3 start			32,390	390	32,289	33,241	31,803			
Interval Phase 2 - Phase 3			1,092	556	1,119	0	1,972			
Phase 2										
Boundary Phase 2 end			33,481	495	33,579	34,253	32,440			
D-AMS037003	29,499 ± 164	34,070	34,107	171	34,122	34,422	33,760	102.7	99.9	Coprolite
D-AMS037005	29,736 ± 150	34,273	34,279	136	34,288	34,543	33,993	101.3	99.9	Coprolite
Beta-506527	30,940 ± 170	35,288	35,288	243	35,306	35,741	34,747	99.8	99.9	Coprolite
Beta-506529	31,640 ± 200	35,963	35,962	229	35,987	36,361	35,479	99.8	99.8	Charcoal
Beta-522263	33,600 ± 230	38,489	38,487	461	38,530	39,244	37,627	100.0	99.7	GRR
1026/UCIAMS-266014	34,260 ± 770	39,218	38,895	838	38,997	40,413	37,187	104.3	99.5	GRR*
Beta-522264	34,380 ± 250	39,568	39,501	254	39,493	40,059	39,035	101.9	99.8	GRR
Boundary Phase 2 start			40,219	577	40,130	41,447	39,269			
Interval Phase 1 - Phase 2			1,177	675	1,149	0	2,351			
Phase 1										
Boundary Phase 1 end			41,396	550	41,442	42,414	40,213			
1064/UCIAMS-266010	36,040 ± 970	40,983	41,849	504	41,871	42,820	40,765	81.7	99.6	GRR*
989/UCIAMS-266011	37,300 ± 1100	41,857	42,206	609	42,155	43,784	41,012	103.7	99.6	GRR*
677/UCIAMS-266012	37,800 ± 1200	42,253	42,470	706	42,365	44,121	41,227	105.8	99.7	GRR*
COL6825.1.1	39,414 ± 544	42,978	42,976	403	42,882	43,931	42,372	100.3	99.8	Charcoal
COL6824.1.1	39,675 ± 540	43,160	43,154	434	43,050	44,077	42,476	100.6	99.8	Charcoal
678/UCIAMS-266009	39,700 ± 1500	43,754	43,400	776	43,338	44,946	42,021	112.9	99.7	GRR*
681/UCIAMS-266008	39,900 ± 1600	43,982	43,470	789	43,418	45,033	42,058	116.5	99.6	GRR*
COL6826.2.1	40,286 ± 579	43,552	43,531	445	43,505	44,386	42,755	101.0	99.8	Charcoal
COL5451.1.1	42,086 ± 711	44,907	44,460	525	44,520	45,371	43,265	93.3	99.7	Charcoal
COL6827.1.1	42,351 ± 736	45,128	44,557	522	44,604	45,467	43,305	88.0	99.6	Charcoal
Boundary Phase 1 start			45,053	637	45,010	46,324	43,598			

Table S6: Summary table of giant root-rat bone collagen stable carbon (δ^{13}C) and nitrogen (δ^{15}N) isotope values for the Fincha Habera specimens (n = 17) and the contemporary samples in north (n = 10) and south (n = 20).

Samples	δ^{13}C (‰)					δ^{15}N (‰)				
	Min.	Max.	Median	Mean	sd	Min.	Max.	Median	Mean	sd
Fincha Habera	-21.31	-19.03	-20.25	-20.16	0.55	4.03	9.23	5.65	5.99	1.33
North	-21.01	-16.50	-20.44	-19.91	1.49	3.11	6.07	4.53	4.51	0.99
South	-21.90	-19.50	-20.46	-20.50	0.73	2.41	8.16	4.54	4.68	1.78

Deutsche Zusammenfassung

Wechselwirkungen zwischen Arten und ihrer Umwelt sind das Fundament von Biodiversität und Ökosystemstabilität. Diese Interaktionen gestalten die räumliche Verteilung von Arten und deren Populationsdynamik, wobei aktuelle und frühere Umweltbedingungen sowie evolutionäre Mechanismen wie die Fähigkeit zur Ausbreitung eine entscheidende Rolle spielen. Zu verstehen, wie Arten durch die Umwelt und menschliche Aktivitäten über verschiedene räumliche und zeitliche Skalen hinweg geformt werden, ist eine Voraussetzung, um den anhaltenden Rückgang der globalen biologischen Vielfalt vorherzusagen und umzukehren.

Bodenwühlende, überwiegend unteririsch lebende Arten stehen in der Regel in enger Wechselwirkung mit ihrer Umwelt. Ihre Wühltätigkeit prägt Ökosystemprozesse, schränkt jedoch gleichzeitig ihre Ausbreitungsmöglichkeiten ein. Dies kann sich in Hochgebirgen noch verschärfen, wo die Geomorphologie der Landschaft Verbreitungsgebiete weiter einschränkt. Darüber hinaus können vom Menschen verursachte Umweltveränderungen in Hochgebirgen das Fortbestehen vieler Arten beeinträchtigen.

Um die komplexen Wechselwirkungen zwischen Arten und Umwelt unter dem Einfluss des Menschen zu entschlüsseln, ist eine Kombination von Methoden erforderlich, die verschiedene räumliche Maßstäbe abdeckt und auch berücksichtigt, wie die Umwelt im Laufe der Zeit die Arten geformt hat. In dieser Dissertation habe ich Riesenmaulwurfsatte (Tachyoryctes macrocephalus) untersucht, eine endemische, bodenwühlende Nagetierart mit stark begrenztem Verbreitungsgebiet in den afro-alpinen Bale-Mountains in Südäthiopien. Mithilfe von ökologischen und genetischen Analysen habe ich das Zusammenspiel von Umwelt und menschlichen Aktivitäten auf zeitlicher Skala beleuchtet, dass sowohl die lokale als auch die gesamte Verbreitung der Art formt, ebenso wie ihre genetische Struktur, Diversität und Demografie.

Im Rahmen meiner Studie konnte ich eine Skalenabhängigkeit der Interaktionen zwischen Art und Umwelt aufzeigen, wobei historische und evolutionäre Faktoren die Interaktionen auf lokaler und landschaftlicher Ebene unterschiedlich prägen. Mithilfe ökologischer Feldstudien (Kapitel II) konnte ich eine enge Wechselwirkung zwischen der Riesenmaulwurfsratte, den lokalen Umweltbedingungen und der menschlichen Landnutzung nachweisen. Während die Aktivität der Riesenmaulwurfsratte die Vegetationsbedeckung reduziert, steigt die lokale Aktivität der Art bei geringerer Vegetationsbedeckung und vermehrter Beweidung durch Vieh, welches die Präferenz der Art für offene Lebensräume verdeutlicht. Durch Hochskalierung

dieser Untersuchungen auf Landschaftsebene mit Hilfe von satellitengestützter Fernerkundung und detaillierten Vegetationsdaten (Kapitel III) konnte ich jedoch feststellen, dass die Textur Metriken, die topografische Unterschiede in der Landschaft beschreiben, das gesamte Verbreitungsgebiet der Art bestimmen. Daher unterschieden sich die Umweltbedingungen, die die lokalen Aktivitäten prägen, von denen, die die Gesamtverbreitung der Art beeinflussen.

Populationsgenetische Untersuchungen zur genetischen Strukturierung und Diversität (Kapitel IV) zeigten die Auswirkungen von Topografie auf die Ausbreitungsfähigkeit der Art. Ich konnte eine starke Unterteilung der Art in zwei Populationen feststellen, wobei es keine Anzeichen für einen Genfluss zwischen diesen gab. Landschaftsgenetische Analysen ergaben, dass topografische Barrieren die treibende Kraft auf der Landschaftsebene hierfür waren, während Umweltbedingungen eine untergeordnete Rolle spielten, selbst für die genetische Substruktur innerhalb der jeweiligen Population.

Die Untersuchungen historischer DNA aus subfossilen Überresten der Riesenmaulwurfsratte aus dem späten Pleistozän (Kapitel V) verdeutlichen, wie Umweltveränderungen und menschliche Aktivitäten über Jahrtausende hinweg die phylogenetische Divergenz und demografische Geschichte der Art beeinflussten. Dir letzte Vergletscherung des Bale-Mountains, sowie menschliche Jagdaktivitäten auf die Riesenmaulwurfsratte während dieser Zeit, führten vermutlich zu einem Rückgang der nördlichen, bzw. der südlichen Population. Darüber hinaus zeigte sich in der nördlichen Population ein anhaltender Rückgang und verringerte Nukleotiddiversität seit dem Ende der letzten Eiszeit, was möglicherweise auf durch Umweltveränderungen bedingte Lebensraumverluste zurückzuführen ist.

Die in dieser Arbeit vorgestellten Studien zeigen die direkten Auswirkungen der lokalen Umweltbedingungen und der menschlichen Aktivitäten auf die Riesenmaulwurfsratte. Meiner Ergebnisse haben verdeutlicht, dass die Art nur begrenzt in der Lage ist, ihr Verbreitungsgebiet unter sich ändernden Umweltbedingungen zu verlagern, da topografischer Barrieren in der Landschaft dies erschwert. Daraus lässt sich schließen, dass veränderte Umweltbedingungen in der Zukunft und zunehmende menschliche Aktivitäten negative Auswirkungen auf die Art, und dadurch auch auf die Funktionalität des Ökosystems im afro-alpinen Ökosystem haben könnten. Das Verständnis dieser komplexen Zusammenhänge ist von entscheidender Bedeutung für effektives Schutzmanagement zur Bewahrung der Biodiversität in Hochgebirgen und zur Erhaltung der Ökosystemfunktionalität.

References

Acharya, Bipin Kumar, Wei Chen, Zengliang Ruan, Gobind Prasad Pant, Yin Yang, Lalan Prasad Shah, Chunxiang Cao, Zhiwei Xu, Meghnath Dhimal, and Hualiang Lin. 2019. "Mapping Environmental Suitability of Scrub in Nepal Using Maxent and Random Forest Models." *International Journal of Environmental Research and Public Health* 16(23):4845.

Aguirre-Gutiérrez, Jesús, Luísa G. Carvalheiro, Chiara Polce, E. Emiel van Loon, Niels Raes, Menno Reemer, and Jacobus C. Biesmeijer. 2014. "Fit-for-Purpose: Species Distribution Model Performance Depends on Evaluation Criteria - Dutch Hoverflies as a Case Study." *PLoS ONE* 8(5):e63708.

Akaike, Hirotugu. 1974. "A New Look at the Statistical Model Identification." *IEEE Transactions on Automatic Control* 19(6):716–23.

Alexander, Alana. 2017. "Genetic_diversity_diffs v1.0.3."

Allentoft, Morten E., Martin Sikora, Karl Göran Sjögren, Simon Rasmussen, Morten Rasmussen, Jesper Stenderup, Peter B. Damgaard, Hannes Schroeder, Torbjörn Ahlström, Lasse Vinner, Anna Sapfo Malaspinas, Ashot Margaryan, Tom Higham, David Chivall, Niels Lynnerup, Lise Harvig, Justyna Baron, Philippe Della Casa, Paweł Dąbrowski, Paul R. Duffy, Alexander V. Ebel, Andrey Epimakhov, Karin Frei, Mirosław Furmanek, Tomasz Gralak, Andrey Gromov, Stanisław Gronkiewicz, Gisela Grupe, Tamás Hajdu, Radosław Jarysz, Valeri Khartanovich, Alexandr Khokhlov, Viktória Kiss, Jan Kolář, Aivar Kriiska, Irena Lasak, Cristina Longhi, George McGlynn, Algimantas Merkevicius, Inga Merkyte, Mait Metspalu, Ruzan Mkrtchyan, Vyacheslav Moiseyev, László Paja, György Pálfi, Dalia Pokutta, Łukasz Pospieszny, T. Douglas Price, Lehti Saag, Mikhail Sablin, Natalia Shishlina, Václav Smrčka, Vasilii I. Soenov, Vajk Szeverényi, Gusztáv Tóth, Synaru V. Trifanova, Liivi Varul, Magdolna Vicze, Levon Yepiskoposyan, Vladislav Zhitenev, Ludovic Orlando, Thomas Sicheritz-Pontén, Søren Brunak, Rasmus Nielsen, Kristian Kristiansen, and Eske Willerslev. 2015. "Population Genomics of Bronze Age Eurasia." *Nature* 522(7555):167–72.

Andrade, Analia, and Pablo Marcelo Fernández. 2017. "Rodent Consumption by Hunter-Gatherers in North Patagonian Andean Forests (Argentina): Insights from the Small Vertebrate Taphonomic Analysis of Two Late Holocene Archaeological Sites." *Journal*

of Archaeological Science: Reports 11:390–99.

Asefa, Addisu, Victoria Reuber, Georg Miehe, Melaku Wondafrash, Luise Wraase, Tilaye Wube, Nina Farwig, and Dana G. Schabo. 2022. "The Activity of a Subterranean Small Mammal Alters Afroalpine Vegetation Patterns and Is Positively Affected by Livestock Grazing." *Basic and Applied Ecology*.

Asefa, Addisu, Victoria Reuber, Georg Miehe, Luise Wraase, Tilaye Wube, Dana G. Schabo, and Nina Farwig. 2023. "Human Activities Modulate Reciprocal Effects of a Subterranean Ecological Engineer Rodent, Tachyoryctes Macrocephalus, on Afroalpine Vegetation Cover." *Ecology and Evolution* 13(7).

Avise, John C. 2000. *Phylogeography: The History and Formation of Species*. Cambridge, MA: Havard University Press.

Baca, Mateusz, Danijela Popović, Alexander K. Agadzhanyan, Katarzyna Baca, Nicholas J. Conard, Helen Fewlass, Thomas Filek, Michał Golubiński, Ivan Horáček, Monika V Knul, Magdalena Krajcarz, Maria Krokhaleva, Loïc Lebreton, Anna Lemanik, Lutz C. Maul, Doris Nagel, Pierre Noiret, Jérome Primault, Leonid Rekovets, Sara E. Rhodes, Aurélien Royer, Natalia V Serdyuk, Marie Soressi, John R. Stewart, Tatiana Strukova, Sahra Talamo, Jarosław Wilczyński, and Adam Nadachowski. 2023. "Ancient DNA of Narrow-Headed Vole Reveal Common Features of the Late Pleistocene Population Dynamics in Cold-Adapted Small Mammals." *Proceedings of the Royal Society B: Biological Sciences* 290(1993).

Baca, Mateusz, Danijela Popović, Anna Lemanik, Sandra Bañuls-Cardona, Nicholas J. Conard, Gloria Cuenca-Bescós, Emmanuel Desclaux, Helen Fewlass, Jesus T. Garcia, Tereza Hadravova, Gerald Heckel, Ivan Horáček, Monika Vlasta Knul, Loïc Lebreton, Juan Manuel López-García, Elisa Luzi, Zoran Marković, Jadranka Mauch Lenardić, Xabier Murelaga, Pierre Noiret, Alexandru Petculescu, Vasil Popov, Sara E. Rhodes, Bogdan Ridush, Aurélien Royer, John R. Stewart, Joanna Stojak, Sahra Talamo, Xuejing Wang, Jan M. Wójcik, and Adam Nadachowski. 2023. "Ancient DNA Reveals Interstadials as a Driver of Common Vole Population Dynamics during the Last Glacial Period." *Journal of Biogeography* 50(1):183–96.

Badgley, Catherine, Tara M. Smiley, Rebecca Terry, Edward B. Davis, Larisa R. G. DeSantis, David L. Fox, Samantha S. B. Hopkins, Tereza Jezkova, Marjorie D. Matocq, Nick

Matzke, Jenny L. McGuire, Andreas Mulch, Brett R. Riddle, V. Louise Roth, Joshua X. Samuels, Caroline A. E. Strömberg, and Brian J. Yanites. 2017. "Biodiversity and Topographic Complexity: Modern and Geohistorical Perspectives." *Trends in Ecology and Evolution* 32(3):211–26.

Bakker, E. S., H. Olff, and J. M. Gleichman. 2009. "Contrasting Effects of Large Herbivore Grazing on Smaller Herbivores." *Basic and Applied Ecology* 10(2):141–50.

Barber-Meyer, Shannon M., Gerald L. Kooyman, and Paul J. Ponganis. 2007. "Estimating the Relative Abundance of Emperor Penguins at Inaccessible Colonies Using Satellite Imagery." *Polar Biology* 30(12):1565–70.

Begall, Sabine., Hynek Burda, and Cristian E. Schleich. 2007. *Subterranean Rodents : News from Underground*. Springer.

Bektas, Volkan, Pete Bettinger, Nate Nibbelink, Jacek Siry, Krista Merry, Katrina Ariel Henn, and Jonathan Stober. 2022. "Habitat Suitability Modeling of Rare Turkeybeard (Xerophyllum Asphodeloides) Species in the Talladega National Forest, Alabama, USA." *Forests* 13(4):490.

Bellis, Laura M., Anna M. Pidgeon, Volker C. Radeloff, Véronique St-Louis, Joaquín L. Navarro, and Mónica B. Martella. 2008. "Modeling Habitat Suitability for Greater Rheas Based on Satellite Image Texture." *Ecological Applications* 18(8):1956–66.

Benítez-López, A., R. Alkemade, A. M. Schipper, D. J. Ingram, P. A. Verweij, J. A. J. Eikelboom, and M. A. J. Huijbregts. 2017. "The Impact of Hunting on Tropical Mammal and Bird Populations." *Science* 356(6334):180–83.

Berhane, Tedros M., Hugo Costa, Charles R. Lane, Oleg A. Anenkhonov, Victor V Chepinoga, and Bradley C. Autrey. 2019. "The Influence of Region of Interest Heterogeneity on Classification Accuracy in Wetland Systems." *Remote Sensing* 11(5):551.

Bernt, Matthias, Alexander Donath, Frank Jühling, Fabian Externbrink, Catherine Florentz, Guido Fritzsch, Joern Pütz, Martin Middendorf, and Peter F. Stadler. 2013. "MITOS: Improved de Novo Metazoan Mitochondrial Genome Annotation." *Molecular Phylogenetics and Evolution* 69(2):313–19.

Berthier, K., M. Galan, J. C. Foltête, N. Charbonnel, and J. F. Cosson. 2005. "Genetic Structure of the Cyclic Fossorial Water Vole (Arvicola Terrestris): Landscape and Demographic

Influences." *Molecular Ecology* 14(9):2861–71.

Beyene, Shimelis. 1986. "A Study on Some Ecological Aspects of the Giants Mole Rat Tachyorctes Macrocephalus in the Bale Mountains, Ethiopia." Addis Ababa University.

Birky, William C., Takeo Maruyama, and Paul Fuerst. 1983. "An Approach to Population and Evolutionary Genetic Theory for Genes in Mitochondria and Chloroplasts, and Some Results." *Genetics* 103:513–27.

BMNP. 2017. *Bale Mountains National Park: General Management Plan 2017-2027.*

Bocherens, Hervé. 2003. "Isotopic Biogeochemistry and the Paleoecology of the Mammoth Steppe Fauna." *Deinsea* 117:42–71.

Boivin, Nicole L., Melinda A. Zeder, Dorian Q. Fuller, Alison Crowther, Greger Larson, Jon M. Erlandson, Tim Denhami, and Michael D. Petraglia. 2016. "Ecological Consequences of Human Niche Construction: Examining Long-Term Anthropogenic Shaping of Global Species Distributions." *Proceedings of the National Academy of Sciences of the United States of America* 113(23):6388–96.

Bollongino, Ruth, Anne Tresset, and Jean Denis Vigne. 2008. "Environment and Excavation: Pre-Lab Impacts on Ancient DNA Analyses." *Comptes Rendus - Palevol* 7(2–3):91–98.

Botta--Dukát, Zoltán. 2005. "Rao's Quadratic Entropy as a Measure of Functional Diversity Based on Multiple Traits." *Journal of Vegetation Science* 16(5):533–40.

Boulangeat, Isabelle, Dominique Gravel, and Wilfried Thuiller. 2012. "Accounting for Dispersal and Biotic Interactions to Disentangle the Drivers of Species Distributions and Their Abundances." *Ecology Letters* 15(6):584–93.

ter Braak, Cajo J. F. 1987. "The Analysis of Vegetation-Environment Relationships by Canonical Correspondence Analysis." *Vegetatio* 69(1–3):69–77.

Brandt, Steven, Elisabeth Hildebrand, Ralf Vogelsang, Jesse Wolfhagen, and Hong Wang. 2017. "A New MIS 3 Radiocarbon Chronology for Mochena Borago Rockshelter, SW Ethiopia: Implications for the Interpretation of Late Pleistocene Chronostratigraphy and Human Behavior." *Journal of Archaeological Science: Reports* 11:352–69.

Breiman, Leo. 2001. "Random Forests." *Machine Learning* 45(1):5–32.

Bronk Ramsey, Christopher. 2009. "Bayesian Analysis of Radiocarbon Dates." *Radiocarbon* 51(1):337–60.

Brooks, Mollie E., Kasper Kristensen, Koen J. van Benthem, Arni Magnusson, Casper W. Berg, Anders Nielsen, Hans J. Skaug, Martin Mächler, and Benjamin M. Bolker. 2017. "GlmmTMB Balances Speed and Flexibility among Packages for Zero-Inflated Generalized Linear Mixed Modeling." *R Journal* 9(2):378–400.

Brown, James H. 2001. "Mammals on Mountainsides: Elevational Patterns of Diversity." *Global Ecology and Biogeography* 10(1):101–9.

Brown, James H., George C. Stevens, and Dawn M. Kaufman. 1996. "The Geographic Range: Size, Shape, Boundaries, and Internal Structure." *Source: Annual Review of Ecology and Systematics* 27:597–623.

Brus, D. J. 2019. "Sampling for Digital Soil Mapping: A Tutorial Supported by R Scripts." *Geoderma* 338:464–80.

Brus, D. J., J. J. de Gruijter, and J. W. van Groenigen. 2006. "Designing Spatial Coverage Samples Using the K-Means Clustering Algorithm." *Developments in Soil Science* 31:183–92.

Bryja, J., L. Granjon, G. Dobigny, H. Patzenhauerová, A. Konečný, J. M. Duplantier, P. Gauthier, M. Colyn, L. Durnez, A. Lalis, and V. Nicolas. 2010. "Plio-Pleistocene History of West African Sudanian Savanna and the Phylogeography of the Praomys Daltoni Complex (Rodentia): The Environment/Geography/Genetic Interplay." *Molecular Ecology* 19(21):4783–99.

Campmas, E., E. Stoetzel, and C. Denys. 2018. "African Carnivores as Taphonomic Agents: Contribution of Modern Coprogenic Sample Analysis to Their Identification." *International Journal of Osteoarchaeology* 28(3):237–63.

Campos, Paula F., Eske Willerslev, Andrei Sher, Ludovic Orlando, Erik Axelsson, Alexei Tikhonov, Kim Aaris-Sørensen, Alex D. Greenwood, Ralf Dietrich Kahlke, Pavel Kosintsev, Tatiana Krakhmalnaya, Tatyana Kuznetsova, Philippe Lemey, Ross MacPhee, Christopher A. Norris, Kieran Shepherd, Marc A. Suchard, Grant D. Zazula, Beth Shapiro, and M. Thomas P. Gilbert. 2010. "Ancient DNA Analyses Exclude Humans as the Driving Force behind Late Pleistocene Musk Ox (Ovibos Moschatus) Population Dynamics."

Proceedings of the National Academy of Sciences of the United States of America 107(12):5675–80.

Carøe, Christian, Shyam Gopalakrishnan, Lasse Vinner, Sarah S. T. Mak, Mikkel Holger S. Sinding, José A. Samaniego, Nathan Wales, Thomas Sicheritz-Pontén, and M. Thomas P. Gilbert. 2018. "Single-Tube Library Preparation for Degraded DNA." *Methods in Ecology and Evolution* 9(2):410–19.

Casas-Gallego, Manuel, Karen Hahn, Katharina Neumann, Sebsebe Demissew, Marco Schmidt, Stéphanie C. Bodin, and Angela A. Bruch. 2023. "Cooling-Induced Expansions of Afromontane Forests in the Horn of Africa since the Last Glacial Maximum." *Scientific Reports* 13(1):10323.

Ceballos, Gerardo, Paul R. Ehrlich, Anthony D. Barnosky, Andrés García, Robert M. Pringle, and Todd M. Palmer. 2015. "Accelerated Modern Human-Induced Species Losses: Entering the Sixth Mass Extinction." *Science Advances* 1(5).

Chala, Desalegn, Christian Brochmann, Achilleas Psomas, Dorothee Ehrich, Abel Gizaw, Catherine A. Masao, Vegar Bakkestuen, and Niklaus E. Zimmermann. 2016. "Good-Bye to Tropical Alpine Plant Giants under Warmer Climates? Loss of Range and Genetic Diversity in Lobelia Rhynchopetalum." *Ecology and Evolution* 6(24):8931–41.

Chen, Jianjun, Shuhua Yi, and Yu Qin. 2017. "The Contribution of Plateau Pika Disturbance and Erosion on Patchy Alpine Grassland Soil on the Qinghai-Tibetan Plateau: Implications for Grassland Restoration." *Geoderma* 297:1–9.

Chu, Bin, Chengpeng Ji, Jianwei Zhou, Yanshan Zhou, and Limin Hua. 2021. "Why Does the Plateau Zokor (Myospalax Fontanieri: Rodentia: Spalacidae) Move on the Ground in Summer in the Eastern Qilian Mountains?" *Journal of Mammalogy* 102(1):346–57.

Clarke, Ralph T., Peter Rothery, and Alan F. Raybould. 2002. "Confidence Limits for Regression Relationships between Distance Matrices: Estimating Gene Flow with Distance." *Journal of Agricultural, Biological, and Environmental Statistics* 7(3):361–72.

Cohen, Jacob. 1960. "A Coefficient of Agreement for Nominal Scales." *Educational and Psychological Measurement* 20(1):37–46.

Cohen, K. M., S. C. Finney, P. L. Gibbard, and J. X. Fan. 2013b. "The ICS International Chronostratigraphic Chart." *Episodes Journal of International Geoscience* 36(3):199–

204.

Conrad, O., B. Bechtel, M. Bock, H. Dietrich, E. Fischer, L. Gerlitz, J. Wehberg, V. Wichmann, and J. Böhner. 2015. "System for Automated Geoscientific Analyses (SAGA) v. 2.1.4." *Geoscientific Model Development* 8(7):1991–2007.

Contreras, Luis, Julio Gutiérrez, Víctor Valverde, and George Cox. 1993. "Ecological Relevance of Subterranean Herbivorous Rodents in Semiarid Coastal Chile." *Revista Chilena de Historia Natural* 66(3):357–68.

Corenblit, Dov, Andreas C. W. Baas, Gudrun Bornette, José Darrozes, Sébastien Delmotte, Robert A. Francis, Angela M. Gurnell, Frédéric Julien, Robert J. Naiman, and Johannes Steiger. 2011. "Feedbacks between Geomorphology and Biota Controlling Earth Surface Processes and Landforms: A Review of Foundation Concepts and Current Understandings." *Earth-Science Reviews* 106(3–4):307–31.

Crawford, C. S., W. P. Mackay, and J. G. Cepeda-Pizarro. 1993. "Detritivores of the Chilean Arid Zone and the Namib Desert: A Preliminary Comparison." *Revista Chilena de Historia Natural* (66):283–89.

Culbert, Patrick D., Volker C. Radeloff, Véronique St-Louis, Curtis H. Flather, Chadwick D. Rittenhouse, Thomas P. Albright, and Anna M. Pidgeon. 2012. "Modeling Broad-Scale Patterns of Avian Species Richness across the Midwestern United States with Measures of Satellite Image Texture." *Remote Sensing of Environment* 118:140–50.

Cunningham, Heather R., Leslie J. Rissler, Lauren B. Buckley, and Mark C. Urban. 2016. "Abiotic and Biotic Constraints across Reptile and Amphibian Ranges." *Ecography* 39(1):1–8.

Cushman, Samuel A., and Erin L. Landguth. 2010. "Spurious Correlations and Inference in Landscape Genetics." *Molecular Ecology* 19(17):3592–3602.

Cushman, Samuel A., and Jesse S. Lewis. 2010. "Movement Behavior Explains Genetic Differentiation in American Black Bears." *Landscape Ecology* 25(10):1613–25.

Cushman, Samuel A., Kevin S. McKelvey, Jim Hayden, and Michael K. Schwartz. 2006. "Gene Flow in Complex Landscapes: Testing Multiple Hypotheses with Causal Modeling." *American Naturalist* 168(4):486–99.

Cutrera, A. P., E. A. Lacey, and C. Busch. 2005. "Genetic Structure in a Solitary Rodent (Ctenomys Talarum): Implications for Kinship and Dispersal." *Molecular Ecology* 14(8):2511–23.

Davies, T. Jonathan, Andy Purvis, and John L. Gittleman. 2009. "Quaternary Climate Change and the Geographic Ranges of Mammals." *American Naturalist* 174(3):297–307.

DeLuca, Thomas H., and Gregory H. Aplet. 2008. "Charcoal and Carbon Storage in Forest Soils of the Rocky Mountain West." *Frontiers in Ecology and the Environment* 6(1):18–24.

Desmet, P. G., and R. M. Cowling. 1999. "Patch Creation by Fossorial Rodents: A Key Process in the Revegetation of Phytotoxic Arid Soils." *Journal of Arid Environments* 43(1):35–45.

Dombrosky, Jonathan. 2020. "A ~1000-Year 13C Suess Correction Model for the Study of Past Ecosystems." *Holocene* 30(3):474–78.

Drummond, A. J., A. Rambaut, B. Shapiro, and O. G. Pybus. 2005. "Bayesian Coalescent Inference of Past Population Dynamics from Molecular Sequences." *Molecular Biology and Evolution* 22(5):1185–92.

Dupont, Lydie. 2011. "Orbital Scale Vegetation Change in Africa." *Quaternary Science Reviews* 30(25–26):3589–3602.

Eldridge, David J., and Walter G. Whitford. 2014. "Disturbances by Desert Rodents Are More Strongly Associated with Spatial Changes in Soil Texture than Woody Encroachment." *Plant and Soil* 381(1–2):395–404.

Elith, Jane, Steven J. Phillips, Trevor Hastie, Miroslav Dudík, Yung En Chee, and Colin J. Yates. 2011. "A Statistical Explanation of MaxEnt for Ecologists." *Diversity and Distributions* 17(1):43–57.

Ersmark, Erik, Gennady Baryshnikov, Thomas Higham, Alain Argant, Pedro Castaños, Doris Döppes, Mihaly Gasparik, Mietje Germonpré, Kerstin Lidén, Grzegorz Lipecki, Adrian Marciszak, Rebecca Miller, Marta Moreno-García, Martina Pacher, Marius Robu, Ricardo Rodriguez-Varela, Manuel Rojo Guerra, Martin Sabol, Nikolai Spassov, Jan Storå, Christina Valdiosera, Aritza Villaluenga, John R. Stewart, and Love Dalén. 2019. "Genetic Turnovers and Northern Survival during the Last Glacial Maximum in European Brown Bears." *Ecology and Evolution* 9(10):5891–5905.

Estes, L. D., P. R. Reillo, A. G. Mwangi, G. S. Okin, and H. H. Shugart. 2010. "Remote Sensing of Structural Complexity Indices for Habitat and Species Distribution Modeling." *Remote Sensing of Environment* 114(4):792–804.

Excoffier, Laurent, and Heidi E. L. Lischer. 2010. "Arlequin Suite Ver 3.5: A New Series of Programs to Perform Population Genetics Analyses under Linux and Windows." *Molecular Ecology Resources* 10(3):564–67.

Exposito-Alonso, Moises, Tom R. Booker, Lucas Czech, Lauren Gillespie, Shannon Hateley, Christopher C. Kyriazis, Patricia L. M. Lang, Laura Leventhal, David Nogues-Bravo, Veronica Pagowski, Megan Ruffley, Jeffrey P. Spence, Sebastian E. Toro Arana, Clemens L. WeiÃŸ, and Erin Zess. 2022. "Genetic Diversity Loss in the Anthropocene." *Science* 377(6613):1431–35.

Faith, J. Tyler. 2014. "Late Pleistocene and Holocene Mammal Extinctions on Continental Africa." *Earth-Science Reviews* 128:105–21.

Farwell, Laura S., David Gudex-Cross, Ilianna E. Anise, Michael J. Bosch, Ashley M. Olah, Volker C. Radeloff, Elena Razenkova, Natalia Rogova, Eduarda M. O. Silveira, Matthew M. Smith, and Anna M. Pidgeon. 2021. "Satellite Image Texture Captures Vegetation Heterogeneity and Explains Patterns of Bird Richness." *Remote Sensing of Environment* 253:112175.

Fauteux, Dominique, Louis Imbeau, Pierre Drapeau, and Marc J. Mazerolle. 2012. "Small Mammal Responses to Coarse Woody Debris Distribution at Different Spatial Scales in Managed and Unmanaged Boreal Forests." *Forest Ecology and Management* 266:194–205.

Feilhauer, Hannes, and Sebastian Schmidtlein. 2009. "Mapping Continuous Fields of Forest Alpha and Beta Diversity." *Applied Vegetation Science* 12(4):429–39.

Fellows Yates, James A., Dorothée G. Drucker, Ella Reiter, Simon Heumos, Frido Welker, Susanne C. Münzel, Piotr Wojtal, Martina Lázničková-Galetová, Nicholas J. Conard, Alexander Herbig, Hervé Bocherens, and Johannes Krause. 2017. "Central European Woolly Mammoth Population Dynamics: Insights from Late Pleistocene Mitochondrial Genomes." *Scientific Reports* 7(1):1–10.

Feng, Xiao, Jianjun Qu, Qingbin Fan, Lihai Tan, and Yaoquan Dun. 2020. "Response of Soil

Water Content and Temperature to Rangeland Desertification in an Alpine Region with Seasonally Frozen Soil and Plateau Pika (Ochotona Curzoniae) Burrows." *Journal of Soils and Sediments* 20(10):3722–32.

Fernández-Stolz, Gabriela P., J. F. B. Stolz, and Thales R. O. De Freitas. 2007. "Bottlenecks and Dispersal in the Tuco-Tuco Das Dunas, Ctenomys Flamarioni (Rodentia: Ctenomyidae), in Southern Brazil." *Journal of Mammalogy* 88(4):935–45.

Fiedler, K., G. Brehm, N. Hilt, D. Süßenbach, and C. L. Häuser. 2008. "Variation of Diversity Patterns Across Moth Families Along a Tropical Altitudinal Gradient." *Gradients in a Tropical Mountain Ecosystem of Ecuador* 198:167–79.

Fiedler, Lynwood A. 1990. "Rodents as a Food Source." *Proceedings of the Vertebrate Pest Conference* 14(14):14.

Filipponi, Federico. 2018. "BAIS2: Burned Area Index for Sentinel-2." *Proceedings* 2(7):364.

Finn, Kyle T., Jack Thorley, Hanna M. Bensch, and Markus Zöttl. 2022. "Subterranean Life-Style Does Not Limit Long Distance Dispersal in African Mole-Rats." *Frontiers in Ecology and Evolution* 10.

Foley, Jonathan A., Ruth DeFries, Gregory P. Asner, Carol Barford, Gordon Bonan, Stephen R. Carpenter, F. Stuart Chapin, Michael T. Coe, Gretchen C. Daily, Holly K. Gibbs, Joseph H. Helkowski, Tracey Holloway, Erica A. Howard, Christopher J. Kucharik, Chad Monfreda, Jonathan A. Patz, I. Colin Prentice, Navin Ramankutty, and Peter K. Snyder. 2005. "Global Consequences of Land Use." *Science* 309(5734):570–74.

Frankham, Richard, Jonathan D. Ballou, David A. Briscoe, and Karina H. McInnes. 2002. "Introduction to Conservation Genetics." *Introduction to Conservation Genetics*.

Fretwell, Peter T., Michelle A. LaRue, Paul Morin, Gerald L. Kooyman, Barbara Wienecke, Norman Ratcliffe, Adrian J. Fox, Andrew H. Fleming, Claire Porter, and Phil N. Trathan. 2012. "An Emperor Penguin Population Estimate: The First Global, Synoptic Survey of a Species from Space." *PLoS ONE* 7(4):e33751.

Fretwell, Peter T., Iain J. Staniland, and Jaume Forcada. 2014. "Whales from Space: Counting Southern Right Whales by Satellite." *PLOS ONE* 9(2):1–9.

Gabet, Emmanuel J., O. J. Reichman, and Eric W. Seabloom. 2003. "The Effects of

Bioturbation on Soil Processes and Sediment Transport." *Annual Review of Earth and Planetary Sciences* 31(1):249–73.

Gallego Llorente, M., E. R. Jones, A. Eriksson, V. Siska, K. W. Arthur, J. W. Arthur, M. C. Curtis, J. T. Stock, M. Coltorti, P. Pieruccini, S. Stretton, F. Brock, T. Higham, Y. Park, M. Hofreiter, D. G. Bradley, J. Bhak, R. Pinhasi, and A. Manica. 2015. "Ancient Ethiopian Genome Reveals Extensive Eurasian Admixture throughout the African Continent." *Science* 350(6262):820–22.

Le Galliard, Jean François, Alice Rémy, Rolf A. Ims, and Xavier Lambin. 2012. "Patterns and Processes of Dispersal Behaviour in Arvicoline Rodents." *Molecular Ecology* 21(3):505–23.

Gao, Qing zhu, Yun fan Wan, Hong mei Xu, Yue Li, Wang zha Jiangcun, and Almaz Borjigidai. 2010. "Alpine Grassland Degradation Index and Its Response to Recent Climate Variability in Northern Tibet, China." *Quaternary International* 226(1–2):143–50.

Gashaw, Temesgen. 2015. "Threats of Bale Mountains National Park and Solutions, Ethiopia." *Journal of Physical Science and Environmental Studies* 1(2):10–16.

Gaston, K. J. 2009. "Geographic Range Limits of Species." *Proceedings of the Royal Society B: Biological Sciences* 276(1661):1391–93.

Gaston, Kevin J. 2003. *The Stucture and Dynamics of Geographic Ranges*. Oxford University Press.

Gebrechorkos, Solomon H., Stephan Hülsmann, and Christian Bernhofer. 2019. "Changes in Temperature and Precipitation Extremes in Ethiopia, Kenya, and Tanzania." *International Journal of Climatology* 39(1):18–30.

Gibbs, H. K., and J. M. Salmon. 2015. "Mapping the World's Degraded Lands." *Applied Geography* 57:12–21.

Gil-Romera, Graciela, Carole Adolf, Blas M. Benito, Lucas Bittner, Maria U. Johansson, David A. Grady, Henry F. Lamb, Bruk Lemma, Mekbib Fekadu, Bruno Glaser, Betelhem Mekonnen, Miguel Sevilla-Callejo, Michael Zech, Wolfgang Zech, and Georg Miehe. 2019. "Long-Term Fire Resilience of the Ericaceous Belt, Bale Mountains, Ethiopia." *Biology Letters* 15(7).

Gitelson, Anatoly A., Daniela Gurlin, Wesley J. Moses, and Tadd Barrow. 2009. "A Bio-Optical Algorithm for the Remote Estimation of the Chlorophyll- a Concentration in Case 2 Waters." *Environmental Research Letters* 4(4):45003.

Gottwald, Jannis, Tim Appelhans, Frank Adorf, Jessica Hillen, and Thomas Nauss. 2017. "High-Resolution MaxEnt Modelling of Habitat Suitability for Maternity Colonies of the Barbastelle Bat Barbastella Barbastellus (Schreber, 1774) in Rhineland-Palatinate, Germany." *Acta Chiropterologica* 19(2):389–98.

Graham, Catherine H., Craig Moritz, and Stephen E. Williams. 2006. "Habitat History Improves Prediction of Biodiversity in Rainforest Fauna." *Proceedings of the National Academy of Sciences of the United States of America* 103(3):632–36.

Graham, Russell W., Ernest L. Lundelius, Mary Ann Graham, Erich K. Schroeder, Rickard S. Toomey, Elaine Anderson, Anthony D. Barnosky, James A. Burns, Charles S. Churcher, Donald K. Grayson, R. Dale Guthrie, C. R. Harington, George T. Jefferson, Larry D. Martin, H. Gregory McDonald, Richard E. Morlan, Holmes A. Semken, S. David Webb, Lars Werdelin, and Michael C. Wilson. 1996. "Spatial Response of Mammals to Late Quaternary Environmental Fluctuations." *Science* 272(5268):1601–6.

Grigusova, Paulina, Annegret Larsen, Sebastian Achilles, Alexander Klug, Robin Fischer, Diana Kraus, Kirstin Übernickel, Leandro Paulino, Patricio Pliscoff, Roland Brandl, Nina Farwig, and Jörg Bendix. 2021. "Area-Wide Prediction of Vertebrate and Invertebrate Hole Density and Depth across a Climate Gradient in Chile Based on Uav and Machine Learning." *Drones* 5(3):86.

Grinnell, J. 1917. "Field Tests of Theories Concerning Distributional Control." *The American Naturalist* 51(602):65–128.

Groos, Alexander R., Naki Akçar, Serdar Yesilyurt, Georg Miehe, Christof Vockenhuber, and Heinz Veit. 2021. "Nonuniform Late Pleistocene Glacier Fluctuations in Tropical Eastern Africa." *Science Advances* 7(11).

Guillera-Arroita, Gurutzeta, José J. Lahoz-Monfort, and Jane Elith. 2014. "Maxent Is Not a Presence-Absence Method: A Comment on Thibaud et Al." *Methods in Ecology and Evolution* 5(11):1192–97.

Guo, Yuan Ting, Jia Zhang, Dong Ming Xu, Li Zhou Tang, and Zhen Liu. 2021. "Phylogenomic

Relationships and Molecular Convergences to Subterranean Life in Rodent Family Spalacidae." *Zoological Research* 42(5):671–74.

Hagenah, N., and N. C. Bennett. 2013. "Mole Rats Act as Ecosystem Engineers within a Biodiversity Hotspot, the Cape Fynbos." *Journal of Zoology* 289(1):19–26.

Hahn, Christoph, Lutz Bachmann, and Bastien Chevreux. 2013. "Reconstructing Mitochondrial Genomes Directly from Genomic Next-Generation Sequencing Reads - A Baiting and Iterative Mapping Approach." *Nucleic Acids Research* 41(13):e129–e129.

Haralick, Robert M., K. Shanmugam, and Its'Hak Dinstein. 1973. "Textural Features for Image Classification." *IEEE Transactions on Systems, Man, and Cybernetics* SMC-3(6):610–21.

Harestad, A. S., and F. L. Bunnel. 1979. "Home Range and Body Weight--A Reevaluation." *Ecology* 60(2):389–402.

Hart, Daniel W., Barry van Jaarsveld, Kiara G. Lasch, Kerryn L. Grenfell, Maria K. Oosthuizen, and Nigel C. Bennett. 2021. "Ambient Temperature as a Strong Zeitgeber of Circadian Rhythms in Response to Temperature Sensitivity and Poor Heat Dissipation Abilities in Subterranean African Mole-Rats." *Journal of Biological Rhythms* 36(5):461–69.

Hartig, Florian. 2021. "Residual Diagnostics for Hierarchical (Multi-Level / Mixed) Regression Models [R Package DHARMa Version 0.4.6]."

Hartigan, J. A., and M. A. Wong. 1979. "Algorithm AS 136: A K-Means Clustering Algorithm." *Journal of the Royal Statistical Society. Series C (Applied Statistics)* 28(1):100–108.

Hartigan, John A. 1975. *Clustering Algorithms (Probability & Mathematical Statistics)*. John Wiley & Sons Inc.

Hastings, Alan, James E. Byers, Jeffrey A. Crooks, Kim Cuddington, Clive G. Jones, John G. Lambrinos, Theresa S. Talley, and William G. Wilson. 2007. "Ecosystem Engineering in Space and Time." *Ecology Letters* 10(2):153–64.

Haussmann, Natalie S. 2017. "Soil Movement by Burrowing Mammals: A Review Comparing Excavation Size and Rate to Body Mass of Excavators." *Progress in Physical Geography* 41(1):29–45.

He, Ya, Shuzhan Hu, Deyan Ge, Qisen Yang, Thomas Connor, and Caiquan Zhou. 2020.

"Evolutionary History of Spalacidae Inferred from Fossil Occurrences and Molecular Phylogeny." *Mammal Review* 50(1):11–24.

Heller, Rasmus, Lounes Chikhi, and Hans Redlef Siegismund. 2013. "The Confounding Effect of Population Structure on Bayesian Skyline Plot Inferences of Demographic History." *PLoS ONE* 8(5).

Hempel, Elisabeth, Faysal Bibi, J. Tyler Faith, Klaus Peter Koepfli, Achim M. Klittich, David A. Duchêne, James S. Brink, Daniela C. Kalthoff, Love DalCrossed D sign©n, Michael Hofreiter, and Michael V. Westbury. 2022a. "Blue Turns to Gray: Paleogenomic Insights into the Evolutionary History and Extinction of the Blue Antelope (Hippotragus Leucophaeus)." *Molecular Biology and Evolution* 39(12):1–16.

Hempel, Elisabeth, Faysal Bibi, J. Tyler Faith, Klaus Peter Koepfli, Achim M. Klittich, David A. Duchêne, James S. Brink, Daniela C. Kalthoff, Love DalCrossed D sign©n, Michael Hofreiter, and Michael V. Westbury. 2022b. "Blue Turns to Gray: Paleogenomic Insights into the Evolutionary History and Extinction of the Blue Antelope (Hippotragus Leucophaeus)." *Molecular Biology and Evolution* 39(12).

Hengl, Tomislav. 2007. *A Practical Guide to Geostatistical Mapping of Environmental Variables*.

Henshilwood, C. S. 1997. "Identifying the Collector: Evidence for Human Processing of the Cape Dune Mole-Rat, Bathyergus Suillus, from Blombos Cave, Southern Cape, South Africa." *Journal of Archaeological Science* 24(7):659–62.

Hewitt, Godfrey M. 1996. "Some Genetic Consequences of Ice Ages, and Their Role in Divergence and Speciation." *Biological Journal of the Linnean Society* 58(3):247–76.

Hewitt, Godfrey M. 2004. "The Structure of Biodiversity - Insights from Molecular Phylogeography." *Frontiers in Zoology* 1:1–16.

Hewitt, Judi E., Simon F. Thrush, and Carolyn Lundquist. 2017. "Scale-Dependence in Ecological Systems." *ELS* 1–7.

Hijmans, Robert J., Steven Phillips, John Leathwick, and Jane Elith. 2017. "Dismo: Species Distribution Modeling. R Package Version 1.1-4." *Cran* 55.

Hillman, Jesse C. 1986. "Conservation in Bale Mountains National Park, Ethiopia." *Oryx*

20(2):89–94.

Hoefs, Christian, Tim van der Meer, Peter Antkowiak, Jonas Hagge, Martin Green, and Jannis Gottwald. 2021. "Exploring the Dotterel Mountains: Improving the Understanding of Breeding Habitat Characteristics of an Arctic-Breeding Specialist Bird." *Wader Study* 128(3):226–37.

Hoffmann, Ary A., Carla M. Sgrò, and Torsten N. Kristensen. 2017. "Revisiting Adaptive Potential, Population Size, and Conservation." *Trends in Ecology and Evolution* 32(7):506–17.

Hofreiter, Michael, Johanna L. A. Paijmans, Helen Goodchild, Camilla F. Speller, Axel Barlow, Gloria G. Fortes, Jessica A. Thomas, Arne Ludwig, and Matthew J. Collins. 2015. "The Future of Ancient DNA: Technical Advances and Conceptual Shifts." *BioEssays* 37(3):284–93.

Hollings, Tracey, Mark Burgman, Mary van Andel, Marius Gilbert, Timothy Robinson, and Andrew Robinson. 2018. "How Do You Find the Green Sheep? A Critical Review of the Use of Remotely Sensed Imagery to Detect and Count Animals." *Methods in Ecology and Evolution* 9(4):881–92.

Hothorn, T., F. Bretz, P. Westfall, R. M. Heiberger, Schuetzenmeister A., and S. Scheibe. 2021. "Package 'Multcomp': Simultaneous Inference in General Parametric Models, Version 1.4-17."

Huntly, N., and O. J. Reichman. 1994. "Effects of Subterranean Mammalian Herbivores on Vegetation." *Journal of Mammalogy* 75(4):852–59.

IPBES. 2019. *Summary for Policymakers of the Global Assessment Report on Biodiversity and Ecosystem Services*. Vol. 45.

IPCC. 2023. *Climate Change 2022 – Impacts, Adaptation and Vulnerability*. edited by H.-O. Pörtner, D. C. Roberts, M. Tignor, E. S. Poloczanska, K. Mintenbeck, A. Alegría, M. Craig, S. Langsdorf, S. Löschke, V. Möller, A. Okem, and B. Rama. Cambridge University Press.

Jansen, Jan, Skipton N. C. Woolley, Piers K. Dunstan, Scott D. Foster, Nicole A. Hill, Marcus Haward, and Craig R. Johnson. 2022. "Stop Ignoring Map Uncertainty in Biodiversity Science and Conservation Policy." *Nature Ecology and Evolution* 6(July):828–29.

Jarvis, J. U. M. 2013. "Genus Tachyoryctes - Root-Rats." Pp. 148–52 in *Mammals of Africa : Rodents, Hares and Rabbits*, edited by H. D. C. . Bloomsbury. Bloomsbury Publishing.

Jiang, Hongshan, Rong Lei, Shou Wei Ding, and Shuifang Zhu. 2014. "Skewer: A Fast and Accurate Adapter Trimmer for next-Generation Sequencing Paired-End Reads." *BMC Bioinformatics* 15(1):1–12.

Jones, Clive G., John H. Lawron, and Moshe Shachak. 1997. "Positive and Negative Effects of Organisms as Physical Ecosystem Engineers." *Ecology* 78(7):1946–57.

Jones, Clive G., John H. Lawton, and Moshe Shachak. 1994. "Organisms as Ecosystem Engineers." *Oikos* 130–47.

Jones, E. P., K. Skirnisson, T. H. McGovern, M. T. P. Gilbert, E. Willerslev, and J. B. Searle. 2012. "Fellow Travellers: A Concordance of Colonization Patterns between Mice and Men in the North Atlantic Region." *BMC Evolutionary Biology* 12(1).

Jónsson, Hákon, Aurélien Ginolhac, Mikkel Schubert, Philip L. F. Johnson, and Ludovic Orlando. 2013. "MapDamage2.0: Fast Approximate Bayesian Estimates of Ancient DNA Damage Parameters." *Bioinformatics (Oxford, England)* 29(13):1682–84.

Jueterbock, Alexander, Irina Smolina, James A. Coyer, and Galice Hoarau. 2016. "The Fate of the Arctic Seaweed Fucus Distichus under Climate Change: An Ecological Niche Modeling Approach." *Ecology and Evolution* 6(6):1712–24.

Jury, Mark R., and Chris Funk. 2013. "Climatic Trends over Ethiopia: Regional Signals and Drivers." *International Journal of Climatology* 33(8):1924–35.

Kaky, Emad, and Francis Gilbert. 2016. "Using Species Distribution Models to Assess the Importance of Egypt's Protected Areas for the Conservation of Medicinal Plants." *Journal of Arid Environments* 135:140–46.

Kaky, Emad, Victoria Nolan, Abdulaziz Alatawi, and Francis Gilbert. 2020. "A Comparison between Ensemble and MaxEnt Species Distribution Modelling Approaches for Conservation: A Case Study with Egyptian Medicinal Plants." *Ecological Informatics* 60:101150.

Katoh, Kazutaka, and Daron M. Standley. 2013. "MAFFT Multiple Sequence Alignment Software Version 7: Improvements in Performance and Usability." *Molecular Biology and*

Evolution 30(4):772–80.

Kawalika, Mathias, and Hynek Burda. 2007. "Giant Mole-Rats, Fukomys Mechowii, 13 Years on the Stage." Pp. 205–19 in *Subterranean Rodents: News from Underground*, edited by S. Begall, H. Burda, and C. E. Schleich. Berlin, Heidelberg: Springer.

Keesing, Felicia. 1998. "Impacts of Ungulates on the Demography and Diversity of Small Mammals in Central Kenya." *Oecologia* 116(3):381–89.

Kellenberger, Benjamin, Diego Marcos, and Devis Tuia. 2018. "Detecting Mammals in UAV Images: Best Practices to Address a Substantially Imbalanced Dataset with Deep Learning." *Remote Sensing of Environment* 216:139–53.

Keller, F., F. Kienast, and M. Beniston. 2000. "Evidence of Response of Vegetation to Environmental Change on High-Elevation Sites in the Swiss Alps." *Regional Environmental Change* 1(2):70–77.

Kelt, Douglas A., and Dirk Van Vuren. 1999. "Energetic Constraints and the Relationship between Body Size and Home Range Area in Mammals." *Ecology* 80(1):337–40.

Kerley, Graham I. H., Walter G. Whitford, and Fenton R. Kay. 2004. "Effects of Pocket Gophers on Desert Soils and Vegetation." *Journal of Arid Environments* 58(2):155–66.

Kidane, Yohannes O., Samuel Hoffmann, Anja Jaeschke, Mirela Beloiu, and Carl Beierkuhnlein. 2022. "Ericaceous Vegetation of the Bale Mountains of Ethiopia Will Prevail in the Face of Climate Change." *Scientific Reports 2022 12:1* 12(1):1–17.

Kimura, Birgitta, Fiona B. Marshall, Shanyuan Chen, Sónia Rosenbom, Patricia D. Moehlman, Noreen Tuross, Richard C. Sabin, Joris Peters, Barbara Barich, Hagos Yohannes, Fanuel Kebede, Redae Teclai, Albano Beja-Pereira, and Connie J. Mulligan. 2011. "Ancient DNA from Nubian and Somali Wild Ass Provides Insights into Donkey Ancestry and Domestication." *Proceedings of the Royal Society B: Biological Sciences* 278(1702):50–57.

Koch, Paul L., and Anthony D. Barnosky. 2006. "Late Quaternary Extinctions: State of the Debate."

Korneliussen, Thorfinn Sand, Anders Albrechtsen, and Rasmus Nielsen. 2014. "ANGSD: Analysis of Next Generation Sequencing Data." *BMC Bioinformatics* 15(1):1–13.

Koshkina, Alyona, Irina Grigoryeva, Viktor Tokarsky, Ruslan Urazaliyev, Tobias Kuemmerle, Norbert Hölzel, and Johannes Kamp. 2020. "Marmots from Space: Assessing Population Size and Habitat Use of a Burrowing Mammal Using Publicly Available Satellite Images." *Remote Sensing in Ecology and Conservation* 6(2):153–67.

Kraus, Diana, Roland Brandl, Sebastian Achilles, Jörg Bendix, Paulina Grigusova, Annegret Larsen, Patricio Pliscoff, Kirstin Übernickel, and Nina Farwig. 2022. "Vegetation and Vertebrate Abundance as Drivers of Bioturbation Patterns along a Climate Gradient." *PLOS ONE* 17(3):e0264408.

Krystufek, Boris, and Vladimir Vohralik. 2013. "Taxonomic Revision of the Palaearctic Rodents (Rodentia). Part 2. Sciuridae: Uricotellus, Marmota, and Sciurotamias." Pp. 27–138 in *Lynx*. Vol. 44.

Kuhn, Max, and Kjell Johnson. 2013. *Applied Predictive Modeling*. New York: Springer.

Kupidura, Przemysław. 2019. "The Comparison of Different Methods of Texture Analysis for Their Efficacy for Land Use Classification in Satellite Imagery." *Remote Sensing* 11(10):1233.

Lacey, Eileen A., and John R. Wieczorek. 2003. "Ecology of Sociality in Rodents: A Ctenomyid Perspective." *Journal of Mammalogy* 84(4):1198–1211.

Lamprecht, Andrea, Philipp Robert Semenchuk, Klaus Steinbauer, Manuela Winkler, and Harald Pauli. 2018. "Climate Change Leads to Accelerated Transformation of High-Elevation Vegetation in the Central Alps." *The New Phytologist* 220(2):447–59.

Lande, Russell. 1988. "Genetics and Demography in Biological Conservation." *Science* 241(4872):1455–60.

Lanfear, Robert, Paul B. Frandsen, April M. Wright, Tereza Senfeld, and Brett Calcott. 2017. "Partitionfinder 2: New Methods for Selecting Partitioned Models of Evolution for Molecular and Morphological Phylogenetic Analyses." *Molecular Biology and Evolution* 34(3):772–73.

LaRue, M. A., H. J. Lynch, P. O. B. Lyver, K. Barton, D. G. Ainley, A. Pollard, W. R. Fraser, and G. Ballard. 2014. "A Method for Estimating Colony Sizes of Adélie Penguins Using Remote Sensing Imagery." *Polar Biology* 37(4):507–17.

Latinne, Alice, Christine N. Meynard, Vincent Herbreteau, Surachit Waengsothorn, Serge Morand, and Johan R. Michaux. 2015. "Influence of Past and Future Climate Changes on the Distribution of Three Southeast Asian Murine Rodents." *Journal of Biogeography* 42(9):1714–26.

Lavrenchenko, L., and R. Kennerley. 2016. "Tachyoryctes Macrocephalus, The IUCN Red List of Threatened Species 2016: E.T21293A115161321."

Lawton, John H. 1994. "What Do Species Do in Ecosystems?" *Oikos* 71(3):367.

Lazagabaster, Ignacio A., Valentina Rovelli, Pierre Henri Fabre, Roi Porat, Micka Ullman, Uri Davidovich, Tal Lavi, Amir Ganor, Eitan Klein, Keren Weiss, Perach Nuriel, Meirav Meiri, and Nimrod Marom. 2021. "Rare Crested Rat Subfossils Unveil Afro-Eurasian Ecological Corridors Synchronous with Early Human Dispersals." *Proceedings of the National Academy of Sciences of the United States of America* 118(31):e2105719118.

Lefcheck, Jon. 2021. "4 Coefficients | Composite Variables." Retrieved August 14, 2023 (https://jslefche.github.io/sem_book/coefficients.html).

Lehmann, Sophie B., David R. Braun, Kate J. Dennis, David B. Patterson, Deano D. Stynder, Laura C. Bishop, Frances Forrest, and Naomi E. Levin. 2016. "Stable Isotopic Composition of Fossil Mammal Teeth and Environmental Change in Southwestern South Africa during the Pliocene and Pleistocene." *Palaeogeography, Palaeoclimatology, Palaeoecology* 457:396–408.

Leigh, Jessica W., and David Bryant. 2015. "POPART: Full-Feature Software for Haplotype Network Construction." *Methods in Ecology and Evolution* 6(9):1110–16.

Lenoir, J., J. C. Gégout, P. A. Marquet, P. De Ruffray, and H. Brisse. 2008. "A Significant Upward Shift in Plant Species Optimum Elevation during the 20th Century." *Science (New York, N.Y.)* 320(5884):1768–71.

Leutner, Benjamin, Ned Horning, Jakob Schwalb-Willmann, and Robert J. Hijmans. 2017. "Package 'RStoolbox.'" *R Foundation for Statistical Computing* Version 0.1.

Leyer, Ilona, and Karsten Wesche. 2007. *Multivariate Statistik in Der Ökologie: Eine Einführung*. Springer-Verlag.

Li, Heng, and Richard Durbin. 2009. "Fast and Accurate Short Read Alignment with Burrows–

Wheeler Transform." *Bioinformatics* 25(14):1754–60.

Li, Heng, Bob Handsaker, Alec Wysoker, Tim Fennell, Jue Ruan, Nils Homer, Gabor Marth, Goncalo Abecasis, and Richard Durbin. 2009. "The Sequence Alignment/Map Format and SAMtools." *Bioinformatics* 25(16):2078–79.

Loarie, Scott R., Craig J. Tambling, and Gregory P. Asner. 2013. "Lion Hunting Behaviour and Vegetation Structure in an African Savanna." *Animal Behaviour* 85(5):899–906.

Lord, Edana, Aurelio Marangoni, Mateusz Baca, Danijela Popović, Anna V. Goropashnaya, John R. Stewart, Monika V. Knul, Pierre Noiret, Mietje Germonpré, Elodie Laure Jimenez, Natalia I. Abramson, Sergey Vartanyan, Stefan Prost, Nickolay G. Smirnov, Elena A. Kuzmina, Remi André Olsen, Vadim B. Fedorov, and Love Dalén. 2022. "Population Dynamics and Demographic History of Eurasian Collared Lemmings." *BMC Ecology and Evolution* 22(1):1–13.

Lorenzen, Eline D., David Nogués-Bravo, Ludovic Orlando, Jaco Weinstock, Jonas Binladen, Katharine A. Marske, Andrew Ugan, Michael K. Borregaard, M. Thomas P. Gilbert, Rasmus Nielsen, Simon Y. W. Ho, Ted Goebel, Kelly E. Graf, David Byers, Jesper T. Stenderup, Morten Rasmussen, Paula F. Campos, Jennifer A. Leonard, Klaus Peter Koepfli, Duane Froese, Grant Zazula, Thomas W. Stafford, Kim Aaris-Sørensen, Persaram Batra, Alan M. Haywood, Joy S. Singarayer, Paul J. Valdes, Gennady Boeskorov, James A. Burns, Sergey P. Davydov, James Haile, Dennis L. Jenkins, Pavel Kosintsev, Tatyana Kuznetsova, Xulong Lai, Larry D. Martin, H. Gregory McDonald, Dick Mol, Morten Meldgaard, Kasper Munch, Elisabeth Stephan, Mikhail Sablin, Robert S. Sommer, Taras Sipko, Eric Scott, Marc A. Suchard, Alexei Tikhonov, Rane Willerslev, Robert K. Wayne, Alan Cooper, Michael Hofreiter, Andrei Sher, Beth Shapiro, Carsten Rahbek, and Eske Willerslev. 2011. "Species-Specific Responses of Late Quaternary Megafauna to Climate and Humans." *Nature* 479(7373):359–64.

Lüdecke, Tina, Andreas Mulch, Ottmar Kullmer, Oliver Sandrock, Heinrich Thiemeyer, Jens Fiebig, and Friedemann Schrenk. 2016. "Stable Isotope Dietary Reconstructions of Herbivore Enamel Reveal Heterogeneous Savanna Ecosystems in the Plio-Pleistocene Malawi Rift." *Palaeogeography, Palaeoclimatology, Palaeoecology* 459:170–81.

Lynn, Joshua S., Samuel Canfield, Ross R. Conover, Jeremy Keene, and Jennifer A. Rudgers. 2018. "Pocket Gopher (Thomomys Talpoides) Soil Disturbance Peaks at Mid-Elevation

and Is Associated with Air Temperature, Forb Cover, and Plant Diversity." *Arctic, Antarctic, and Alpine Research* 50(1).

Magoč, Tanja, and Steven L. Salzberg. 2011. "FLASH: Fast Length Adjustment of Short Reads to Improve Genome Assemblies." *Bioinformatics* 27(21):2957–63.

Manel, Stéphanie, Felix Gugerli, Wilfried Thuiller, Nadir Alvarez, Pierre Legendre, Rolf Holderegger, Ludovic Gielly, and Pierre Taberlet. 2012. "Broad-Scale Adaptive Genetic Variation in Alpine Plants Is Driven by Temperature and Precipitation." *Molecular Ecology* 21(15):3729–38.

Manel, Stéphanie, Michael K. Schwartz, Gordon Luikart, and Pierre Taberlet. 2003. "Landscape Genetics: Combining Landscape Ecology and Population Genetics." *Trends in Ecology and Evolution* 18(4):189–97.

Mapelli, Fernando J., Matías S. Mora, Patricia M. Mirol, and Marcelo J. Kittlein. 2012. "Population Structure and Landscape Genetics in the Endangered Subterranean Rodent Ctenomys Porteousi." *Conservation Genetics* 13(1):165–81.

Marcy, Ariel E., Scott Fendorf, James L. Patton, and Elizabeth A. Hadly. 2013. "Morphological Adaptations for Digging and Climate-Impacted Soil Properties Define Pocket Gopher (Thomomys Spp.) Distributions." *PLoS ONE* 8(5).

Martínez-Navarro, Bienvenido, Tegenu Gossa, Francesco Carotenuto, Saverio Bartolini-Lucenti, Paul Palmqvist, Asfawossen Asrat, Borja Figueirido, Lorenzo Rook, Elizabeth M. Niespolo, Paul R. Renne, Gadi Herzlinger, and Erella Hovers. 2023. "The Earliest Ethiopian Wolf: Implications for the Species Evolution and Its Future Survival." *Communications Biology 2023 6:1* 6(1):1–14.

Massada, Avi Bar, Alexandra D. Syphard, Susan I. Stewart, Volker C. Radeloff, Avi Bar Massada, Alexandra D. Syphard, Susan I. Stewart, and Volker C. Radeloff. 2012. "Wildfire Ignition-Distribution Modelling: A Comparative Study in the Huron–Manistee National Forest, Michigan, USA." *International Journal of Wildland Fire* 22(2):174–83.

Meisner, Jonas, and Anders Albrechtsen. 2018. "Inferring Population Structure and Admixture Proportions in Low-Depth NGS Data." *Genetics* 210(2):719–31.

Mekonen, Sefi. 2020. "Coexistence between Human and Wildlife: The Nature, Causes and Mitigations of Human Wildlife Conflict around Bale Mountains National Park, Southeast

Ethiopia." *BMC Ecology* 20(1):1–9.

Mekonnen, Betelhem, Bruno Glaser, Roland Zech, Michael Zech, Frank Schlütz, Robert Bussert, Agerie Addis, Graciela Gil-Romera, Sileshi Nemomissa, Tamrat Bekele, Lucas Bittner, Dawit Solomon, Andreas Manhart, and Wolfgang Zech. 2022. "Climate, Vegetation and Fire History during the Past 18,000 Years, Recorded in High Altitude Lacustrine Sediments on the Sanetti Plateau, Bale Mountains (Ethiopia)." *Progress in Earth and Planetary Science* 9(1):1–19.

Merow, Cory, Matthew J. Smith, and John A. Silander. 2013. "A Practical Guide to MaxEnt for Modeling Species' Distributions: What It Does, and Why Inputs and Settings Matter." *Ecography* 36(10):1058–69.

Mertes, Katherine, and Walter Jetz. 2018. "Disentangling Scale Dependencies in Species Environmental Niches and Distributions." *Ecography* 41(10):1604–15.

Meyer, Hanna, and Edzer Pebesma. 2021. "Predicting into Unknown Space? Estimating the Area of Applicability of Spatial Prediction Models." *Methods in Ecology and Evolution* 12(9):1620–33.

Meyer, Hanna, Christoph Reudenbach, Tomislav Hengl, Marwan Katurji, and Thomas Nauss. 2018. "Improving Performance of Spatio-Temporal Machine Learning Models Using Forward Feature Selection and Target-Oriented Validation." *Environmental Modelling Software* 101:1–9.

Mi, Chunrong, Falk Huettmann, Yumin Guo, Xuesong Han, and Lijia Wen. 2017. "Why Choose Random Forest to Predict Rare Species Distribution with Few Samples in Large Undersampled Areas? Three Asian Crane Species Models Provide Supporting Evidence." *PeerJ* 2017(1):e2849.

Miehe, Georg, Sabine Miene, Knut Kaiser, Liu Jianquan, and Xinquan Zhao. 2008. "Status and Dynamics of the Kobresia Pygmaea Ecosystem on the Tibetan Plateau." *Ambio* 37(4):272–79.

Miehe, Sabine, and Georg Miehe. 1994. *Ericaceous Forests and Heathlands in the Bale Mountains of South Ethiopia*. Hamburg: Traute Warnke, Hamburg.

Miller, Mark A., Wayne Pfeiffer, and Terri Schwartz. 2010. *Creating the CIPRES Science Gateway for Inference of Large Phylogenetic Trees*. New Orleans (LA).

Miranda, Victoria, Carolina Rothen, Natalia Yela, Adriana Aranda-Rickert, Johana Barros, Javier Calcagno, and Sebastián Fracchia. 2019. "Subterranean Desert Rodents (Genus Ctenomys) Create Soil Patches Enriched in Root Endophytic Fungal Propagules." *Microbial Ecology* 77(2):451–59.

Mirol, Patricia, Mabel D. Giménez, Jeremy B. Searle, Claudio J. Bidau, and Chris G. Faulkes. 2010. "Population and Species Boundaries in the South American Subterranean Rodent Ctenomys in a Dynamic Environment." *Biological Journal of the Linnean Society* 100(2):368–83.

Mishra, Varun Narayan, Rajendra Prasad, Praveen Kumar Rai, Ajeet Kumar Vishwakarma, and Aman Arora. 2019. "Performance Evaluation of Textural Features in Improving Land Use/Land Cover Classification Accuracy of Heterogeneous Landscape Using Multi-Sensor Remote Sensing Data." *Earth Science Informatics* 12(1):71–86.

Mokotjomela, Thabiso, Ute Schwaibold, and Neville Pillay. 2009. "Does the Ice Rat Otomys Sloggetti Robertsi Contribute to Habitat Change in Lesotho?" *Acta Oecologica* 35(3):437–43.

Monadjem, Ara, Peter J. Taylor, Christiane Denys, and Fenton P. D. Cotterill. 2015. *Rodents of Sub-Saharan Africa: A Biogeographic and Taxonomic Synthesis*. Berlin, Boston: Walter de Gruyter GmbH & Co KG.

Mooney, Jazlyn A., Clare D. Marsden, Abigail Yohannes, Robert K. Wayne, and Kirk E. Lohmueller. 2023. "Long-Term Small Population Size, Deleterious Variation, and Altitude Adaptation in the Ethiopian Wolf, a Severely Endangered Canid." *Molecular Biology and Evolution* 40(1):1–14.

Mora, Matías S., Fernando J. Mapelli, Oscar E. Gaggiotti, Marcelo J. Kittlein, and Enrique P. Lessa. 2010. "Dispersal and Population Structure at Different Spatial Scales in the Subterranean Rodent Ctenomys Australis." *BMC Genetics* 11(9).

Morales, Narkis S., Ignacio C. Fernández, and Victoria Baca-González. 2017. "MaxEnt's Parameter Configuration and Small Samples: Are We Paying Attention to Recommendations? A Systematic Review." *PeerJ* (3):1–16.

Mueller-Dombois, D., and D. Ellenberg. 1974. *Community Sampling: The Relevé Method*. New York: John Wiley and Sons.

Myers, Norman, Russell A. Mittermeler, Cristina G. Mittermeler, Gustavo A. B. Da Fonseca, and Jennifer Kent. 2000. "Biodiversity Hotspots for Conservation Priorities." *Nature 2000 403:6772* 403(6772):853–58.

Nevo, Eviatar. 1999. *Mosaic Evolution of Subterranean Mammals: Regression, Progression and Global Convergence*. Oxford: Oxford Univ Press.

Nottingham, Andrew T., Noah Fierer, Benjamin L. Turner, Jeanette Whitaker, Nick J. Ostle, Niall P. McNamara, Richard D. Bardgett, Jonathan W. Leff, Norma Salinas, Miles R. Silman, Loeske E. B. Kruuk, and Patrick Meir. 2018. "Microbes Follow Humboldt: Temperature Drives Plant and Soil Microbial Diversity Patterns from the Amazon to the Andes." *Ecology* 99(11):2455–66.

Oksanen, Jari, Pierre Legendre, Bob O'Hara, M. Henry H. Stevens, Maintainer Jari Oksanen, and MASS Suggests. 2020. "Vegan: Community Ecology Package. R Package Version 2.5-7." *Community Ecology Package* 10:631–37.

Olofsson, Johan, Hans Tommervik, and Terry V. Callaghan. 2012. "Vole and Lemming Activity Observed from Space." *Nature Climate Change* 2(12):880–83.

Oppel, Steffen, Ana Meirinho, Iván Ramírez, Beth Gardner, Allan F. O'Connell, Peter I. Miller, and Maite Louzao. 2012. "Comparison of Five Modelling Techniques to Predict the Spatial Distribution and Abundance of Seabirds." *Biological Conservation* 156:94–104.

Orrock, John L., John F. Pagels, William J. McShea, and Elizabeth K. Harper. 2000. "Predicting Presence and Abundance of a Small Mammal Species: The Effect of Scale and Resolution." *Ecological Applications* 10(5):1356–66.

Ossendorf, Götz, Alexander R. Groos, Tobias Bromm, Minassie Girma Tekelemariam, Bruno Glaser, Joséphine Lesur, Joachim Schmidt, Naki Akçar, Tamrat Bekele, Alemseged Beldados, Sebsebe Demissew, Trhas Hadush Kahsay, Barbara P. Nash, Thomas Nauss, Agazi Negash, Sileshi Nemomissa, Heinz Veit, Ralf Vogelsang, Zerihun Woldu, Wolfgang Zech, Lars Opgenoorth, and Georg Miehe. 2019. "Middle Stone Age Foragers Resided in High Elevations of the Glaciated Bale Mountains, Ethiopia." *Science* 365(6453):583–87.

Ossendorf, Götz, Minassie Girma Tekelemariam, Joséphine Lesur, and Ralf Vogelsang. 2023. "Fincha Habera, Ethiopia." Pp. 315–25 in *Handbook of Pleistocene Archaeology of*

Africa: Hominin behavior, geography, and chronology, edited by A. Beyin, D. K. Wright, J. Wilkins, and D. I. Olszewski. Cham: Springer.

Padilla, Francisco M., Beatriz Vidal, Joaquín Sánchez, and Francisco I. Pugnaire. 2010. "Land-Use Changes and Carbon Sequestration through the Twentieth Century in a Mediterranean Mountain Ecosystem: Implications for Land Management." *Journal of Environmental Management* 91(12):2688–95.

Palkopoulou, Eleftheria, Love Dalén, Adrian M. Lister, Sergey Vartanyan, Mikhail Sablin, Andrei Sher, Veronica Nyström Edmark, Mikael D. Brandström, Mietje Germonpré, Ian Barnes, and Jessica A. Thomas. 2013. "Holarctic Genetic Structure and Range Dynamics in the Woolly Mammoth." *Proceedings of the Royal Society B: Biological Sciences* 280(1770).

Palmeirim, Ana Filipa, Manoel Santos-Filho, and Carlos A. Peres. 2020. "Marked Decline in Forest-Dependent Small Mammals Following Habitat Loss and Fragmentation in an Amazonian Deforestation Frontier." *PLOS ONE* 15(3):e0230209.

Paradis, Emmanuel, and Jeffrey Barrett. 2010. "Pegas: An R Package for Population Genetics with an Integrated–Modular Approach." *Bioinformatics* 26(3):419–20.

Parmesan, Camille. 2006. "Ecological and Evolutionary Responses to Recent Climate Change." *Annual Review of Ecology, Evolution, and Systematics* 37:637–69.

Pauls, Steffen U., Carsten Nowak, Miklõs Bálint, and Markus Pfenninger. 2013. "The Impact of Global Climate Change on Genetic Diversity within Populations and Species." *Molecular Ecology* 22(4):925–46.

Payne, Davnah, Eva M. Spehn, Mark Snethlage, and Markus Fischer. 2017. "Opportunities for Research on Mountain Biodiversity under Global Change." *Current Opinion in Environmental Sustainability* 29:40–47.

Peterman, William E. 2018. "ResistanceGA: An R Package for the Optimization of Resistance Surfaces Using Genetic Algorithms." *Methods in Ecology and Evolution* 9(6):1638–47.

Peterman, William E., Grant M. Connette, Raymond D. Semlitsch, and Lori S. Eggert. 2014. "Ecological Resistance Surfaces Predict Fine-Scale Genetic Differentiation in a Terrestrial Woodland Salamander." *Molecular Ecology* 23(10):2402–13.

Phillips, Steven, Robert P. Anderson, and Robert E. Schapire. 2006. "Maximum Entropy Modeling of Species Geographic Distribution." *Ecological Modelling* 190(3–4):231–59.

Pielke, Roger A., Andy Pitman, Dev Niyogi, Rezaul Mahmood, Clive McAlpine, Faisal Hossain, Kees Klein Goldewijk, Udaysankar Nair, Richard Betts, Souleymane Fall, Markus Reichstein, Pavel Kabat, and Nathalie de Noblet. 2011. "Land Use/Land Cover Changes and Climate: Modeling Analysis and Observational Evidence." *Wiley Interdisciplinary Reviews: Climate Change* 2(6):828–50.

Pinheiro, José, and Douglas Bates. 2019. "Nlme: Linear and Nonlinear Mixed Effects Models." *Mixed-Effects Models in S and S-PLUS*.

Porcasi, X., G. Calderón, M. Lamfri, N. Gardenal, J. Polop, M. Sabattini, and C. M. Scavuzzo. 2005. "The Use of Satellite Data in Modeling Population Dynamics and Prevalence of Infection in the Rodent Reservoir of Junin Virus." *Ecological Modelling* 185(2–4):437–49.

Pöyry, Juha, Kristin Böttcher, Stefan Fronzek, Nadine Gobron, Reima Leinonen, Sari Metsämäki, and Raimo Virkkala. 2018. "Predictive Power of Remote Sensing versus Temperature-Derived Variables in Modelling Phenology of Herbivorous Insects." *Remote Sensing in Ecology and Conservation* 4(2):113–26.

Prendergast, Mary E., Jennifer Miller, Ogeto Mwebi, Emmanuel Ndiema, Ceri Shipton, Nicole Boivin, and Michael Petraglia. 2023. "Small Game Forgotten: Late Pleistocene Foraging Strategies in Eastern Africa, and Remote Capture at Panga Ya Saidi, Kenya." *Quaternary Science Reviews* 305:108032.

Price, Mary V, and Robert H. Podolsky. 1989. "Mechanisms of Seed Harvest by Heteromyid Rodents: Soil Texture Effects on Harvest Rate and Seed Size Selection." *Oecologia* 81(2):267–73.

Quaglietta, Lorenzo, Vania C. Fonseca, Petra Hájková, António Mira, and Luigi Boitani. 2013. "Fine-Scale Population Genetic Structure and Short-Range Sex-Biased Dispersal in a Solitary Carnivore, Lutra Lutra." *Journal of Mammalogy* 94(3):561–71.

R Core Team. 2021. "R: A Language and Environment for Statistical Computing. R Foundation for Statistical Computing."

Rahbek, Carsten, Michael K. Borregaard, Alexandre Antonelli, Robert K. Colwell, Ben G. Holt,

David Nogues-Bravo, Christian M. Ø. Rasmussen, Katherine Richardson, Minik T. Rosing, Robert J. Whittaker, and Jon Fjeldså. 2019. "Building Mountain Biodiversity: Geological and Evolutionary Processes." *Science* 365(6458):1114–19.

Rahbek, Carsten, Michael K. Borregaard, Robert K. Colwell, Bo Dalsgaard, Ben G. Holt, Naia Morueta-Holme, David Nogues-Bravo, Robert J. Whittaker, and Jon Fjeldså. 2019. "Humboldt's Enigma: What Causes Global Patterns of Mountain Biodiversity?" *Science* 365(6458):1108–13.

Rambaut, Andrew, Alexei J. Drummond, Dong Xie, Guy Baele, and Marc A. Suchard. 2018. "Posterior Summarization in Bayesian Phylogenetics Using Tracer 1.7." *Systematic Biology* 67(5):901–4.

Rangwala, Imtiaz, and James R. Miller. 2012. "Climate Change in Mountains: A Review of Elevation-Dependent Warming and Its Possible Causes." *Climatic Change* 114(3–4):527–47.

Rao, C. Radhakrishn. 1982. "Diversity and Dissimilarity Coefficients: A Unified Approach." *Theoretical Population Biology* 21(1):24–43.

Rehling, Finn, Anna Delius, Julia Ellerbrok, Nina Farwig, and Franziska Peter. 2023. "Wind Turbines in Managed Forests Partially Displace Common Birds." *Journal of Environmental Management* 328:116968.

Rehling, Finn, Eelke Jongejans, Jan Schlautmann, Jörg Albrecht, Hubert Fassbender, Bogdan Jaroszewicz, Diethart Matthies, Lina Waldschmidt, Nina Farwig, and Dana G. Schabo. 2023. "Common Seed Dispersers Contribute Most to the Persistence of a Fleshy-Fruited Tree." *Communications Biology* 6(1).

Reichman, O. J. 1975. "Relation of Desert Rodent Diets to Available Resources." *Journal of Mammalogy* 56(4):731–51.

Reichman, O. J., and Eric W. Seabloom. 2002. "The Role of Pocket Gophers as Subterranean Ecosystem Engineers." *Trends in Ecology and Evolution* 17(1):44–49.

Reichman, O. J., and S. C. Smith. 1985. "Impact of Pocket Gopher Burrows on Overlying Vegetation." *Journal of Mammalogy* 66(4):720–25.

Reimer, Paula J., William E. N. Austin, Edouard Bard, Alex Bayliss, Paul G. Blackwell,

Christopher Bronk Ramsey, Martin Butzin, Hai Cheng, R. Lawrence Edwards, Michael Friedrich, Pieter M. Grootes, Thomas P. Guilderson, Irka Hajdas, Timothy J. Heaton, Alan G. Hogg, Konrad A. Hughen, Bernd Kromer, Sturt W. Manning, Raimund Muscheler, Jonathan G. Palmer, Charlotte Pearson, Johannes Van Der Plicht, Ron W. Reimer, David A. Richards, E. Marian Scott, John R. Southon, Christian S. M. Turney, Lukas Wacker, Florian Adolphi, Ulf Büntgen, Manuela Capano, Simon M. Fahrni, Alexandra Fogtmann-Schulz, Ronny Friedrich, Peter Köhler, Sabrina Kudsk, Fusa Miyake, Jesper Olsen, Frederick Reinig, Minoru Sakamoto, Adam Sookdeo, and Sahra Talamo. 2020. "The IntCal20 Northern Hemisphere Radiocarbon Age Calibration Curve (0–55 Cal KBP)." *Radiocarbon* 62(4):725–57.

Reuber, Victoria M., Alba Rey-Iglesia, Michael V. Westbury, Andrea A. Cabrera, Nina Farwig, Mikkel Skovrind, Radim Šumbera, Tilaye Wube, Lars Opgenoorth, Dana G. Schabo, and Eline D. Lorenzen. 2021. "Complete Mitochondrial Genome of the Giant Root-Rat (Tachyoryctes Macrocephalus)." *Mitochondrial DNA Part B: Resources* 6(8):2191–93.

Reuber, Victoria M., Michael V. Westbury, Alba Rey-Iglesia, Addisu Asefa, Nina Farwig, Georg Miehe, Lars Opgenoorth, Radim Sumbera, Luise Wraase, Tilaye Wube, Eline D. Lorenzen, and Dana G. Schabo. 2023. "Topographic Barriers Drive the Pronounced Genetic Subdivision of a Range-Limited Fossorial Rodent." *BioRxiv* 2023.04.06.535856.

Rey-Iglesia, Alba, Adrian M. Lister, Anthony J. Stuart, Hervé Bocherens, Paul Szpak, Eske Willerslev, and Eline D. Lorenzen. 2021. "Late Pleistocene Paleoecology and Phylogeography of Woolly Rhinoceroses." *Quaternary Science Reviews* 263.

Rice, William R. 1989. "Analyzing Tables of Statistical Tests." *Evolution* 43:223–25.

Rieux, Adrien, and Camilo E. Khatchikian. 2017. "Tipdatingbeast: An r Package to Assist the Implementation of Phylogenetic Tip-Dating Tests Using Beast." *Molecular Ecology Resources* 17(4):608–13.

Rocchini, Duccio, Giovanni Bacaro, Gherardo Chirici, Daniele Da Re, Hannes Feilhauer, Giles M. Foody, Marta Galluzzi, Carol X. Garzon-Lopez, Thomas W. Gillespie, Kate S. He, Jonathan Lenoir, Matteo Marcantonio, Harini Nagendra, Carlo Ricotta, Edvinas Rommel, Sebastian Schmidtlein, Andrew K. Skidmore, Ruben Van De Kerchove, Martin Wegmann, and Benedetto Rugani. 2018. "Remotely Sensed Spatial Heterogeneity as an Exploratory Tool for Taxonomic and Functional Diversity Study." *Ecological Indicators* 85(June

2017):983–90.

Romero, Gustavo Q., Thiago Gonçalves-Souza, Camila Vieira, and Julia Koricheva. 2015. "Ecosystem Engineering Effects on Species Diversity across Ecosystems: A Meta-Analysis." *Biological Reviews* 90(3):877–90.

Ronquist, Fredrik, and John P. Huelsenbeck. 2003. "MrBayes 3: Bayesian Phylogenetic Inference under Mixed Models." *Bioinformatics* 19(12):1572–74.

Rosengren, Erika, Arina Acatrinei, Nicolae Cruceru, Marianne Dehasque, Aritina Haliuc, Edana Lord, Cristina I. Mircea, Ioana Rusu, Emilio Mármol-Sánchez, Beatrice S. Kelemen, and Ioana N. Meleg. 2021. "Ancient Faunal History Revealed by Interdisciplinary Biomolecular Approaches." *Diversity* 13(8):1–31.

Rosenzweig, Michael L. 1995. *Species Diversity in Space and Time*. Cambridge University Press.

Rousset, François. 1997. "Genetic Differentiation and Estimation of Gene Flow from F-Statistics under Isolation by Distance." *Genetics* 145(4):1219–28.

Rozas, Julio, Juan C. Sánchez-DelBarrio, Xavier Messeguer, and Ricardo Rozas. 2003. "DnaSP, DNA Polymorphism Analyses by the Coalescent and Other Methods." *Bioinformatics* 19(18):2496–97.

Ruiz-Gonzalez, Aritz, Samuel A. Cushman, María José Madeira, Ettore Randi, and Benjamín J. Gómez-Moliner. 2015. "Isolation by Distance, Resistance and/or Clusters? Lessons Learned from a Forest-Dwelling Carnivore Inhabiting a Heterogeneous Landscape." *Molecular Ecology* 24(20):5110–29.

Ruiz, Daniel, Hernán Alonso Moreno, María Elena Gutiérrez, and Paula Andrea Zapata. 2008. "Changing Climate and Endangered High Mountain Ecosystems in Colombia." *Science of the Total Environment* 398(1–3):122–32.

Sandel, B., L. Arge, B. Dalsgaard, R. G. Davies, K. J. Gaston, W. J. Sutherland, and J. C. Svenning. 2011. "The Influence of Late Quaternary Climate-Change Velocity on Species Endemism." *Science* 334(6056):660–64.

Sandel, Brody. 2015. "Towards a Taxonomy of Spatial Scale-Dependence." *Ecography* 38(4):358–69.

Schaebitz, Frank, Asfawossen Asrat, Henry F. Lamb, Andrew S. Cohen, Verena Foerster, Walter Duesing, Stefanie Kaboth-Bahr, Stephan Opitz, Finn A. Viehberg, Ralf Vogelsang, Jonathan Dean, Melanie J. Leng, Annett Junginger, Christopher Bronk Ramsey, Melissa S. Chapot, Alan Deino, Christine S. Lane, Helen M. Roberts, Céline Vidal, Ralph Tiedemann, and Martin H. Trauth. 2021. "Hydroclimate Changes in Eastern Africa over the Past 200,000 Years May Have Influenced Early Human Dispersal." *Communications Earth and Environment* 2(1):1–10.

Schaffers, Andre P., Ivo P. Raemakers, Karle V. Sykora, and Cajo J. F. Ter Braak. 2008. "Arthropod Assemblages Are Best Predicted By Plant." *Ecology* 89(3):782–94.

Schmieder, Robert, and Robert Edwards. 2011. "Quality Control and Preprocessing of Metagenomic Datasets." *Bioinformatics* 27(6):863–64.

Schubert, Mikkel, Luca Ermini, Clio Der Sarkissian, Hákon Jónsson, Aurélien Ginolhac, Robert Schaefer, Michael D. Martin, Ruth Fernández, Martin Kircher, Molly McCue, Eske Willerslev, and Ludovic Orlando. 2014. "Characterization of Ancient and Modern Genomes by SNP Detection and Phylogenomic and Metagenomic Analysis Using PALEOMIX." *Nature Protocols 2014 9:5* 9(5):1056–82.

Schubert, Mikkel, Stinus Lindgreen, and Ludovic Orlando. 2016. "AdapterRemoval v2: Rapid Adapter Trimming, Identification, and Read Merging." *BMC Research Notes* 9(1).

Schweizer, Manuel, Laurent Excoffier, and Gerald Heckel. 2007. "Fine-Scale Genetic Structure and Dispersal in the Common Vole (Microtus Arvalis)." *Molecular Ecology* 16(12):2463–73.

Scrucca, Luca. 2013. "GA: A Package for Genetic Algorithms in R." *Journal of Statistical Software* 53(4):1–37.

Sexton, Jason P., Patrick J. McIntyre, Amy L. Angert, and Kevin J. Rice. 2009. "Evolution and Ecology of Species Range Limits." *Annual Review of Ecology, Evolution, and Systematics* 40:415–36.

Shenbrot, Georgy I., and Boris R. Krasnov. 2005. "An Atlas of the Geographic Distribution of the Arvicoline Rodents of the World (Rodentia, Muridae: Arvicolinae)." 336.

Sherrod, Susan K., and Timothy R. Seastedt. 2001. "Effects of the Northern Pocket Gopher (Thomomys Talpoides) on Alpine Soil Characteristics, Niwot Ridge, CO."

Biogeochemistry 55(2):195–218.

Shipley, Bill. 2009. "Confirmatory Path Analysis in a Generalized Multilevel Context." *Ecology* 90(2):363–68.

Shirk, Andrew J., Erin L. Landguth, and Samuel A. Cushman. 2018. "A Comparison of Regression Methods for Model Selection in Individual-Based Landscape Genetic Analysis." *Molecular Ecology Resources* 18(1):55–67.

Sillero-Zubiri, C., and D. Gottelli. 1995. "Diet and Feeding Behavior of Ethiopian Wolves (Canis Simensis)." *Journal of Mammalogy* 76(2):531–41.

Sillero-Zubiri, C., F. H. Tattersall, and D. W. Macdonald. 1995. "Habitat Selection and Daily Activity of Giant Molerats Tachyoryctes Macrocephalus: Significance to the Ethiopian Wolf Canis Simensis in the Afroalpine Ecosystem." *Biological Conservation* 72(1):77–84.

Simonetti, Javier A., and Luis E. Cornejo. 1991. "Archaeological Evidence of Rodent Consumption in Central Chile." *Latin American Antiquity* 2(1):92–96.

Šklíba, Jan, T. Vlasatá, M. Lövy, E. Hrouzková, Y. Meheretu, C. Sillero-Zubiri, and R. Šumbera. 2020. "The Giant That Makes Do with Little: Small and Easy-to-Leave Home Ranges Found in the Giant Root-Rat." *Journal of Zoology* 310(1):64–70.

Šklíba, Jan, Tereza Vlasatá, Matěj Lövy, Ema Hrouzková, Yonas Meheretu, Claudio Sillero-Zubiri, and Radim Šumbera. 2017. "Ecological Role of the Giant Root-Rat (Tachyoryctes Macrocephalus) in the Afroalpine Ecosystem." *Integrative Zoology* 12(4):333–44.

Skoglund, Pontus, Jessica C. Thompson, Mary E. Prendergast, Alissa Mittnik, Kendra Sirak, Mateja Hajdinjak, Tasneem Salie, Nadin Rohland, Swapan Mallick, Alexander Peltzer, Anja Heinze, Iñigo Olalde, Matthew Ferry, Eadaoin Harney, Megan Michel, Kristin Stewardson, Jessica I. Cerezo-Román, Chrissy Chiumia, Alison Crowther, Elizabeth Gomani-Chindebvu, Agness O. Gidna, Katherine M. Grillo, I. Taneli Helenius, Garrett Hellenthal, Richard Helm, Mark Horton, Saioa López, Audax Z. P. Mabulla, John Parkington, Ceri Shipton, Mark G. Thomas, Ruth Tibesasa, Menno Welling, Vanessa M. Hayes, Douglas J. Kennett, Raj Ramesar, Matthias Meyer, Svante Pääbo, Nick Patterson, Alan G. Morris, Nicole Boivin, Ron Pinhasi, Johannes Krause, and David Reich. 2017. "Reconstructing Prehistoric African Population Structure." *Cell* 171(1):59-71.e21.

Skotte, Line, Thorfinn Sand Korneliussen, and Anders Albrechtsen. 2013. "Estimating Individual Admixture Proportions from next Generation Sequencing Data." *Genetics* 195(3):693–702.

Slatyer, Rachel A., Megan Hirst, and Jason P. Sexton. 2013. "Niche Breadth Predicts Geographical Range Size: A General Ecological Pattern." *Ecology Letters* 16(8):1104–14.

Smith, AT, NA Formozov, RS Hoffmann, Z. Changlin, and MA Erbajeva. 1990. "The Pikas." Pp. 14–60 in *Rabbits, Hares and Pikas: Status Survey and Conservation Action Plan*. International Union for Conservation of Nature and Natural Resources.

Stamatakis, Alexandros. 2014. "RAxML Version 8: A Tool for Phylogenetic Analysis and Post-Analysis of Large Phylogenies." *Bioinformatics* 30(9):1312–13.

Steinbauer, Manuel J., John Arvid Grytnes, Gerald Jurasinski, Aino Kulonen, Jonathan Lenoir, Harald Pauli, Christian Rixen, Manuela Winkler, Manfred Bardy-Durchhalter, Elena Barni, Anne D. Bjorkman, Frank T. Breiner, Sarah Burg, Patryk Czortek, Melissa A. Dawes, Anna Delimat, Stefan Dullinger, Brigitta Erschbamer, Vivian A. Felde, Olatz Fernández-Arberas, Kjetil F. Fossheim, Daniel Gómez-García, Damien Georges, Erlend T. Grindrud, Sylvia Haider, Siri V. Haugum, Hanne Henriksen, María J. Herreros, Bogdan Jaroszewicz, Francesca Jaroszynska, Robert Kanka, Jutta Kapfer, Kari Klanderud, Ingolf Kühn, Andrea Lamprecht, Magali Matteodo, Umberto Morra Di Cella, Signe Normand, Arvid Odland, Siri L. Olsen, Sara Palacio, Martina Petey, Veronika Piscová, Blazena Sedlakova, Klaus Steinbauer, Veronika Stöckli, Jens Christian Svenning, Guido Teppa, Jean Paul Theurillat, Pascal Vittoz, Sarah J. Woodin, Niklaus E. Zimmermann, and Sonja Wipf. 2018. "Accelerated Increase in Plant Species Richness on Mountain Summits Is Linked to Warming." *Nature 2018 556:7700* 556(7700):231–34.

Stephens, Philip A., Candy A. D'Sa, Claudio Sillero-Zubiri, and Nigel Leader-Williams. 2001. "Impact of Livestock and Settlement on the Large Mammalian Wildlife of Bale Mountains National Park, Southern Ethiopia." *Biological Conservation* 100(3):307–22.

Stevens, Rhiannon E., Roger Jacobi, Martin Street, Mietje Germonpré, Nicholas J. Conard, Susanne C. Münzel, and Robert E. M. Hedges. 2008. "Nitrogen Isotope Analyses of Reindeer (Rangifer Tarandus), 45,000 BP to 9,000 BP: Palaeoenvironmental Reconstructions." *Palaeogeography, Palaeoclimatology, Palaeoecology* 262(1–2):32–45.

Stewart, Alan J. A., Tristan M. Bantock, Björn C. Beckmann, Marc S. Botham, David Hubble,

and David B. Roy. 2015. "The Role of Ecological Interactions in Determining Species Ranges and Range Changes." *Biological Journal of the Linnean Society* 115(3):647–63.

Stewart, G. R., M. H. Turnbull, S. Schmidt, and P. D. Erskine. 1995. "13C Natural Abundance in Plant Communities Along a Rainfall Gradient: A Biological Integrator of Water Availability." *Functional Plant Biology* 22(1):51–55.

Suchard, Marc A., Philippe Lemey, Guy Baele, Daniel L. Ayres, Alexei J. Drummond, and Andrew Rambaut. 2018. "Bayesian Phylogenetic and Phylodynamic Data Integration Using BEAST 1.10." *Virus Evolution* 4(1).

Šumbera, Radim, Jarmila Krásová, Leonid A. Lavrenchenko, Sewnet Mengistu, Afework Bekele, Ondřej Mikula, and Josef Bryja. 2018. "Ethiopian Highlands as a Cradle of the African Fossorial Root-Rats (Genus Tachyoryctes), the Genetic Evidence." *Molecular Phylogenetics and Evolution* 126:105–15.

Šumbera, Radim, Matěj Lövy, Jorgelina Marino, Miloslav Šimek, and Jan Šklíba. 2020. "Gas Composition and Its Daily Changes within Burrows and Nests of an Afroalpine Fossorial Rodent, the Giant Root-Rat Tachyoryctes Macrocephalus." *Zoology* 142:125819.

Swift, Jillian A., Michael Bunce, Joe Dortch, Kristina Douglass, J. Tyler Faith, James A. Fellows Yates, Judith Field, Simon G. Haberle, Eileen Jacob, Chris N. Johnson, Emily Lindsey, Eline D. Lorenzen, Julien Louys, Gifford Miller, Alexis M. Mychajliw, Viviane Slon, Natalia A. Villavicencio, Michael R. Waters, Frido Welker, Rachel Wood, Michael Petraglia, Nicole Boivin, and Patrick Roberts. 2019. "Micro Methods for Megafauna: Novel Approaches to Late Quaternary Extinctions and Their Contributions to Faunal Conservation in the Anthropocene." *BioScience* 69(11):877–87.

Tallents, Lucy A., and David W. Macdonald. 2011. "Mapping High-Altitude Vegetation in the Bale Mountains, Ethiopia." *Walia—Special Edition on the Bale Mountains* 97–117.

Tang, Ze, Yangjian Zhang, Nan Cong, Michael Wimberly, Li Wang, Ke Huang, Junxiang Li, Jiaxing Zu, Yixuan Zhu, and Ning Chen. 2019. "Spatial Pattern of Pika Holes and Their Effects on Vegetation Coverage on the Tibetan Plateau: An Analysis Using Unmanned Aerial Vehicle Imagery." *Ecological Indicators* 107:105551.

Tariku, Z. .. 2021. "Analysis of Faunal Collections from Simbero Rock Shelter in the Bale Mountains National Park. Unpublished M.A. Theses." University of Cologne.

Taylor, Peter John, Aluwani Nengovhela, Jabulani Linden, and Roderick M. Baxter. 2016. "Past, Present, and Future Distribution of Afromontane Rodents (Muridae: Otomys) Reflect Climate-Change Predicted Biome Changes." *Mammalia* 80(4):359–75.

Teklehaimanot, Gebremeskel, and M. Balakrishnan. 2018. "Distribution and Population Status of the Endemic Rock Hyrax Sub-Species Distribution and Population Status of the Endemic Rock Hyrax Sub-Species (Procavia Capensis Capillosa) of the Bale Mountains, Ethiopia." *International Journal of Ecology and Environmental Sciences* 44(1):1–10.

Teshome, Eyob, Deborah Randall, and Anouska Kinahan. 2011. "The Changing Face of the Bate Mountains National Park over 32 Years: A Study of Land Cover Change." *Walia* 2011:118–30.

Tierney, Jessica E., James M. Russell, Yongsong Huang, Jaap S. Sinninghe Damsté, Ellen C. Hopmans, and Andrew S. Cohen. 2008. "Northern Hemisphere Controls on Tropical Southeast African Climate during the Past 60,000 Years." *Science* 322(5899):252–55.

Torre, Ignacio, Mario Díaz, Jesús Martínez-Padilla, Raúl Bonal, Javier Viñuela, and Juan A. Fargallo. 2007. "Cattle Grazing, Raptor Abundance and Small Mammal Communities in Mediterranean Grasslands." *Basic and Applied Ecology* 8(6):565–75.

Tromp-van Meerveld, H. J., and Jeff J. McDonnell. 2006. "On the Interrelations between Topography, Soil Depth, Soil Moisture, Transpiration Rates and Species Distribution at the Hillslope Scale." *Advances in Water Resources* 29(2):293–310.

Tuanmu, Mao-Ning, and Walter Jetz. 2015. "A Global, Remote Sensing-Based Characterization of Terrestrial Habitat Heterogeneity for Biodiversity and Ecosystem Modelling." *Global Ecology and Biogeography* 24(11):1329–39.

Tucker, Marlee A., Terry J. Ord, and Tracey L. Rogers. 2014. "Evolutionary Predictors of Mammalian Home Range Size: Body Mass, Diet and the Environment." *Global Ecology and Biogeography* 23(10):1105–14.

Umer, M., H. F. Lamb, R. Bonnefille, A. M. Lézine, J. J. Tiercelin, E. Gibert, J. P. Cazet, and J. Watrin. 2007. "Late Pleistocene and Holocene Vegetation History of the Bale Mountains, Ethiopia." *Quaternary Science Reviews* 26(17–18):2229–46.

Vial, D. T. 2011. "Livestock Grazing in Bale Mountains National Park, Ethiopia: Past, Present and Future." *Walia—Special Edition on the Bale Mountains* 197–207.

Vial, Flavie, David W. Macdonald, and Daniel T. Haydon. 2011. "Response of Endemic Afroalpine Rodents to the Removal of Livestock Grazing Pressure." *Current Zoology* 57(6):741–50.

Vicente, Mário, and Carina M. Schlebusch. 2020. "African Population History: An Ancient DNA Perspective." *Current Opinion in Genetics & Development* 62:8–15.

Vlasatá, T., J. Šklíba, M. Lövy, Y. Meheretu, C. Sillero-Zubiri, and R. Šumbera. 2017. "Daily Activity Patterns in the Giant Root Rat (Tachyoryctes Macrocephalus), a Fossorial Rodent from the Afro-Alpine Zone of the Bale Mountains, Ethiopia." *Journal of Zoology* 302(3):157–63.

Vleck, David. 1979. "The Energy Cost of Burrowing by the Pocket Gopher Thomomys Bottae." *Physiological Zoology*.

Wakulińska, Martyna, and Adriana Marcinkowska-Ochtyra. 2020. "Multi-Temporal Sentinel-2 Data in Classification of Mountain Vegetation." *Remote Sensing* 12(17):2696.

Wallis, Christine I. B., Gunnar Brehm, David A. Donoso, Konrad Fiedler, Jürgen Homeier, Detlev Paulsch, Dirk Süßenbach, Yvonne Tiede, Roland Brandl, Nina Farwig, and Jörg Bendix. 2017. "Remote Sensing Improves Prediction of Tropical Montane Species Diversity but Performance Differs among Taxa." *Ecological Indicators* 83:538–49.

Wan, Xinru, Guangshun Jiang, Chuan Yan, Fangliang He, Rongsheng Wen, Jiayin Gu, Xinhai Li, Jianzhang Ma, Nils Chr Stenseth, and Zhibin Zhang. 2019. "Historical Records Reveal the Distinctive Associations of Human Disturbance and Extreme Climate Change with Local Extinction of Mammals." *Proceedings of the National Academy of Sciences of the United States of America* 116(38):19001–8.

Wang, Dongliang, Quanqin Shao, and Huanyin Yue. 2019. "Surveying Wild Animals from Satellites, Manned Aircraft and Unmanned Aerial Systems (UASs): A Review." *Remote Sensing* 11(11).

Wang, Yingxin, Xinglu Zhang, Y. I. Sun, Shenghua Chang, Zhaofeng Wang, Guang Li, And Fujiang Hou, Y Wang, X Zhang, Y. Sun, S Chang, Z Wang, G Li, and F. Hou. 2020. "Pika Burrow and Zokor Mound Density and Their Relationship with Grazing Management and Sheep Production in Alpine Meadow." *Ecosphere* 11(5):e03088.

Warren, Steven D., Martin Alt, Keith D. Olson, Severin D. H. Irl, Manuel J. Steinbauer, and

Anke Jentsch. 2014. "The Relationship between the Spectral Diversity of Satellite Imagery, Habitat Heterogeneity, and Plant Species Richness." *Ecological Informatics* 24:160–68.

Weir, B. S., and C. Clark Cockerham. 1984. "Estimating F-Statistics for the Analysis of Population Structure." 38(6):1358–70.

Westbury, Michael V., Stefanie Hartmann, Axel Barlow, Ingrid Wiesel, Viyanna Leo, Rebecca Welch, Daniel M. Parker, Florian Sicks, Arne Ludwig, Love Dalen, and Michael Hofreiter. 2018. "Extended and Continuous Decline in Effective Population Size Results in Low Genomic Diversity in the World's Rarest Hyena Species, the Brown Hyena." *Molecular Biology and Evolution* 35(5):1225–37.

Willi, Yvonne, Josh Van Buskirk, and Ary A. Hoffmann. 2006. "Limits to the Adaptive Potential of Small Populations." *Annual Review of Ecology, Evolution, and Systematics* 37:433–58.

Wilson, Don E., and DeeAnn M. Reeder. 2005. *Mammal Species of the World*. 3rd ed. Baltimore, Maryland: Johns Hopkins University Press.

Wilson, Robert J., and David Gutiérres. 2016. "Effects of Climate Change on the Elevational Limits of Species Ranges." Pp. 107–32 in *Ecological Consequences of Climate Change: Mechanisms, Conservation, and Management*.

Wisz, Mary Susanne, Julien Pottier, W. Daniel Kissling, Loïc Pellissier, Jonathan Lenoir, Christian F. Damgaard, Carsten F. Dormann, Mads C. Forchhammer, John Arvid Grytnes, Antoine Guisan, Risto K. Heikkinen, Toke T. Høye, Ingolf Kühn, Miska Luoto, Luigi Maiorano, Marie Charlotte Nilsson, Signe Normand, Erik Öckinger, Niels M. Schmidt, Mette Termansen, Allan Timmermann, David A. Wardle, Peter Aastrup, and Jens Christian Svenning. 2013. "The Role of Biotic Interactions in Shaping Distributions and Realised Assemblages of Species: Implications for Species Distribution Modelling." *Biological Reviews* 88(1):15–30.

Wood, Eric M., Anna M. Pidgeon, Volker C. Radeloff, and Nicholas S. Keuler. 2013. "Image Texture Predicts Avian Density and Species Richness." *PLOS ONE* 8(5):e63211.

Wraase, Luise, Victoria M. Reuber, Philipp Kurth, Mekbib Fekadu, Sebsebe Demissew, Georg Miehe, Lars Opgenoorth, Ulrike Selig, Zerihun Woldu, Dirk Zeuss, Dana G. Schabo, Nina

Farwig, and Thomas Nauss. 2022. "Remote Sensing-Supported Mapping of the Activity of a Subterranean Landscape Engineer across an Afro-Alpine Ecosystem." *Remote Sensing in Ecology and Conservation* 1–15.

Wright, Sewall. 1969. *Evolution and the Genetics of Populations, Vol. 2, The Theory of Gene Frequencies*. Chicago: University of Chicago Press.

Wright, Sewall. 1978. *Evolution and the Genetics of Populations, Vol. 4: Variability within and among Natural Populations*. Chicago: University of Chicago Press.

Wu, Ruixin, Qi Chai, Jianquan Zhang, Mengying Zhong, Yuehua Liu, Xiaoting Wei, Duo Pan, and Xinqing Shao. 2015. "Impacts of Burrows and Mounds Formed by Plateau Rodents on Plant Species Diversity on the Qinghai-Tibetan Plateau." *Rangeland Journal* 37(1):117–23.

Yaba, Mohammed, Tariku Mekonnen, Afework Bekele, and James Malcolm. 2011. "Food Selection and Feeding Behavior of Giant Mole Rat (Tachyoryctes Macrocephalus, Ruppell, 1842) from the Sanetti Plateau of Bale Mountains National Park, Ethiopia." *Asian Journal of Applied Sciences* 4(7):735–40.

Yalden, D. W. 1975. "Some Observations on the Giant Mole-Rat Tachyoryctes Macrocephalus (Rüppel 1842)(Mammalia Rhizomydae) of Ethiopia." *Monitore Zoologico Italiano. Supplemento* 6(1):275–303.

Yalden, D. W. 1983. "The Extent of High Ground in Ethiopia Compared to the Rest of Africa." *SINET: Ethiopian Journal of Science* 6:35–38.

Yalden, D. W. 1985. "Tachyoryctes Macrocephalus." *Mammalian Species* (237):1–3.

Yalden, D. W., and M. J. Largen. 1992. "The Endemic Mammals of Ethiopia." *Mammal Review* 22(3–4):115–50.

Yang, Tao, Xiaobo Hao, Quanxi Shao, Chong Yu Xu, Chenyi Zhao, Xi Chen, and Weiguang Wang. 2012. "Multi-Model Ensemble Projections in Temperature and Precipitation Extremes of the Tibetan Plateau in the 21st Century." *Global and Planetary Change* 80–81:1–13.

Yannic, Glenn, Loïc Pellissier, Joaquín Ortego, Nicolas Lecomte, Serge Couturier, Christine Cuyler, Christian Dussault, Kris J. Hundertmark, R. Justin Irvine, Deborah A. Jenkins,

Leonid Kolpashikov, Karen Mager, Marco Musiani, Katherine L. Parker, Knut H. Røed, Taras Sipko, Skarphéoinn G. Pórisson, Byron V. Weckworth, Antoine Guisan, Louis Bernatchez, and Steeve D. Côté. 2013. "Genetic Diversity in Caribou Linked to Past and Future Climate Change." *Nature Climate Change 2013 4:2* 4(2):132–37.

Yoshihara, Y., T. Okuro, J. Undarmaa, T. Sasaki, and K. Takeuchi. 2009. "Are Small Rodents Key Promoters of Ecosystem Restoration in Harsh Environments? A Case Study of Abandoned Croplands on Mongolian Grasslands." *Journal of Arid Environments* 73(3):364–68.

Yu, He, Alexandra Jamieson, Ardern Hulme-Beaman, Chris J. Conroy, Becky Knight, Camilla Speller, Hiba Al-Jarah, Heidi Eager, Alexandra Trinks, Gamini Adikari, Henriette Baron, Beate Böhlendorf-Arslan, Wijerathne Bohingamuwa, Alison Crowther, Thomas Cucchi, Kinie Esser, Jeffrey Fleisher, Louisa Gidney, Elena Gladilina, Pavel Gol'din, Steven M. Goodman, Sheila Hamilton-Dyer, Richard Helm, Jesse C. Hillman, Nabil Kallala, Hanna Kivikero, Zsófia E. Kovács, Günther Karl Kunst, René Kyselý, Anna Linderholm, Bouthéina Maraoui-Telmini, Nemanja Marković, Arturo Morales-Muñiz, Mariana Nabais, Terry O'Connor, Tarek Oueslati, Eréndira M. Quintana Morales, Kerstin Pasda, Jude Perera, Nimal Perera, Silvia Radbauer, Joan Ramon, Eve Rannamäe, Joan Sanmartí Grego, Edward Treasure, Silvia Valenzuela-Lamas, Inge van der Jagt, Wim Van Neer, Jean Denis Vigne, Thomas Walker, Stephanie Wynne-Jones, Jørn Zeiler, Keith Dobney, Nicole Boivin, Jeremy B. Searle, Ben Krause-Kyora, Johannes Krause, Greger Larson, and David Orton. 2022. "Palaeogenomic Analysis of Black Rat (Rattus Rattus) Reveals Multiple European Introductions Associated with Human Economic History." *Nature Communications 2022 13:1* 13(1):1–13.

Zagorodniuk, I., M. Korobchenko, V. Parkhomenko, and Z. Barkaszi. 2018. "Steppe Rodents at the Edge of Their Range: A Case Study of Spalax Microphthalmus in the North of Ukraine." *Biosystems Diversity* 26(3):188–200.

Zaniewski, A. Elizabeth, Anthony Lehmann, and Jacob Mc C. Overton. 2002. "Predicting Species Spatial Distributions Using Presence-Only Data: A Case Study of Native New Zealand Ferns." *Ecological Modelling* 157(2–3):261–80.

Zhang, Yanming. 2007. "The Biology and Ecology of Plateau Zokors (Eospalax Fontanierii)." Pp. 237–49 in *Subterranean Rodents: News from Underground*, edited by S. Begall, H. Burda, and C. E. Schleich. Berlin, Heidelberg: Springer.

Zhang, Yanming, and Jike Liu. 2003. "Effects of Plateau Zokors (Myospalax Fontanierii) on Plant Community and Soil in an Alpine Meadow." *Journal of Mammalogy* 84(2):644–51.

Zhang, Yanming, Zhibin Zhang, and Jike Liu. 2003. "Burrowing Rodents as Ecosystem Engineers: The Ecology and Management of Plateau Zokors Myospalax Fontanierii in Alpine Meadow Ecosystems on the Tibetan Plateau." *Mammal Review* 33(3–4):284–94.

Zhao, Ziyi, Nengwen Xiao, Mei Shen, and Junsheng Li. 2022. "Comparison between Optimized MaxEnt and Random Forest Modeling in Predicting Potential Distribution: A Case Study with Quasipaa Boulengeri in China." *Science of The Total Environment* 842:156867.

Declaration/Erklärung

Ich versichere, dass ich meine Dissertation mit dem Titel „Linking Scales: Investigations on the interactions between environmental conditions, humans, and a fossorial rodent species across space and time" selbstständig ohne unerlaubte Hilfe angefertigt und mich dabei keiner anderen als der von mir ausdrücklich bezeichneten Quellen und Hilfsmittel bedient habe.

Diese Dissertation wurde in der jetzigen oder einer ähnlichen Form noch bei keiner anderen Hochschule eingereicht und hat noch keinen sonstigen Prüfungszwecken gedient.

Marburg, den 01.09.2023

Victoria Michelle Reuber

Curriculum Vitae

[Here was originally a page on the author's curriculum vitae]

[Here was originally a page on the author's curriculum vitae]